Developing Energy and Nutrient Mass Balances to Inform Value Recovery Options in Municipal Wastewater Treatment Systems

Thesis submitted to Newcastle University for the degree of Doctor of Engineering in the Faculty of Science, Agricultural & Engineering

Author: Ziye Dai

Supervisors: Dr Adam Jarvis

Professor David Graham

Date: June 2019

Abstract

Municipal wastewater contains valuable substances such as energy, organic carbon and nutrients. Recovery of these valuable substances may be a promising approach towards the circular economy. However, their fate in the treatment processes is rarely studied holistically and may have substantial variations between sites. The overall aim of this project is to reliably determine the chemical energy and mass balances of wastewater treatment plants in the UK to inform possible options for recovery of organic carbon (for energy), nitrogen and phosphorus.

This study firstly developed a novel method for rapidly measuring wastewater energy content and determined the relationship between COD and chemical energy as 15.8 kJ/g COD. A similar relationship is estimated for the sludge. Subsequently, chemical energy balance is built on the COD balance. This study discovers only 20-30% of influent chemical energy can be potentially recovered as CH_4 for energy recovery. With this limited amount of energy recovered, wastewater treatment is unable to be energy self-sustaining even that the influent energy is more than 5-14 folds of the electricity consumption. Potential energy recovery opportunities are found in the primary settlement, secondary treatment, sludge return liquor, and digested sludge. In terms of nutrient, 17-41% of influent TN and 33-52% of influent TP are accessible for recovery in the sludge return liquor and biosolid. The potential value recovery option is to increase the capturing of nutrient into the sludge.

The impact of the implementation of energy and nutrient recovery measures on the overall energy balance and mass balance are studied via modelling. The nutrient recovery measure increases the nutrient loading in the sludge return liquor and biosolid and barely impacts the energy balance. However, whilst reducing the electricity deficit, the energy recovery measures tend to reduce the nutrient loading in the sludge return liquor but increase the proportion distributed in biosolid and the final effluent.

The economic feasibility and sensitivity study of the implementation of the biosolid pyrolysis is part of this research. Although it appears not to be economically viable at the current time, it substantially improves the energy balance of the treatment work. Economically viability could be achieved in the future if the influential capital cost can be reduced or better incentive can be granted.

Declaration

I hereby declare that this thesis is my original research work. I truly acknowledged all the sources of literature and information which has been used in this thesis. This thesis has not been submitted for a degree at this or any other University previously.

Ziye Dai

15/03/2019

Acknowledgements

I would like to acknowledge my primary supervisor Dr Adam Jarvis, with thanks for providing me lots of academic and technical support and encouragement. I am very appreciated his enormous patience and help throughout my whole EngD study, especially at the time I failed. Many great thanks to Mrs. Justine Easten, who has always been kind and helpful and have been looking after me in every aspect of this EngD study. I would also like to thank Dr Jaime Amezaga for being such a supportive director of the STREAM centre in Newcastle University

I would like to thank STREAM IDC and my sponsoring company Northumbrian Water and Scottish Water for offering me the funding to complete this EngD. I would like to thank Dr Mark Haffey previously from Scottish Water and especially Mr. Andrew Moore from Northumbrian Water, who have always been supportive and have provided me with all the resources I needed for this project. I also would like to thank Mr. Luke Dennis, Mr. John Robinson, Mr. Andrew Hinsmarsh, and Ms Laura Wilkinson from Northumbrian Water, and Mr. Robert McGinty and Mr. Jamie Lynch for their assistance during the sampling work.

I would like to thank my colleagues and co-workers who have given me advice and help and had fun time together. Particularly, I would like to thank Mr. Dave Race for all his help in the laboratory. I would like to thank my STREAM cohort IV members for their care and love.

I am incredibly thankful to my parents, my families and my friends back in China. Many thanks for their patience and love.

Last but not least, greatest gratitude to my wonderful wife Teng Zhang, who sacrifices a lot for staying in the UK for being me accompany. Without her endless support, I may not be able to get through all the dark moments in this journey.

Table of Contents

List of Figures

List of Tables

Chapter 1 Introduction

This Chapter first introduces the background and drivers for the research undertaken in Section 1.1. The aims and objective are proposed in Section 1.2. The thesis structure is shown in Section 1.3.

1.1 Background and drivers

1.1.1 Wastewater and wastewater treatment

Municipal wastewater comes from the water from toilets, baths, sinks and washing machines in homes, from water used in industry, and from rainwater runoff (DEFRA, 2012). This water is contaminated with organic matter, nutrients, metals, oils, pathogens, and other pollutants (DEFRA, 2012, Tchobanoglous et al., 2003). Direct discharges of wastewater to the environment may cause severe damage to the water environment, such as eutrophication of the receiving waters caused from the excessive input of nutrients, ecosystem damage to receiving waters due to the oxygen depletion during microbial biodegradation of organic matter, and health risks caused by the pathogens from wastewater entering into waters used for recreational purposes e.g. bathing waters (DEFRA, 2012). Therefore, wastewater treatment is crucial to ensure that wastewater quality is of a suitable standard to return to the environment.

Wastewater from different sources is collected in the sewerage network and flows into wastewater treatment works. Wastewater treatment generally has three stages: (1) preliminary treatment (2) primary treatment and (3) secondary treatment (Tchobanoglous et al., 2003, DEFRA, 2012). Preliminary treatment typically involves screening out large solids, such as wood and plastics, and removal of grit. Primary treatment has the objective of settling suspended particulate matter. Secondary treatment is usually biological and is used to remove the residual particulate and soluble contaminants. In some cases tertiary treatment is required for removing specific types of pollutant (Tchobanoglous et al., 2003). Once pollutant concentrations are lowered to below the consent level, wastewater can be discharged back to environment.

The treatment processes, especially the primary and secondary treatment, produce sludge as a by-product. In current practise the produced sludge is commonly sent for anaerobic digestion (AD). Since AD requires the feed sludge to have a certain moisture level (Mills et al., 2014), sludge goes through a thickening process to remove the extra undesired water content. The anaerobic digestion of sludge produced digested sludge and biogas contains biomethane and CO_2 (Smyth et al., 2016, Wan et al., 2016, Tchobanoglous et al., 2003). The digested sludge will be dewatered and usually sent for land application (DEFRA, 2012). The produced biomethane will be commonly used onsite for electricity generation or injected to the gas grid (Mills et al., 2014). A schematic flow diagram of the wastewater and sludge treatment process is shown in Figure 1-1.

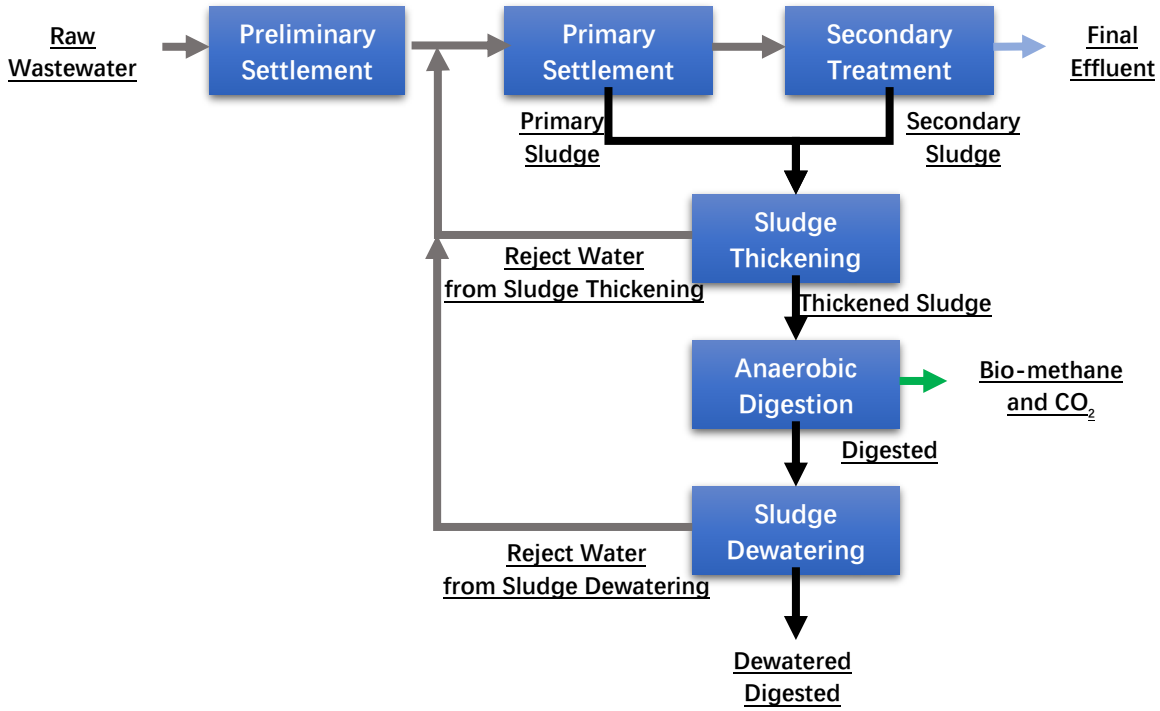

Figure 1-1 Schematic of typical wastewater treatment and sludge treatment

1.1.2 Drivers for value recovery from wastewater

In essence, wastewater is a used resource that is disposed of to a wastewater treatment facility in order to minimize the harm of that disposal. This reflects the conventional economic model of "take-make-consume-dispose": resources are taken from the environment, made into products, consumed by society, and finally disposed back to the environment (IWA, 2016). This economic model heavily relies on the abundance of natural resources (IWA, 2016). If the

natural resource is finite, then this economic model is not sustainable (IWA, 2016). A schematic illustration of the linear economy model is shown in Figure 1-2.

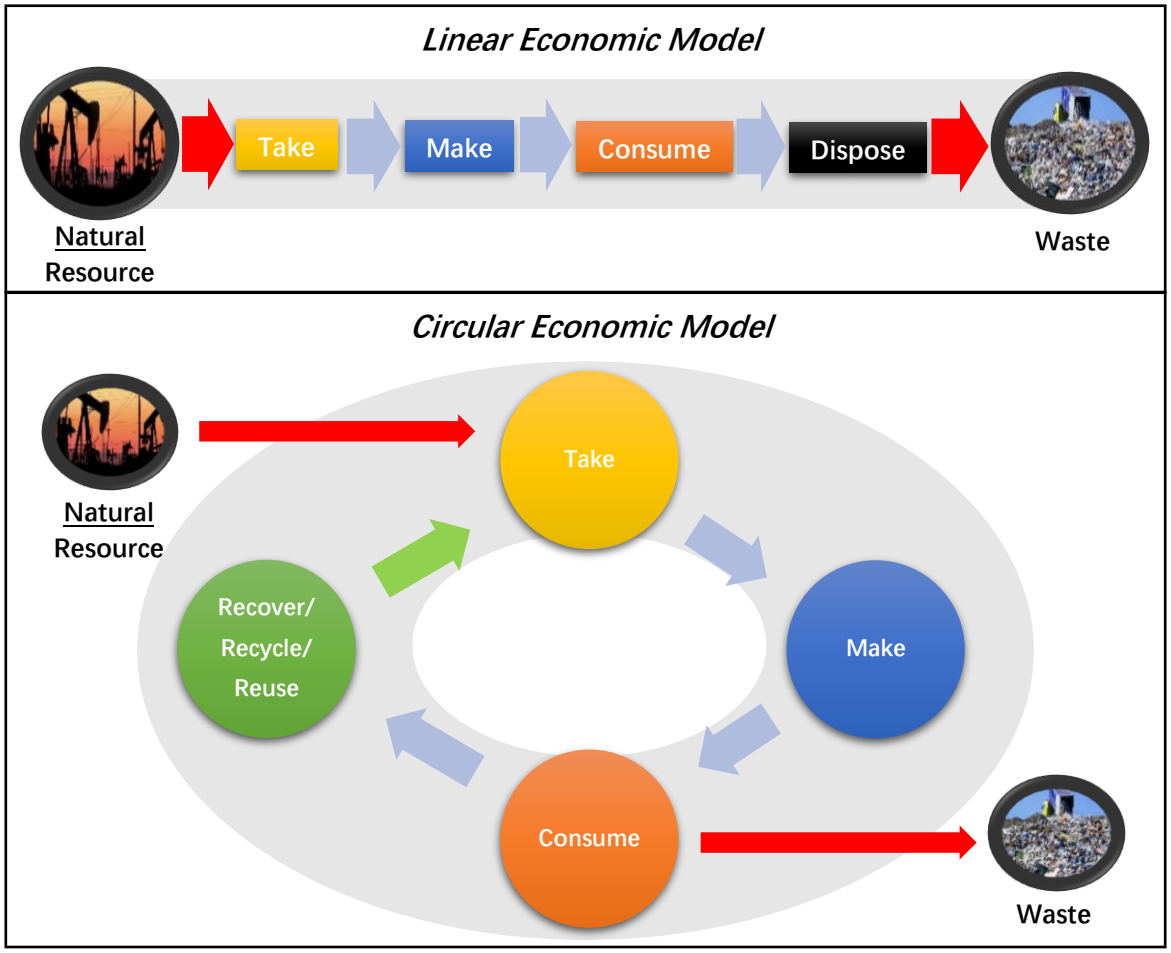

Figure 1-2 The schematic of linear economic model and circular economic model (IWA, 2016)

Pearce and Turner (1990) proposed a concept of circular economy. In 2015, the European Commission defined the circular economy as follows: *"In a circular economy, the value of products and materials is maintained for as long as possible. Waste and resource use are minimised, and when a product reaches the end of its life, it is used again to create further value."* The European Union also set a target to recycle 65% of municipal waste by 2035 (European Commission, 2019). Wastewater is rich in organic carbon, nitrogen and phosphorus content (Ainger et al., 2009). Cellulose, plastics, fertilizers, energy of methane, hydrogen and electricity have all been reported to be recoverable from wastewater (van der Hoek et al., 2016, Scherson and Criddle, 2014, McCarty et al., 2011, Cotterill et al., 2018, van der Hoek et al., 2018). Therefore, wastewater is no longer just a waste to dispose of, but actually a resource to

society. Wastewater treatment works can then be transformed into a chemical process plant for extracting these valuable substances back into products (Ainger et al., 2009). The recovery of chemical energy, nitrogen and phosphorus from wastewater could also bring in environmental benefit, such as tackling the fossil scarcity and the phosphorus shortage (Mayer et al., 2016, Wan et al., 2016). Value recovery from wastewater will therefore play an important role in the circular economy (IWA, 2016).

1.1.3 Current status of value recovery from wastewater

Substances commonly recovered from wastewater are organic carbon, for chemical energy, and nutrients for fertilizer (McCarty et al., 2011, Mayer et al., 2016, Stoll et al., 2018). Currently full-scale value recovery is mainly from wastewater treatment sludge rather than directly from wastewater (Bowen et al., 2010, Smyth et al., 2016, Mills et al., 2014, Münch and Barr, 2001). The approach to energy recovery is anaerobic digestion of the sludge for methane production (Smyth et al., 2016, Bowen et al., 2010, Mills et al., 2011). The approach to nutrient recovery is typically to utilize the digested sludge as fertilizer for agricultural land application. Alternatively phosphate and ammonium may be precipitated to produce the slow release fertilizer struvite (magnesium ammonium phosphate), usually from the reject water produced from digested sludge dewatering (Münch and Barr, 2001, Ostara, 2010, Paz-Ferreiro et al., 2018).

However, current practices only recover limited amounts of the valuable substances flowing into wastewater treatment plant (WWTP). A mass balance study of a Singapore WWTP suggested that only approximately 18% of the organic carbon from the raw wastewater was recovered as methane (Shi, 2011). Meanwhile, 11% of the nitrogen and 20% of the phosphorus from the raw wastewater were found in the reject water produced from the digested sludge dewatering, whilst 12% of nitrogen and 43% of phosphorus from the raw wastewater ended in the dewatered digested sludge (Shi, 2011). It is worth noting that the recovery efficiency can vary substantially from site to site. In another mass balance study of an Austrian WWTP, approximately 36% the organic carbon from the raw wastewater was recovered as methane (Wett et al., 2007).

Mass and energy balance is a very useful technique for process evaluation, designing and benchmarking WWTP (Yeshi et al., 2013). More importantly, it can be used to guide process improvement to promote value recovery from wastewater (Yeshi et al., 2013). However, there are few studies that perform plant wide holistic mass balance investigation of organic carbon, nitrogen and phosphorus together (Yeshi et al., 2013). Meanwhile, the construction of mass and energy balance required proper flow and concentration measurement of each influent and effluent of the treatment process (Tchobanoglous et al., 2003). The construction could be constraint by the poor flow and concentration monitoring, since water companies do not often synchronously measure flow and concentration on each influent and effluent of their treatment process (*personal communication*, M Haffey, Scottish Water, April 2015, *personal communication*, L Wilkinson, Northumbrian Water, June 2015).

As mentioned above the organic carbon recovered from wastewater is used for energy application. Although some efforts have been made to construct chemical energy balances for wastewater treatment works from the organic carbon (expressed as chemical oxygen demand, COD) mass balance, the relationship between chemical energy and the COD of wastewater is yet to be reliably defined (Wan et al., 2016, Wett et al., 2007). The approach to measurement of chemical energy is to dry the wastewater first, and then to measure the calorific value of the dried wastewater via bomb calorimetry (Korth et al., 2017, Shizas and Bagley, 2004, Heidrich et al., 2010). The drying stage is vital to the accuracy of the energy measurement because it has to retain as much of the energetic organic carbon in the dried wastewater and it should be time efficient to allow large amount of measurements (Heidrich et al., 2010, Korth et al., 2017). The current method applied for drying is freeze-drying. However, whilst this is able to retain more than 80% of the organic carbon originally contained in the wastewater it requires approximately 4 weeks to process a sample (Heidrich et al., 2010). Furthermore, neither freeze driers or bomb calorimeters are equipment commonly possessed by water companies (Korth et al., 2017, Schaum et al., 2016). Therefore, to construct a reliable chemical energy balance, a reliable and time efficient drying method is required. With greater amount of sample being analyzed, the relationship between chemical energy and COD or another proper surrogates can be better defined.

The implementation of value recovery initiatives may have a negative impact on existing treatment performance at WWTPs. As stated in Section 1.1.1 and shown Figure 1-1, wastewater and sludge treatment consists of a series of mechanical and biological processes. The introduction of new value recovery technologies, or the improvement of current value recovery technologies at a WWTP, may influence the performance of a process and consequently affect the downstream processes. For instance, if a WWTP has a nutrient discharge consent, the recirculation of its nutrient rich reject water from the digested sludge dewatering back to head of the work, will stress the treatment process (Münch and Barr, 2001). Implementation of struvite recovery, which recovers the nutrient from rejected water (from the sludge dewatering) into fertilizers, will reduce the stress to the wastewater treatment performance (Münch and Barr, 2001). However, in the example of cellulose recovery, if the cellulose, which is an organic carbon resource, is captured prior or post the primary treatment but not sent for digestion, the organic loading carbon loading to the digester will be reduced (van der Hoek et al., 2016). This causes an adverse effect to the current organic carbon recovery as biomethane production becomes smaller (van der Hoek et al., 2016).

1.2 Aims and Objectives

Current efforts to recover value from WWTPs focus on sludge, but the degree to which substances are recovered is variable and/or low (Shi, 2011, Wett et al., 2007). Furthermore, recovery of valuable substances directly from wastewater is currently limited. In this research the following aspects of value recovery were therefore explored:

- The potential for recovery of value directly from municipal wastewaters
- Improving the efficiency of current value recovery approaches used on sludge

The foundation for delivering such improvements in value recovery is a clear quantitative understanding of the chemical and energy mass balances at WWTPs, such that there is a proper appreciation of the fate of potentially valuable organic carbon, nitrogen and phosphorus during wastewater and sludge treatment. Furthermore, knowledge of how these mass balances vary between WWTPs is required. Only then can the benefits of value recovery options be truly evaluated.

Therefore, the overall aim of this project is to reliably determine the chemical energy and mass balances of wastewater treatment plants in the UK to inform possible options for recovery of organic carbon (for energy), nitrogen and phosphorus.

To fulfil this overall aim, the objectives were set, as follows:

1. Develop a reliable and practical method for determination of the chemical energy content of wastewater, and identify a reliable surrogate of the chemical energy in wastewater and in sludge

2. Construct chemical energy and mass balances for 4 WWTPs to determine the fate of chemical energy, organic carbon (expressed as COD), nitrogen and phosphorus in the wastewater and sludge treatment (via modelling)

3. Identify potential waste recovery opportunities and explore the impact of their implementation on the existing treatment process (via modelling)

In order to obtain representative findings, 4 WWTPs from the sponsor companies of Scottish Water and Northumbrian Water were chosen in this study. These 4 WWTPs were intentionally selected as they are varied in terms of population equivalent (P.E.), wastewater treatment processes, and sludge treatment processes. Details for each of them are shown in Table 1-1.

Table 1-1 Overview of the 4 Investigated WWTPs

WWTPs	Population Equivalent	Wastewater Treatment Process	Sludge Treatment Process
WWTP A	40,000	Primary Settlement with Chemical Dosing for Phosphate removal and Activated Sludge with Nitrification	N/A
WWTP B	230,000	Primary Settlement and Activated Sludge	Sludge Thickening and Dewatering
WWTP C	1,000,000	Primary Settlement and Activated Sludge	Sludge Thickening, Dewatering and Advanced Anaerobic Digestion
WWTP D	180,000	Primary Settlement and Activated Sludge with Nitrification	N/A

1.3 Thesis Structure

The remaining 7 chapters of this thesis are arranged as follows:

Chapter 2 - A literature review focusing on the determination of surrogate of chemical energy in wastewater and in sludge and the study of the fate of the valuable organic carbon, nitrogen and phosphorus in the wastewater and sludge treatment processes

Chapter 3 - Field and analytical methods used, the procedure of wastewater and sludge treatment modelling, and the construction of chemical and energy balances

Chapter 4 - Results and Discussion of the method developed for determination of chemical energy in wastewater, and discussion of the surrogates for estimating the chemical energy in wastewater and sludge

Chapter 5 – Results and Discussion of chemical energy and COD mass balance, and discussion of potential chemical energy recovery opportunities from wastewater and the impact of their implementation

Chapter 6 - Results and Discussion of nitrogen and phosphorus mass balance, and discussion of potential nutrient recovery opportunities from wastewater and the impact of their implementation

Chapter 7 – Business case study on biosolid gasification for energy recovery, which includes discussion of the economic evaluation and sensitivity studies on the uncertainties

Chapter 8 – Conclusions and Recommendation

Chapter 2 Literature Review

This chapter first reviews the surrogate of chemical energy in wastewater and in sludge in Section 2.1. It then assesses the fate of valuable organic carbon, nitrogen and phosphorus in the wastewater and sludge treatment processes in Section 2.2. It reviews application of modelling in the mass balance investigation and in studying the impact of process reconfiguration in Section 2.3. The research questions are then proposed in Section 2.4.

2.1 The surrogate of chemical energy in wastewater and in sludge

Chemical energy contained in wastewater is estimated approximately 5 times greater than electricity consumed for during treatment (Wan et al., 2016). Wastewater also contains thermal and kinetic energy (McCarty et al., 2011). Wastewater treatment has the potential to become an energy net producer (McCarty et al., 2011). But, in reality it is the opposite as the chemical energy within wastewater is not used in its full potential. It is worth, then to know the fate of different types of energy during the wastewater.

Recovery of thermal energy requires heat pump which consumes electricity. Alternative fuels for heating, such as natural gas or fuel oil, are equally expensive as electricity, then thermal recovery is costly(McCarty et al., 2011). Kinetic energy is caused by the movement of wastewater and hence it can be recovered by hydropower electricity generation (Power et al., 2014). Kinetic energy recovery has a strict requirement: flow rate of wastewater. Power et al. (2014) reported that only 14 out of 100 Irish wastewater treatment plants are suitable for hydropower electricity generation, and those plants are relatively large. Also, thermal and kinetic energy recovery are rarely conducted.

Currently, energy recovery focus on the chemical energy capture from wastewater and sludge (McCarty et al., 2011, Stoll et al., 2018, Scherson and Criddle, 2014). Therefore, it is useful to understand the chemical energy balance of the wastewater and sludge treatment to discover the potential chemical energy reserve.

The experimental measurement of the chemical energy content of sludge and wastewater is commonly done via bomb calorimetry (Shizas and Bagley, 2004, Heidrich et al., 2010, Korth et al., 2017, Smyth et al., 2016, Schaum et al., 2016). Because more than 70% of the mass in both wastewater and sludge is from non-combustible water, the wastewater and sludge will be dried first and then analyzed for chemical energy content via bomb calorimetry (Korth et al., 2017, Smyth et al., 2016, Shizas and Bagley, 2004, Heidrich et al., 2010, Schaum et al., 2016). However, bomb calorimetry is not commonly possessed in WWTPs due to its cost and complicated set up (for example, it requires oxygen cylinders) (Schaum et al., 2016, Smyth et al., 2016). The chemical energy content of the wastewater and sludge is therefore not able to be routinely measured (Smyth et al., 2016, Schaum et al., 2016). Chemical energy balance is then calculated on the mass balance of a chosen surrogate of wastewater and sludge (Mills et al., 2014, Wan et al., 2016, Wett et al., 2007). The determination of the relationship between chemical energy content and the suitable surrogate of it is crucial to the accuracy of the chemical energy balance.

2.1.1 Surrogate of wastewater chemical energy

Since chemical energy is mainly stored in the organic contaminants and chemical oxygen demand (COD) is commonly used to represent the concentration of the organic contaminant in wastewater, COD is the preferable surrogate of the chemical energy content in wastewater (Owen, 1982, Korth et al., 2017, Scherson and Criddle, 2014, Tchobanoglous et al., 2003).

Owen (1982) firstly proposed the concept of using COD to estimate the energy content of wastewater. The study measured the calorific value of several organic compounds that may exist in wastewater. The oxygen demand of the complete combustion ($COD_{Combustion}$) per gram of those substances were also studied based on both theoretical enthalpy calculation and experimental measurement. It was obtained by diving calorific value by the $COD_{Combustion}$, chemical energy within per gram of COD. The kJ/g COD of the measured organic ranged from 12.6 to 15.5 and the mean value was 14.2 (shown in Table 2-1). The study chose to use the value of 13.9 kJ/g COD for its energy-related calculation. In this case, the energy calculation used by Owen (1982) is based on BTU/lb. 13.9 kJ/g is equivalent to a round up number of 6,000 BTU/lb while 14.2 kJ/g is equivalent to 6,100 BTU/lb. This 13.9 kJ/g COD value was a

reasonable assumption, but it was not selected based on the proportion of the concentration of organic compound in the wastewater.

Table 2-1 The kJ/g COD values of commonly found organics in wastewater studied by Owen (1982)

Name	Chemical Formula	Measured kJ/g COD	Calculated kJ/g COD
Wastewater Organic	$C_{10}H_{18}O_3N$	15.5	13.9
Bacterial Cells	$C_5H_7O_2N$	14.7	15.4
Carbohydrates	$C_6H_{10}O_5$	14.7	12.7
Fats	$C_{18}H_3\,6O_2$	15.1	14.5
Proteins	$C_{71}H_{128}O_{23}S$	N/A	14.1
Acetic Acid	$C_2H_4O_2$	13.6	12.6
Benzene	C_6H_6	13.6	13.8
Benzoic Acid	$C_7H_6O_2$	13.5	13.0
Butyric Acid	$C_4H_8O_2$	13.7	13.8
Carbon Dioxide	CO_2	0	0
Ethanol	C_2H_6O	14.3	14.5
Furfural	$C_5H_4O_2$	14.7	12.8
Hydrogen Sulfide	H_2S	N/A	N/A
Lactic Acid	$C_3H_6O_3$	14.1	12.6
Levulinic Acid	$C_5H_8O_3$	N/A	13.2
Methane	CH_4	13.9	15.4
Methanol	CH_4O	15.2	14.4
Phenol	C_6H_6O	13.7	13.5
Propionic Acid	$C_3H_6O_2$	13.7	13.6
Vanilin	$C_8H_8O_3$	14.0	13.0

Shizas and Bagley (2004) conducted the first study to experimentally measure chemical energy content in wastewater. In this research, wastewater was oven dried at 104°C to remove all the moisture. Subsequently, the dried wastewater was fed to the bomb calorimeter for chemical energy measurement. The study determined a result of 14.7 kJ/g COD, which is higher than the value that Owen (1982) reported. The 14.7 kJ/g COD was estimated based on one raw wastewater sample which could not be considered representative.

Heidrich et al. (2010) also measured chemical energy content in wastewater. The study followed a similar approach by drying the wastewater sample first, and subsequently measuring

its energy content via bomb calorimetry. However, Heidrich et al. (2010) used freeze drying instead of the oven drying method. The study showed that freeze drying was able to retain 73-81% of COD in the dried residue compared to oven drying which only retained 51-56%. Thus, this leads to a higher measured value of chemical energy content of wastewater and a higher value kJ/g COD. In this case, the study experimentally measured two raw wastewater samples and determined values of 17.7 to 28.7 kJ/g COD respectively.

Rather than reporting energy content as kJ/g COD, Korth et al. (2017) used linear regression to determine the mathematical relationship between chemical energy content of wastewater and COD. His experiments concluded that chemical energy content in wastewater (kJ/L) equal to 3.883×COD (g/L) +2.045. The equation was determined by applying 20 data points from which 1 were from data point from Shizas and Bagley (2004) and 2 were from Heidrich et al. (2010). However, whilst acknowledging that freeze-drying is a preferable method for wastewater energy measurement, Korth et al. (2017) nevertheless used oven drying for the majority of samples, because of the long processing time for freeze drying. The r^2 of the linear regression is reported as 0.65 (Korth et al., 2017).

The relationship between chemical energy and COD has only been experimentally studied on 20 raw wastewater samples globally. The experimental measured values reported Shizas and Bagley (2004) and Heidrich et al. (2010) vary by up to 95 % (comparing to the 14.7 KJ/g COD). Meanwhile, Korth et al. (2017) did suggest using linear regression to estimate the chemical energy content of wastewater from COD, but the majority of the data used for linear regression analysis were obtained from the oven drying method which is proven not effectively in retaining COD. Therefore, the relationship between COD and chemical energy was poorly defined and needs to be reliably determined.

Unlike the COD, N and P measurement, which can be conducted on aqueous samples and completed within hours or days, the chemical energy measurement requires dried sample and weeks to complete (Korth et al., 2017, Heidrich et al., 2010). The drying stage is time consuming, as freeze drying takes 4 weeks to dry enough wastewater to generate approximately 0.5 g of dried residue to be used in the bomb calorimetry (Heidrich et al., 2010). The time-consuming drying process hinders the large amount experimental measurement on chemical

energy content of wastewater and the subsequent study of the relationship between chemical energy and COD.

2.1.2 Surrogate of sludge chemical energy

Total solid (TS) content is usually used as a surrogate of sludge chemical energy (Mills et al., 2014, Shizas and Bagley, 2004, Schaum et al., 2016, Smyth et al., 2016). The chemical energy content of the sludge is calculated by multiplying the calorific value of the dried solid content with TS content (Mills et al., 2014). This is because the TS content is routinely measured in sludge treatment and is commonly used to describe the performance and mass balance of the sludge treatment (Smyth et al., 2016, Bowen et al., 2010).

Unlike wastewater, hundreds of sludge samples have been studied for chemical energy content of the TS content (Schaum et al., 2016). The result does vary from types of sludge and studies. The reported chemical energy content of TS content ranges from 15.9 to 17.9 kJ/g for primary sludge, 12.2 to 18.1 kJ/g for surplus activated sludge, and 11.1 to 15.7 kJ/g for digested sludge, respectively (Schaum et al., 2016, Shizas and Bagley, 2004, Smyth et al., 2016). There is a considerable variation in the chemical energy content of TS content in the sludge, especially for the surplus activated sludge and digested sludge.

Moreover, Shizas and Bagley (2004), Schaum et al. (2016) and Smyth et al. (2016) all suggested that the sludge chemical energy is also related to volatile solid (VS) content because most of the energetic organic is contained in the VS. The chemical energy content of VS content reported in these three studies range from 21.0 to 26.6 kJ/g for primary sludge, 20.6 to 21.3 kJ/g for surplus activated sludge, and 20.5 to 30.7 kJ/g for digested sludge, respectively (Schaum et al., 2016, Shizas and Bagley, 2004, Smyth et al., 2016). There is also a considerable variation in the chemical energy content of VS content in the sludge. Therefore, a validation of the relationship between the chemical energy and the TS and VS content of sludge is required.

2.2 Fate of valuables in wastewater treatment work

Naden et al. (2016) estimated 1,460,000 tonnes organic carbon, 263,000 tonnes of nitrogen and 43,600 tonnes of phosphorus flowed through United Kingdom's WWTPs in 2010. Using a ratio

of chemical oxygen demand (COD) to total organic carbon as 3:1 (Henze and Comeau, 2008), 4,380,000 tonnes COD flows into the treatment work. Reportedly, 1 gram of COD contains 13.9 kJ of chemical energy (Owen, 1982). Then, an estimated 16,900 GWh of chemical energy flows into the UK's wastewater treatment. Wastewater treatment uses up to 1% of the national electricity (POST, 2007). According to the Historical electricity data: 1920 to 2017 published by Department for business, Energy & Industrial Strategy, the annual electricity production of the UK in 2010 was 333,205 GWh. This suggests that electricity consumed for wastewater treatment is approximately 3,332 GWh electricity per annum. The energy reserve in the wastewater is approximately 5 times greater than the energy used for treatment purposes. For nutrient, over the same period (2010), the UK's annual fertilizer consumption was approximately 1,000,000 tonnes of nitrogen and 84,000 of phosphorus (AIC, 2011). Indicating, that more than a quarter of the nutrient demand for agricultural consumption can be found in wastewater.

At present, these valuables are not fully recovered into usable resource from wastewater treatment plants. Actually, part of them are converted and emitted into the atmosphere, another portion will be captured in the sludge and ultimately released to land, and only a small part of it is recovered into the products (i.e. CH_4 or fertiliser of struvite) that we can use (Mills et al., 2014, Münch and Barr, 2001, Tchobanoglous et al., 2003, Wett et al., 2007). Besides, part of these valuable products will discharged back to surface water bodies. Naden et al. (2016) estimated that in 2010, 63,000 tonnes of organic carbon, 104,000 tonnes of nitrogen and 14,800 tonnes of phosphorus were discharged to the environment after treatment process.

Since the amount of the valuable organic carbon, nitrogen and phosphorus are substantial but not yet fully utilized, it is worth knowing what the exact fate of these valuables are in the wastewater treatment process. Mass balance is a measure to track a mass loading of a substance in the inlet(s) and in the outlet(s) of a chemical treatment process (Tchobanoglous et al., 2003). It is commonly used to study the fate or the distribution pattern of a substance in the wastewater treatment process (Shi, 2011, Wett et al., 2007, Gans et al., 2007). Commonly, a wastewater treatment process includes mechanical primary settlement and secondary biological treatment (Tchobanoglous et al., 2003). A complete process will also have sludge treatment associated with anaerobic digestion (Shi, 2011, Wett et al., 2007). . Since organic carbon is commonly

expressed as COD in wastewater treatment, COD is used to represent organic carbon in the following content of this chapter.

2.2.1 Fate of COD, N and P in primary settlement

2.2.1.1 Process mechanism

Primary settlement aims to remove the readily settleable solids and floating material by sedimentation, but soluble organic content including contaminants, are not typically removed at this stage, unless there is chemical addition. Theoretically, the settleable particulate contaminants are removed after and end up in the primary sludge (Tchobanoglous et al., 2003).

2.2.1.2 COD, N and P Mass balance of primary settlement

COD

The typical contribution of the particulate fraction to total wastewater COD is approximately 60% (Henze and Comeau, 2008, Tchobanoglous et al., 2003). Commonly, the COD removal rate of primary settlement ranges from 30-40 %, with the remaining 60-70% of COD flowing to secondary treatment (Shi, 2011, Wan et al., 2016, Gans et al., 2007).

Nitrogen

Typically, the soluble ammoniacal nitrogen (NH_4^+-N) contributes 60-75 % to the total nitrogen (TN) content (Tchobanoglous et al., 2003, Henze and Comeau, 2008). Since the soluble nitrites or nitrates are only a minor component of TN, the majority of the remaining 40 % of TN content is present as organic nitrogen (both particulate and soluble fractions) (Henze and Comeau, 2008). Therefore, theoretically no more than 40 % of TN is captured in the primary sludge. In practice the percentage of TN captured in primary sludge is only 10-25 % (Kristensen et al., 2004, Shi, 2011). Therefore, 75-90 % of TN in wastewater treatment works flows to the secondary treatment process.

Phosphorus

The soluble content of phosphate (PO_4^{3-}-P) is the dominant component of the total phosphorus (TP) in raw wastewater, and the typical contribution of it to the TP content is 67% (Tchobanoglous et al., 2003, Henze and Comeau, 2008). Therefore, theoretically less than 33 % of the inflowing TP is captured in the primary sludge. In practice, the percentage of P captured

in primary sludge in a pure mechanical primary settlement is only 10-25 % (Kristensen et al., 2004, Shi, 2011). However, PO_4^{3-}-P can be removed via the addition of aluminum ($AlCl_3$ or $Al_2(SO_4)_3$) or ferric salts ($FeCl_3$ or $Fe_2(SO_4)_3$) (Tchobanoglous et al., 2003). Depending on the chemical dosage, the TP removal rate can be up to 75-95% (Tchobanoglous et al., 2003). The studies of Kristensen et al. (2004) and Grizzetti and Bouraoui (2006) shows that, if chemical dosing is involved in primary treatment, 20-92 % of the TP is removed and captured in the primary sludge. Therefore, if chemical dosing is not in place, 75-90 % of the TP to the treatment works will flow to the secondary treatment; if chemical dosing is used then 18-80% of the TP of the work will flow to secondary treatment. There is a great variation in TP removal in primary settlement.

2.2.2 Fate of COD, N and P in secondary settlement

Secondary biological treatment utilizes microorganisms to treat the COD, nitrogen and TP. In all of the WWTPs investigated the activated sludge process is employed as the secondary treatment process. This Section 2.2.2 therefore only reviews the fate of the targeted substances (COD, N and P) in the activated sludge process.

2.2.2.1 Process mechanism of activated sludge

COD

For COD removal, aerobic heterotrophic microorganisms oxidize organic matter into CO_2 and water (H_2O). These microorganisms assimilate at the same time part of the organic matter present in the secondary treatment for its own growth (Tchobanoglous et al., 2003). Oxidation requires that microorganisms have to be maintained at a constant level to deliver satisfactory COD removal efficiency. However, the excess growth of microorganisms from the organic matter assimilation are removed as Surplus Activated Sludge (SAS). Thus, after the secondary treatment, COD, namely the organic carbon, is distributed between CO_2, the secondary treatment effluent, and the SAS (Puig et al., 2008).

Nitrogen

There are three elements to nitrogen removal (Tchobanoglous et al., 2003):

- Nitrification, in which aerobic autotrophic nitrifiers will oxidize the ammoniacal nitrogen to nitrite (NO_2^-) and nitrate (NO_3^-)

- Denitrification may also occur when wastewater is recirculated to an anoxic zone. Denitrifiers will reduce the NO_2^- and NO_3^- produced during nitrification to N_2
- Assimilation of nitrogen during microorganism growth

Thus, after secondary treatment, nitrification and denitrification may occur, and total nitrogen content may be distributed between N_2, the secondary treatment effluent and the SAS. If denitrification or nitrification do not occur, nitrogen content is distributed between the secondary treatment effluent and the SAS.

Phosphorus

TP removal is accomplished via simultaneous assimilation during microorganism growth, and this effect can be enhanced by installing an anaerobic zone prior to the aerobic zone (Tchobanoglous et al., 2003). Sedlak (1991) describes the process as follow:

1. The Phosphate Accumulated Organism (PAO) in the anaerobic zone break down the energy rich polyphosphate in their cells, for the energy needed for the production of Polyhydroxybutyrate (PHB) through assimilation of the fermented product, such as volatile fatty acid. Meanwhile, phosphate is released through the breakdown of polyphosphate, and hence increasing phosphate in the wastewater.
2. In the aerobic zone, energy is produced by the oxidation of the PHB and phosphate is stored back into the cells. Because some bacteria can store more polyphosphate than they need in their cells, the assimilation during microorganism growth will increase phosphate removal.

TP is only distributed between the secondary treatment effluent and the SAS (Puig et al., 2008).

2.2.2.2 COD, N and P Mass balance of activated sludge

COD

Puig et al. (2008) and Meijer et al. (2001) both experimentally measured the COD loading of influent and effluent of the activated sludge process and SAS. Meijer et al. (2001) suggested that the COD load in the SAS is 30-60% of the total removed COD loading. If activated sludge is able to remove 90% of the influent COD, 27-54 % of the COD to activated sludge will be in SAS, and 36-63 % of the COD is emitted as CO_2. Puig et al. (2008) indicated that

approximately 42.5 % of the inflowing COD to the activated sludge ended in the SAS, and approximately 49.5 % of the COD was emitted as CO_2. Gans et al. (2007) reported a similar pattern as 46.8% of the inflowing COD ends as CO_2 and 43.5% of it is in the SAS. However, Shi (2011) suggested that 67.6% of the COD could be emitted as CO_2, whilst the SAS only captured 23.3% of the COD. Meanwhile, a case study of the Strass WWTP in Austria suggested that, a high rate activated sludge system is able to act as a primary treatment (Wett et al., 2007). It can capture 60% of the inflowing COD into the SAS (Wett et al., 2007). There is a great variation of the COD distribution pattern in the secondary biological treatment of activated sludge.

Nitrogen

Sötemann et al. (2006) modelled the TN mass balance of nitrification of the activated sludge process and suggested that approximately 22% of the N entering the activated sludge process was captured in the SAS. Shi (2011) found approximately 12.3% of influent N was captured in the SAS in an activated sludge process with denitrification, while 47.7% was released as N_2 gas and 40.0% remained in the final effluent. In Gans et al. (2007), 18.2% of the influent in the SAS was TN, 15.0% was found released as N_2 gas, and 67.0% was discharged as final effluent. There was also a great variation of the nitrogen distribution pattern in the secondary treatment.

Phosphorus

Puig et al. (2008) experimentally measured the TP loading of the influent and effluent of an enhanced biological phosphorus removal (EBPR) activated sludge process and found approximately 70% of the influent TP was captured in the SAS. However, this pattern is not likely representative of the P distribution pattern for the WWTPs do not have EBPR. Gans et al. (2007) and Shi (2011) reported a similar pattern that approximately 50% of the influent TP to the activated sludge is captured in the sludge and the rest remains in the final effluent. Similar to the COD and TP, the TP distribution pattern in the secondary treatment varies from site to site.

2.2.3 Fate of COD, N and P in sludge treatment

Sludge thickening and dewatering

Sewage sludge is commonly treated with anaerobic digestion (AD). In 2014/2015, 80% of the UK sewage sludge was treated with digestion (OFWAT, 2016). AD requires that feed sludge contains an adequate moisture level (Mills et al., 2014). Sludge thickening and dewatering is used to increase the solids content and it is achieved by mechanical filtering with the aid of gravity and centrifugation (SNF Floerger, 2003). Because small particles and dissolved chemicals pass through the filter, the filtrate typically retains some COD, N and P (Shi, 2011, Tchobanoglous et al., 2003, Henze and Comeau, 2008). Commonly the filtrate produced from sludge thickening and the centrate produce from sludge dewatering (via centrifuge), usually referred as sludge returned liquor, is recirculated to the head of the works and mixed with raw wastewater for treatment (Shi, 2011). The sludge return liquor can contribute from 20 to 90% of the original COD loading to the WWTP (Jardin et al., 2006, Fattah, 2012, Evans, 2007). Table 2.2 shows the ratio of COD, TN and TP loading in the sludge return liquor to the influent loading found in Gans et al. (2007) and Shi (2011). The data suggests that there is also great variation in the percentage of COD, TN and TP distributed in the sludge return liquor.

Table 2.2 The ratio of COD, TN and TP loading in the sludge return liquor to the influent loading reported in literatures

	COD	TN	TP
Gans et al. (2007)	38.4%	24.6%	62.5%
Shi (2011)	8.3%	11.9%	39.4%

In some cases, sludge thickening and dewatering is conducted prior to the anaerobic digestion (Shi, 2011, Wett et al., 2007), where part of the COD, TN and TP are kept in the sludge return liquor. Loading of COD, TN and TP to the digester shall be less than loading in the sludge generated in the wastewater treatment.

Anaerobic digestion

In anaerobic digestion, the organic matter goes through three decomposition stages:

1. Hydrolysis which converts particulate matter to soluble compounds
2. Fermentation which degrades amino acids, sugars, and some fatty acids into acetate, CO_2 and hydrogen

3. Methanogenesis which converts is the acetate, CO_2 and hydrogen into biogas of CO_2 and methane.

Forty to 53 % of the COD from sludge was reported to be recovered and stored in the form of methane (Shi, 2011, Wett et al., 2007). With respect to TP, its loading in the feed and digested sludge does not change (Shi, 2011). In the case of TN, a portion may be emitted as biogas during digestion, but usually in very small amounts as reported by Rasi (2009).

2.2.4 COD, N and P mass balance of wastewater treatment plants

Apart from the mass balance conducted by Shi (2011), other studies described in previous sections did not present a holistic mass balance approach for COD, N and P in a total wastewater and sludge treatment. For instance, Wett et al. (2007) presented a plant wide (including wastewater treatment and sludge treatment with anaerobic digestion) mass balance for only COD. Gans et al. (2007) showed a plant wide mass balance of COD, N and P, but the investigation did not include anaerobic digestion. Therefore, more holistic mass balance studies cover the COD, N and P are needed.

Wastewater treatment is a sequence process, the variation of material distribution pattern will be amplified after each individual process is combined. If the mass balance is to serve the purpose of process optimization, different recommendation will be given based on different mass balances. Using the mass balances conducted on two WWTPs by Shi (2011) and by Wett et al. (2007) as examples, the former only captured 48.4% of its COD inflowing to the work into the sludge, but the latter was able to capture 74.8%. Later on, Shi (2011) applied a digester that was not as efficient as the one applied by Wett et al. (2007). Shi (2011) only recovers 17.9% of its COD inflowing to the work into biogas whilst Wett et al. (2007) recovers 35.4%.Then, the dewatered digested sludge described in Shi (2011) still contains 22.3% of its COD inflowing to the work, but the percentage in Wett et al. (2007) is 37.6%. In the case of Shi (2011), improvement of the energy balance focused on producing more sludge from the wastewater treatment and to elevate the energy recovery efficiency of its digestion (Shi, 2011). For Wett et al. (2007), improvement of the energy balance focused on the energy saving of the treatment process instead of elevating the biogas production (Wett et al., 2007).

2.3 Applying modelling of mass balance investigation and the impact of waste recovery

In previous sections the mass balance calculation method is used to study the fate of COD, N and P in WWTPs. Since chemical energy recovery is obtained from the chemical organic content, the chemical energy balance comes from COD or TS mass balance (Mills et al., 2014, Wan et al., 2016). Mass balance is therefore a very useful technique for process evaluation, designing and benchmarking WWTP (Yeshi et al., 2013).

For constructing the mass balance of a substance or an element (in a set time period), it is important to know its mass loading in and out of the process. As the mass loading is calculated by multiplying the flow and concentration (Tchobanoglous et al., 2003), both flow and concentration measurements are then crucial to the construction and the accuracy of a mass balance.

2.3.1 Wastewater Mass balance Constraints

The concentration data, such as COD, N and P, can be monitored regularly by onsite operators in a WWTWs, or via a dedicated sampling campaign (Puig et al., 2008). A proper flow measurement is sometimes difficult to conduct. Scottish Water and Northumbrian Water are both Industrial sponsors of this Project and provided required information on the case study sites. Scottish Water regularly monitors 313 of its wastewater treatment facilities and Northumbrian Water regularly monitors 160. However, there is no facility has proper flow measurement on all its wastewater or sludge streams (*personal communication*, M Haffey, Scottish Water, April 2015, *personal communication*, L Wilkinson, Northumbrian Water, June 2015). In some cases, the subtraction method can be used to estimate the non-measured flow or mass loading. For example, the gas product of activated sludge, the N mass loading in the gas product of activated sludge can be calculated by subtracting the combined N loading in the final effluent and the SAS from N loading of the activated sludge influent(Puig et al., 2008). However, if more than one stream, then mass balance calculations will be severely hindered.

In some cases, the concentration data of many chemical parameters is also difficult to obtain because it is difficult to collect a sample. For instance, some WWTPs discharge its primary sludge through underground pipes, then the discharged primary sludge will instantly mix with

other sludge once it reaches the sludge storage tank Then, it is impossible to collect the primary sludge sample in those WWTPs. Constructing mass balance via direct measurement of flow and concentration sometimes is hindered by operational design and physical structure of the WWTPs.

2.3.2 Applying modelling for mass balance construction

Modelling is a good tool for constructing the mass balance of wastewater and sludge treatment. A model is comprised of mathematical equations (Henze et al., 2000, Takács et al., 1991). It is used to represent the construction and operation of a system (Maria, 1997). In wastewater modelling, data of tank sizes, flow rate, dissolved oxygen level of the biological treatment, are used to construct the model that represent the construction of the treatment work (Langergraber et al., 2004, Rieger et al., 2012). After the model is constructed, it requires a calibration stage (Langergraber et al., 2004). The principle of the calibration is to provide the model the known input, then compare the modelled output to the known output (Maria, 1997). The know input is the measured flow rate and contaminant concentration of the raw wastewater, and the outputs are usually the contaminant concentration of the effluent of treatment process (Liwarska-Bizukojc et al., 2011, Fall et al., 2011). If there is a substantial difference between the known input and the modelled output, then the parameters which are found influential to the modelled output will be adjusted to a level which can leads to a convergence (Fall et al., 2011, Liwarska-Bizukojc et al., 2011, Rieger et al., 2012, Sin et al., 2011). Once the model is validated, it can be used to describe the behavior of the system and to predict the unmeasurable physical and chemical variables, for instance flow and contaminant concentrations (Jones et al., 1989, Gasso et al., 2002).

The wastewater model includes the Takacs model for settler modelling and Activated sludge model No.1 (ASM1), ASM2, ASM2d, ASM3, and the Anaerobic Digestion Model No.1 (ADM1) for the biological wastewater and sludge treatment modelling (Takács et al., 1991, Batstone et al., 2002, Henze et al., 2000). In the Takacs model, the mathematical equation is used to express the settling velocity of the solid in ten virtual layers of settler for modelling the solid settling (Takács et al., 1991). In the biological models, the COD, nitrogen and phosphorus are first characterized into the state variables which can or cannot contain biological reactions. The biological reactions which are expressed in mathematical equations consist of the

concentrations of the state variables and kinetics to form a matrix (Henze et al., 2000). Solving the matrix will predict the COD, nitrogen and phosphorus concentrations of the treated effluent (Fall et al., 2011, Petersen et al., 2002, Liwarska-Bizukojc et al., 2011). Moreover, inorganic precipitation, such as struvite, can be also modelled (Musvoto et al., 2000, Hydromantis, 2017). Hence, wastewater modelling can be applied for wide mass balance studies. For instance, the COD mass balance conducted in Strass WWTP was performed by modelling (Wett et al., 2007). Puchongkawarin et al. (2015) also used modelling to predict the mass balances of COD, nitrogen derivatives, and phosphorus derives under different operational strategies.

Wastewater modelling is usually conducted by dedicated commercial software (Gernaey et al., 2004). Commonly used wastewater modelling software includes Aquasim developed by Eawag (Tas et al., 2009), BioWin developed by EnviroSim (Liwarska-Bizukojc et al., 2011), GPS-X developed by Hydromantis (Fall et al., 2011), SIMBA developed by inCTRL Solutions (Wett et al., 2007), STOAT developed by Water Research Centre (Sarkar et al., 2010), and WEST developed by Mike powered by DHI (Vanhooren et al., 2003) as some examples.

2.3.3 Applying modelling for studying waste recovery

Mass balance of WWTPs is required to understand the fate of valuable substances including energy during the treatment process. More importantly, it could aid to identify the potential waste recovery opportunities, namely where and how to recover the valuables. Sometimes, implementation of new processes or technologies may solve one problem but raise new ones at the same time. Yeshi et al. (2013) reported that after applying modelling techniques, predicted results such as capturing more COD in the primary sludge lead to a better chemical energy recovery but weaken denitrification in the subsequent biological process since less carbon source is available to the denitrification. Anaerobic treatment may bring a better energy balance to the wastewater treatment work but it is usually incapable of removing nutrients and hence post treatment polishing is required (Chernicharo, 2006).

Wastewater modelling provides convenience on studying the impact caused by the implementation of a new process. This is because, reconfiguration and experimentation are impractical and too costly to do on a real system but can be done theoretically on a model with low budget (Maria, 1997).

Wastewater modelling has been used for studying the impact of implementing waste recovery technologies. Drewnowski et al. (2018) applies modelling to predict the increase of biogas production over the increase of suspended solid removal efficiency of the primary settlement. Sutton et al. (2011) modelled a better the energy balance due to the virtual implementation of anaerobic digestion for sludge treatment. Puchongkawarin et al. (2015) designed a WWTP that consists of recovery technologies of up-flow anaerobic sludge blanket for energy recovery and ion exchange associated with struvite crystallizer for nutrient recovery. It then used modelling to determine mass and energy balance under different operational configurations and discovered the best one with the greatest cost benefits. Fabiyi et al. (2016) modelled the WASSTRIP process which aims to release the ortho-phosphate stored in the SAS produced from the EBPR process. The modelling robustly predicted the ortho-phosphate release in the sludge handling process and provided insight for phosphate recovery for fertilizers.

2.4 Research Questions

According to Section 2.1, although COD is well used as a surrogate of wastewater chemical energy, the relationship between the two is poorly defined due to the time-consuming drying process hinders the large amount of experimental measurements. Moreover, the relationship between the TS and VS content and the sludge chemical energy needs to be validated. On this basis, the research questions proposed are:

I. Is there a reliable and practical method to dry the wastewater but without losing a substantial amount of energetic COD?
II. What is the best surrogate(s) of the chemical energy content of wastewater?
III. What is the relationship between the surrogates and chemical energy content of wastewater and sludge four investigated WWTPs of the sponsor companies?

According to Section 2.2, although the fate of the COD, TN and TP has been studied based on theory and in real treatment works, there may be a substantial variation of their distribution patterns in each individual treatment process. Furthermore, there are few studies that perform plant wide holistic mass balance investigation of COD, N and P together. The related research questions proposed is:

I. What are the chemical energy balance and COD, TN and TP mass balances of the four investigated WWTPs of the sponsor companies?

Understanding the fate of chemical energy, COD, N and P is to discover the potential opportunities to improve value recovery. However, according to Section 2.3, the implementation of new processes or technologies may cause issues to the treatment performance. Therefore, the related research questions are:

I. From the chemical energy balance and mass balance studies, what are the opportunities for improving the current value recovery?

If the measures for improving value recovery are implemented, what are the impact on the current chemical energy and mass balance and on the value recovery?

Chapter 3 Methodology

This chapter describes the sample collection (Section 3.1), the experimental procedures for chemical analysis (Section 3.2), the statistical analysis (Section 3.3), the procedures used for wastewater and sludge modelling (Section 3.4), and the construction of mass and chemical energy balances for the wastewater treatment plants (Section 3.5).

3.1 Sample and data collection methods

3.1.1 Wastewater and sludge sampling

3.1.1.1 24-hour composite sample collection

Four wastewater treatment plants (WWTP) were sampled. Each WWTP wastewater has mechanical primary settlement and activated sludge as secondary biological treatment. Apart from WWTP A's Trickling Filter process, each wastewater and sludge stream was sampled, but with varied sampling methods.

Composite sampling was applied to the collection of:

1. Raw inlet wastewater, after it had been screened and de-gritted
2. Effluent from primary treatment
3. Effluent from secondary biological treatment

Samples were collected hourly using an Aquacell (Aquamatic, UK) autosampler over a period of 24 hours from the open channel flows in or out of the process. Hourly samples of 400 mL were collected in 24 clean plastic 800 mL containers in the autosampler. 200 mL of sample from each container was taken and combined to form a 24-hour composite sample of 4.8 L volume. The compositing was time proportional rather than flow proportional.

The sludge is essentially a liquid since commonly more than 50% of its mass is water content (Tchobanoglous et al., 2003). It is therefore collectable in the same way as a wastewater sample. Sludge and sludge return liquor (the rejected wastewater generated from sludge thickening and dewatering) was collected by grab sampling as they are pumped through underground piping which is not accessible to the autosampler.

In an effort to sample the same wastewater during its passage through the treatment plant (i.e. to take account of hydraulic residence time (HRT)), sampling of the raw wastewater, primary effluent and secondary effluent was staggered according to the estimated HRT of each unit process.

Both WWTP C and D have onsite sludge thickening and dewatering. The removed water (called filtrate or centrate in this thesis) was recirculated to the head of the works for treatment. The recirculation is through underground pipe and goes into the primary settlement separately from the raw inlet. Therefore, the filtrate or centrate was sampled separately. Using WWTP C as an example, if the sample period of the raw inlet is from 08:00 day 1 to 08:00 day 2, the sludge return liquor of primary sludge thickening is sampled by grab sampling during the period of 08:00 day 1 to 08:00 day 2.

3.1.1.2 24-hour spot sample collection

In order to understand the diurnal variation of flow and chemical composition of raw wastewater hourly samples were collected over 24 hours using an Aquacell autosampler (Aquamatic, UK). Unlike the composite sampling, each hourly sample had a volume of 800 mL and was retained in separate sample bottles.

3.1.2 Sample storage

The grab wastewater samples and the sample of the 24-hour study were stored in 1 L Polyethylene Terephthalate (PET) rectangular sample bottles (Medfor, UK). The grab sludge sample was stored in 500 mL Polypropylene (PP) sample jars.

Samples were stored in a cool box with ice packs during transportation. The transportation time was from 30 minutes to 4 hours. All sludge and wastewater samples were stored in a fridge at 4 ^{o}C immediately upon arrival back at the laboratory.

Chemical analysis was typically expected to be done within 48 hours after sample collection. If not, samples were frozen at -20^{o}C to inhibit microbial activity which affects the chemical composition of the sample.

3.1.3 Flow and energy consumption data collection

3.1.3.1 Flow data collection

Flow data were downloaded from water companies' database after sampling was completed. Downloaded flow data were either a series of instantaneous flow rate values recorded every 15 minutes or daily total flow from 00:00:00 to 23:59:59.

Since the sampling period for composite samples was 24 hours the 24-hour total flow was also appropriate for the mass and energy balance study. For treatment plants that recorded flow at 15-minute intervals, these measurements were summed to provide a 24 hour total.

Because most of the composite sampling did not start at exactly 00:00:00 and typically spanned two days, if only daily total flow was available, the daily total flow of those two consecutive days was collected. 24 hour flow for the period of sampling was then calculated proportionately according to the individual flows on the two days e.g. if sampling was undertaken for 14 hours during a day when the flow was 10 000 m^3/d and 10 hours when flow was 8 000 m^3/d then the daily flow was calculated as: [10 000 × (14÷24)]+[8 000 × (10÷24)].This calculation is based on an assumption that the hourly flow is the same during a day. The flow of WWTP D is calculated through this approach.

3.1.3.2 Energy consumption data collection

All the energy data were downloaded from water companies' databases after the sampling was finished. Original energy data downloaded were either a series of half-hourly consumption or daily total which counts energy consumption from 00:00:00 to 23:59:59 of a day.

For data recorded as half-hourly consumption, the 24-hour consumption was then obtained by summing the half-hourly consumption during the sampling period.

If only daily total energy consumption was available, based on the assumption that the energy consumption rate stays constant during a day, the 24-hour consumption was then calculated proportionately according to the individual consumption on the two days, e.g. if sampling was undertaken for 14 hours during a day when the electricity consumption was 6,000 kWh/d and 10 hours when flow was 7,200 kWh/d, then the daily electricity consumption was calculated

as [6,000 × (14÷24)]+[7200 × (10÷24)]. The electricity consumption of WWTP A, C and D are calculated through this approach.

3.2 Chemical analysis

3.2.1 Chemical analysis of wastewater

Chemical analysis of wastewater included Chemical Oxygen Demand (COD), soluble COD (sCOD), particulate COD (pCOD), Total Organic Carbon (TOC), Dissolved Organic Carbon (DOC), particulate Organic Carbon (POC), Ammoniacal Nitrogen (NH_4^+-N), Total Kjeldahl Nitrogen (TKN), Nitrite Nitrogen (NO_2^--N), Nitrate Nitrogen (NO_3^--N), Total Nitrogen (TN), Phosphorus as Phosphate (PO_4^{3-}-P), Total Solid (TS) by oven drying, Volatile Solid (VS), Total Solid (TS_{cve}) by centrifugal vacuum evaporation, and chemical energy content.

Composite samples collected in the mass and energy balance sampling were analysed for all the variables. The grab samples of sludge return liquor were also analysed for all variables except for TS_{cve} and chemical energy content.

Samples collected in the 24-hour study were analysed for COD, sCOD, pCOD, NH_4^+-N and PO_4^{3-}-P. Starting with the 1st hourly sample, in total 6 samples were selected at 4-hourly intervals and measured for TS_{cve} and chemical energy content.

NO_2^--N and NO_3^--N were measured in duplicate, TS_{cve} was measured in either duplicate or triplicate, chemical energy was measured once on each sample, and all other parameters were measured in triplicate.

3.2.1.1 Sample preparation

Samples for sCOD, DOC, NH_4^+-N and PO_4^{3-}-P were filtered through 0.45 µm Polyether Sulfone (PES) syringe filters (VWR, US). Samples for NO_2^--N and NO_3^--N were filtered through 0.20 µm Polyether Sulfone (PES) syringe filters (VWR, US). There was no sample preparation for other variables.

3.2.1.2 COD measurement

COD measurement required 0.3-3.0 mL of sample and was conducted with a Spectroquant ® COD Cell Test (Merck Millipore, Germany) with measuring ranges of 4-40 mg/L, 5-80 mg/L and 25-1500 mg/L and Spectroquant ® Phare 300 Spectrometer (Merck Millipore, Germany).

For sCOD measurement, 0.45 µm filtered sample was analysed following the COD measurement procedure. pCOD is calculated by subtracting sCOD from COD.

3.2.1.3 Organic carbon measurement

TOC measurement required 0.1-2.0 mL of sample and was conducted with a TOC Cuvette Test (Purging Method) (Hach, US) with measuring range of 3 – 30 mg/L and 30-300 mg/L and DR1900 Portable Spectrometer (Hach, US).

For DOC measurement, 0.45 µm filtered samples were analysed following the TOC measurement procedure. POC is calculated by subtracting the DOC from TOC.

3.2.1.4 Nitrogen measurement

NH_4^+-N measurement required 0.2-1.0 mL of 0.45 µm filtered sample and was conducted with a Spectroquant ® Ammonium Cell Test (Merck Millipore, Germany) with a measuring range of 0.2-8.0 mg/L and Spectroquant ® Ammonium Test (Merck Millipore, Germany) with a measuring range of 2-75 mg/L. NH_4^+-N was analysed with a Spectroquant ® Phare 300 Spectrometer (Merck Millipore, Germany)

TKN measurement was adapted from standard method 4500-N_{Org} C (APHA, 2012). For this measurement 0.1–10 mL of sample was required. It was mixed in a Kjeldahl Flask with 14 mL of concentrated H_2SO_4 and 2 tablets each containing 5 g of K_2SO_4 and 0.5 g $CuSO_4 \cdot 5H_2O$ (Gerhardt, Germany). The solution was digested at 400 ^oC for 60 minutes with a Turbotherm heater (Gerhardt, Germany) to convert TKN into ammonium. After the digested solution was cooled to ambient temperature it was mixed with 80 mL 40% NaOH solution and distilled in Vapodest 30s (Gerhardt, Germany) to convert NH_4^+ into free NH_3 and transferred to a flask containing 50 mL of a 20 g/L H_3BO_3 solution. The H_3BO_3 solution was then titrated with 0.05 N H_2SO_4 solution to determine the TKN concentration.

NO_2^--N and NO_3^--N measurement required 5-6 mL of 0.20 µm filtered sample and were analsyed using an Ion Chromatograph (IC) Dionex ICS-1000 with Ionpack AS 14A as column and carbonate as eluent.

TN is the sum of TKN, NO_2^--N and NO_3^--N.

3.2.1.5 Orthophosphate measurement

PO_4^{3-}-P measurement requires 0.2-1.0 mL of 0.45 µm filtered sample and was conducted with Spectroquant ® Phosphate Cell Test (Merck Millipore, Germany) with measuring ranges of 0.05-5.0 mg/L, 0.5-25.0 mg/L and 3.0 – 100.0 mg/L and Spectroquant ® Phare 300 Spectrometer (Merck Millipore, Germany).

3.2.1.6 Solids measurement

TS and VS measurement used 40 mL of sample and follows standard method 2540 B and 2540 E (APHA, 2012).

For the TS_{cve} measuremernt the sample flask (Genevac, UK) was pre-dried at 103-105 ^oC until its weight change was less than 4% which is the allowable variation between two TS measurement in standard method 2540 B (APHA, 2012). The weight of the pre-dried container was recorded as $\boldsymbol{m_f}$. Sample with a volume ($\boldsymbol{v}$) of 300-400 mL was placed into the pre-dried container and dried by centrifugal vacuum evaporation using a Rocket 4D Synergy (Genevac, UK) at 18 mbar, 30^{o}C and 1,800 rpm for 19 hours and 40 minutes to remove all the visible water. After the centrifugal evaporator drying, the container (with dried residue in it) was further dried in a dessicator at ambient temperature for at least two days until its weight change was less than 4%. The weight of the container was recorded as $\boldsymbol{m_{f+dr}}$. TS_{cve} was calculated by Equation 3-1.

Equation 3-1

$$TS_{cve} = \frac{(m_{f+dr} - \mathrm{m}_f) \times 1000}{V}$$

Where $\boldsymbol{m_{f+dr}}$ is the weight of the container with dried residue in it, $\boldsymbol{m_f}$ is the weight of the container, $\boldsymbol{V}$ is the volume of the sample placed into the container.

3.2.1.7 Chemical energy measurement of wastewater

The dried residue produced from the TS_{cve} measurement was used for analysis of the chemical energy content of the same aliquot.

A Parr 6100 Compensated Jacket Calorimeter (Parr Instrument Company, USA) was used for energy measurement. The bomb calorimeter requires approximately 26 kJ of heat in one measurement but no more than 2 g of sample input. Thus, the calorific value of the sample in the calorimeter has to be higher than 13 kJ/g. Previous reports of the calorific value of dried wastewater are in the range 3.2 to 10.5 kJ/g (Shizas and Bagley, 2004, Heidrich et al., 2010), and therefore the dried residue needed to be co-combusted with a high calorific value substance. Paraffin wax, which has been used as the combustion aid in the combustion study (via bomb calorimetry) of Germanium metal (Sunner and Månsson, 1979), was chosen as the combustion aid in this study. Its calorific value was determined as a mean value of 46.7344 kJ/g via experimental bomb calorimetry on 8 samples with weight 0.6001–0.6409 g.

0.15 – 0.60 g of dried wastewater sample was then mixed with 0.40 – 0.60 g of Paraffin wax to form approximately 1 g of combustible sample to be introduced to the bomb calorimeter. The weight of the dried sample, and the weight and calorific value of the paraffin wax, were entered into the instrument, and the calorimeter then automatically calculated the dried sample's calorific value (kJ/g) after each measurement. The chemical energy content of wastewater (E_{ww}) was calculated by multiplying the calorific value of the dried wastewater (E_{dww} in kJ/g) of the dried sample with TS_{cve} (in mg/L) of the sample, as shown in Equation 3-2.

Equation 3-2

$$E_{ww} = E_{dww} \times TS_{cve}$$

Where $\boldsymbol{E_{dww}}$ is the caloric value of the dried residue, $\boldsymbol{TS_{cve}}$ is the TS concentration measured by the centrifugal vacuum。

40 mL of the same wastewater sample used for the TS_{cve} and chemical energy measurement was also separately dried by the Rocket 4D Synergy under the same conditions. After drying, 40 mL of deionised water was added into the flask for rehydration. The samples underwent

sonication for 10 minutes to ensure complete rehydration. COD concentration of the rehydrated sample was then measured in triplicate. The COD recovery rate was then calculated by dividing the original COD by the rehydrated COD. Multiplied by 100 this gave the percentage of COD retained in the dried sample. Calculation of COD recovery rate is shown in Equation 3-3

Equation 3-3

$$COD\ Recovery\ Rate = \frac{COD_{(o)}}{COD_{(rehy)}}$$

Where $\boldsymbol{COD_{(o)}}$ is the COD concentration of the original wastewater before drying, and $\boldsymbol{COD_{(rehy)}}$ the COD concentration of the rehydrated wastewater.

The energy content so determined (E_{ww}) was that used to explore the relationship with COD and to calculate the energy balance of the WWTPs.

3.2.2 Chemical analysis of sludge

All the sludge samples collected were analysed for Total Solid percentage (TS%), Volatile Solid percentage to TS (VS/TS%), Total Organic Carbon percentage to TS (TOC/TS%), Total Nitrogen percentage to TS (TN/TS%), Total Phosphorus percentage to TS (TP/TS%) and chemical energy content. However, in some specific cases variables were not measured due to insufficient sample size. These individual cases are highlighted in the Results & Discussion chapters.

3.2.2.1 Sample preparation

Apart from the TS% and VS% measurement and TOC% measurement of the SAS, sludge was dried in an oven at 103-105 ^{o}C until constant weight was reached prior to any further measurements.

For TOC%, TN% and TP%, the dried sample was ground to a fine powder using a James Martin ZX809X Spice and Coffee Grinder (Wahl Clipper Corporation, USA) before measurement.

3.2.2.2 Solid measurement

TS% and VS/TS% were measured in the same set of experiments. Triplicate analyses of both variables were undertaken on each sludge sample.

The method of TS% and VS/TS% measurement is adapted from standard method 2450 G (APHA, 2012). The adaptation is that the sample mass is reduced from the recommended 25-50 g to 3-5 g due to limited oven and muffle furnace space. In terms of procedures, a crucible was dried in a muffle furnace at 550°C for 1 hour and then stored and cooled in a desiccator overnight. After the weight (m_c) of the crucible was recorded, 2.0 to 5.0 g of sludge sample was added to the crucible. The crucible was weighed again to obtain m_{c+s}. The crucible was then dried in the oven at 103-105 °C overnight. After drying, the crucible was cooled in a dessiccator until its weight change was less than 4%. The weight of the crucible was recorded as m_{104}. TS% was then calculated using Equation 3-4.

Equation 3-4

$$\text{TS\%} = \frac{m_{104} - m_c}{m_{c+s} - m_c} \times 100\%$$

Where m_{104} is the weight of the crucible with dried residue after oven drying, m_{c+s} is the weight of the crucible with wet sludge sample, m_c is the weight of the crucible after 550°C muffle furnace drying.

The crucible was then dried in a muffle furnace at 550°C for at least 30 minutes. After drying, the crucible was cooled in a dessiccator until its weight change was less than 4%. The weight of the crucible was recorded as m_{550}. VS/TS% was the calculated by using Equation 3-5.

Equation 3-5

$$\text{VS/TS\%} = (1 - \frac{m_{550} - m_c}{m_{104} - m_c}) \times 100\%$$

Where m_{550} is the weight of the crucible with dried residue after 550°C muffle furnace drying, m_{104} is the weight of the crucible with dried residue after oven drying, and m_c is the weight of the crucible after 550°C muffle furnace drying.

3.2.2.3 TOC/TS% measurement

TOC/TS% was determined using 0.1 g of 103-105 °C oven dried and ground sample. 1 mL of 4.0 mol/L HCl was added to each crucible. The HCl was then removed from the sample after4 hours. The sample was then oven dried at 60 to 70 °C for 16 – 24 hours. A Leco CS230 Carbon/Sulphur Analyser was used to measure the carbon percentage of the sample and the blank. The TOC/TS% was calculated using Equation 3-6.

Equation 3-6

$$\text{TOC/TS\%} = \frac{TC_S\% - TC_B\%}{D}$$

Where ***TCs%*** is the measured carbon percentage of the sample, ***TC_B%*** is the measured carbon percentage of the blank, and D is the dry matter factor.

The solid content in the SAS was lower than 1% (equivalent to 1,000 mg/L). For generating 0.1 g of dried solid for the TOC% measurement, it was therefore necessary to use more than 100 mL of sample. Because of restrictions on oven drying space in the laboratory the TOC content of SAS was measured following the experimental procedure shown in Section 3.2.1.3 and is in units of mg/L. TOC/TS% of the SAS is then calculated via Equation 3-7.

Equation 3-7

$$\text{TOC/TS\%} = \frac{TOC}{TS\% \div 100\% \times 1000 \times 1000}$$

Where ***TOC*** (mg/L) is the total organic carbon of the SAS and ***TS%*** is the total solid content of the SAS.

3.2.2.4 TN/TS% measurement

TN/TS% was measured by the Scientific Service of Scottish Water (SSSW). Samples were dried and ground before posting. A single measurement was done on each sample.

0.05 g of sample was microwave-digested with 25 ml of $Na_2S_2O_8$ or NaOH solution. The digestion was conducted at 140^{o}C for 40 minutes. The digested sample was then diluted to 100 mL with deionised water, and subsequently analysed with standard method 4500-N B In-Line UV/Persulfate Digestion and Oxidation with Flow Injection Analysis (APHA, 2012). The method firstly breaks down the simple nitrogen compound (i.e. Ammonia) and the complex nitrogen compound to Nitrate. All the Nitrate is then reduced to Nitrite which is quantified for determining the TN/TS% of the sample.

Although the analytical method measures the TN/TS% of the sample, NH_4^+-N may be lost due to evaporation during preliminary drying at 103-105^{o}C. Hence, the measured TN% may be lower than the real value. Assuming only NH_4^+-N is lost during the drying, actual mass of TN

of sludge is the sum of the mass of TN in the dried solid and the mass of NH_4^+-N lost. Assuming the NH_4^+-N is only within the liquid fraction of the sludge and its concentration is C^{AmmN}, the adjusted TN% of sludge is calculated by Equation 3-8.

Equation 3-8

$$TN\%_{adjusted} = \frac{TN\% \times TS\% + C^{AmmN} \times (1 - TS\%) \times \rho_{Sludge}}{TS\%}$$

where ***TN/TS%*** is the measured TN content in the dried solid of sludge, ***TS%*** is the total solid percentage of sludge, $\boldsymbol{C^{AmmN}}$ is NH_4^+-N concentration of the corresponding sludge return liquor, and the $\boldsymbol{\rho_{Sludge}}$ is the density of the sludge.

As all other component of Equation 3-8 were measured, the key to the calculation is the NH_4^+-N concentration in the water content of sludge. In sludge thickening and dewatering, water fraction is removed and the NH_4^+-N of it is measured. By assuming the NH_4^+-N of the water content of the wet and thickened/dewatered sludge are the identical to the NH_4^+-N of the removed water fraction, $TN\%_{adjusted}$ of the sludge before and after thickening or dewatering can be obtained.

However, only WWTP C has sludge thickening and dewatering on each of the primary sludge, SAS, sludge fed to the digester and the digested sludge. As sampling and analysis of the thickening and dewatering facilities was undertaken on multiple occasions the $TN\%:TN\%_{adjusted}$ of each type of sludge was determined and an average value calculated. The $TN\%_{adjusted}$ of sludge produced in other WWTPs was adjusted by multiplying its TN% with the $TN\%:TN\%_{adjusted}$ of a corresponding type of sludge：the $TN\%:TN\%_{adjusted}$ of the primary sludge calculated from the primary sludge of WWTP C will be applied to the primary sludge produced in other three WWTPs; the the $TN\%:TN\%_{adjusted}$ of the SAS calculated from the SAS of WWTP C will be applied to the SAS produced in WWTP A and D. The result of the $TN\%:TN\%_{adjusted}$ and the adjusted TN% of sludges are presented in Appendix A.

3.2.2.5 TP/TS% measurement

TP% was also measured by SSSW. Samples were dried and ground before posting. A single measurement was done on each sample.

0.5g of sample was mixed with 4 mL of concentrated HNO_3 and 4 mL of concentrated HCl. The solution was pre-digested in the uncapped vessel for at least 30 minutes or until any visible reaction had ceased. The pre-digested solution was then microwave-digested in a capped vessel at 175 ^oC for 15 minutes. The digested solution was filtered through a 540 filter paper (Whatman) and then diluted to 100 mL with deionised water. The phosphorus content was then measured using a Perkin Elmer Nexion 300X ICPMS Spectrometer at 30.994 AMU with KED (Collision) Helium Gas flow of 5.4 mL/min and is corrected for using Scandium as an internal standard measured at 45 AMU.

3.2.2.6 Chemical energy measurement

Chemical energy measurement of sludge followed the experimental procedure described in Section 3.2.1.7. 0.4-0.7 g of dried sludge sample was mixed with 0.4-0.6 g of Parafin Wax to form approximately 1.0 - 1.2 g of combustible sample which was measured for its calorific value by the same bomb calorimeter described in *Section 3.2.1.7*. The chemical energy content of dried sludge (E_{ds}) is expressed as KJ/g. The chemical energy of the wet sludge (E_s) is calculated via Equation 3-9.

Equation 3-9

$$E_s = \rho_s \times TS\% \times E_{ds}$$

Where $\boldsymbol{\rho_s}$ is the density of the sludge and is taken as 1 g/cm^3, ***TS%*** is the total solid content of the sludge, and $\boldsymbol{E_{ds}}$ is the energy content of the dried sludge.

3.3 Statistical analysis

Descriptive statistics, such as mean value and standard deviation was conducted using Minitab 2018.

For the study of relationships between energy content and chemical constituents of wastewater or sludge the Correlation and Best Subset functions of Minitab 2018 were used to determine which parameter(s) best reflect the wastewater or sludge energy content via single or multiple regression. The graphs of regressions were produced in Minitab 2018.

3.4 Wastewater and sludge treatment modelling

Constructing correct mass and energy balance requires measurement of both flow and concentration on every inflow and outflow stream of the wastewater and sludge treatment process. However, such comprehensive sampling is not undertaken by the water companies. Thus, existing available data is used here, first to predict the unknown flows and concentrations, then to construct models of the four wastewater and sludge treatments for, and ultimately construct mass and energy balances for each of them.

There are three steps to the wastewater and sludge treatment modelling in this thesis:

1. model construction (in Section 3.4.1)
2. influent characterization (in Section 3.4.2)
3. model calibration and validation (in Section 3.4.3)

In the following sections the experimentally measured values (of flow and concentration) are referred to as 'observed values', and the modelled, simulated values are referred to as 'predicted values'.

3.4.1 Model construction

3.4.1.1 Operating model/library

The modelling work in this research was undertaken in software GPS-X 7.0. All the wastewater and sludge treatment modelling were conducted under library "Comprehensive Carbon, Nitrogen, Phosphorus (mantis2lib)". All the biological processes are modelled with "mantis2" which is an in-house model developed by the software company Hydromantis and is developed from biological models of Activated Sludge Model 2d (ASM2d) and Anaerobic Digestion Model 1 (ADM1) (Hydromantis, 2017). The "mantis2" is able to model the COD, nitrogen and phosphorus mass balance of the wastewater and sludge treatment (Fall et al., 2011, Drewnowski et al., 2018). Moreover, it can also model the application of advanced technologies such as anaerobic wastewater treatment and Struvite recovery treatment which are not included in the classic ASM2d model or ADM model (Hydromantis, 2017).

3.4.1.2 Modelling of individual treatment processes

3.4.1.2.1 Chemical dosing

The chemical dosing in the modelling is for two purposes. One is for mimicking the actual phosphate removal by intentional chemical dosing in the real world. The other one is for virtually removing sCOD and phosphate for the modelling purpose.

Actual Ferric dosing for phosphate removal

WWTP A does have an actual chemical dosing process for phosphate removal. Therefore, its model uses the "In-line Chemical Dosing" unit for mimicking the process. Ferric sulphate ($Fe_2(SO_4)_3 \cdot 9H_2O$) is chosen as the chemical. The "percent hydrated ferric sulphate" is set as 100%. The dosage method is mass based, and the dosage rate is 236 kg/d according to the historical data (*personal communication,* J McCowan, Scottish Water, August 2018).

Virtual aluminum dosing for sCOD removal

It is possible that there is a considerable reduction of sCOD after the primary treatment because part of the sCOD first flocculates into pCOD and subsequently settles (Gernaey et al., 2001). For mimicking this process, the "In-line Chemical Dosing" unit uses aluminum sulphate ($Al_2(SO_4)_3 \cdot 18H_2O$) to coagulate and flocculate the soluble inert COD and the soluble colloidal COD into pCOD in its default settings. This research uses this unit for the purpose of virtual sCOD removal. The dosage aimed for is the minimum required to remove sCOD. The kineticrelated to the sCOD removal are obtained via the "Optimization" function that aims to remove all the soluble inert COD (21.5 mg/L) and the soluble colloidal COD (39.99 mg/L) from a wastewater with a flowrate of 10,000 m^3/d, 430 mg/L COD and 147.5 mg/L sCOD via 1 kg/d dosage of $Al_2(SO_4)_3.18H_2O$ (*personal communication,* S Snowling, Hydromantis, November 2018). The kinetics of the process of sCOD removal obtained will then be applied in the virtual sCOD removal unit if the sCOD reduction is greater than 15 mg/L after primary settlement. The default and adjusted value of related kinetic of the process of sCOD removal via the $Al_2(SO_4)_3 \cdot 18H_2O$ dosing are shown in Table 3-1.

Table 3-1 The default and adjusted values of related kinetic of the $Al_2(SO_4)_3 \cdot 18H_2O$ for virtual sCOD removal

	Default Value	Adjusted Value
pKsp, apparent - Log of soluility product of AlPO4	13.6	0.00000000
Minimum metal to colloidal organic ratio (at high concentration), g Metal/g COD removal	4.0	0.00012632
Minimum metal to colloidal organic ratio (at high concentration), g Metal/g COD removal	20.0	33.71681100
Affinity factor for colloidal organic, m3/g removal	0.5	1.19473060
Minimum metal to snd ratio (at high concentration), g Metal/g COD removal	4.0	0.00000000
Minimum metal to snd ratio (at high concentration), g Metal/g COD removal	20.0	0.00000000
Affinity factor for snd, m3/g removal	0.5	0.00000000
Minimum metal to si (at high concentration), g Metal/g COD removal	4.0	0.00020201
Minimum metal to si (at high concentration), g Metal/g COD removal	20.0	34.96696400
Affinity factor for si, m3/g removal	0.5	1.37120470

As the unit serves a virtual sCOD removal purpose, the chemical shall not react with other possible reactive chemicals, namely the phosphate. Therefore, the k_{sp} value of the $AlPO_4$ is set as "0" to prevent any phosphate reacting with the $Al_2(SO_4)_3 \cdot 18H_2O$.

Virtual ferric dosing for phosphate removal

It is also possible that there is a considerable reduction of phosphate after the primary treatment. This is because some phosphate may react with unexpected iron content in the primary settlers, which scavenges phosphate and results in settling of iron phosphate (*personal communication*, L Wilkinson, Northumbrian Water, October 2018). If phosphate reduction is greater than 1.5 mg/L after primary settlement, the "In-line Chemical Dosing" unit, using $Fe_2(SO_4)_3 \cdot 9H_2O$, will be applied. The "percent hydrated ferric sulphate" is set as 100%. The dosing method is mass based.

3.4.1.2.2 Primary settlement

The current library has three types of primary settlers, the "Circular Primary Settlers", the "Rectangular Primary Settlers", and the "High Rate Treatment". The appropriate unit, and its dimensions, is chosen according to the configuration of the actual WWTPs.

The Simple1D model that developed from Takács model is used in all the models (Takács et al., 1991). The primary de-sludging process can be initiated and controlled through a variety of triggers, such as a given discharge rate, a rate that is proportional to a specific discharge rate (i.e. to the inflowing wastewater), or a proportional–integral–derivative (PID) controller which is able to control the COD of the discharged primary sludge. The WWTP A and D are controlled via the PID controller using the COD (estimated from the VS content via Equation 4-4, explanation given in Section 4.2.3) of the primary sludge as the control variable. WWTP B is controlled via a TSS concentration because the primary settlement unit used is unable to be controlled by the COD concentration. WWTP C is controlled via a given discharge rate according to the historical data because the primary sludge was not measured during the sampling campaign.

Considering WWTPs A and D have surplus activated sludge recirculation, their primary settlers are converted into a reactive settler whose biological reactions are controlled by an independent "Plug Flow Tank" unit. The primary settlers of WWTP B and C are pure mechanical settlers.

In reality, the majority of WWTPs have more than one settler. In order to simplify the modelling, only one primary settler is used in each modelling exercise. Its centre depth and the side wall depth are the same as the actual ones and inputted into the model. The surface area inputted to the model is the sum of the surface area of all the actual settlers (Hydromantis, 2017). The inlet point of the wastewater is set equal to the water level of the tanks. The configuration of the primary settlement tanks of each WWTP are shown in Table 3-2.

Table 3-2 The configuration of the primary settlement tanks of each WWTP

	WWTP A	WWTP B	WWTP C	WWTP D
Tank Dimension	Circular sloping bottom settler Centre depth - 3.6m Sidewall depth - 2.0m Surface Area - 1,029m^2	High rate treatment	Rectangular sloping bottom settler Water depth - 3.3m Surface Area - 9750m^2	Circular settler Centre depth - 3.75m Sidewall depth - 1.8m Surface Area - 6,945m^2
Control Method	Target COD of primary Sludge – 34,844 mg/L Sampling interval - 15 minutes Proportional gain - 0.001 Integral time - 0.01	Target TSS concentration of primary sludge – 30,000 mg/L (the predicted COD of 43,120 mg/L which is close the target COD of 43,951 mg/L)	Set flowrate of primary sludge - 1,548 m3/d	Target COD of primary Sludge – 24,225 mg/L Sampling interval - 15 minutes Proportional gain - 0.001 Integral time - 0.01

3.4.1.2.2 Secondary biological treatment

The main biological treatment process used in all four WWTPs is the aerobic suspended activated sludge process (consisting of an aerobic zone only). Therefore the “Plug Flow Tank” unit and the subsequent secondary clarifier unit are chosen to model the biological treatment process. The dimension of the “Plug Flow Tank”, dissolved oxygen (DO) concentration, mixed liquor suspended solid (MLSS) concentration, and the volume or the ratio of the return activated sludge (RAS) are set according to the actual configuration and/or the historical data of each WWTP. The discharge of SAS is controlled by a PID controller using the measured MLSS of the mixed liquor in the activated process as the control variable.

In WWTP A and D the secondary settlers are biologically active and linked to an independent “Plug Flow Tank” unit which controls the biological reactions. Similar to the primary settlers, there is only one secondary settler used in each modelling exercise. The center depth and the side wall depth of the secondary settlers are set to be the same as the actual ones, and the surface

area of each is the sum of the surface area of all actual settlers. The inlet point of the wastewater is set 2/3 of the center depth from the bottom according to recommendations provided by the engineer from the Hydromantis (*personal communication,* S Snowling, Hydromantis, August 2018). The configuration of the activated sludge process and the subsequent clarifier for each WWTP is shown in Table 3-3.

Table 3-3 The configuration of the activated sludge process and the subsequent clarification process for each WWTP

	WWTP A	**WWTP B**	**WWTP C**	**WWTP D**
Tank Dimension of Activated Sludge	Volume - 1,924 m^3 Depth – 3.93 m	Volume – 22,291 m^3 Depth – 8.6 m	Volume - 33,203 m^3 Depth – 6.5 m	Volume - 21136.5m^3 Depth – 4.5 m
DO	2.0 mg/L	2.0 mg/L	2.5 mg/L	0.66 mg/L
RAS Control	71% to the Primary Effluent	64,694 m^3/d	225,152 m^3/d	87,452 m^3/d
Control Method	Target MLSS- 2,405 mg/L Sampling interval - 10 minutes Proportional gain - 0.1 Integral time - 0.01	Target MLSS- 2,540 mg/L Sampling interval - 5 minutes Proportional gain - 0.8 Integral time - 0.01	Target MLSS- 2,805 mg/L Sampling interval - 15 minutes Proportional gain - 0.5 Integral time - 0.01	Target MLSS-1,733 mg/L Sampling interval - 5 minutes Proportional gain - 0.2 Integral time - 0.1
Tank Dimension of Final Clarifiers	Circular sloping bottom settler Centre depth - 3.45m Sidewall depth - 1.85m Surface Area - 1,078.0m^2	Circular flat bottom settler Centre depth - 4.5m Surface Area - 5,606 m^2	Circular flat bottom settler Centre depth - 4.5m Surface Area - 16,120 m^2	Circular sloping bottom settler Centre depth - 5.25m Sidewall depth - 1.75m Surface Area - 6801.0 m^2

In WWTP A the aerobic suspended activated sludge only treats 83% of the treated primary effluent. The remaining 17% is treated by the trickling filter with subsequent clarification.

Although the sampling campaign did not measure the concentration of the effluent of the trickling filter process, a “Trickling Filter” unit was included in WWTP A’s model. However, the performance of the trickling filter will not be calibrated.

The “Trickling Filter” unit has a bed depth of 1.8m and a bed surface of 173m^2. The subsequent clarifier has a flat-bottomed shape, with a surface area of 117m^2 and a water depth of 2.5m (inlet point is 1.25 m from the bottom of the clarifier). The biological model stoichiometry of the “Trickling Filter” unit was left as its default value in the model. No biological reactions were enabled in the clarifier.

3.4.1.2.3 Sludge treatment modelling

Although both WWTP B and C have sludge treatment and receives imported sludge from satellites WWTPs, the flowrate of the imported sludge to WWTP B is absent. Therefore, only the sludge treatments of WWTP C is modelled in this research.

Sludge storage tank

The sludge imported to, or produced in, WWTP C is stored in the “Plug Flow Tank” unit which acts as the storage tank, with biological reactions available for modelling the potential fermentation process (*personal communication*, S Snowling, Hydromantis, December 2018). The volume of the tanks is set according to the actual configuration with a universal depth of 5 metres. The volume of the storage tanks is shown in Table 3-4.

Table 3-4 The volume of the sludge storage tanks

Tanks	Volume, m^3
Imported sludge tanks*	17,000
Primary sludge tank	390
SAS tank	250
Raw sludge tank	40,000
Digested sludge tank	4,500

*: The volume of imported sludge tank is calculated based on the historical flow of 857 m^3 and the potential storage time before it reaches WWTP C is estimated as 14 days (*personal communication* L Wilkinson, Northumbrian Water, August 2018).

In order to mimic anoxic or anaerobic conditions, the DO of the tanks is set to 0. The "Plug Flow Tank" unit is originally designed for the suspended growth wastewater treatment and hence reactive biomasses are assumed present in the tank initially. In this application, in order to mimic the fermentation that is caused simultaneously by the biomass contained in the sludge itself rather than by the biomass initially in the tank, the initial concentration of all the biomass in the "Plug Flow Tank" unit is set to "0" (*personal communication,* S Snowling, Hydromantis, December 2018).

Sludge thickening and dewatering

WWTP C has both sludge thickening via drum thickening and sludge dewatering via centrifuge. GPS-X does include modelling options for such processes, via the "Drum Microscreen" and the "Hydrocyclone Solid Separation" units, which are corresponding to the actual process used at WWTP C. In GPS-x, the "Drum Microscreen" and the "Hydrocyclone Solid Separation" share the same set of operational parameters that control the modelling of thickening and dewatering, though the default values are different. Considering the parameters will be tested for sensitivity and adjusted later on, for simplification purpose the "Drum Microscreen" unit is used for modelling of all thickening and dewatering processes regardless what the actual process is.

Anaerobic Digestion

In WWTP C, the indigenous primary sludge will be thickened with the imported sludge together. The indigenous SAS only is thickened alone. The thickened SAS and thickened primary sludge will be combined and stored. The combined sludge is called Raw sludge. The Raw sludge will

then be dewatered and fed to the Thermal Hydrolysis Process (THP). The THP treated sludge will then be fed to the digester. The digested sludge will be stored in the storage tank prior to its dewatering.

In this research, the complete model of WWTP C only includes the wastewater treatment, the thickening of primary sludge and SAS, and the dewatering of raw sludge. The anaerobic digestion and the subsequent dewatering of the digested sludge are modelled in a separated layout. The reason for separating the models is that both the TOC:COD ratios and the organic fraction are found influential to the flow and quality of the produced biogas, and to the soluble nutrients content of the sludge liquor from the digested sludge dewatering (Hydromantis, 2015). However, the appropriate TOC:COD ratio fits for the digestion process may not be the same as the appropriate TOC:COD ratio fits for the modelling of the wastewater treatment. Moreover, the predicted organic fraction of the dewatered raw sludge generated from the wastewater treatment model may be substantially to the appropriate organic fraction for the digester feed, which it is not possible to adjust.

The “Anaerobic Digestion” unit is used to model the sludge anaerobic digestion in WWTP C. According to the actual configuration, the volume of the digester is set at 18,463 m^3 with 1,000 m^3 head space. Because there is not enough information, such as the sCOD of sludge treated before and after the THP process, the THP process is not included in the model.

3.4.2 Influent characterization

The “codstate” model in the “mantis2” library is used for all the wastewater and sludge modelling. The flow, concentration and fractions of the components of the raw wastewater and sludge are required to initiate the modelling.

In total, it is necessary to input 66 variables of composite variables, state variables and fractions in the “codstate” model to thoroughly specify every state variable required by the model (Hydromantis, 2017). Due to the limited number of parameters actually measured in the sampling campaign, only flow, COD, TKN and TP, nitrogen-related state variable of NH_4^+-N and nitrite and nitrate, phosphorus-related state variable of phosphate, the VSS/TSS ratio, the organic fractions of COD, the nitrogen fraction, the phosphorus fraction, and the ratios of TOCs

to CODs are input to the model. This research assumes that there is no reactive biomass in the raw wastewater and the variables of store poly-phosphate in PAO inorganic compounds, organic fractions of volatile fatty acids, methanol and biomasses, inorganic compounds, inorganic precipitates and soluble gases remain at their default values.

3.4.2.1Influent characterization of wastewater modelling

3.4.2.1.1 Flow

The raw wastewater fed to the wastewater treatment process has been screened and de-gritted, and hence the screening and de-gritting were not included in the models.

Five sampling campaigns were undertaken for each WWTP. However, some wastewater and sludge samples were unable to collect in some sampling campaigns. Data from three sampling campaigns was used for modelling at WWTP A and D, four campaigns for WWTP C, and five campaigns for WWTP B. The mean flowrate of the raw wastewater of those selected campaigns will be inputted to the model.

WWTP B and C have sludge return liquor recirculated back to the primary settlement. For these sites the flow and mass loading from the sludge return liquor is counted in the flow and concentration of the actual raw wastewater for the purposes of modelling, as per Equation 3-33 and Equation 3-34 in Section 3.5.6.

3.4.2.1.2 COD and its fractions

The composite variable of total COD is experimentally measured or calculated. The soluble inert fraction to total COD, readily biodegradable fraction to total COD, and the particulate fraction to total COD remains as default values of 0.05, 0.20 and 0.13 initially.

The key task of the COD characterization is to match the input sCOD and pCOD to the experimentally measured values. This is achieved via adjusting the colloidal fraction of slowly biodegradable COD (*frscol*), which is a type of sCOD, using Equation 3-11.

Equation 3-10

$$frscol = \frac{sCOD - COD \times frsi - COD \times frss}{COD \times (1 - frsi - frss - frxi)}$$

Where ***sCOD*** and ***COD*** is experimental measured sCOD and COD, ***frsi*** is soluble inert fraction to total COD, ***frss*** is readily biodegradable fraction to total COD, and ***frxi*** is the particulate fraction to total COD.

3.4.2.1.3 Nitrogen compounds and its fractions

TKN and NH_4^+-N were experimentally measured on all the wastewater samples for the modelling. Nitrite and nitrate were not experimentally measured on all of the wastewater samples collected from WWTP B and only for some of the wastewater samples collected from WWTP C. For those raw wastewater samples for which nitrite and nitrate were not measured their contents are assumed to be 0 mg/L. Nitrite and nitrate were not measured on the primary effluent and final effluent from WWTPs B and C. Neither WWTP has SAS recirculated back to the primary settlement and nitrification does not occur in their aerobic activated sludge process. Therefore, nitrite and nitrate content of the primary settlement and final clarification were also assumed to be 0 mg/L.

Soluble TKN was not measured on all raw wastewater samples. The default value of 0.9 is used.

The N content of the soluble inert material is set as 0.10 for WWTP A, C and D given that there is a relatively big difference between the observed TKN and NH_4^+-N in the final effluent (Roeleveld and van Loosdrecht, 2002, El Sheikh et al., 2016). The default value of 0.05 is set for WWTP B because difference between the observed TKN and NH_4^+-N in the final effluent is small. The N content of inert particulate material is set as 0.03 according to Roeleveld and van Loosdrecht (2002).

3.4.2.1.4 Phosphorus compounds and its fraction

Phosphate was experimentally measured on all the raw wastewater samples. The original sampling campaign focused on understanding the phosphate flux through the wastewater treatment works and hence TP was not measured. TP is therefore estimated using COD data.

Both WWTP A and C have historical data for COD and TP of their raw influents. There are strong positive relationships ($p<0.05$, examined with Minitab 2018) between TP and COD in both cases, as shown in Figure 3-1 and 3-2.

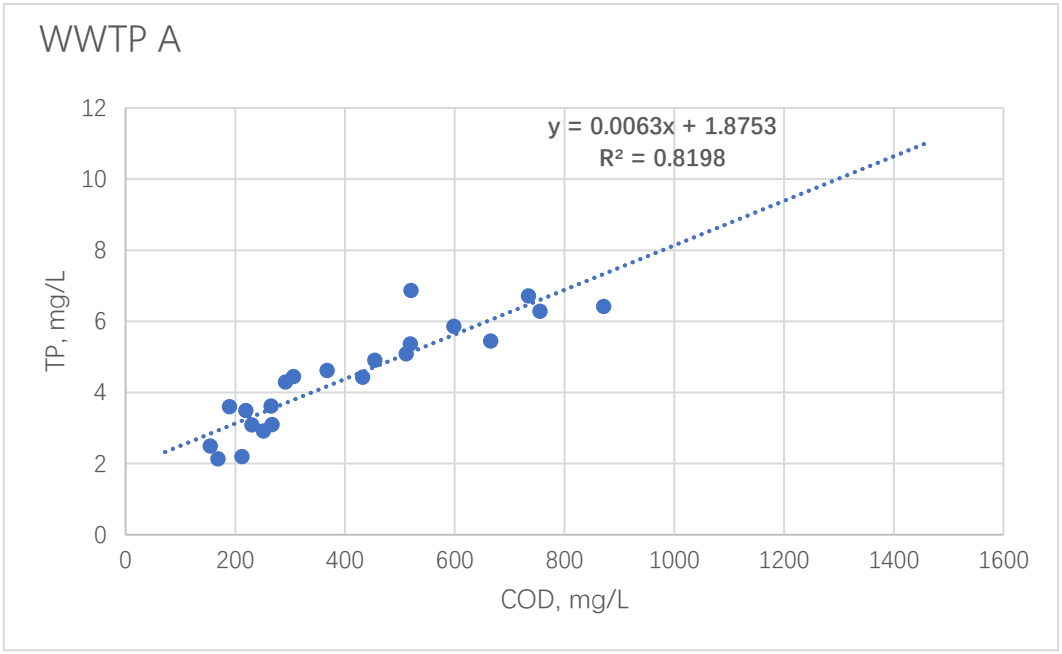

Figure 3-1 Relationship between TP and COD of WWTP C

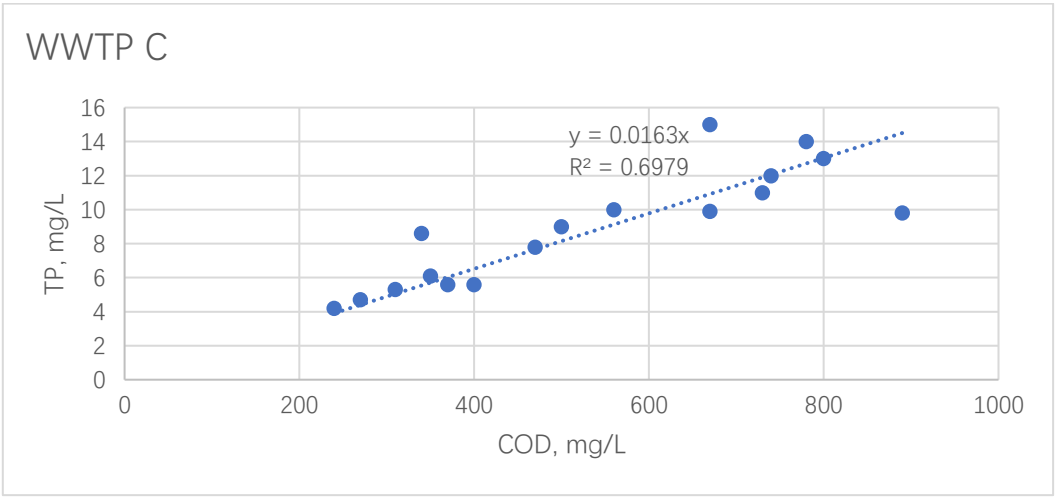

Figure 3-2 Relationship between TP and COD of WWTP C

Considering WWTP A and WWTP D both receives domestic wastewater with limited industrial wastewater and WWTP D is geographically close (approximately 12 miles) to WWTP A (*personal communication,* J McCowan, Scottish Water, July 2016), the TP of the raw wastewater of WWTPs A and D is estimated via COD through the linear regression equation of TP (mg/L) = 0.0063×COD+1.875 determined by historical data of WWTP A. The same approach applies to WWTP B and C as they receive substantial amount of industrial wastewater and are close (approximately 7.5 miles) to each other (*personal communication,* L Wilkinson, Northumbrian Water, March 2017). The equation is TP (mg/L) =0.00163×COD.

Both the P content of soluble inert material and inert particulate material are set as 0.005 according to Roeleveld and van Loosdrecht (2002).

3.4.2.1.5 The VSS/TSS ratio

Neither VSS nor TSS were measured on all the wastewater samples. The VSS and TSS values are not directly input to the model but are calculated by multiplying the inert particulate and particulate substrate concentrations by a default ratio value of 1.8 g particulate COD/g VSS. This ratio was not adjusted at any point during the modelling. Because the primary settlement settles the suspended solids (Tchobanoglous et al., 2003), the VSS/TSS ratio of the inflowing wastewaters are assumed to be the same as the VS/TS% of their primary sludge.

3.4.2.1.6 The Carbon content in substrates

The Carbon content of soluble inert material, inert particulate material, slowly biodegradable substrate, soluble substrate, and colloidal material can be defined individually. Similar to the default setting in GPS-X, for this research a common value was used for all five parameters. The value given is site specific and is determined by dividing the TOC by the COD of the raw wastewater.

3.4.2.2 Influent characterization of sludge treatment

Only the sludge treatment of WWTP C was modelled in this research. The sludge treatment prior to anaerobic digestion was modelled in the wastewater treatment model of WWTP C. Thus, the flow and quality of majority of the sludge streams were predicted generated in the model simultaneously. However, there were two occasions that the sludge is like the raw wastewater need to be characterized for their fractions. The first one is the imported sludge that is combined with the indigenous primary sludge and fed to the primary sludge thickening. The other is the digester feed sludge.

3.4.2.2.1 Imported sludge

The characterization of the imported sludge focuses on three aspects: COD, TN and TP. The concentration of each parameter (C_{ImpS}) is calculated according to the predicted flow and quality of the primary sludge and the measured flow and quality of the feed sludge to the primary sludge drum thickener, and is calculated via Equation 3-11

Equation 3-11

$$C_{ImpS} = \frac{Q_{PF} \times C_{PF} - Q_{PS} \times C_{PS}}{Q_{ImpS}}$$

Where $\boldsymbol{Q_{PF}}$ is the measured flowrate of the feed sludge to the primary sludge thickening, $\boldsymbol{C_{PF}}$ is the measured or estimated concentration of COD, TN and TP of the feed sludge to the primary sludge thickening, $\boldsymbol{Q_{PS}}$ is the predicted flowrate of the primary sludge, $\boldsymbol{C_{PS}}$ is predicted concentration of COD, TN and TP of the primary sludge, $\boldsymbol{Q_{ImpS}}$ is measured flowrate of the imported sludge.

In GPS-X, the TS and VS of the sludge is not possible to predicted by modeling (Hydromantis, 2017). Rather, they are estimated from the COD. By default, the software considers that a gram of pCOD is equal to 0.56 gram of VSS. Thus, a value of the COD of the digester feed sludge and the measured VSS/TSS ratio will be input to the "Influent Advisor" in GPS-X and will then be manually adjusted to a proper value that leads to an adequate TS and VS which are close to the calculated result.

The characterization of the imported sludge is based on the WWTP A and D's primary sludges that are co-settled with the indigenous biological sludge recirculated to the primary tanks. This is because the primary sludge produced in WWTP A and D is actually exported to other treatment works for thickening and dewatering. The phosphate, ammonium, organic fractions (such as the inert particulate COD to total COD, the inert soluble COD to total COD, etc.), nitrogen and phosphorus fraction, and part of the inorganic compounds are the component of interest to characterize. The values of the components and fractions used for the imported sludge are taken the mean value of the primary sludge generated from WWTP A and D. Details are listed in Table 3-5.

Table 3-5 The concentration and fraction used for characterizing the imported sludge

Parameter	Unit	Value of primary sludge of WWTP A	Value of primary sludge of WWTP D	Value used for Imported sludge
ammonia nitrogen	gN/m3	72.77	39.85	56.31
ortho-phosphate	gP/m3	15.68	10.21	12.95
soluble inert fraction of total COD	-	0.00	0.00	0.00
readily biodegradable fraction of total COD	-	0.00	0.00	0.00
particulate inert fraction of total COD	-	0.21	0.23	0.22
colloidal fraction of slowly biodegradable COD	-	0.00	0.00	0.00
acetate fraction of total COD	-	0.02	0.02	0.02
propionate fraction of total COD	-	0.01	0.00	0.01
unbiodegradable cell products fraction of total COD	-	0.02	0.07	0.04
iron hydroxide	gFe(OH)3/m3	311.10	0.00	155.55
iron phosphate	gFePO4/m3	444.70	0.00	222.35
magnesium hydrogen phosphate (newberyite)	gMgHPO4/m3	0.49	0.32	0.40
magnesium ammonium phosphate (struvite)	gMgNH4PO4/m3	39.07	0.41	19.74

3.4.2.2.2 Digester feed sludge

The characterization of the imported sludge focuses on four aspect, the COD, TN and TP, and the flowrate.

In theory, the digester feed sludge comes from dewatered raw sludge, and therefore the COD, TN and TP mass loading of the two should be the same. Because dewatered sludge is occasionally imported, and combined with the dewatered raw sludge, the mass loading of the

two may be different. However, this is not known for certain because flowrate and quality of sludge going through the THP process was not measured. If the mass loading of the predicted dewatered Raw sludge is smaller than the mass loading of the digester feed, then the measured concentration of the digested feed will be used to characterize the sludge. If the opposite is the case, the concentration of the digester feed will be estimated from the mass loading of the dewatered raw sludge via Equation 3-12.

Equation 3-12

$$C_{DF} = C_{DRS} \times \frac{Q_{DRS(P)}}{Q_{DF(O)}}$$

where $\boldsymbol{C_{DRS}}$ is the concentration of COD, TN and TP in the dewatered Raw sludge, $\boldsymbol{Q_{DRS(P)}}$ is the predicted flowrate of the dewatered Raw sludge and $\boldsymbol{Q_{DF(O)}}$is the experimentally measured volume observed of the digester feed.

The observed COD (estimated via VS via Equation 4-4), TN and the TP obtained from the five sampling campaigns done in this study are 113,137.1 mg/L, 4,315.4 mg/L and 1109.7 mg/L, respectively. The flowrate is collected from Northumbrian Water and is 876 m^3/d (*personal communication*, L Wilkinson, Northumbrian Water, 01 March 2017).

The NH_4^+-N and PO_4^{3-}-P content of the digester feed sludge will be estimated based on the predicted value of the dewatered raw sludge through the Equation 3-12.

The soluble inert fraction to total COD, readily biodegradable fraction to total COD, the particulate fraction to total COD, and the colloidal fraction of slowly biodegradable COD are given values of 0.0, 0.0, 0.20 and 0.0, respectively. Default values were used for all other fractions and concentrations.

3.4.3 Model calibration and validation

The aim of the calibration process is to match the simulated flow and quality of the effluent wastewater and sludge to the experimentally measured values, and then to predict the flow and quality of the unmeasured streams, and finally to study the mass and chemical energy balance of the WWTPs (Petersen et al., 2002, Hulsbeek et al., 2002).

There are two stages in the calibration process, the first is to screen the most influential parameters that affects the predicted result, and the second stage is to adjust those screened parameters to a reasonable value that makes the predicted flow and quality of the wastewater and sludge match experimental observed values.

3.4.3.1 Parameter screening

According to Brun et al. (2002) and Liwarska-Bizukojc et al. (2011), a sensitivity coefficient ($S_{i,j}$) is used to demonstrate how influential a parameter is to the predicted result. The $S_{i,j}$ is calculated via Equation 3-13 .

Equation 3-13

$$S_{i,j} = \left| \frac{\triangle y_i / y_i}{\triangle x_i / x_i} \right|$$

where y_i is predicted result (output variable), and x_i is the input parameter variable which can be a kinetic of the mechanical settling, mechanical thickening and dewatering, chemical reaction or biological reaction, a model stoichiometry or a fraction.

Like Liwarska-Bizukojc et al. (2011), a 10% increase is first given to the input parameter variable x_i for obtaining a new predicted result y_i. Meanwhile, the $\triangle x_i / x_i$ is constant as 0.1. The $S_{i,j}$ is then calculated. The $S_{i,j}$ is studied on every output variable of the model. If the $S_{i,j}$ is greater than 0.25, then the input parameter is considered as influential to the predicted parameter (Liwarska-Bizukojc et al., 2011).

The $S_{i,j}$ is then used to calculate the mean square sensitivity measure δ_j^{msqr}. This is used to demonstrate the influence of a change in a single parameter to the overall predicted results (Liwarska-Bizukojc et al., 2011). The δ_j^{msqr} is calculated using Equation 3-14.

Equation 3-14

$$\delta_j^{msqr} = \sqrt{\frac{1}{n} \sum_{n=1}^{n} S_{i,j}^2}$$

Where n is the number of the target variables that characterizes the quality of the wastewater and sludge.

The parameters controlling the settling, biological reactions in the settlers, activated sludge, sludge storage tanks, anaerobic digestion, and sludge thickening and dewatering will be studied for both $S_{i,j}$ and δ_j^{msqr}. According to Liwarska-Bizukojc et al. (2011), if a parameter has a δ_j^{msqr} greater than 0.1000 or ranks top 10-20th among all the studied parameters, then it will be selected for adjustment.

3.4.3.2 Parameter adjustment

3.4.3.2.1 Calibration algorithm

GPS-X has an Optimization function to numerically adjust the influential control variable to a value (within a given range) that makes the predict value of the target variables fit closely to their observed value (Hydromantis, 2017, Drewnowski et al., 2018). The Nelder-Mead algorithm is used in Optimization function (Hydromantis, 2017, Drewnowski et al., 2018). The control variables are commonly kinetics and model stoichiometry of a mechanical process or a biological reaction.

There are three objective functions in the Optimization function that are used in the calibration conducted in this research:

1. The "Relative Difference" (Equation 3-15),
2. The "Relative Sum of Squares" (Equation 3-16) and
3. The "Absolute Difference" (Equation 3-17).

Equation 3-15

$$F = \sum_{j=1}^{m} \sum_{i=1}^{n_j} \left| z_{i,j} - f_{i,j} \right|$$

Equation 3-16

$$F = \sum_{j=1}^{m} \sum_{i=1}^{n_j} \left| \frac{z_{i,j} - f_{i,j}}{z_{i,j}} \right|$$

Equation 3-17

$$F = \sum_{j=1}^{m} \sum_{i=1}^{n_j} \left(\frac{z_{i,j} - f_{i,j}}{z_{i,j}} \right)^2$$

Where $z_{i,j}$ is the measured value of response j in experiment i, $f_{i,j}$ is the value of response variable j predicted by the process model in experiment i, m is the number of measured response variables, and the number of experiments for response j.

The "Relative Difference" and "Relative Sum of Squares" aim to minimize the percentage difference between the predicted values and the observed values of all the target variables. However, the drawback of these two objective functions is that they prioritize the target variable that is present at low concentrations as a small numerical change will leads to a big percentage change. For example, the targeted concentration of A substance is 10 mg/L and or B substance is 10,000 mg/L. The initial prediction of A and B is 9 mg/L and 10,000 mg/L. The total relative difference between the initial prediction and the observation is |(9-10)/10)+(10,000-10,000)/10,000)|=10%. A given change of a kinetic of a mechanical or biological reaction is able to increase the prediction of A by 1 mg/L and the prediction of B by 10 mg/L. If "Relative Difference" is the objective function, the Optimization will not make the change of the kinetic because the total numerical difference would be increased to |(10-10)/10)+(10,000-10,010)/10,000|=0.1%. This also applies to the optimization using "Relative Sum of Square" as objective function.

The "Absolute Difference" objective aims to minimize the numerical difference between the predicted values and the observed values of all the target variables. The drawback of this is that it will prioritize those target variables that have high concentrations (in thousands or tens of thousands mg/L), since the change in them can be hundreds or thousands mg/L and therefore leads to a substantial numerical difference. Using the same example stated in last paragraph for demonstration, the total numerical difference between the initial prediction and the observation is |(10-9)+(10,000-10,000)|=1 mg/L. A given change of a kinetic of a mechanical or biological reaction is still able to increase the prediction of A by 1 mg/L and the prediction of B by 10 mg/L. If Absolute Difference is the objective function, the Optimization will not make the change of the kinetic because the total numerical difference would be increased to |(10-10)+(10,000-10,010)|=10 mg/L.

Regarding the given value range of the control variable, for the biological models the upper boundary is set as 120% of the default value and the lower boundary is set as 80% of the default value. If a value range is reported, then the reported range will be used. In some cases, instead of a value range a single value is reported. If the reported value is higher than 120% or lower than 80% of the default value, then it becomes the boundary. If the control variable is the operational efficiency of a mechanical process, the range given is 0-1. The value ranges of the kinetic and stoichiometry of the biological models are given in Appendix B.

3.4.3.2.2 Calibration procedures

The calibration procedures for the wastewater treatment modelling

The calibration procedures is developed from Fall et al. (2011) and is stepwise. The calibration procedures of the wastewater treatment are slightly different for WWTP A and D, which have SAS recirculation to their primary settlers, compared to WWTPs B and C which do not. The calibration procedures are listed below.

Step 1

If there is substantial change of sCOD and phosphate after primary treatment, then a virtual unit for sCOD removal and phosphate removal is added between the influent unit and the primary settlers.

For the virtual sCOD removal, the soluble inert fraction of total COD, colloidal fraction of slowly biodegradable COD, readily biodegradable fraction of total COD and the chemical dosage rate of $Al_2(SO_4)_3 \cdot 18H_2O$ are the control variables. The sCOD and pCOD of the raw wastewater, sCOD and the soluble inert sCOD of the primary effluent, are the target variable. The soluble inert sCOD, which is not experimentally measured, is set as 90% of the observed sCOD of the effluent from final clarification (Hulsbeek et al., 2002).

For the virtual ferric dosing for phosphate removal, the chemical dosage rate of $Fe_2(SO_4)_3 \cdot 9H_2O$ is the control variable and the measured phosphate concentration of the primary effluent is the target variable.

The objective function of the “Optimization” is “Absolute Difference”.

Step 2

For WWTP B and C (o SAS recirculated back to the primary settlement) the influential parameters on the primary settlers are chosen first. The target variables of this tuning are the pCOD, sCOD, TKN of the primary effluent and the TSS, VSS, TN and TP of the primary sludge. The objective function of the Optimization is “Relative Sum of Squares”.

The influential parameters of the activated sludge and final settlers are then chosen for the adjustment. However, if the influential parameter is from the ammonium oxidizers group or the nitrite oxidizer group of the biological model, or is only influential (with a $S_{i,j} > 0.25$) to the nitrogen derivatives of ammonium, nitrite and nitrate, then it is not adjusted. This was the approach taken by (Fall et al., 2011). The target variables are the pCOD, sCOD, TKN, and phosphate of the final effluent and the flow, TSS, VSS, TN and TP of the WAS. The objective function of the “Optimization” is “Relative Sum of Squares”.

For WWTP A and D (SAS recirculated back to the primary settlement) the influential parameters of the primary settlers, activated sludge, and final settlers are chosen for calibration all at onceat this step.The target variables are the pCOD, sCOD, TKN, and phosphate of the primary effluent, the pCOD, sCOD and phosphate of the final effluent, the TSS, VSS, TN and TP of the primary sludge and SAS, and the flow of the SAS. The objective function of the “Optimization” is “Relative Sum of Squares”.The same approach is taken for the ammonium and nitrite oxidizer groups as for WWTPs B and C.

Step 3

The nitrogen related parameter will be adjusted. The target variables are the pCOD, sCOD, TKN, and phosphate of the primary effluent, the pCOD, sCOD, ammonium, TKN, Nitrate, TN, and phosphate of the final effluent, the TSS, VSS, TN and TP of the primary sludge and SAS, and the flow of the SAS. The objective function of the “Optimization” is “Relative Sum of Squares”.

The calibration procedures for the sludge thickening and dewatering treatment prior to anaerobic digestion

The influential parameters of the biological model of the sludge storage tank and sludge thickening and dewatering will be adjusted at the same time. The target variables are commonly the COD, sCOD, pCOD, ammonium, TKN and phosphate of the filtrate and centrate and the COD, TN and TP of the thickened and dewatered sludge. In the case of the raw sludge dewatering, the COD, TN and TP of the stored sludge (prior to dewatering) will also be chosen as target variables in the tuning. That is because the stored sludge was what was sampled and measured in the sampling campaign. The objective function of the "Optimization" is "Relative Difference".

The calibration procedures for anaerobic treatment and subsequent digestion

The influential parameters for the biological model as it relates to the anaerobic digestion and dewatering of digested sludge are adjusted at the same time. The fraction of inflowing sludge and the ratio of TOC content to per gram particulate CODs are also adjusted at this time. The target variables are the TOC content of the feed sludge, the flow of the produced CO_2, CH_4 and total biogas, the COD, sCOD, pCOD, ammonium, TKN and phosphate of the filtrate and centrate, and the COD, TN and TP of both the stored and dewatered digested sludge. The objective function of the "Optimization" is "Relative Difference".

3.4.3.3 Validation

Rieger et al. (2012) considers that it is acceptable to have ± 5-15 % difference between the predicted data and the observed data. However, current literatures rarely reported a quantitative method for validating predicted data generated from the steady state modeling to the observed data. But Liwarska-Bizukojc et al. (2011) reported a quantitative method for validating the goodness of fit between the observed values and the predicted values produced in the dynamic modelling. The method is to calculate the average relative difference by comparing a set of predicted values to the corresponding observed values via Equation 3-18.

Equation 3-18

$$ARD = \frac{\sum_{n=1}^{n}(\left|\frac{OV - PV}{OV}\right| \times 100\%)}{n}$$

where ***OV*** is the observed value, ***PV*** is the predicted value, *n* is the number of target variables selected in the optimization.

In the example of Fall et al. (2011) which reported both the observed value and the predicted values generated from steady state modeling, the ARD calculated is 23%. For this research an ARD of no greater than 15% was deemed acceptable, to be consistent with the range of values observed by Rieger et al. (2012).

Furthermore, a visualization aid developed by Fall et al (2011) was also used to demonstrate the goodness of fit of the predicted values. The method is to use the observed value (in y-axis) to plot against the predicted value. A diagonal line with a slope of 1 is drawn on all plots to use as a reference line. The graphs are produced via Matlab 2017.

3.5 Construction of mass and chemical energy balances

The wastewater and sludge treatment in the investigated WWTPs consists of primary settlement, aerobic activated sludge as secondary biological treatment, secondary clarification, sludge storage and subsequent thickening and dewatering, and anaerobic digestion. This study firstly examines the mass and energy balance of each individual process and then investigates the balances of the entire WWTPs.

3.5.1 Calculation of mass loading

Mass loading within wastewater is calculated by multiplying flow (Q, m^3/day) by concentration (*C*, mg/L) in a sample collected simultaneously to the flow measurement (Equation 3-19). Mass load is reported in units of kg/day or tonne/day, as appropriate.

Equation 3-19

$$M = Q \times C$$

Where ***Q*** is the flow of the wastewater, and ***C*** is the concentration of a given contaminant.

The concentration (*C%*) of sludge is expressed as percentage weight in dried solid and is therefore a weight to weight unit. Thus, the mass loading within sludge is calculated by multiplying the flow by the specific density (ρ, ton/m^3) of sludge first, and then by its TS% and the corresponding concentration, as shown in Equation 3-20.

Equation 3-20

$$M = Q \times \rho_{Sludge} \times TS\% \times C\%$$

Where $\boldsymbol{Q}$ is the flow of the sludge, $\boldsymbol{\rho_{Sludge}}$ is the specific density of sludge, $\boldsymbol{TS\%}$ is the dried solid percentage of the sludge, and $\boldsymbol{C\%}$ is the percentage concentration to the dried solid.

However, the observed sludge concentration is to serve the modelling. In the modelling software GPS-X, the component concentration is expressed weight to volume (w/v) concentration in unit of mg/L. Therefore, the w/w concentration has to be converted in to mg/L concentration.

In the sludge density calculation shown in Appendix C, the sludges sampled have a TS% varies from 0.5% to 24.0%, and VS/TS% varies from 60% to 80%. In this range of TS% and VS/TS%, the specific density of sludge falls in the range of 1,001 to 1,061 g/L. Thus, the specific density of all the sludges in this study were assumed as 1,000 g/L. A 1,000g/L sludge specific density is also applied in Lu (2006).

Therefore, the w/v TS content of the sludge (TS_s, g/L) is calculated via Equation 3-21.

Equation 3-21

$$TS_s = TS\% * 1{,}000$$

For other sludge component of VS, TOC, TN and TP, their w/v concentration is calculated via multiplying the TS_s with their weight percentage to TS. For example, the w/v VS content of the sludge is calculated by multiplying the TS with VS/TS%.

3.5.2 Calculation of chemical energy loading

As chemical energy content of wastewater (E_{ww}, kJ/L) is also a concentration, chemical energy (E) loading within wastewater is calculated by multiplying flow with the corresponding E_{ww} (as shown in Equation 3-22).

Equation 3-22

$$E = Q \times E_{ww}$$

where $\boldsymbol{Q}$ is the flow of the wastewater and $\boldsymbol{E_{ww}}$

Since chemical energy content (E_{ds}, kJ/g) of sludge is the calorific value of the dried solid, chemical energy loading within the sludge is calculated by multiplying flow by the specific density (ρ, ton/m^3) of sludge first, and then by its TS% and the corresponding E_{ds} (as shown in Equation 3-23).

Equation 3-23

$$E = Q \times \rho_{Sludge} \times TS\% \times E_{ds}$$

where $\boldsymbol{Q}$ is the flow of the wastewater, $\boldsymbol{\rho_{Sludge}}$ is the density of sludge and is assumed 1,000g/L, $\boldsymbol{TS\%}$ is the dried solid percentage of the sludge, and $\boldsymbol{E_{ds}}$ is the chemical energy content (kJ/g) of the dried sludge.

The chemical energy loading may also be estimated through the relationship between the chemical energy content (in kJ/L or kJ/g) and the TS, VS and COD determined in Chapter 4.

3.5.3 Flow balance

As shown in Section 3.5.1 and 3.5.2 flow is the key element for acquiring mass and energy loading. In this study, flow of all the raw inlet and SAS sludge, feed sludge to thickening and dewatering process, and in-flowing and out-flowing sludge to the digester were measured and collected by water companies (stated in Section 3.1.3). However, the flow of primary effluent of WWTP A, B and D, secondary effluent of WWTP A and D, the primary sludge of WWTP B and C, and the out-flowing sludge of WWTP B and C's sludge thickening and dewatering were not measured by water companies. Neither was it possible to measure these variables with a portable flow meter. Given that the total inlet flowrate should equal the total outlet flow (Puig et al., 2008), in this study the effluent wastewater flow rate is therefore calculated using Equation 3-24.

Equation 3-24

$$Q_{In} = Q_{Eff} + Q_S$$

where $\boldsymbol{Q_{in}}$ is the flow of all influents, $\boldsymbol{Q_{Eff}}$ is the flow of all the effluent wastewater streams, and $\boldsymbol{Q_S}$ is the flow of all the effluent sludge streams. The influent liquid streams, effluent wastewater

streams and sludge streams of the flow balance of each individual process are listed in Table 3-6.

Table 3-6 The influent liquid streams, effluent wastewater streams and sludge streams of the flow balance of each individual process

Process	Q_{In}	Q_{Eff}	Q_S
Primary	WWTP A and D: Raw wastewater plus recirculated biological sludge WWTP B and C: Raw wastewater plus sludge return liquor	Primary effluent	Primary sludge
Activated Sludge	Primary effluent RAS	Mixed liquor	N/A
Secondary Clarifier	Mixed liquor	Final Effluent	RAS SAS
Activated Sludge + Secondary Clarifier	Primary effluent	Final Effluent	SAS
Whole Wastewater treatment work	WWTP A and D: Raw wastewater WWTP B and C: Raw wastewater and sludge return liquor	Final Effluent	WWTP A and D: Primary Sludge WWTP B and C: Primary Sludge + SAS
Sludge Holding Tank	Sludge	N/A	Stored sludge
Sludge Thickening and Dewatering	Sludge	Return Liquor	Thickened or Dewatered sludge
Anaerobic Digestion	Sludge feed	N/A	Digested Sludge
Wastewater treatment + Sludge Treatment	Raw wastewater and sludge return liquor	Final Effluent Return liquor	Digested Sludge

3.5.4 Mass balance

This study investigates the mass balances of COD, TN and TP of all the processes and the mass balances of TS and VS of the sludge thickening and dewatering processes. In wastewater and sludge treatment there are commonly multiple outflows: (1) treated effluent, (2) sludge and (3)

gaseous emissions (captured or otherwise). Therefore, the mass balance of a process is expressed as shown in Equation 3-25.

Equation 3-25

$$M_{In} = M_{Eff} + M_G + M_S$$

Where $\boldsymbol{M_{In}}$ is the influent mass, $\boldsymbol{M_{Eff}}$ is the effluent mass in the treated effluent, $\boldsymbol{M_G}$ is the effluent mass in the gaseous emission, and $\boldsymbol{M_S}$ is the effluent mass in the removed sludge. The influent liquid streams, effluent wastewater streams and sludge streams used in the mass balance of each individual process are listed in Table 3-7.

Table 3-7 The influent and effluent wastewater streams and sludge streams used in the mass balance of each individual process

Process	M_{In}	M_{Eff}	M_G	M_S
Primary Settlement	WWTP A and D: Raw wastewater and recirculated biological sludge WWTP B and C: Raw wastewater and sludge return liquor	Primary effluent	N/A	Primary Sludge
Activated Sludge	Primary effluent RAS	Mixed liquor	CO_2 and N2	N/A
Secondary Clarification	Mixed liquor	Final Effluent	CO_2 and N2	RAS WAS
Activated Sludge + Secondary Clarifier	Primary effluent	Final Effluent	CO_2 and N2	WAS
Whole Wastewater treatment work	WWTP A and D: Raw wastewater WWTP B and C: Raw wastewater and sludge return liquor	Final Effluent	CO_2 and N2	WWTP A and D: Primary Sludge WWTP B and C: Primary Sludge + WAS
Sludge Holding Tank	Sludge	N/A	CO_2 and N2	Stored sludge
Sludge Thickening and Dewatering	Sludge	Return Liquor	N/A	Thickened and Dewatered sludge
Anaerobic Digestion	Sludge feed	N/A	Biogas (CH_4 and CO_2)	Digester Sludge
Wastewater treatment + Sludge Treatment	Raw wastewater and sludge return liquor	Final Effluent Return liquor	Biogas, CO_2 and N2	Digester Sludge

To investigate the distribution pattern of COD, TN and TP in individual process, in Chapters 4 and the proportionate mass flows of substances as treated effluent, sludge, or gaseous emission are expressed as percentages of the total influent mass.

If both flow and concentration of all inflow and outflow streams are directly measured or modelled, the mass balance is considered as closed. Nevertheless, as there may be error in both flow and concentration measurement it is not always the case that inflowing mass is exactly equalled by mass flows out. The error of the closed mass balance is studied by comparing the numerical difference between the right and the left of Equation 3-26. Considering flow measurement may be subject to errors of ± 15% (Agu et al., 2017), if the difference is within ± 15%, the mass balance is considered as balanced and correct. If the difference is outside of ± 15%, the mass balance is considered as incorrect, and discussion is provided on the possible causes of the inaccuracy.

If an individual mass loading is calculated by directly subtracting the sum of all out-flowing mass loadings from the inflows (as shown in Equation 3-26), that mass balance is always balanced. This type of mass balance is considered as open mass balance. Its accuracy is examined via comparing the percentage mass loading of each component to the theoretical or reported value in literature.

Equation 3-26

$$M_{Out(unknown)} = M_{In} - \sum M_{Out(known)}$$

Where $\boldsymbol{M_{Out(unknown)}}$ is the effluent mass which is neither measured or calculated, $\boldsymbol{M_{In}}$ is the influent mass, and $\sum \boldsymbol{M_{Out(known)}}$ is the sum of measured or calculated effluent mass. This method has mainly been applied to the activated sludge and its subsequent final clarification and sludge storage. This is because flows and concentrations of their potential gaseous products were not measured.

3.5.5 Chemical energy balance

If there is no chemical energy consumed during the process then the chemical energy balance is expressed as the Equation 3-27.

Equation 3-27

$$E_{In} = E_{Eff} + E_G + E_S$$

Where E_{In} is the influent chemical energy, E_{Eff} is the effluent chemical energy in the treated effluent wastewater, E_G is the effluent chemical energy in the gaseous emission, and E_S is the effluent chemical energy in the sludge retained in the treatment process. Although gaseous products are generated in some processes, if the gaseous product (such as CO_2 and N_2) has a calorific value of zero then they are not accounted for in the energy balance calculation. The influent liquid streams, effluent wastewater streams and sludge streams of the energy balance of each individual process are listed in Table 3-8.

Table 3-8 The influent and effluent wastewater streams and sludge streams of the energy balance for each individual process

Process	E_{In}	E_{Eff}	E_G	E_S
Primary Settlement	WWTP A and D: Raw wastewater and recirculated biological sludge WWTP B and C: Raw wastewater and sludge return liquor	Primary effluent	N/A	Primary Sludge
Activated Sludge	Primary effluent RAS	Mixed liquor	N/A	N/A
Secondary Clarification	Mixed liquor	Final Effluent	N/A	RAS WAS
Activated Sludge + Secondary Clarifier	Primary effluent	Final Effluent	N/A	WAS
Whole Wastewater treatment work	WWTP A and D: Raw wastewater WWTP B and C: Raw wastewater and sludge return liquor	Final Effluent	N/A	WWTP A and D: Primary Sludge WWTP B and C: Primary Sludge + WAS
Sludge Holding Tank	Sludge	N/A	N/A	Stored sludge
Sludge Thickening and Dewatering	Sludge	Return Liquor	N/A	Thickened or Dewatered sludge
Anaerobic Digestion	Sludge feed	N/A	Biogas (CH_4)	Digester Sludge
Wastewater treatment + Sludge Treatment	Raw wastewater and sludge return liquor	Final Effluent Return liquor	Biogas (CH_4)	Digester Sludge

The biological elements of secondary treatment and anaerobic digestion may consume part of the influent chemical energy. Specifically, the difference between the in-flowing energy and the out-flowing energy is considered as loss of energy. Their energy balance is expressed as Equation 3-28.

Equation 3-28

$$E_{In} = E_{Eff} + E_G + E_S + E_{Loss}$$

where $\boldsymbol{E_{In}}$ is the influent chemical energy, $\boldsymbol{E_{Eff}}$ is the effluent chemical energy in the treated effluent wastewater, $\boldsymbol{E_G}$ is the effluent chemical energy in the gaseous emission, $\boldsymbol{E_S}$ is the effluent chemical energy in the removed sludge, and $\boldsymbol{E_{Loss}}$ is the difference between the in-flowing chemical energy and the out-flowing chemical energy.

If the chemical energy loading of all the inflows and outflows are calculated by multiplying flow and concentration the balance is considered as closed. The examination of its accuracy is described in Section 3.5.4.

3.5.6 Calculations related to the primary treatment

In the construction of the balances the major complexity is within the primary settlement, as the influent not only consists of raw inlet wastewater but also of recirculated biological sludge, or sludge return liquor. Therefore, two issues need resolving: the first is to calculate the actual primary sludge produced due to the sedimentation of the particulates from the raw wastewater, and the second is to estimate the flow of the sludge return liquor as it is not measured by the water companies.

For the first issue, this study assumes that all of the biological sludge recirculated back to the primary settlement will completely settle and be completely discharged within the primary sludge. The mass of actual primary sludge is therefore calculated by subtracting the mass of biological sludge from primary sludge in the mass balance, as indicated in Equation 3-29. An equivalent expression applies to energy (Equation 3-30) and nutrients.

Equation 3-29

$$M_{RI} = M_{PE} + M_{APS} = M_{PE} + (M_{PS} - M_{BS})$$

Where $\boldsymbol{M_{RI}}$ is the influent mass in the raw inlet, $\boldsymbol{M_{PE}}$ is the effluent mass within the primary effluent, $\boldsymbol{M_{APS}}$ is the is effluent mass of the actual primary sludge, $\boldsymbol{M_{PS}}$ is effluent mass within the primary sludge combined with actual primary sludge and biological sludges, and $\boldsymbol{M_{BS}}$ is the mass of all the biological sludge recirculated back to the primary settlement tank.

Equation 3-30

$$E_{RI} = E_{PE} + E_{APS} = E_{PE} + (E_{PS} - E_{BS})$$

Where $\boldsymbol{E_{RI}}$ is the influent chemical energy with in raw inlet, $\boldsymbol{E_{PE}}$ is the effluent chemical energy within the primary effluent, $\boldsymbol{E_{APS}}$ is the is effluent chemical energy of the actual primary sludge, $\boldsymbol{E_{PS}}$ is effluent chemical energy within the primary sludge combined with actual primary sludge and biological sludges, and $\boldsymbol{E_{BS}}$ is the chemical energy of all the biological sludge recirculated back to the primary settlement.

For the second issue the flow of the return liquor is estimated through the flow balance and the TS mass balance. The flow and TS mass balance of a sludge thickening or dewatering facility can be described as in Equations 3-31 and 3-32.

Equation 3-31

$$Q_{WS} = Q_{RL} + Q_{DewS}$$

Where $\boldsymbol{Q_{WS}}$is the influent wet sludge flow, $\boldsymbol{Q_{RL}}$is the flow of the return liquor (the removed wastewater), and $\boldsymbol{Q_{DewS}}$ is the flow of the effluent thickened or dewatered sludge.

Equation 3-32

$$M_{WS}^{TS} = M_{RL}^{TS} + M_{DewS}^{TS}$$

Where $\boldsymbol{M_{WS}^{TS}}$is the influent TS mass, $\boldsymbol{M_{RL}^{TS}}$ is the TS mass within the return liquor (the removed wastewater), and $\boldsymbol{M_{DewS}^{TS}}$ is the TS mass within thickened or dewatered sludge.

According to Equation 3-20 and 3-31, the Equation 3-32 is derived into Equation 33 as

Equation 3-33

$$Q_{WS} \times TS_{WS}\% = Q_{RL} \times C_{RL}^{TS} + (Q_{WS} - Q_{RL}) \times TS_{Dew}\%$$

$$Q_{RL} = \frac{Q_{WS} \times (TS_{WS}\% - TS_{DewS}\%)}{(C_{RL}^{TS} - TS_{DewS}\%)}$$

where $\boldsymbol{Q_{RL}}$is the flow of the return liquor (the removed wastewater), $\boldsymbol{Q_{WS}}$is the influent wet sludge flow, $\boldsymbol{TS_{DewS}}\%$ is the TS% of the thickened or dewatered sludge, $\boldsymbol{TS_{WS}}\%$ is the TS% of the wet sludge, and $\boldsymbol{C_{RL}^{TS}}$ is the TS concentration of the return liquor. Because this study considers the specific density of the sludge to be 1 g/L of the sludge, 1% TS% is equal to 10,000 mg/L of TS.

Once the flow of the sludge return liquor is known, the concentration of the actual in-flowing wastewater containing sludge return liquor can be calculated using Equation 3-34.

Equation 3-34

$$C_{In(actual)} = \frac{M_{RI} + \sum M_{SRL}}{Q_{In(actual)}}$$

Where $\boldsymbol{M_{RI}}$ is the mass within the raw inlet, $\sum M_{SRL}$ is the sum of mass with the sludge return liquor, $\boldsymbol{Q_{In(actual)}}$ is the actual flow which includes all the raw wastewater, filtrates and centrates to primary settlement.

Chapter 4 Results and Discussion: Chemical energy of wastewater and sludge

This chapter discusses the chemical energy within wastewater and sludge. It examines the performance of an innovative wastewater drying method developed in this research (in Section 4.1.1). It presents the energy-related characteristics of wastewater (in Section 4.1.2) and sludge (in Section 4.2.1), and then investigates the relationships between routinely measured variables and wastewater energy (in Section 4.1.3 and 4.1.4) or sludge energy (in Section 4.2.2).

4.1 Chemical energy of wastewater

4.1.1 Method Improvement

A key objective of this research was to develop a more reliable method for the routine determination of municipal wastewater energy content. The method should be effective in retaining the COD in the dried wastewater because any loss of COD will result in loss of energy and therefore an erroneously low value for energy content will result (Heidrich et al., 2010). Moreover, the method should be also time efficient since the current measurement could take approximately weeks to finish (Heidrich et al., 2010).

COD loss is primarily associated with the sample drying process (Heidrich et al., 2011). In this study, the centrifugal evaporation is used to dry the wastewater and therefore the effect of drying by centrifugal evaporation was tested. Results indicated that the centrifugal evaporation drying of samples has a greater COD recovery (mean 84.8%, n=36) than both freeze-drying (73.8 – 81.7%) and oven-drying (51.3 – 56.2%) (Heidrich et al., 2010). Using the centrifugal evaporation drying process, there was no particular difference in COD loss during drying of raw wastewater, primary treated and secondary treated, despite the large differences in initial COD: 87.4% (n=16), 82.6% (n=12) and 82.9% (n=8), respectively. Losses of COD during drying have previously been ascribed to loss of volatile organic compounds such as acetate (Heidrich et al., 2010), and that may be the case with losses during centrifugal

evaporation drying also. Nevertheless, centrifugal evaporation still incurs lower losses than the freeze-drying process.

In terms of the drying time, centrifugal evaporation is able to simultaneously dry six 400 mL wastewater samples typically less than 72 hours. Comparing to freeze-drying which requires 28 days to dry 1.5 L wastewater sample (Heidrich et al., 2010), centrifugal evaporation is a far quicker drying process but does not compromise the effectiveness in retaining COD.

4.1.2 Wastewater characteristics

Summary statistics for the COD and energy content of the wastewaters (spot raw, composite raw, composite primary treated and composite final effluent) of all four study sites are shown in Table 4-1.

The CODs of raw wastewaters A, B and C are significantly higher than that of wastewater D ($p < 0.05$), and the COD of Wastewater B is statistically higher than Wastewater C ($p < 0.05$). Notwithstanding these differences, the four domestic wastewaters sampled are typical of COD concentrations of domestic wastewaters internationally (430 mg/L to 800 mg/L for medium and high strength wastewaters respectively) (Tchobanoglous et al., 2003). Unsurprisingly, given that organic matter is removed through the treatment process, there is a consistent decrease in COD, at all wastewater treatment plants, from raw wastewater to final effluent.

The overall mean energy content of the spot raw and composite raw wastewaters falls in the previously reported range of 1.12 kJ/L and 41.11 kJ/L (Korth et al., 2017, Heidrich et al., 2010, Shizas and Bagley, 2004). Similar to the COD, there is a consistent decrease in chemical energy content of wastewater (E_{ww}, kJ/L), at all wastewater treatment plants, from raw wastewater to final effluent, with the overall mean for the latter being < 1.5 kJ/L.

Table 4-1 Mean COD and E_{ww} (± standard deviation) of wastewater samples from this research compared to literature values

	Parameter	Spot Raw	Composite Raw	Composite Primary Treated	Composite Final Effluent
Centrifugal Vacuum Dried					
WWTP A	COD, mg/L	530.1 ±276.3 (n=12)	758.0 ±433 (n= 5)	312.3 ±158.0 (n=5)	38.24 ±10.07 (n=5)
	E_{ww}, kJ/L	10.20 ±4.20 (n11)	12.22 ±8.30 (n=5)	4.65 ±2.83 (n=5)	0.14 ±0.09 (n=5)
WWTP B	COD, mg/L	714.7 ±229.1 (n=12)	613.1 ±57.7 (n=5)	392.2 ±40.7 (n=5)	57.5 ±28.4 (n=5)
	E_{ww}, kJ/L	11.94 ±4.70 (n=12)	11.00 ±1.57 (n=5)	6.39 ±0.71 (n=5)	0.54 ±0.25 (n=5)
WWTP C	COD, mg/L	568.9 ±148.1 (n=12)	522.8 ±109.3 (n=9)	450.0 ±96.2 (n=5)	93.8 ±27.4 (n=5)
	E_{ww}, kJ/L	6.85 ±2.77 (n= 12)	7.86 ±2.63 (n=9)	6.87 ±2.15 (n=5)	1.31 ±0.16 (n=3)
WWTP D	COD, mg/L	409.6 ±189.8 (n=12)	305.4 ±113.5 (n=5)	150.0 ±55.9 (n=5)	24.89 ±6.75 (n=5)
	E_{ww}, kJ/L	6.53 ±6.08 (n=11)	4.40 ±1.01 (n=5)	2.17 ±0.96 (n=5)	0.11 ±0.10 (n=4)
Overall	COD, mg/L	555.8 ±236.3 (n=48)	545.4 ±251.4 (n=24)	326.1±147.0 (n=20)	51.51 ±31.48 (n=19)
	E_{ww}, kJ/L	8.90 ±4.98 (n=46)	8.70 ±4.88 (n=24)	5.02 ±2.56 (n=20)	0.46 ±0.48 (n=17)
Oven Dried					
Heidrich et al. (2010)	COD, mg/L		647.3 ± 100.6 (n=2)		
	E_{ww}, kJ/L		6.95 ± 1.91 (n=2)		
Korth et al. (2017)	COD, mg/L		1275 ± 915 (n=17)		
	E_{ww}, kJ/L		6.30 ± 4.19 (n=23)		
Shizas and Bagley (2004)	COD, mg/L	431(n= 1)			
	E_{ww}, kJ/L	6.30 (n= 1)			
Freeze Dried					
Heidrich et al. (2010)	COD, mg/L		647.3 ± 100.6 (n= 2)		
	E_{ww}, kJ/L		12.20 ± 6.51 (n= 2)		
Korth et al. (2017)	COD, mg/L		1817 ± 1091 (n= 3)		
	E_{ww}, kJ/L		20.22 ± 10.65 (n= 6)		

4.1.3 The relationship between COD and chemical energy content of wastewater

For the purposes of data analysis samples were grouped into four categories: (1) composite raw wastewater samples only (2) all composite samples i.e. raw, settled and final effluent (3) individual spot raw wastewater samples collected at different times through a day, and (4) all wastewater samples (both composite and spot samples).

The tested variables (stated in Section 3.2.1) were first analyzed for their correlation with E_{ww}. For the composite raw samples COD, pCOD, TOC, DOC and VS all had a strong correlation with E_{ww} (Spearmen Rho >0.85, $p<0.05$). For all composite samples COD, pCOD, TOC, POC, T_{ce} and chemical energy content of dried wastewater (E_{dww}, kJ/g) all have a strong correlation with E_{ww} (Spearmen Rho >0.90, $p<0.05$). For the spot raw samples COD and E_{dww} have the strongest correlation with E_{ww} (Spearmen Rho >0.70, $p<0.05$), and for all composite and spot samples combined COD, pCOD and E_{dww} all have strong positive correlations with E_{ww} (Spearmen Rho >0.85, $p<0.05$). COD has a ubiquitously strong correlation with E_{ww}, irrespective of sample group.

The variables with the strongest correlation with the E_{ww} were analysed by the Best Subset function of Minitab to identify the most appropriate variables (in terms of r^2 and the adjusted r^2 (r^2_{adj})) to use in a regression model. Although an increase in the number of variables might improve the value of r^2, if r^2_{adj} is not simultaneously increased, then the variable tested could be excluded in the regression (Minitab Inc., 2017b). The best regression model was considered that having the highest r^2_{adj} but with as few variables as possible. The results of the Best Subset study are shown in Table 4-2.

Table 4-2, Best regression for estimating wastewater energy

No. of Variables	r^2	r^2_{adj}	Parameter Required
Composite raw, n=24			
1	88.9	88.4	pCOD
1	86.5	85.9	COD
1	83.7	83.0	TOC
2	91.1	90.2	pCOD, DOC
3	91.9	90.7*	COD, pCOD, DOC
4	92.1	90.4	COD, pCOD, DOC, VS
5	92.1	89.9	COD, pCOD, TOC, DOC, VS
All composite, n=59			
1	92.9	92.8	COD
1	92.7	92.5	pCOD
1	91.4	91.2	TOC
2	93.9	93.7	COD, pCOD
3	95.0	94.8*	pCOD, TOC, VS
4	95.2	94.8	COD, pCOD, TOC, VS
5	95.3	94.8	COD, pCOD, TOC, VS, TS_{cve}
6	95.3	94.8	COD, pCOD, TOC, VS, TS_{cve}, E_{dww}
Spot raw, n=46			
1	51.3	50.1	E_{dr}
1	50.8	49.7	COD
1	41.1	39.8	TS_{cve}
2	89.7	89.2	TS_{cve}, E_{dww}
3	90.8	90.1*	sCOD, TS_{cve}, E_{dww}
4	90.8	90.0	COD, sCOD, TS_{cve}, E_{dr}
All samples, n=107			
1	77.2	77.0	COD
1	68.3	68.0	E_{dww}
1	52.7	52.2	TS_{cve}
2	90.9	90.7	TS_{cve}, E_{dww}
3	91.5	91.2*	COD, TS_{cve}, E_{dww}
4	91.5	91.2	COD, $P\text{-}PO_4^{3-}$, TS_{cve}, E_{dww}
5	91.5	91.1	COD, sCOD, $P\text{-}PO_4^{3-}$, TS_{cve}, E_{dww}

*: The regression with highest r^2_{adj} but as few variables as possible

For both the composite raw and composite of all samples, the r^2 of all the single or multiple regression analyses varies within a narrow range 88.9%-92.1% and 92.9%-95.3%, respectively. For the composite raw, the r^2 of the regression determined solely by COD, pCOD or TOC with $E_{ww,}$ of the composite raw samples are all above 80.0 % ($p<0.05$). For all composite samples

the r^2 values for the regression of COD, pCOD or TOC with E_{ww} are over 90% in all cases ($p<0.05$).

In both cases of the spot raw and all samples, the best regression comprises the TS_{cve} and E_{dww}. In fact, E_{ww} is calculated by multiplying TS_{cve} and E_{dww} together. If both TS_{cve} and E_{dww} are known, there is no need to use regression to estimate E_{ww}. For both sample groups, regressions determined solely by COD still result in the strongest single variable regressions.

Regression based solely on COD always ranks in the top 2 of single variable regressions for each sample group, and the r^2 of regression determined by pCOD or TOC of the composite samples is always greater than 90%. Hence, COD is selected to plot against the E_{ww} of different sample groups, and pCOD and TOC are chosen to plot against the E_{ww} of the composite samples. The plot, regression line (red solid line), the confidence interval (green dash line) and the prediction interval (purple dash line) of each individual regression are shown in Figure 4-1. The regression equations of each individual regression are listed in Table 4-3. It is worth noting that the Minitab 18 can only display the confidence interval and prediction interval on regressions has intercept in its regression equation. However, in 5 out of 6 cases shown in Figure 4-1, the intercept is not statistically significant ($p>0.05$) and can be potentially removed from the regression equation (Minitab Blog Editor, 2013). Thus, the regression equation with no intercept is also worked out and listed in the Table 4-3. Although the regression with no intercept has a higher r^2 than the regression with intercept does, That is because of the r^2 is calculated differently and it does not mean the quality of the former is better than the latter (Minitab Inc., 2017a).

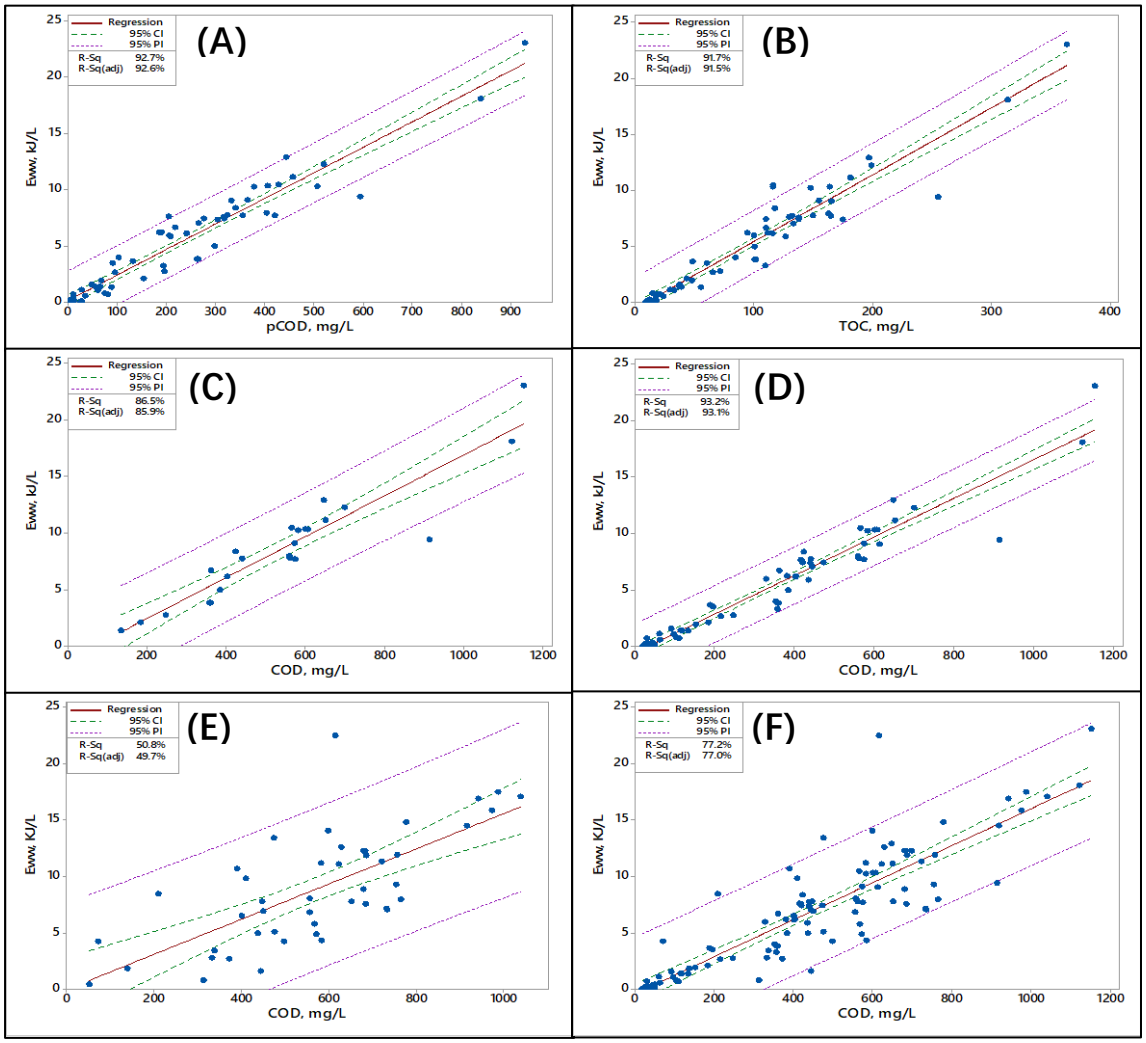

Figure 4-1 Plots of E_{ww} of different sample groups against COD, pCOD or TOC. (A) E_{ww} of Composite Samples against pCOD, (B) E_{ww} of Composite Samples against TOC, (C) E_{ww} of Composite Raw against COD, (D) E_{ww} of Composite Samples against COD; (E) E_{ww} of Spot Raw against COD, and (F) E_{ww} of All Samples against COD

Table 4-3 Regression equations of regressions between E_{ww} and pCOD, TOC and COD shown in Figure 4-1

	n	Regression Equation with intercept*	Regression Equation without intercept*
Figure 4-1 (A)	60	E_{ww}=0.172+0.0227 pCOD(r^2=92.7%)	E_{ww}=0.0231 pCOD (r^2=96.7%)
Figure 4-1 (B)	61	E_{ww}= -0.560+0.0599 TOC(r^2=91.7%)	E_{ww}=0.0562 TOC (r^2=96.0%)
Figure 4-1 (C)	24	E_{ww}= -1.149+0.0181 COD(r^2=86.5%)	E_{ww}=0.0163 COD (r^2=96.6%)
Figure 4-1 (D)	61	E_{ww}= -0.549+0.0171 COD(r^2=93.2%)**	E_{ww}=0.0161 COD (r^2=96.7%)
Figure 4-1 (E)	46	E_{ww}= 0.02+0.0155 COD(r^2=50.9%)	E_{ww}=0.0156 COD (r^2=88.5%)
Figure 4-1 (F)	107	E_{ww}= -0.382+0.0164 COD(r^2=77.2%)	E_{ww}=0.0158 COD (r^2=91.6%)

*: E_{ww} is unit of kJ/L. pCOD, TOC and COD are in unit of mg/L.
**: The intercept of the regression equation is found statistically significant.

In Figure 4-1 the sample sizes of the 6 datasets shown vary from 24 to 107, compared to a sample size of only 19 in the work of Korth et al (2017). Moreover, apart from the regression determined by COD for the spot raw sample (Figure 4-1 (C)), the r^2 of the regression models shown in Table 4-3 are also stronger than those reported for the COD (n=14, r^2=65%) and TOC (n=19, r^2=66%) models in Korth et al. (2017). Since the univariate regressions determined by the single variables of COD, pCOD or TOC are almost as strong as the multivariate regression, using these individual variables appears to be a very reliable means of estimating the inflowing chemical energy to a WWTP.

The regression equations shown in bottom 4 rows of Table 4-3 indicate the numerical relationship between the E_{ww} and COD. Because the E_{ww} is in unit of kJ/L and the COD is in unit of mg COD/L, the slope will be in unit of kJ/mg COD. If the slope is simply considered as how many kJ of chemical energy is contained in 1 mg of COD, then the measured values are likely to be smaller than the actual value because approximately 15% of the COD is lost during the centrifugal drying process. Nevertheless, the slope of the regression equation with no intercept (from 15.6-16.3 kJ/g COD) still indicates a greater energy per gram of COD than is present in a selection of organic compounds commonly found in municipal wastewaters (Table 4-4) (Huang et al., 2010). The rest of the content of this Section 4.1.3 will discuss the cause of this difference.

Table 4-4. Common organic compounds and their calculated energy values

Compounds[a]	**Type**	**Formula**	**ΔH/gCOD**[b]
Glutamic	Proteins	$C_5H_9NO_4$	13.4
Aspartic		$C_4H_7NO_4$	13.3
Glucose	Sugars	$C_6H_{12}O_6$	14.6
Xylose		$C_5H_{10}O_5$	14.7
Acetic acid	Volatile Fatty Acids	CH_3COOH	13.6
Butyric Acid		$CH_3CH_2CH_2COOH$	13.6
Fulvics	Humic substances	$C_{33}H_{32}O_{19}$	15.7
Humics		$C_{34}H_{34}O_{16}N_2$	11.6-14.5
Cellulose	Others	$(C_6H_{12}O_6)_n$	14.6
Lignin		$(C_9H_{10}O_2)_n$, $(C_{10}H_{12}O_3)_n$ or $(C_{11}H_{14}O_4)_n$	14.1

[a]A selection of different compound types selected, but all have been shown to be present at high concentration in municipal wastewater by Huang et al. (2010).
[b]ΔH/gCOD is calculated from deoxygenation enthalpy values presented by Sato (1990), except for Fulvics which is based on data in Reddy et al. (1989). Values for energy content of additional organic compounds can be found in Heidrich et al. (2010).

In principle, the kJ/g COD can be calculated via the Equation 4-1.

Equation 4-1

$$kJ/g\ COD\ = \frac{E_{ww}}{COD}$$

Where $\boldsymbol{E_{ww}}$ (kJ/L) is the chemical energy of a wastewater and $\boldsymbol{COD}$ (g/L) is the COD concentration of that wastewater.

There are three main issues that might compromise the accuracy of the determination of the kJ/g COD value:

A. Whether the bomb calorimeter is able to combust all the energy-containing substances
B. Whether the dichromate method of COD analysis is able to oxidize all the substances that contribute energy and
C. How much of the substances that contribute to energy is lost during the drying process.

The quite a few common organic compounds listed in Table 4-3 have been measured for their calorific value via bomb calorimetry, for instance, Shizas and Bagley (2004) measured glucose, Evans and Skinner (1959) measured the acetic acid, Ribeiro da Silva et al. (2013) measured cellulose, Colbert et al. (1981) measured cellulose, Tsuzuki and Hunt (1957) and (Tsuzuki and Hunt, 1957) measured aspartic acid and glutamic acid. In those studies, the measured caloric values of the tested substances well match those substances' standard enthalpy of combustion since the difference between the two is less than 5% (Shizas and Bagley, 2004, Colbert et al., 1981, Evans and Skinner, 1959, Ribeiro da Silva et al., 2013, Wu Yang et al., 1999). This indicates the bomb calorimeter is able to fully combust those substances in the wastewater and deliver a reliable calorific value.

Regarding the second issue that may compromise accuracy (B), in this research the COD was tested using the dichromate method, in which the contaminants are oxidized in a solution rich in the dichromate ion ($Cr_2O_7^{2-}$) (APHA, 2012). During the reaction, the oxidant $Cr_2O_7^{2-}$ is reduced to Cr^{3+}, which results in a color change in the solution (APHA, 2012). Subsequently, the quantification of the extent of the color change indicates the COD concentration of a sample (APHA, 2012). But the dichromate is unable to fully oxidize every oxidizable substance, and yet some of these oxidizable substances can contribute chemical energy (APHA, 2012, Li et al., 2012, Boyles, 1991). In this sense, the COD measured by the dichromate method may be

lower than the theoretical COD of a sample completely oxidized via combustion. This could therefore result in an erroneously high value of kJ/g COD.

The substances that contain energy but are resistant to $Cr_2O_7^{2-}$ oxidation include benzene, toluene, pyridine, ammonia and its derivatives (considered as the TKN). (Li et al., 2012, Scherson and Criddle, 2014, Boyles, 1991). The contribution of these substances to the total E_{ww} varies. Although the calorific value of benzene, toluene and pyridine can be up to two times greater than that of TKN, their combined contribution is actually less than 1% because of their low concentrations in wastewater (Huang et al., 2010, Li et al., 2012, Thornton et al., 2001, Zalat and Elsayed, 2013). Consequently their contribution to energy is less than one tenth of the energy contained in TKN (shown in Table 4-5). Scherson and Criddle (2014) suggested that approximately 15% of chemical energy in raw wastewater is from TKN. Hence, this research considers that the energy contributed from the unmeasurable COD is mainly from TKN. Total wastewater energy content is considered to come mainly from TKN and the measurable COD.

Table 4-5 Chemical energy contributed by commonly found substances unaccounted for in the COD measurement

	Concentration in raw wastewater, mg/L[a]	**Calorific value, kJ/g[b]**	**Chemical Energy, kJ**	**Proportion to the total E_{ww}, %[c]**
Benzene	0.2	41.8	0.01	0.1%
Toluene	0.6	42.4	0.03	0.3%
Pyridine	1.0	33.5	0.03	0.4%
NH_4^+-N [c]	27.2	22.5	0.61	7.0%
TKN [c]	40.77	22.5	0.92	10.6%

[a] For benzene and toluene, the listed value is the reported in Thornton et al. (2001). For Pyridine, the listed value is based on data reported in Zalat and Elsayed (2013). For N-NH_4^+ and TKN, the listed values are the mean concentration of the composite raw.
[b] The caloric value is calculated by dividing the enthalpy of combustion by the molar weight (NIH, 2018b, NIH, 2018a, NIST, 2018b, NIST, 2018a).
[c] The proportion is calculated by diving the chemical energy by the mean E_{ww} of the composite raw (listed in Table 4-2).

Ammonia is volatile and is likely to be evaporated during the drying process along with other volatile compounds that contribute to COD (Maurer and Müller, 2012, Huett, 1997). Hence, its contribution to the subsequent energy measurement will be cancelled. But the nitrogen containing protein may still stay in the dried residue after evaporation (Singh, 2007). The exact

amount of NH_4^+-N and TKN that remained in the dried residue was not determined as part of this research. Hence, it was not possible to calculate the exact energy contributed by the NH_4^+-N and TKN compared to that contributed by the measurable COD. In this sense, the slope no longer indicates how many kJ of chemical energy is contained in a gram of COD but just the empirical mathematical relationship between COD and E_{ww}. Based on the regression determined in the Figure 4-1, the E_{ww} of wastewater can be estimated via Equation 4-2 which is the regression equation from plotting E_{ww} of All Samples against COD .

Equation 4-2

$$E_{ww} = COD \times 0.0158 \text{ kJ/mg}$$

where ***COD*** is the chemical oxygen demand of a wastewater and is in unit of mg/L.

Fundamentally, to measure the chemical energy content of wastewater it is necessary is calculate the product of the concentration and heating value of each energy-containing chemical within the wastewater, and then sum the products for all such chemicals in the wastewater. This would be particularly useful for the purposes of energy audits and decision-making regarding selection and implementation of energy recovery technologies. Taking a lignin-rich wastewater as an example, mechanical separation and subsequent recovery would be a better option than anaerobic treatment which is less efficient at breaking down lignin (Stoica et al., 2009). However, wastewater is a mixed waste and the number of individual compounds it contains could be measurable in hundreds or thousands (Huang et al., 2010). It is likely that the composition of the energy-containing chemicals are site-specific (Heidrich et al., 2010). Therefore, the work required for understanding the concentration and heating value of each energy-containing chemical would be substantial and does not tend to be practical, or cost-effective, for a general energy audit of numerous WWTPs or for initial technical feasibility assessment of a particular technology. But the regression equations derived as part of this research, which are determined from various types of samples collected from four WWTPs of varied population equivalents and locations, indicates that a reliable determination of energy content can be derived from the COD alone, which is quickly and cost-effectively determined.

4.1.4 The impact from diurnal variation to the chemical energy in wastewater

The diurnal variation of influent wastewater quality has a direct bearing on the relationship between E_{ww} and COD. As shown in Figure 4-1 (F), the inclusion of spot raw sample data in

the regression does not result in any substantial change in the relationship (i.e the slope of the regression line) between E_{ww} and COD. However, Figure 4-1(E) shows that the regression plots using spot raw water sample data only has more scatter than those regressions using composite sample data. This research did not perform a detailed study of the variance of organic load of the spot raw wastewater samples, but the ratio between pCOD and COD of each spot and composite raw sample have been analyzed. Although there is no statistical difference between the mean value of the pCOD:COD ratio of all spot raw samples compared to all the composite raw samples (p=0.308), there is significant difference in the variance (Levene test, p>0.05) (Minitab Inc., 2017c). Individual value plots of two groups of data is shown Figure 4-2. Diurnal variability is considered to be the cause of the greater scatter in the regressions involving spot raw analyses only, but further investigation of the exact reasons for this variation of chemical composition is recommended.

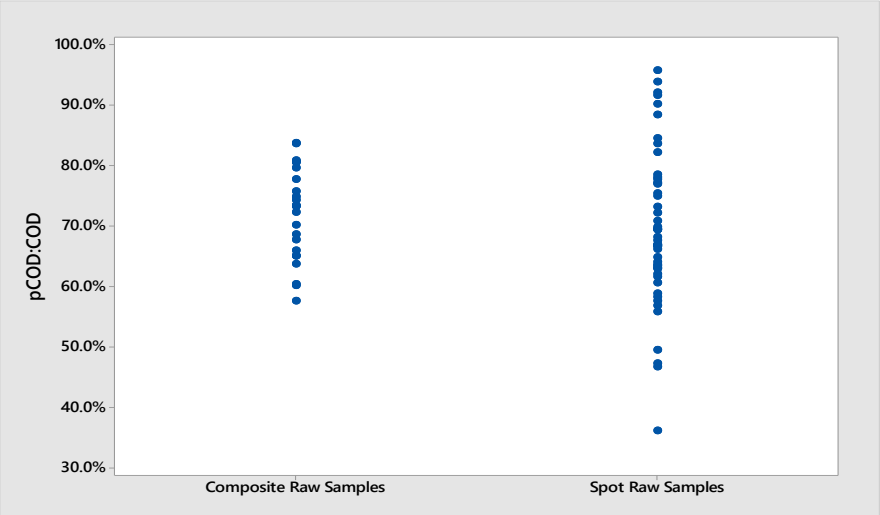

Figure 4-2 Individual value plot of pCOD:COD of Composite Raw and Spot Raw

Apart from influencing the determination of relationship between E_{ww} and COD, the diurnal variation also impacts the chemical loading to the WWTPs. The hourly chemical energy loading to WWTP A and WWTP C were investigated as part of this research. These plants have population equivalents of 40,000 and 1,000,000, respectively. The hourly flow, COD and energy loading to WWTPs A and C are shown in Figure 4-3.

For those hourly samples for which E_{ww} was not directly measured, it was estimated via Equation 4-2 i.e. by multiplying the hourly flow by COD (mg/L) and by 0.0158 kJ/mg COD (shown in Table 4-3, row 6)

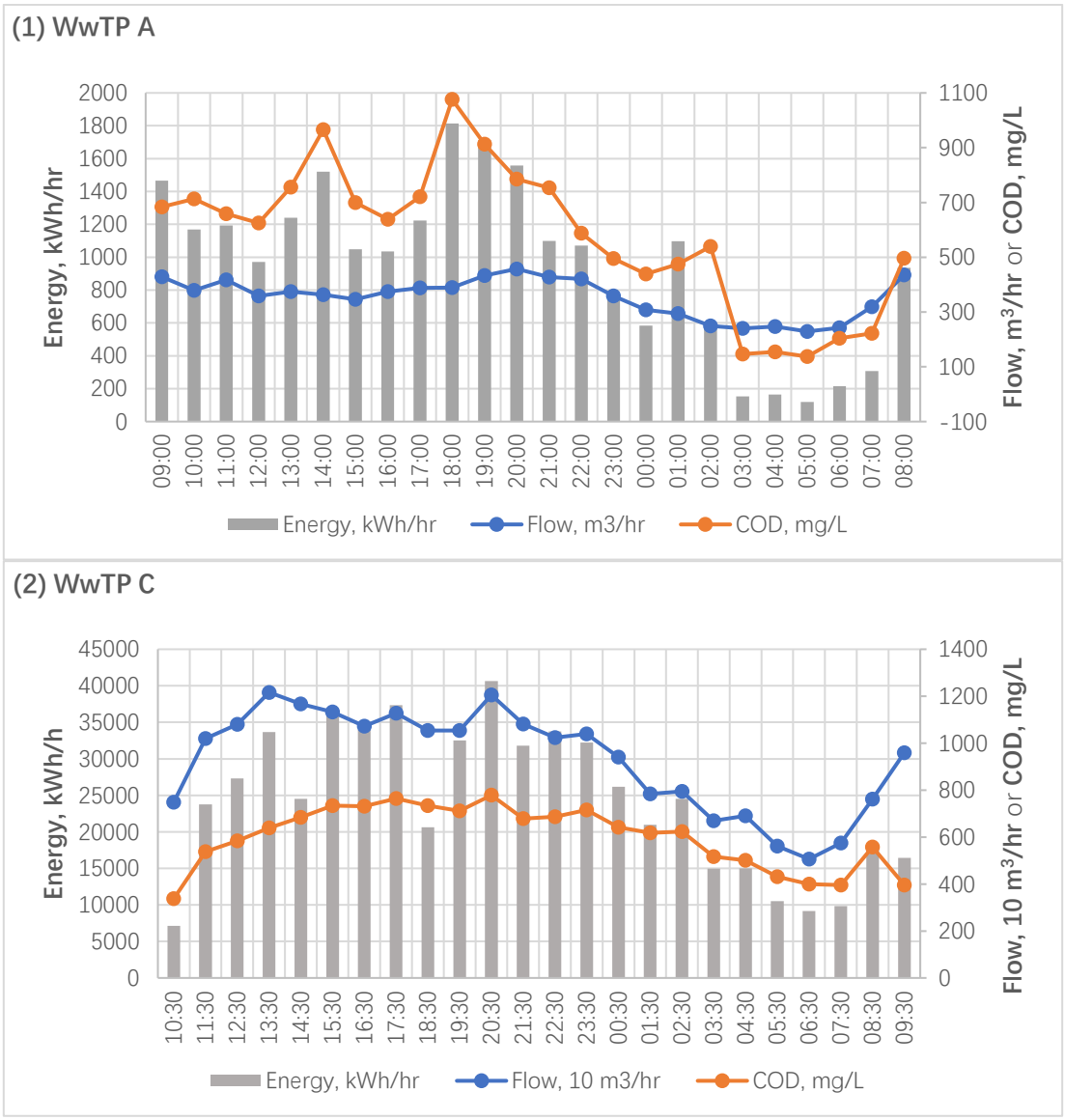

Figure 4-3 The hourly flow, COD and energy loading to the WWTP A and C

The pattern of hourly energy loading to the WWTPs is site specific. In terms of the hourly flowrate, variation is similar for the two sites; using the ratio of maximum flow to minimum flow as a metric, 2.0 for WWTP A and 2.4 for WWTP C. But WWTP A has a greater diurnal variation of COD concentration, as its ration maximum to minimum COD is 7.8, while for WWTP C it is only 2.3. This phenomenon matches the reported finding that the diurnal variation of COD can be large in small treatment works (Raboni et al., 2013). For the hourly

energy loading, the maximum to minimum ratio is 15.2 for WWTP A and 5.7 for WWTP C. Hence, at smaller sites it can tentatively be concluded that there will be greater variability in energy load.

There is an increasing need to recover energy from wastewater (Scherson and Criddle, 2014, Wan et al., 2016). COD is not only an indicator of the E_{ww} of municipal wastewater but also one of the decisive factors determining the feasibility of an energy recovering technology. Stoll et al. (2018) report that microbial fuel cells (MFCs) will only be energy neutral or energy positive if the inflowing COD concentration is high enough and if there is high enough removal of COD. The diurnal fluctuation of COD is therefore likely to affect the energy balance of the MFC (Stoll et al., 2018). To recover energy effectively a successive technology should be able to convert the COD into an energy product efficiently and be able to adapt to the diurnal variation of both loading and types of COD. Therefore, more work should be done to understand the diurnal fluctuations of COD and energy loading and the variation of types of COD or energy material flows to the WWTP.

4.2 Chemical energy of sludge

4.2.1 Sludge Characteristic

Summary statistics for TS%, VS/TS%, TOC/TS%, TN/TS%, TP/TS%, and the chemical energy content of the sludge of all four study sites are shown in Table 4-6.

To begin with the primary sludge and Surplus Activated Sludge (SAS) as secondary sludge generated from 4 WWTPs are compared. Although the primary sludge produced in WWTP A and WWTP D both contain SAS which gets recirculated from the final clarifiers to the primary settlement for co-settling, there is no statistical difference (two Sample T test, $p>0.05$) in chemical energy content of dried sludge (E_{ds}, kJ/g) of primary sludge and SAS between the four WWTPs.

WWTP B and WWTP C are both district sludge thickening and dewatering centers and have mechanical sludge thickening and dewatering treatment comprising drum thickening and

centrifugal dewatering. WWTP C also uses thermal treatment via CAMBI thermal hydrolysis, and biological sludge processing using anaerobic digestion. The E_{ds} of the sludge before and after each sludge treatment process was studied in this research. There is no significant difference ($p>0.05$) in E_{ds} of the sludges before and after the mechanical and thermal-chemical treatment. But the E_{ds} of the sludge fed to the digester is significantly higher than the energy content of digested sludge. The same applies to VS/TS% and TOC/TS%. Therefore, anaerobic digestion appears to be lowering the E_{ds} of the sludge. The mean value of the energy content of the dried and wet sludges and TS%, VS/TS%, TOC/TS%, TN/TS% and TP/TS% of the sludge collected are shown in Table 4-6.

Table 4-6 The mean value (± standard deviation) of TS%, VS/TS%, TOC/TS%, TN/TS%, TP/TS% and chemical energy content of the dried sludge and wet sludge

Type	*n*	*TS%*	*VS/TS%*	*TOC/TS%*	*TN/TS%*	*TP/TS%*	*E_{ds}, kJ/g**	*E_s, kJ/kg***
Primary Sludge	20	3.3±0.7 %	82.6±3.5 %	42.6±3.1 %	3.2±0.6 %	1.2±0.3 %	16.8±1.2	563.8±124.8
Thickened Primary Sludge	5	5.8±1.0 %	81.5±2.5 %	40.8±1.7 %	2.9±0.5 %	1.0±0.2 %	16.5±0.9	950.2±135.6
SAS	20	0.5±0.2 %	78.2±5.1 %	31.6±2.9 %	6.2±0.5 %	2.2±0.8 %	16.4±1.1	72.9±31.5
Thickened SAS	10	3.9±1.2 %	83.2±1.4 %	38.5±2.6 %	6.7±0.5 %	2.7±0.6 %	18.1±0.5	714.2±226.4
Stored Sludge	10	3.6±0.7%	78.3±6.1 %	38.9±3.3 %	4.6±0.8 %	1.6±0.1 %	17.3±1.4	620.6±120.9
Dewatered Stored Sludge	10	23.5±2.0 %	82.9±1.6 %	41.3±2.7 %	3.7±0.4 %	1.3±0.2 %	18.2±0.5	4266.0±367.0
THP Feed	5	15.7±1.3 %	82.0±1.0 %	39.9±0.7 %	3.2±1.1 %	1.8±1.1 %	18.1±0.9	2861.0±322.0
Digester Feed	5	10.3±0.9 %	82.2±1.2 %	42.2±1.3 %	4.1±0.5 %	1.1±0.1 %	18.6±0.8	1921.0±212.4
Digested Sludge	5	5.3±0.4 %	67.8±1.6 %	35.5±1.1 %	8.6±1.4 %	2.1±0.3 %	15.6±0.7	824.0±90.1
Dewatered Digested Sludge	5	28.5±3.4 %	70.1±7.7 %	34.8±1.1 %	5.2±0.2 %	1.8±0.0 %	15.2±0.3	4322.0±485.0

*: E_{ds} is the acronym of chemical energy content of dried sludge

**: E_s is the acronym of the chemical energy content of the wet sludge

4.2.2 The relationship between solids and chemical energy content of sludge

As with the study of E_{ww}, surrogates that could be used to reliably indicate sludge energy content were evaluated. The weight to weight (w/w) concentration to the total solid content, such as VS/TS%, TOC/TS%, and the weight to volume (w/v) concentration, such as the TS_s, VS_s, are analyzed for their relationship with the chemical energy content of the dried sludge (E_{ds}, kJ/g) and with the chemical energy content of wet sludge (E_s, kJ/L).

In all cases the w/w concentration to the total solid content (i.e. VS/TS%, TN/TS%, etc.) had a weak (<0.50) correlation with both E_{ds} and E_{ws}. All the w/v concentrations to the sludge (in unit mg/L) are found with a weak correlation with the E_{ds}, but with strong correlation (>0.89, $p<0.05$) with the E_s. All the w/v concentrations are found highly correlated with each other (Spearman Rho, >0.900, $p<0.05$). Therefore, the w/v concentrations are selected to proceed the best subset study. The results of the Best Subset study are shown in Table 4-7.

Table 4-7 Best regression for estimating wastewater energy

No. of Predictor	r^2	r^2_{adj}	Parameter Required
1	99.4	99.4	TOC_s
1	99.4	99.4	VS_s
1	98.5	98.5	TS_s
1	83.4	83.2	TN_s
1	80.8	80.6	TP_s
2	99.6	99.6	VS_s, TOC_s
3	99.6	99.6	TS_s, VS_s, TOC_s
4	99.6	99.6	TS_s, VS_s, TOC_s, TN_s, TP_s
5	99.6	99.6	TS_s, VS_s, TOC_s, TN_s

The single variable regressions determined by each w/v concentration to sludge energy has strong linear relationship ($r^2>0.80$, $p<0.05$) with E_s. The r^2 of the best three single variable regressions, determined by TOC%, VS% or TS%, are nearly identical to the r^2 (99.6%) of the best model. Therefore, the single variable regression is already good enough to predict the E_s. The plot, regression line, confidence interval and prediction interval of the regression determined by TOC_s, VS_s or TS_s are shown in Figure 4-4. All the regression shown in Figure 4-4 considered intercept in the regression equation. The determined regression equations with and without intercept are shown in Table 4-8. It is worth noting that the intercept is found not statistically significant ($p>0.05$) in all three cases.

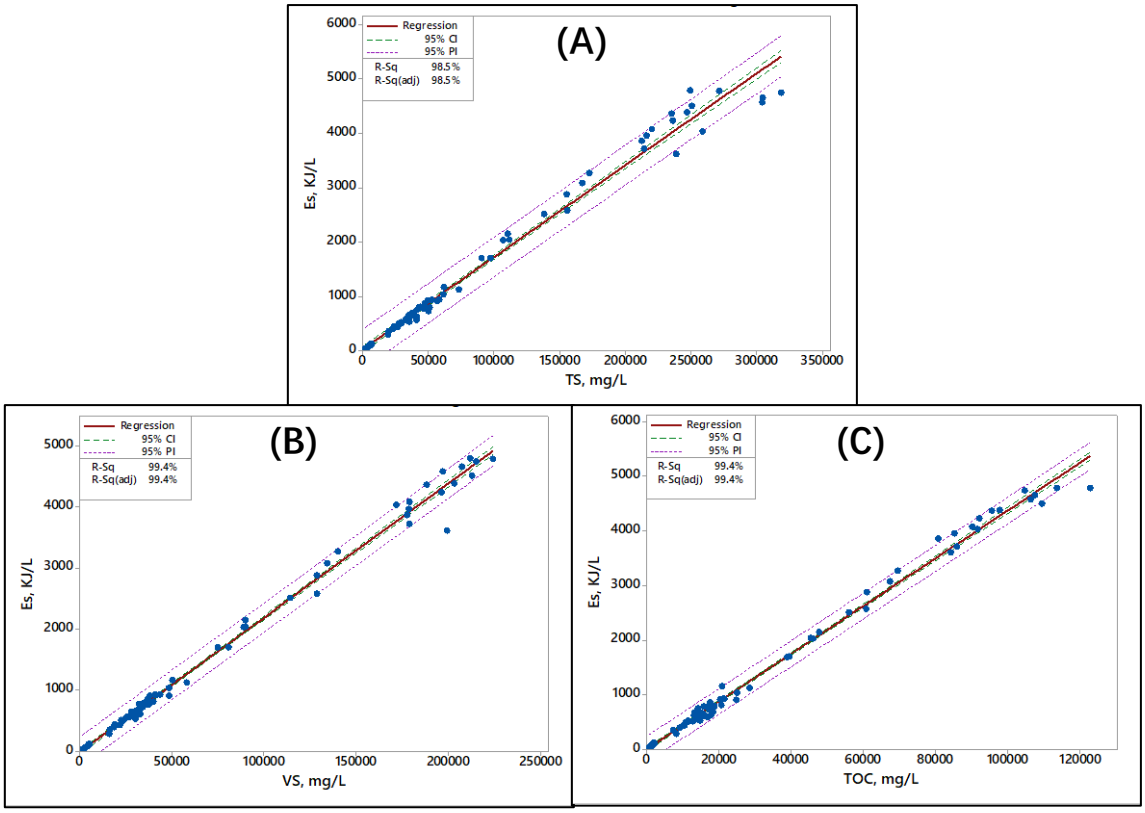

Figure 4-4 Plots of E_s against TS_s, VS_s and TOC_s (A) E_s against TS_s, (B) E_s against VS_s, and (C) E_s against TOC_s

Table 4-8 Regression equations of regressions between E_s and TS_s, VS_s and TOC_s shown in Figure 4-4

	n	Regression Equation with intercept*	Regression Equation without intercept*
Figure 4-4 (A)	87	E_s=23.8+0.0170 TS_s (r^2=98.5%)	E_s= 0.0171 TS_s (r^2=99.2%)
Figure 4-4 (B)	87	E_s=-10.5+0.0220 VS_s (r^2=99.4%)	E_s= 0.0219 VS_s (r^2=99.7%)
Figure 4-4 (C)	87	E_s=2.5+0.0437 TOC_s (r^2=99.4%)	E_s= 0.0438 TOC_s (r^2=99.7%)

*: E_s is in unit of kJ/L. TS, VS and TOC are in unit of mg/L.

Similar to the study of the chemical energy of wastewater, this research aimed to identify a reliable empirical method to quickly estimate the energy content or loading of a sludge using routinely analysed variables such as TS% and VS/TS%, or TS_s and VS_s that are interpreted from TS% and VS/TS%. Figure 4-4 suggests that the E_s can be estimated from TS_s, VS_s and TOC_s. Using the TS_s for estimation would be the simplest and quickest because both the VS_s and TOC_s is measured on top of the measurement of TS_s.

In regression equation shown in Table 4-8, E_s is in unit of kJ/L and TS_s is in unit of g/L, thus the slope should be in unit of kJ/g TS. The slope 17.1 kJ/g TS_s (in Figure 4-4 (A)) is nearly

identical to 17.11±1.33 kJ/g which is the mean value of E_{ds} of all the sludge sample analyzed in this study. It is likely that the calorific value of the dried sludge, the E_{ds}, determines the slope. However, E_{ds} values from literatures are substantially varied, as shown in Table 4-9. The mean E_{ds} values determined by Shizas and Bagley (2004) and Schaum et al. (2016) are significantly smaller (Two Sample T Test, $p<0.05$) than the mean E_{ds} found in this research. Thus, there may be risks of errors associated with using 17.10 kJ/g TS_s to evaluate the E_s.

Table 4-9 Energy related characteristic of sludge reported in literature

	Primary Sludge			**SAS**			**Digested Sludge**		
	E_{ds}, kJ/g	VS/TS%, %	kJ/g VS	E_{ds}, kJ/g	VS/TS%, %	kJ/g VS	E_{ds}, kJ/g	VS/TS%, %	kJ/g VS
Shizas and Bagley (2004)	15.90	67.00	23.73	12.40	60.00	20.66	12.70	51.00	24.90
Schaum et al. (2016)	16.40	78.00	21.02	14.30	69.00	20.72	11.10	59.00	18.81

By dividing the E_{ds} with VS/TS%, kJ/g VS is obtained and illustrates how many kJ of energy is contained in a gram of VS. There is no significant difference (Two Sample T test, $p>0.05$) between the mean kJ/g VS found in this study and that found by Shizas and Bagley (2004) and Schaum et al. (2016). Moreover, the mean value of kJ/g VS of this study is 21.48 kJ/g. It is also nearly identical to 21.89 kJ/g VS which is the slope of the regression equation determined by VS_s (shown in Figure 4-4 (B)). Therefore, E_s can be estimated from VS_s using a value of 21.9 kJ/g VS and Equation 4-3.

Equation 4-3

$$E_s = VS_s \times 21.9 = TS_s \times VS/TS\% \times 21.9$$

The major components in the sludge are the carbohydrate-lignin organic compounds, such as cellulose, hemicellulose and lignin (Ogilvie, 1998). Considering they can be fully combusted, their caloric values are the same as their kJ/g VS values, which are 16.5 kJ/g for cellulose, 13.9 kJ/g for hemicellulose, and 20.7 kJ/g for lignin (Kim et al., 2017). Although they are lower than the value of 21.48 kJ/g VS, sludges also contains substances with higher caloric values such as the grease (Ogilvie, 1998). The grease can consist of Myristic Acid, Palmitic Acid, Stearic Acid, Oleic Acid and Linoleic Acid (Dong, 2015). Their calorific values range from 37

to 40 kJ/g (Demirbas, 2016). Therefore, estimated E_s via Equation 4-4 appears to be a reasonable approach.

Current practice is mainly to recover energy from wastewater via anaerobic digestion of sludge. Maximizing the sludge production from wastewater treatment is one of the measures to improve the energy recovery and energy efficiency of a WWTP (Wan et al., 2016). Via Equation 4-1 and 4-4, researchers and operators can quickly estimate the energy flux of a treatment process or a treatment work using the routinely measured parameters of COD and VS/TS%. This will help identifying potential opportunities for maximizing sludge production and discovering potential opportunities for energy recovery.

4.2.3 The relationship between COD and chemical energy content of sludge

Although the E_S can be estimated via VS_s, there is still difficulty in applying modelling to construct the chemical energy balance, since VS_s is not able to predict in the modelling software GPS-X. Thus, a relationship between the VS_s and the COD in the sludge has to be defined.

By definition, the COD of the sludge is contributed from the VS (as shown in Figure 4-5) (Foladori et al., 2010). The VS_s of the sludge, which consists of both pCOD and sCOD, is originally from the wastewater. If in the wastewater there is a strong relationship between COD and VS, this relationship will possibly pass on to the sludge. Subsequently, the relationship of COD and E_s can be determined.

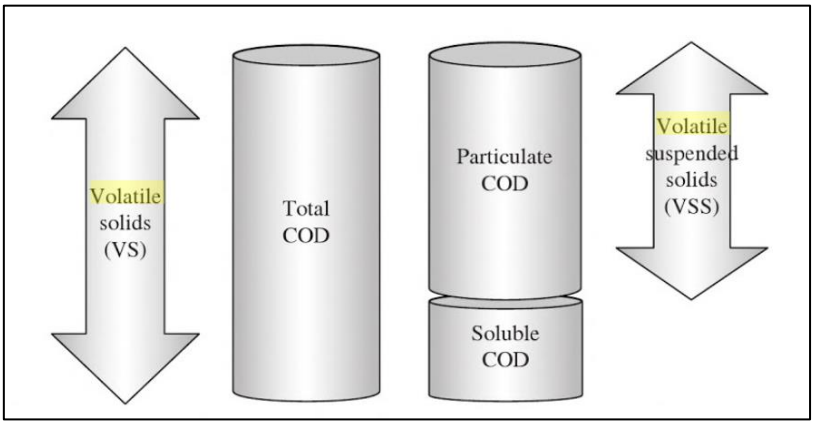

Figure 4-5 Physico-chemical fractionation of total COD in the sludge (Foladori et al., 2010)

The composite samples are used for this investigation since both COD and VS are measured on them. The statistical analysis suggests that there is a strong linear relationship (n=61, r^2=92.13%, p<0.05) between the two as shown in Figure 4-6.

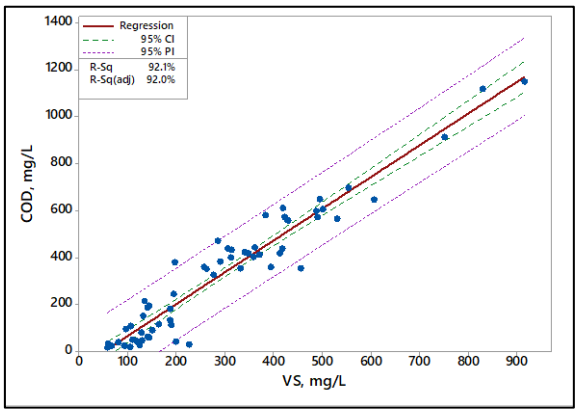

Figure 4-6 The relationship between COD and VS in wastewater

In the wastewater, COD (mg/L) can be estimated via VS (mg/L) via Equation 4-4

Equation 4-4

$$\mathrm{COD} = -66.5 + 1.3526\ \mathrm{VS}$$

The study then applied Equation 4-4 to estimate the sludge COD. The estimated sludge COD is found having a strong linear relationship (r^2=99.66, p<0.05) with the sludge energy E_s (kJ/L), as shown in Figure 4-7. The regression equation determined are E_s= -9.5+0.0162 COD or E_s= 0.0162 COD. The slope 0.0162 falls the range of 0.0156 to 0.0171 which are the slope determined for the COD and E_{ww} via different sample groups (shown in Table 4-3). The relationship between the energy content (kJ/L) and COD (mg/L) in both wastewater and sludge are nearly identical. The implication of it is that the chemical energy balance is very likely to be the same as the COD mass balance in the wastewater treatment and in the sludge treatment in this four studied WWTPs. Therefore, this study will use Equation 4-2 to estimate the wastewater and sludge energy and will use the COD mass balance to express the chemical energy balance.

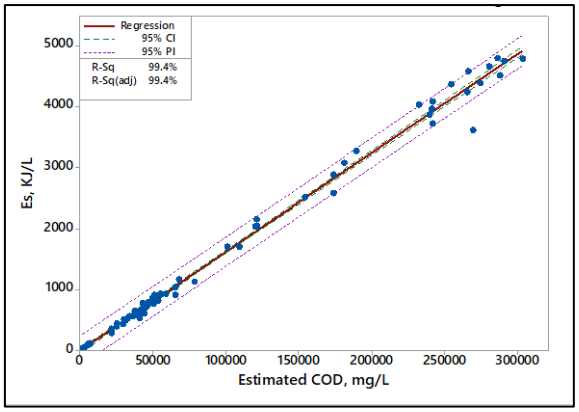

Figure 4-7 The relationship between energy content (kJ/g) and COD in sludge

4.3 Chapter Summary

This research successfully developed a new wastewater drying method that is at least as good as the proven method of freeze drying for retaining the energy-containing material but is a far less time-consuming method.

Subsequently, this research conducted statistical analysis (correlation and Best Subset of regression) to investigate the relationship between E_{ww} and commonly analysed wastewater variables. COD was found to be the best surrogate of energy content of wastewater. It has a ubiquitously (across the four WWTPs) strong linear relationship (77-93%, $p<0.05$, excluding the spot raw) with E_{ww}. Therefore, an empirical equation is proposed for estimating the wastewater energy from COD.

A similar statistical study was also conducted for understanding the relationship between E_s and the other commonly analysed sludge variables. Strong linear relationships (>85%, $p<0.05$) were found between the E_s and TS_s, VS_s or TOC_s. Empirical equations are proposed for estimating the sludge chemical energy from the TS_s and VS_s. Moreover, via assuming the wastewater and sludge share the same relationship between COD and VS, the sludge COD was estimated. Subsequently, the relationship between chemical energy and COD in the sludge is found similar in the wastewater. This implies that chemical energy balance of a WWTP shall follows the COD mass balance.

The research aims to develop a quick but reliable method of estimating wastewater energy content using routinely analyzed variables has been fulfilled. As the energy of wastewater and sludge can be estimated much more quickly as a consequence, an energy audit of a treatment process or a treatment works can now be easily conducted. This will help researchers and operators to better monitor the energy recovery performance and discover potential opportunities for improvement in energy recovery.

Wastewater is a mixture and hence its energy source is from multiple types or groups of chemicals. This research did not investigate the breakdown of the energy contribution from different groups of chemicals as it was not a primary aim of the research. Nevertheless, that is an area recommended for future research because it may help target energy recovery technologies to specific energy containing materials that are not recovered using current methods.

Chapter 5 COD Mass Balance and Energy Balance of Wastewater Treatment Plants

This chapter first presents the calibration and validation of the wastewater and sludge modelling of four WWTPs (Section 5.1). The COD and energy balances of each process are shown in Section 5.2. Based on these balances, in Section 5.3 there is a discussion of the potential for energy recovery from wastewater and sludge. Section 5.4 builds four case studies to examine how energy recovery approaches might impact on the electricity balance of a conceptual WWTP.

5.1 Model calibration and validation

5.1.1 Wastewater and sludge treatment models

5.1.1.1 Wastewater treatment models

Wastewater treatment models were built for WWTP A, WWTP B, WWTP C, and WWTP D. Screen shots of the models are shown in Figure 5-1 to 5-4. In each case the process, the flow diagram represents the actual treatment units at each WWTP, with the exception of the virtual units added for sCOD and PO_4^{3-}-P removal, the virtual unit added for controlling the biological reaction in the settlers, and the simplication of the trickling filter process of WWTP A (explained in Section 3.4.1.2.2).

It is worth noting that in all four WWTPs there is an sCOD decrease of 15 mg/L during primary settlment. This is considered to be due to flocculation and subsequent settling of the sCOD (Gernaey et al., 2001). Thus, a virtual removal unit is added to each wastewater treatment model to ensure this sCOD decrease is reflected in the model.

In WWTP B there is also a decrease of >1.5 mg/L PO_4^{3-}-P during primary treatment. This is thought to be due to sorption of phosphate by iron and subsequent settlement. The elevated iron concentration is thought to be due to mining-related waters entering the WWTP (L Wilkinson, personal communication, 29 October 2018). A virtual PO_4^{3-}-P unit is added to the WWTP B model, prior to its primary settlement, to simulate this.

In the case of WWTPs A and D, biological sludges is recirculated back to the primary settlement. Moreover, their activated sludge process has nitrification and potential denitrification may occurred in final clarification. Thus, the primary settlements and final clarifications of WWTPs A and D are biological reactive. In their model, virtual activated sludge tanks ("Plug Flow Tank" unit) are added to control the biological reaction.

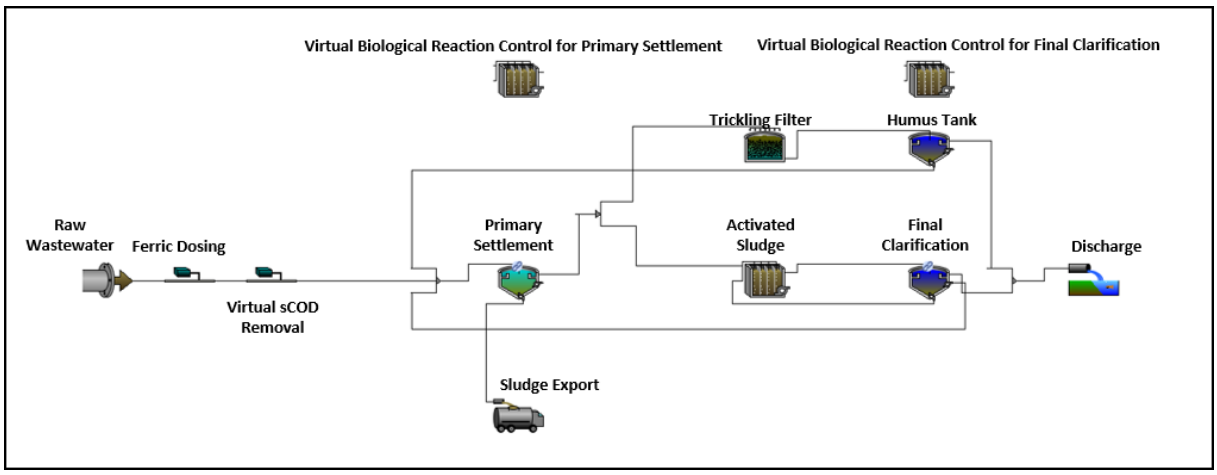

Figure 5-1 The wastewater treatment model of WWTP A

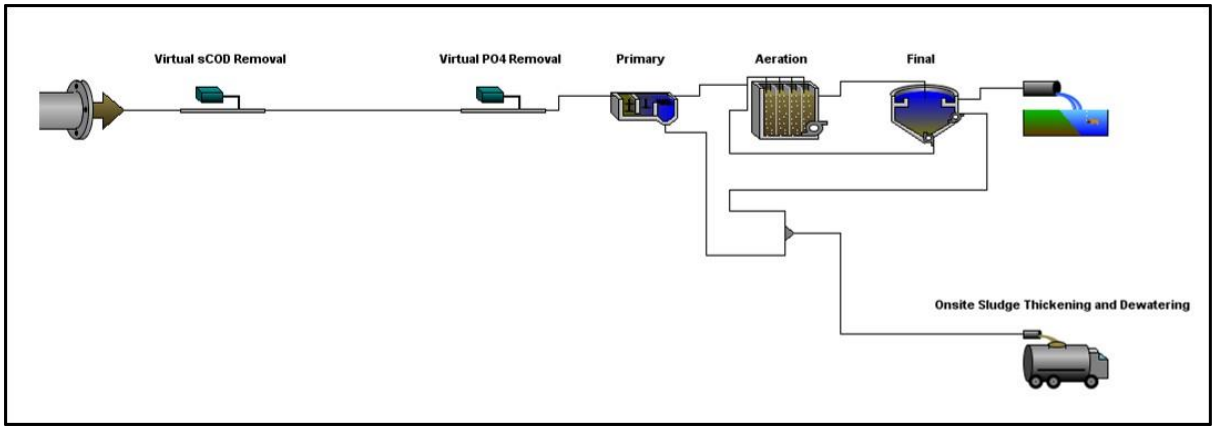

Figure 5-2 The wastewater treatment model of WWTP B

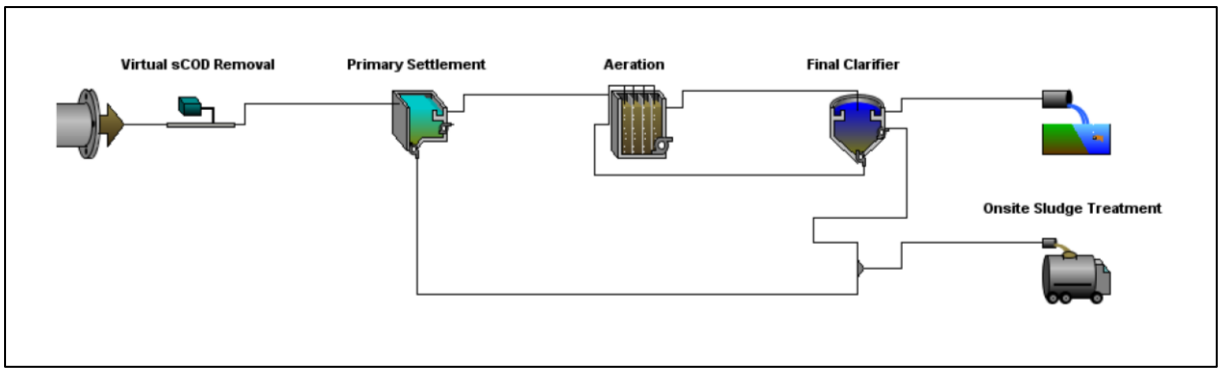

Figure 5-3 The wastewater treatment model of WWTP C

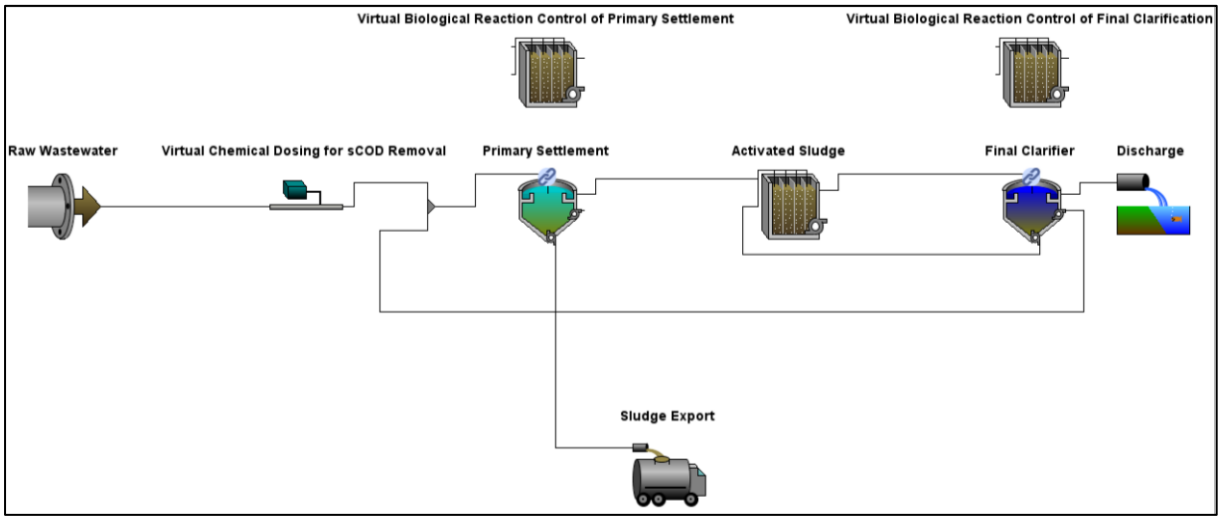

Figure 5-4 The wastewater treatment model of WWTP D

The influent water quality data, and other input variables, used for the modelling of each of the WWTPs are listed in Table 5-1.

Table 5-1 The influent water quality, and other input variables, used for the modelling of each WWTP

Parameter	WWTP A	WWTP B	WWTP C	WWTP D
Flow, m^3/d	9052	49624	278954	37312
COD, mg/L	1061.4	727.1	665.0	336.6
TKN, mg/L	50.9	56.9	55.50	31.8
TP, mg/L	8.5	9.1	10.8	4.0
NH_4^--N, mg/L	30.1	37.7	41.8	19.9
Nitrite-N, mg/L	0.03	0.0	0.00	0.02
Nitrate-N, mg/L	0.23	0.0	0.00	0.28
PO_4^{3-}-P, mg/L	3.8	7.1	6.65	1.50
VSS/TSS	0.83	0.85	0.81	0.78
Soluble inert fraction of total COD (frsi)	0.050	0.050	0.050	0.050
Readily biodegradable fraction of total COD (frss)	0.200	0.200	0.200	0.200
Particulate inert fraction of total COD (frxi)	0.130	0.130	0.130	0.130
Colloidal fraction of slowly biodegradable COD (frscol)	0.014	0.148	0.075	0.161
NH4:sTKN	0.800	0.900	0.800	0.800
N content of soluble inert material (iNSI) , gN/gCOD	0.100	0.050	0.100	0.100
N content of inert particulate inert material (iNXI) , gN/gCOD	0.030	0.030	0.030	0.030
P content of soluble inert material (iPSI) , gN/gCOD	0.005	0.005	0.005	0.005
P content of inert particulate inert material (iPXI) , gN/gCOD	0.005	0.005	0.005	0.005
TOC/COD	0.293	0.323	0.311	0.341

5.1.1.2 Sludge treatment models

Although both WWTPs B and C have sludge thickening and dewatering, because of lack of data of the sludge thickening and dewatering of WWTP B, only the sludge dewatering of WWTP C has been modelled. The sludge thickening and dewatering prior to digestion is built on the wastewater treatment model of WWTP C (Figure 5-3). It is worth noting that 300 m^3 of pure water is virtually added to the raw sludge tank in order to make up the flow of the raw

sludge to approximately 2,300 m^3 that matches the historical data. The anaerobic digestion model is built separately. The sludge treatment models are shown in Figure 5-5 and 5-6.

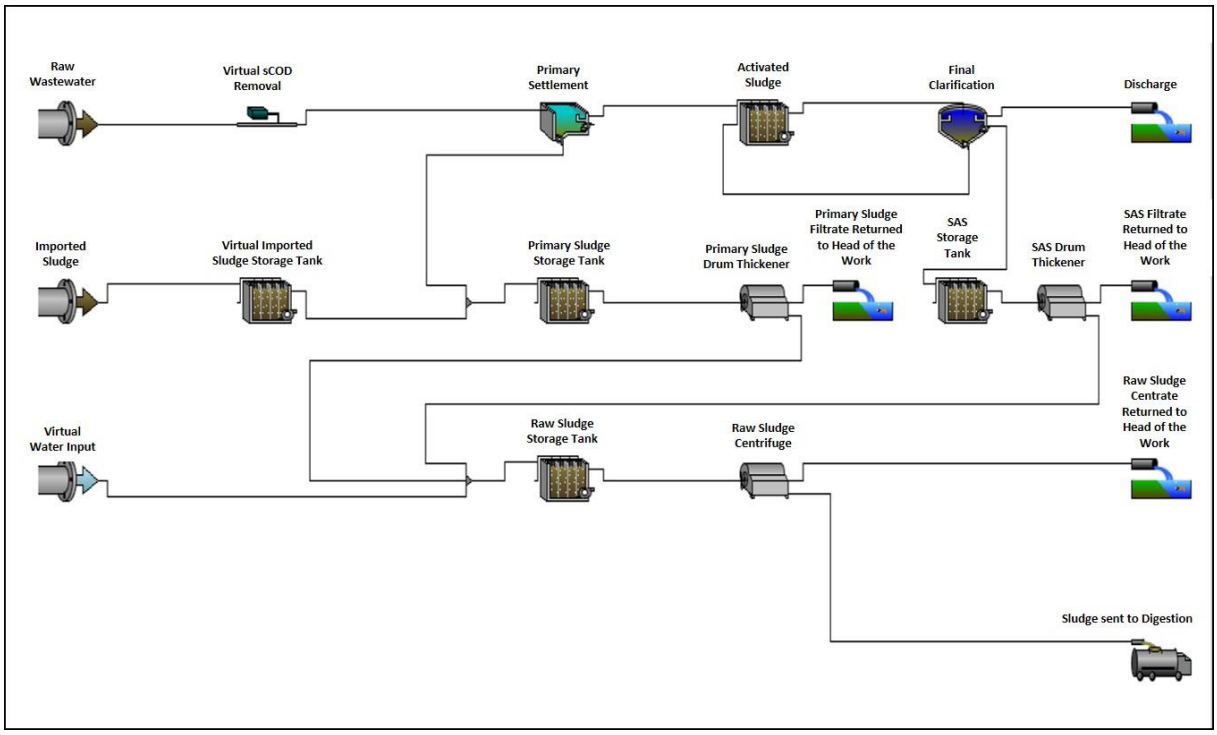

Figure 5-5 The model of WWTP C's wastewater treatment and sludge thickening and dewatering prior to anaerobic digestion

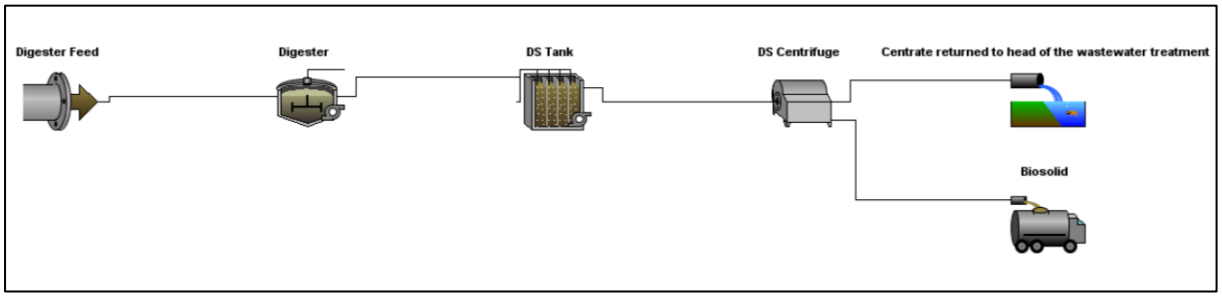

Figure 5-6 The model of WWTP C's anaerobic digestion and the subsequent sludge dewatering

5.1.2 Calibration and validation of the wastewater treatment models

5.1.2.1 Calibration of the wastewater treatment models

In all four WWTPs the *aerobic heterotrophic yield on soluble substrate* always ranks in the top three. That is because it is influential to variety of the targeted variables and the the most important ones found in this study are the flow of SAS, sCOD, PO_4^{3-}-P concentration. This

phenomenon has been identified in previous studies (Cosenza et al., 2014, Sin et al., 2011, Mannina et al., 2011).

The settling parameters of the primary settlers and final clarification are classified as influential. That is because the settling parameters of the primary settler control quantity of slowly biodegradable flows to the activated sludge process and the parameters of the final clarification control the concentration of the pCOD.

Maximum growth rate for ammonia oxidizer and ammonia oxidizer aerobic decay rate were found to be influential to ammonium content of the final effluent (Sin et al., 2011, Cosenza et al., 2014). The modelling of WWTP A, B and D agrees this phenomenon, but not for WWTP C. The reason is that the HRT of WWTP C's activated sludge process is too short to allow ammonium oxidation to happen. Because nitrification occurs in WWTPs A and D, some of the nitrification and denitrification related parameters are found to be influential in these two WWTPs.

However, the parameters controlling phosphate removal by phosphate accumulating organism (PAOs)re rarely ranked in the top 20 or 30. That is because none of the WWTPs have an anaerobic or anoxic section in their activated sludge process (Tchobanoglous et al., 2003). Phosphate removal by PAO therefore rarely happens.

The most important parameters of influent fraction, kinetic and stoichiometric that influence the modelling results, and are therefore subject to adjustment in the model for each WWTP, are listed in the Tables D-1 to D-4 in Appendix D. The table also presents the δ_j^{msqr} (that indicates the influence of the parameter to the entire model), the adjusted value, the order of adjustment, and the category each adjusted parameter belongs to.

5.1.2.2 Validation of wastewater treatment models

For the wastewater treatment modelling, the ARD between the predicted results and the observed results of WWTPs are:

- WWTP A: 28.1%
- WWTP B: 11.3 %
- WWTP C: 3.9%
- WWTP B: 13.8%

The high ARD of WWTP A is due to the predicted NH_4^+-N concentration (0.88 mg/L) is 338% greater than the observed NH_4^+-N concentration (0.22 mg/L). However, Rieger et al. (2012) suggested that it is allowable to have a 1 mg/L difference between the predicted result and the observed result when the concentration is low. In this case, the observed and predicted NH_4^+-N concentration is lower than 1 mg/L and the difference between the two is only 0.68 mg/L which is smaller than the allowable difference. If the NH_4^+-N concentration is excluded, the ARD of WWTP A becomes 10.8%. Then, the ARD of the modelling of all four WWTPs are then no greater than 15%. As shown in Figure 5-7, the observed results well match the model predictions.

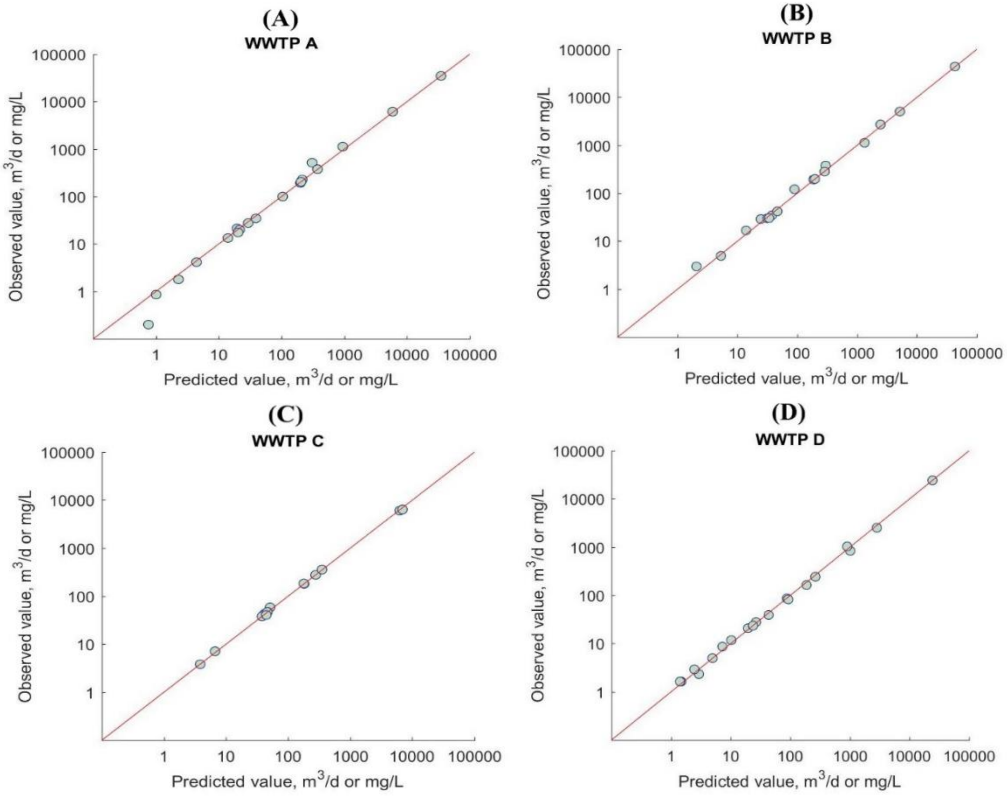

Figure 5-7 Comparison between the observed results and predicted results of the modelling of four WWTPs (A)WWTP A,(B) WWTP B, (C)WWTP C and (D) WWTP D

Hence, the model constructed for the wastewater treatment plants is considered representative of the actual performance and the material mass balance of the WWTPs. The predicted flowrate and concentrations are therefore used in the mass and energy balance calculations for the WWTPs in this chapter and in Chapter 6.

The observed and predicted result of the wastewater modelling are shown in Table E-1 in Appendix E.

5.1.3 Calibration and validation of the sludge treatment models

5.1.3.1 Calibration of the sludge treatment models prior to anaerobic digestion

In the sludge storage, thickening and dewatering prior to the digestion, the following factors are found to be most influential on the biological reactions of the sludge storage tank: yield of fermentative biomass, aerobic heterotrophic decay rate, anaerobic reduction factor for decay rate (in Heterotrophic Biomass section of the biological model), hydrolysis rate constant for xs, saturation coefficient for particulate COD, anaerobic reduction factor for decay rate (in Heterotrophic Biomass section of the biological model). These factors are influential because the majority of the reactive biomass within the sludge is heterotrophic biomass. They affect the solubilization of the particulate substrate and ultimately impact the soluble component of sCOD, ammonium and phosphate of the filtrate and centrate.

For the thickening and dewatering, the parameter fraction of influent flow of the sludge thickening and dewatering is always found to be influential as it affects the TS content of the thickened or dewatered sludge. The removal efficiency of slowly biodegradable substrate, inert particulate material and heterotrophic biomass (particularly in the SAS thickening) are found to be influential on the modelling results, especially to the pCOD content in the filtrate and centrate. The removal efficiency of nitrogen in slowly biodegradable substrate and phosphorus in slowly biodegradable substrate mainly impacts on the TP and TN content of the thickened and dewatered sludge and the TKN content of the filtrate and centrate.

The parameters of kinetic and stoichiometric parameters that influence the biological modelling results of the sludge storage and sludge thickening and dewatering processes prior to digestion,

and are therefore subject to adjustment in the model for each WWTP, are listed in the Tables D-5 to D-7 in Appendix D. The table also presents the adjusted value and the category those adjusted parameter belongs to.

5.1.3.2 Calibration of the sludge treatment models of anaerobic digestion and the subsequent sludge dewatering

In the modelling of the anaerobic digestion and its subsequent dewatering, the particulate inert fraction of total COD and yield of fermentative biomass is found to be influential on the extent of the digestion and the volume of biogas produced. The C content of inert particulate material and of the slowly biodegradable substrate are influential to the ratio of CO_2 and CH_4 in the biogas (Hydromantis, 2015).

For the digested sludge centrate, N and P content of the inert particulate material influences the amount of N and P in the particulate biodegradable substrate which can be digested and release ammonium and phosphate. Therefore, these two fractions are influential to the ammonium and phosphate content of the centrate. The fraction of inert COD during slow biodegradable organic hydrolysis affects the production of inert sCOD and influences the sCOD concentration in the centrate.

Like sludge dewatering, the fraction of influent flow and removal efficiency of particulate inert material of the sludge dewatering unit are influential the solids content of the dewatered sludge and the pCOD concentration of the filtrate and centrate. Unlike the sludge thickening and dewatering prior to digestion, the wet digested sludge is rich in unbiodegradable cells and biomass related to the digestion process but has limited heterotrophic biomass or slowly biodegradable substrate (since it has been digested), as shown in Table 5-2. Therefore, the removal efficiency of the unbiodegradable cell product, fermentative biomass, acetogenic biomass, acetolactic methanogenic biomass, and hydrogenotrophic methanogenic biomass also influences the particulate content of filtrate and centrate.

Table 5-2 The predicted different type of CODs of the feed sludge to different sludge thickening and dewatering

	Feed Sludge of primary sludge drum thickening	Feed Sludge of SAS drum thickening	Feed Sludge of raw sludge centrifuge	Feed Sludge of digested sludge centrifuge
Total COD, mg/L	37490.0	6948.0	46870.0	40830.0
Particulate inert material, mg/COD	7694.0	1830.0	12720.0	23810.0
Unbiodegradable cell product, mg/COD	669.1	81.5	1408.0	3072.0
Slowly biodegradable substrate, mg/COD	26210.0	1306.0	23060.0	28.3
Heterotrophic biomass, mg/COD	255.2	3683.0	3443.0	0.0
Fermenting biomass, mg/COD	0.0	0.0	0.0	7406.0
Acetongenic biomass, mg/COD	0.0	0.0	37.9	14.7
Acetoclastic methanogenic biomass, mg/COD	0.0	0.0	0.0	1433.0
Hydrogenotrophic methanogenic biomass, mg/COD	0.0	0.0	139.1	1073.0

The parameter of influent fraction (of digester feed sludge), kinetic and stoichiometric parameters that influence the biological modelling results of the sludge storage, sludge thickening and dewatering processes and the anaerobic digestion, and are therefore subject to adjustment in the model for each WWTP, are listed in the Tables D-8 in Appendix D. The table also presents the adjusted value and the category those adjusted parameter belongs to.

5.1.3.3 Validation of the sludge treatment models

For the sludge treatment modelling, the ARD between the predicted result and the observed results are also no higher than the allowable value of 15.0%. The ARDs of the various treatment stages are as follows:

- primary sludge thickening: 7.4%
- SAS thickening: 12.1%
- raw sludge dewatering: 5.2%
- anaerobic digestion and the subsequent digested sludge dewatering: 5.2%

As can be seen in Figure 5-8, the observed results match the model predictions well.

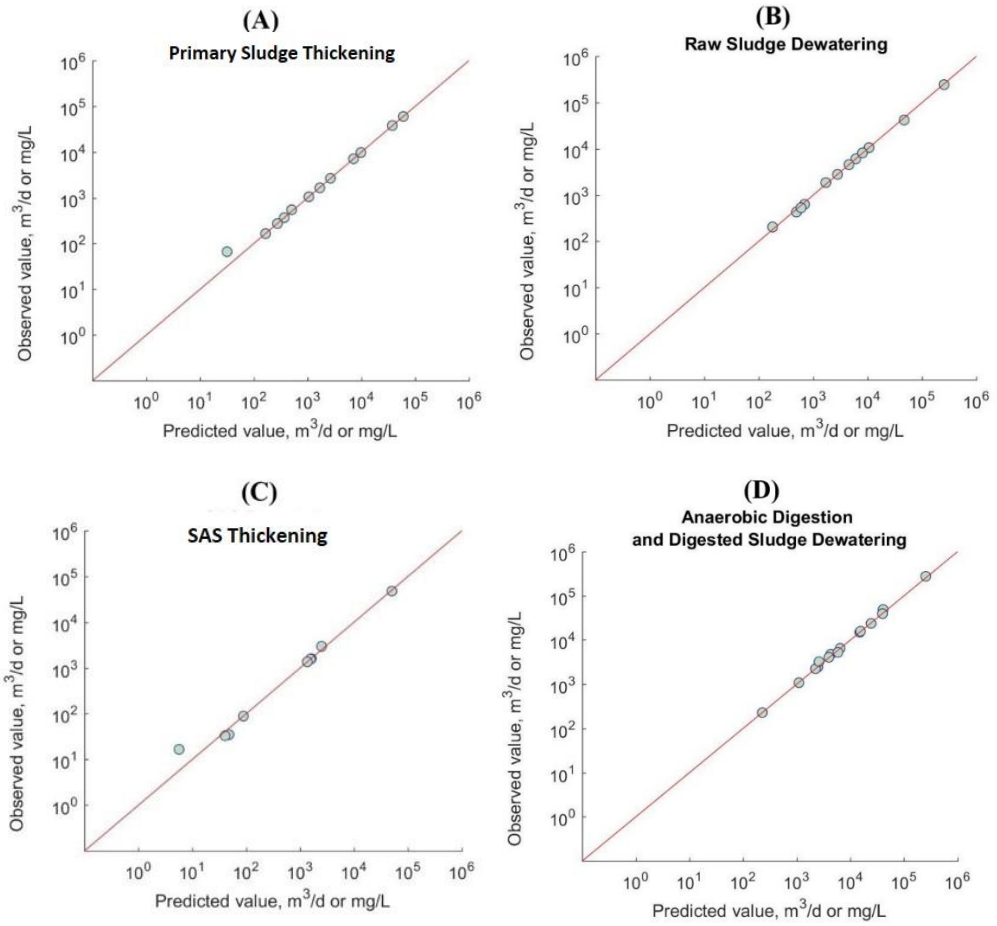

Figure 5-8 Comparison between the observed results and predicted results of the modelling of sludge treatment (A) Primary sludge thickening, (B)Raw sludge dewatering, (C) SAS thickening, and (D) Anaerobic digestion and digested sludge dewatering

Hence, the models constructed for modelling the sludge treatment including thickening, dewatering and anaerobic digestion are considered representative of the actual performance and the material mass balance of the WWTPs. The predicted flowrate and concentrations are therefore used in the mass and energy balance calculations of the sludge treatment in this chapter and Chapter 6.

The observed and predicted result of the sludge treatment modelling are shown in Table E-2 in Appendix E.

5.2 The COD mass balance and chemical energy balance of treatment processes

5.2.1 The COD mass balance and chemical energy balance of primary settlement units

The flow and concentration data predicted via modelling were used in the construction of the COD mass balance and chemical energy balances of primary settlement units.

In the four study WWTPs, the chemical energy of both wastewater and sludge have strong linear relationships with COD (stated in Section 4.1.3 and 4.2.3). Therefore, the chemical energy of the wastewater and sludge are estimated from the predicted COD (from modelling) via Equation 4-2 (shown in Section 4.1.3).

In the case of WWTP A and D, which have reactive settlers, the outflowing COD mass and chemical energy within the sludge and effluent wastewater is >1% smaller than the inflowing COD mass and chemical energy. The missing COD and chemical energy are considered as loss and are considered being caused by the biological reactions. However, the loss is less than 1% Therefore even though biological sludge is recirculated back to the primary settlement tanks, the COD loss caused by the biological reactions can be ignored. In the case of WWTPs B and C, which have no biological sludge is recirculated back to the primary settlement tanks, the outflowing COD mass and chemical energy within the sludge and effluent wastewater equals the inflowing.

The COD mass and the chemical energy flows through the primary settlement units of all four treatment plants can be balanced Hence, the COD mass and the chemical energy balances are considered reliable. The COD mass balance and the chemical energy balance of the primary settlement units of all four WWTPs are shown in Figure 5-9. In Figure 5-9, the C.E. presented stands for chemical energy.

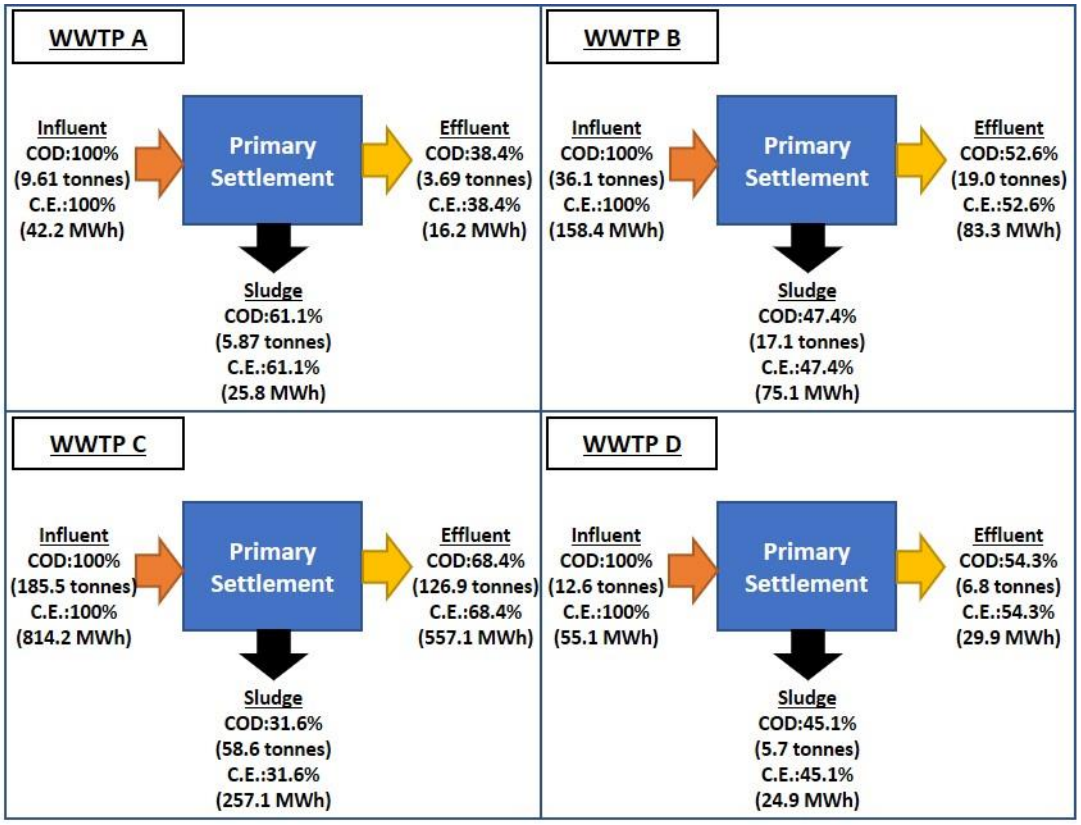

Figure 5-9 The COD mass and chemical energy balances of primary settlement in a daily basis at the four WWTPs investigated

Typically COD removal efficiencies for primary settlement tanks are approximately 30-40 %, with the remaining 60-70% of COD flowing to secondary treatment units (Wan et al., 2016, Shi, 2011, Yeshi et al., 2013). The COD removal efficiencies of WWTPs B, C and D are similar to this typical value. However, WWTP A removes about 60% of the COD in the primary settlement process. This is probably because WWTP A doses ferric sulfate to its screened raw wastewater. Although the ferric dosing solely aims to remove the phosphate (*personal communication*, J McCowan, Scottish Water, April 2016), it may improve the sedimentation of colloidal or particular matter and therefore potentially settles a greater proportion of COD from the raw wastewater into the primary sludge (Ismail et al., 2012, Tchobanoglous et al., 2003).

As shown in Table 5-3, a higher pCOD removal leads to a higher COD removal. However, there do not appear to be any relationships between the hydraulic retention time (HRT), the ratio of pCOD:COD, the COD, sCOD or pCOD concentration and the efficiency of COD removal in the primary tanks (shown in Figures 5-10 and 5-11), though this is based on rather limited data and would therefore need further investigation.

Table 5-3 The predicted influent and effluent CODs concertation and the CODs removal efficiency of primary settlement in four WWTPs

	WWTP A	WWTP B	WWTP C	WWTP D
pCOD in raw wastewater, mg/L	786.8	478.4	467.7	218.9
pCOD in primary effluent, mg/L	206.4	197.8	276.9	92.9
pCOD removal efficiency*	73.8%	58.7%	40.8%	57.5%
sCOD in raw wastewater, mg/L	274.6	248.7	197.3	117.7
sCOD in primary effluent, mg/L	200.1	187.4	180.7	87.1
sCOD removal efficiency*	27.1%	24.6%	8.4%	26.0%
COD removal efficiency*	61.7%	47.0%	31.2%	46.5%

*: Removal efficiency = (Influent Concentration – Effluent Concentration) ÷ Influent Concentration

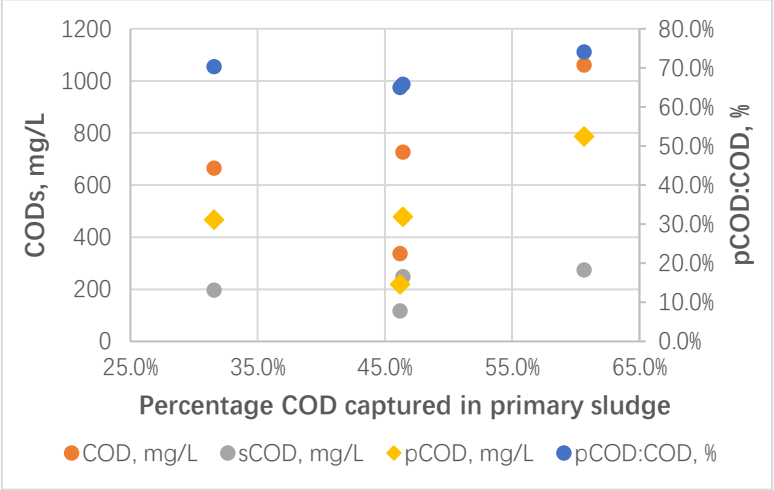

Figure 5-10 The impact of CODs concentration and fractions to the percentage COD captured in primary sludge

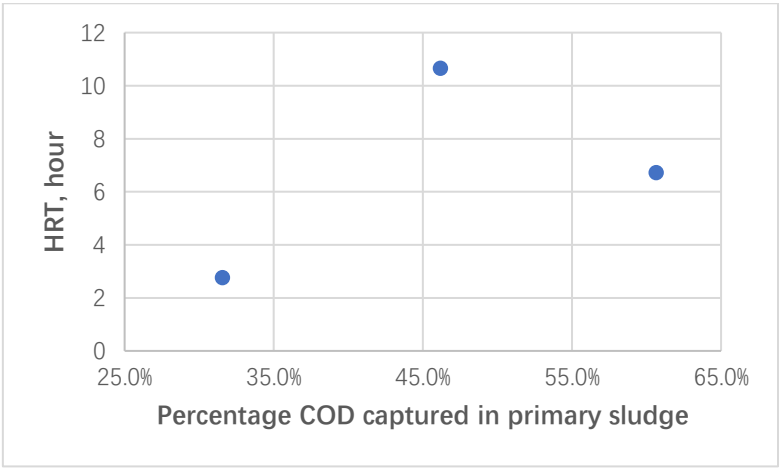

Figure 5-11 The impact of HRT to the percentage COD captured in primary sludge

In summary, for the four WWTPs investigated in this study, primary settlement captured 46.3 ± 12.1% of influent COD and chemical energy in the primary sludge, with the remainder flowing to the secondary treatment processes.

5.2.2 The COD mass balance and chemical energy balance of secondary biological treatment (activated sludge)

The flow and concentration data predicted via modelling were used in the construction of the COD mass balance and chemical energy balances of secondary biological treatment as activated sludge. The chemical energy of the wastewater and sludge are estimated from the predicted COD (from modelling) via Equation 4-2 (shown in Section 4.1.3).

In the four study WWTPs, the COD mass and chemical energy within the effluent sludge and wastewater flows into activated sludge process is substantially smaller than the inflowing COD mass and chemical energy. Considering the activated sludge can remove organic matter via oxidation (Tchobanoglous et al., 2003), the missing COD mass and chemical energy is due to the organic carbon being oxidized to CO_2 as gaseous product and emitted to the atmosphere.

In the case of WWTPs B and C, which do not have biological reactive final clarification, the outflowing and inflowing COD mass and chemical energy of the final clarification balances. But in the case of WWTPs A and D, which have biological reactive final clarification, the outflowing COD mass and chemical energy within the effluent sludge and wastewater flows into final clarification is 1-2% smaller than the inflowing. The possible reason for this is that some of the COD may be consumed by denitrification occurring in the final clarifiers (Yeshi et al., 2013, Tchobanoglous et al., 2003). Considering the loss of COD mass and chemical energy in the final clarifier is small, the activated sludge process and the final clarification process are combined for the calculation of mass and energy balance. The COD mass balance and chemical energy balances for the four WWTPs are shown in Figure 5-12. In Figure 5-12, the C.E. presented stands for chemical energy.

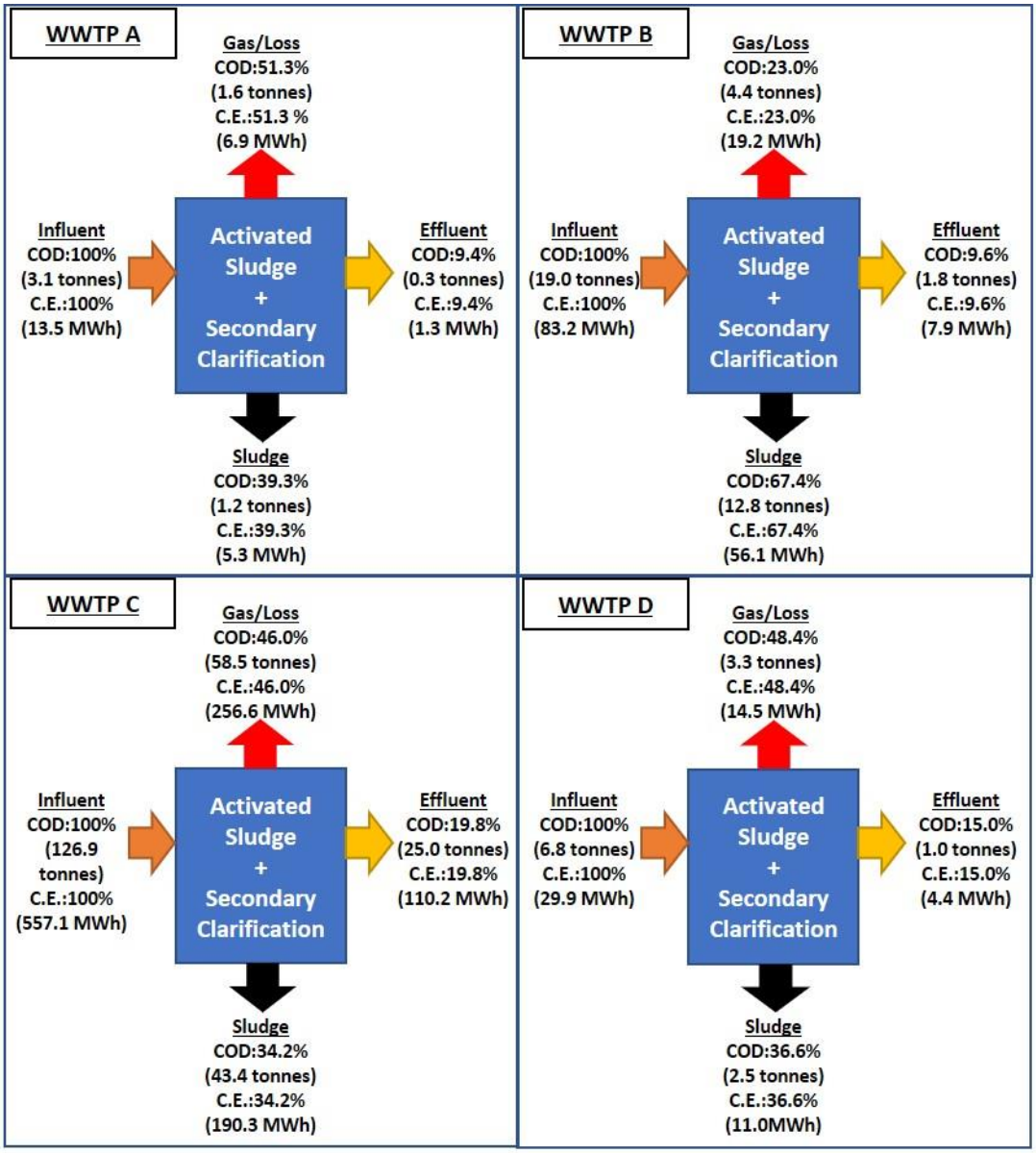

Figure 5-12 The COD mass and chemical energy balances of activated sludge in a daily basis at the four WWTPs investigated

Nowak et al. (1999) suggested that 25.0 - 60.0 % of the COD removed was stored in new growth biomass, and the rest was lost as CO_2. Hence, the ratio of COD in surplus activated sludge (SAS, displays as sludge in Figure 5-12) and COD lost as CO_2 was in the range 0.33 (25%:75%) to 1.50 (60%:40%). From the data shown in Figure 5-12, the calculated ratios of WWTPs A (1.30), B (0.34), C (1.35) and D (1.32) fall in this range. One possible reason for this high ratio in WWTP B was that both biomass assimilation and bio-flocculation participated in capturing the COD into the SAS (Jimenez et al., 2015). The bio-flocculation captures the COD without oxidizing it and can be enhanced via iron dosing (Jimenez et al., 2015). The raw

wastewater of WWTP B possibly has a high iron content because the part of the wastewater could be from the runoff from abandoned metal mine (*personal communication*, L Wilkinson, Northumbrian Water, 29 October 2018). Hence, it is possible that unexpected bio-flocculation took place in WWTP B.

In summary, this study finds that activated sludge captures 44.4 ± 15.5% of influent COD and chemical energy in the SAS. Simultaneously, 42.2 ± 13.0% of the influent COD and chemical energy is lost, potentially as CO_2. The remaining 13.7± 5.4% will leave the treatment works as final effluent if there is no tertiary treatment.

5.2.3 The COD mass balance and chemical energy balance of sludge thickening and dewatering facilities

The flow and concentration data predicted via modelling were used in the construction of the COD mass balance and chemical energy balances of sludge thickening and dewatering facilities.

The TSS, VSS, COD mass balance and chemical energy balance are constructed for all four sludge thickening and dewatering processes of WWTP C. All the mass flows are balanced, as shown in Figure 5-13. In Figure 5-13, the C.E. presented stands for chemical energy.

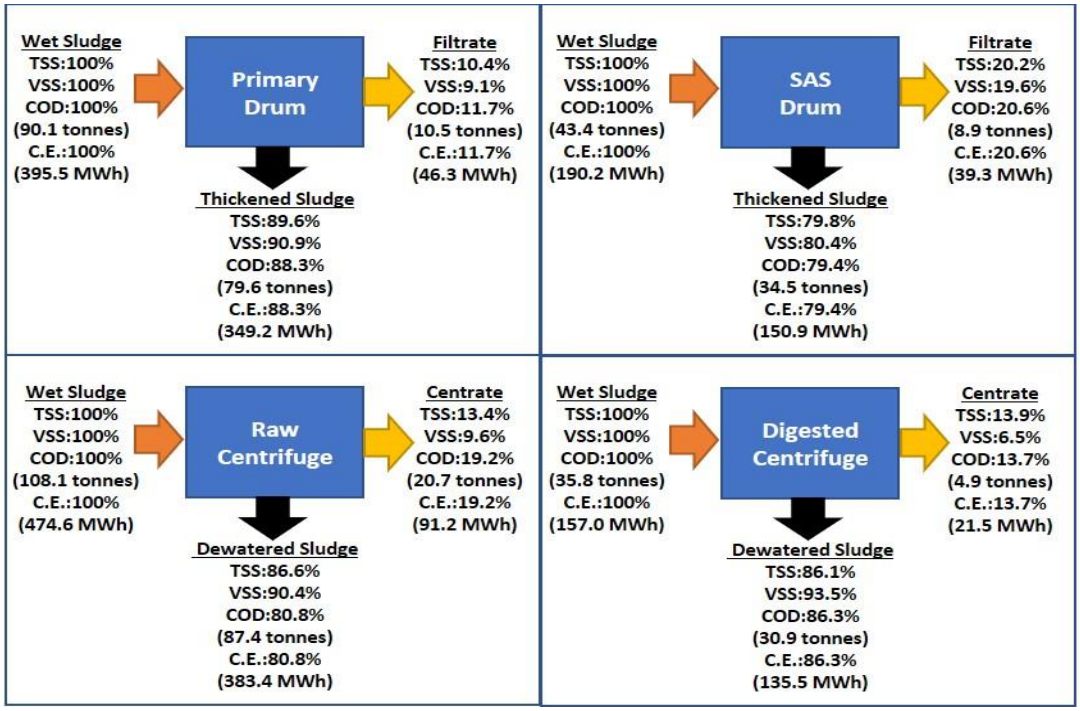

Figure 5-13 The TSS, VSS, COD mass balances and chemical energy balance of the sludge thickening and dewatering processes in WWTP C

TS and VS were measured in the sampling campaign, but not the TSS and VSS. Here, the predicted TSS and VSS are used as reference values to demonstrate the distribution of the particulate material.

In GPS-X, VSS contributes to pCOD (Hydromantis, 2017). As shown in Figure 5-4, in the thickening of primary sludge and SAS, the distribution pattern of the VSS and COD are in good agreement. But in the raw sludge and digested sludge dewatering, the percentage of the total COD in the centrate of the raw centrifuge and the digested centrifuge is substantially greater than the percentage of total VSS. That is likely due to the large proportion of COD in centrate present as sCOD (as shown in Table 5-4). The sCOD is produced from the solubilization of the particulate materials due to the hydrolysis and fermentation after long storage times or digestion prior to the sludge dewatering (Tchobanoglous et al., 2003, Ubay-Cokgor et al., 2005). In the case of primary sludge thickening and raw sludge dewatering, although similar percentages of the VSS ends in the filtrate or centrate, because the raw sludge contains more sCOD, a greater percentage of the COD ends in the raw sludge centrate than in the primary sludge filtrate.

Table 5-4 The predicted sCOD and COD concentration in different filtrates and centrates

	sCOD, mg/L	COD, mg/L	sCOD:COD
Primary Sludge Filtrate	2661.9	9777.2	27.2%
SAS Filtrate	47.8	1603.0	3.0%
Raw Sludge Centrate	6027.2	10536.7	57.2%
Digested Sludge Centrate	4059.1	6722.3	60.4%

The thickening of primary sludge, SAS and the dewatering of raw sludge take place before digestion. Although approximately 80% or more of COD and chemical energy is captured in the thickened and dewatered sludge, since part of the COD and chemical energy ends in the filtrates or centrates, it suggests that not all the COD and chemical energy captured in the primary sludge and secondary sludge will reach the digester. Therefore, sludge thickening and dewatering appears to reduce the chemical energy input to the digester.

5.2.4 The COD mass balance and chemical energy balance of anaerobic digestion

The flow and concentration data predicted via modelling were used in the construction of the COD mass balance and chemical energy balances of anaerobic digestion.

The percentage difference between the inflowing and outflowing COD and chemical energy balances is no greater than ± 7.0% (Figure 5-14). Therefore, both the COD mass balance and chemical energy balances appear to be reliable. However, unlike in the as the primary settlement (Section 5.2.1), activated sludge (Section 5.2.2) and sludge thickening and dewatering (Section 5.2.3), the chemical energy balance no longer fully follows the COD balance as the percentage of chemical energy in the biogas is less than the percentage of COD.

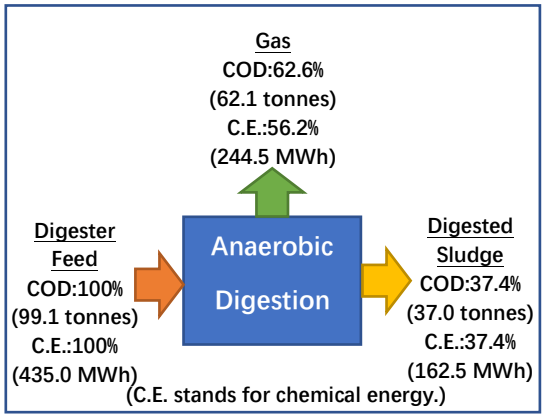

Figure 5-14 The COD and chemical energy balance of anaerobic digestion in WWTP C

The chemical energy balance suggests that 56.2 % of the chemical energy in the sludge is recovered as CH_4. Mills et al. (2014) suggested that a typical advanced AD (AAD) process is able to recover 51.0 % of the sludge energy into CH_4, and Barber (2016) reported a figure of 60.0 %. The findings of this study therefore approximately match these literature values.

In this study, the outflowing chemical energy within the bio-methane and in the digested sludge is 6.4% less than the inflowing. Mills et al. (2014) suggested a similar pattern: the outflowing chemical energy within the bio-methane and in the digested sludge is 5.2% less than the inflowing. In theory, the chemical energy loss during the anaerobic digestion is possible. This thesis uses glucose ($C_6H_{12}O_6$) as an example (shown in Example 5-1) to demonstrate this phenomenon in theory.

Example 5-1

$$C_6H_{12}O_6 = 3CH_4 + 3CO_2$$

$$C_6H_{12}O_6(s) + 6O_2(g) = 6CO_2(g) + 6H_2O(lq)$$

-1281 0 -393.51×6 -285.83×6 $\triangle_r H$=-2,804.04 kJ/mol

$$3CH_4(g) + 6O_2(g) = 3CO_2(g) + 6H_2O(lq)$$

-74.81×3 0 -393.51×3 -285.83×6 $\triangle_r H$=-2,671.08 kJ/mol

As shown in Example 5-1

- The complete anaerobic digestion of 1 mole of $C_6H_{12}O_6$ produces 3 moles of CH_4 and 3 moles of CO_2. A complete oxidation of 1 mole of $C_6H_{12}O_6$ and 3 moles of CH_4 consumes the same amount of oxygen (O_2).
- Based on the enthalpy calculation, although 3 moles of CH_4 has the same amount of COD as 1 mole of $C_6H_{12}O_6$, the heat release from the combustion ($\triangle_r H$) of 3 moles of CH_4 is only 2,671.08 ÷ 2,804,04 = 95.2% of the heat released from the combustion of 1 mole of $C_6H_{12}O_6$.

The result found in study (shown in Figure 5-14) and reported by Mills et al. (2014) agrees with the theory.

5.3 Energy recovery opportunities based on WWTP mass balances

5.3.1 Energy product of wastewater treatment

Based on the results presented in Sections 5.2.1 and 5.2.2, the COD and chemical energy mass balances are shown in Figure 5-15.

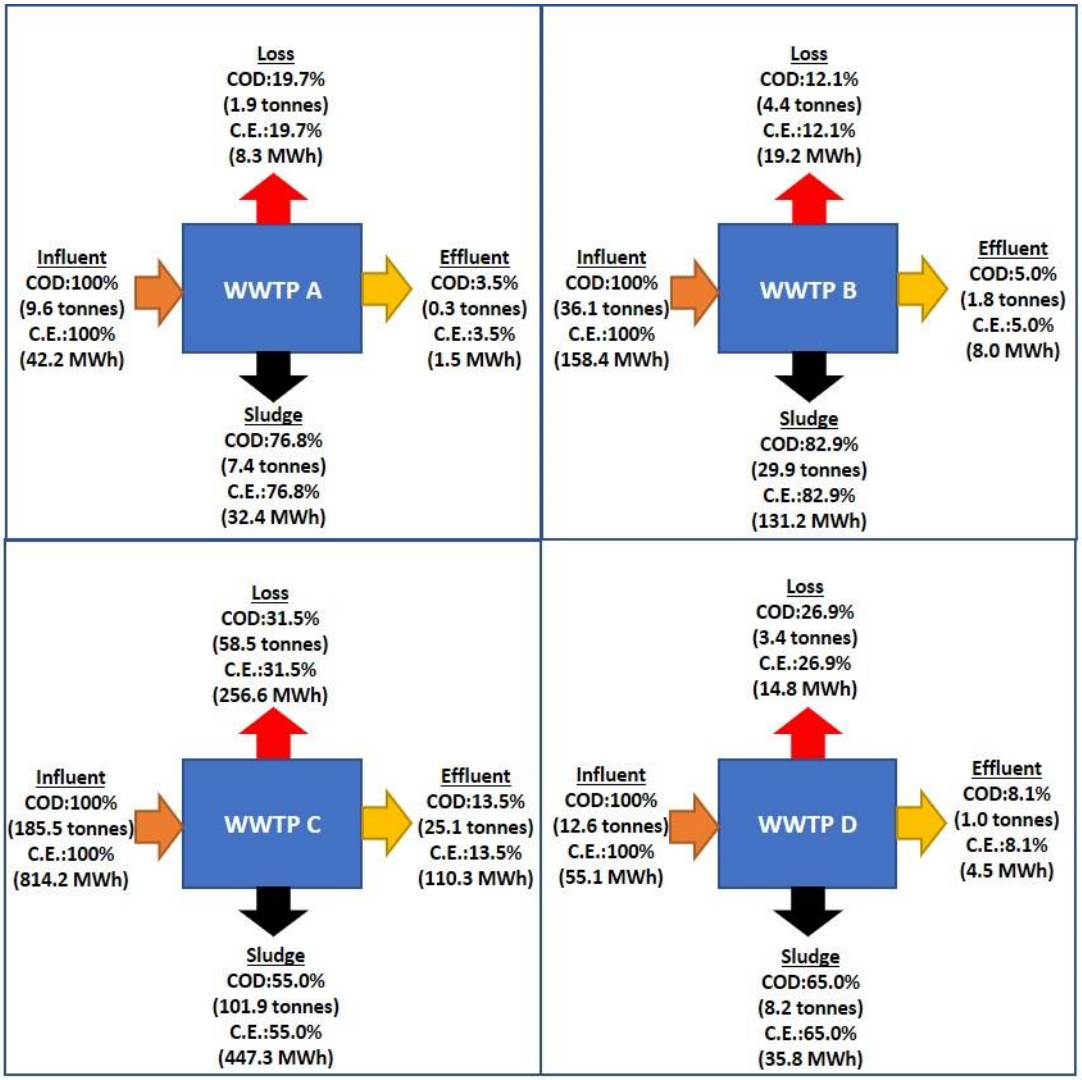

Figure 5-15 The COD and chemical energy mass balance of the four WWTPs investigated

WWTPs can be considered as reactors that convert their feedstock, the energetic raw wastewater, into three outputs: (1) sludge, (2) treated wastewater as final effluent, and (3) gaseous emissions. From an energy recovery perspective, not every output can be considered as a product. What is critical is whether the output contains considerable amounts of chemical energy and whether there is potential to recover it.

As shown in Figure 5-15, apart from WWTP C no more than 15.0% the COD and chemical energy flowing into the WWTPs is present in the final effluent. Meanwhile, the COD concentration of the final effluents are lower than 100 mg/L, which is too low for energy self-sufficient recovery, i.e. the energy consumption for energy recovery would be greater than the value of the energy recovered(Stoll et al., 2018). The final effluent is not therefore considered to be a potential product at any of the WWTPs. The gas produced from the energetic organic carbon is mainly CO_2 which contains no chemical energy, and hence it is not a product neither (Tchobanoglous et al., 2003). In these four WWTPs, 31.2 ± 14.5% of COD and chemical energy flowing into the works is lost via a combination of oxidation in the aerobic activated sludge process and final effluent discharge.

In current practice energy recovery from wastewater is commonly achieved via anaerobic digestion of sludge (Pearce et al., 2014), in which case sludge is the only energy product. However, the energy cannot be produced directly from the sludge. Rather, it is an intermediate product, in the same way that gasoline can be combusted for producing heat or to drive a vehicle. In the four study WWTPs, 68.6 ± 14.4% of COD and chemical energy flowing into the works is captured in the sludge and sent for digestion.

5.3.2 Energy product of sludge treatment

In the four WWTPs investigated only WWTP C has anaerobic digestion onsite for energy recovery from sludge. Therefore, the sludge treatment of WWTP C is used here for illustrative purposes. Sludge treatment can be considered as a reactor. Its feedstock is the sludge, and the outputs are the biogas, filtrates, centrates and digested cake. The COD mass and chemical energy balance are constructed based on the predicted result obtained via modelling and are as shown in Figure 5-16. As can be seen, the outflowing COD and chemical energy to the sludge is smaller than the inflowing. The loss of COD and chemical energy during the sludge treatment is likely due to the biological reactions occurred in the sludge storage and digestion.

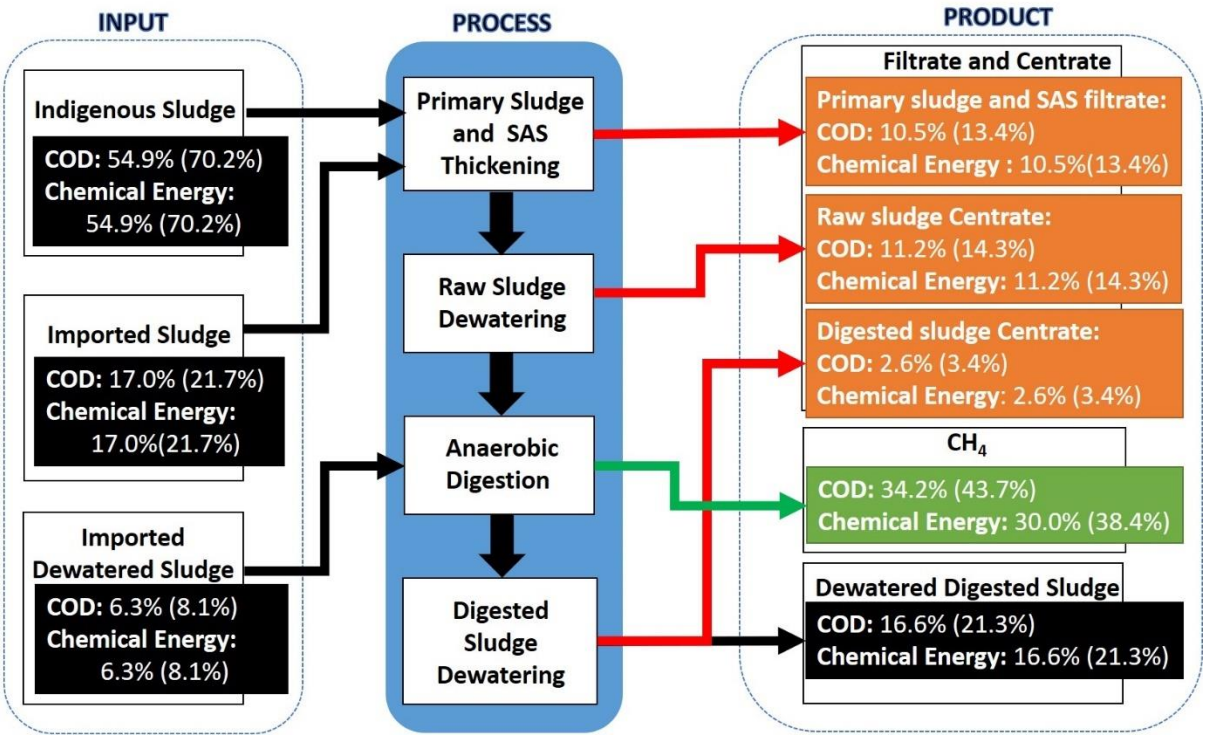

Figure 5-16 The COD and chemical energy balance of the sludge treatment in WWTP C
(The value shows in the () are the percentage mass balance using the total COD and chemical energy inputted to the sludge treatment as reference)

As shown in Figure 5-16, WWTP C treats the indigenous sludge and also the imported wet sludge and imported dewatered sludge. The imported sludge contains the equivalent of 17.0.0% of the inflowing COD and chemical energy to the works. Meanwhile, the imported dewatered sludge contains the equivalent of 6.3% of the inflowing COD and chemical energy to the works. Unlike the wastewater treatment, the sludge treatment distributes its influent COD and chemical energy to its three outputs more evenly:

- 21.3 % of the sludge COD and sludge chemical energy ends in the dewatered digested sludge
- 31.1% of the sludge COD and sludge chemical energy is retained in the filtrates and centrates
- 43.7% of the sludge COD and 38.4% of the sludge chemical energy is recovered as CH_4.

Although dewatered digested sludge, filtrates and centrates contain considerable amounts of chemical energy, they are not available for direct energy use. Currently, at WWTP C, the filtrates and centrates are recirculated back to the head of the works, and the dewatered digested cake is sent for agricultural land use (*personal communication*, L Wilkinson, Northumbrian

Water, October 2015). Therefore, CH_4 is the only energy product of the combined wastewater and sludge treatment. It is worth noting that the percentage sludge COD retained in the filtrates and centrates are substantially greater that the value reported by Shi (2011) (17.1%) and Wett et al. (2007) (2.4%).

As shown in the Figure 5-16, the COD and energy outputs do not equal the inputs. That is because part of the COD and chemical energy is lost during sludge storage and digestion but is not accounted for in Figure 5-16.

5.3.3 Energy recovery potential from wastewater

5.3.3.1 Chemical energy recovery potential of wastewater

If the wastewater treatment and sludge treatment are considered as two reactors in sequence, the chemical energy that could potentially be generated (E_{CEGen}) from 1 m^3 of wastewater can be empirically estimated by Equation 5-1.

Equation 5-1

$$E_{CEGen} = E_{ww} \times \eta_{SfWW} \times \eta_{CEfS}$$

Where $\boldsymbol{E_{ww}}$ is the chemical energy content of 1 m^3 of wastewater and can be estimated via multiplying its COD concentration by 0.0158 kJ/mg COD (0.0044 kWh/g COD),

$\boldsymbol{\eta_{SfWW}}$ is the percentage of the chemical energy flowing into the works that is captured in the indigenous sludge, and

$\boldsymbol{\eta_{CEfS}}$ is the percentage of the sludge chemical energy recovered in the energy product from the sludge treatment.

η_{CEfS} is affected by the two factors;

1. the percentage of sludge chemical energy that could reach the digester after several stages of thickening and dewatering (η_{CErD})
2. the energy recovery efficiency of the digester (η_{CEfD}). η_{CEfS} can be expressed as Equation 5-2.

   Equation 5-2

$$\eta_{CEfS} = \eta_{CErD} \times \eta_{CEfD}$$

Because WWTPs A, B and D has no sludge digestion, and hence these WWTPs has no studied η_{CErD} and η_{CEfD}. In the estimation of the E_{CEGen} from the raw wastewater of WWTPs A, B and D, the universal values of η_{CErD} and η_{CEfD} are used based on the chemical energy balance of the sludge treatment WWTP C. As shown in Figure 5-16, 91.9 units of sludge energy are first fed to the sludge treatment, but after several stages of thickening and dewatering only 60.2 units reaches the AAD. The η_{CErD} is 65.5%. After 8.1 units of sludge energy from the imported dewatered sludge is added, the AAD receives 68.3 units of sludge energy and generates CH_4, which is equivalent to 38.4 units of sludge energy. Thus, the η_{CEfD} is 56.2%. The E_{CEGen} values of all four WWTPs are estimated from the COD concentration of the raw wastewater (shown in Table 5-1) via Equation 5-1 and listed in Table 5-5.

Table 5-5 The estimated chemical energy production potential from the four study WWTPs

	COD, mg/L	E_{ww}, kWh/m^3	η_{SfWW}**	E_{CEGen}, kWh/m^3	E_{CEGen}:E_{ww}
WWTP A	**1061.4**	4.66	76.8%	1.32	28.3%
WWTP B	**727.1**	3.19	82.9%	0.97	30.5%
WWTP C	**665.0**	2.92	54.9%	0.59	20.2%
WWTP D	**336.6**	1.48	65.0%	0.35	23.9%

*: The percentage chemical energy capture in the sludge shown in Figure 5-15

As shown in Table 5-5, both the COD of the raw wastewater and the η_{SfWW} influence the E_{CH4Gen}. In the case of WWTP C and WWTP D, although WWTP D has a higher η_{SfWW} than WWTP C (65.0% compared to 54.9%), since the COD of WWTP C raw wastewater is approximately double that of WWTP D, the E_{CEGen} of WWTP C is higher than E_{CH4Gen} of WWTP D. In the case of WWTP B and C, although the COD of their raw wastewater is similar, since the η_{SfWW} of WWTP B is about 1.5 times greater than WWTP C, the E_{CEGen} of WWTP B is much higher than that of WWTP C (0.97 kWh/m^3 compared to 0.59 kWh/m^3). The values of E_{CEGen}:E_{ww} in Table 5-4 suggest that only approximately 20-30% of the chemical energy contained in the raw wastewaters of these WWTPs can be recovered as CH_4 energy. In reality, the E_{CEGen}:E_{ww} of WWTP C is 30.0% (shown in Figure 5-16). This higher ratio is attributed to the extra sludge imported to the sludge treatment.

5.3.3.1 Electrical energy recovery potential of wastewater

Wastewater and sludge treatment have the potential to produce energy, but they also consume energy. Energy used in wastewater treatment is usually in the form of electrical energy, and for

sludge treatment both electrical and heat energy may be used (Wan et al., 2016, Mills et al., 2014). However, the energy balance of a WWTP is usually expressed as a function of kWh electricity used per m^3 of wastewater. Current practice in the wastewater treatment sector is to recover electrical energy from wastewater by feeding the CH_4 produced in sludge digestion to an electricity generator (Rawlinson et al., 2012, Gu et al., 2017). To construct a more meaningful energy balance it is therefore useful to convert the energy of wastewater and sludge, in units of heat or chemical energy, into units of electrical energy, so that a direct comparison of electricity consumed to potential electricity available can be made for individual wastewater treatment plants (Wan et al., 2016). For this research this has been done by combining the total chemical energy potentially available in the wastewater and sludge treatment processes, thus producing a single figure for available electricity.

One of the key tasks to implement this approach is to convert the heat energy consumed during the advanced anaerobic digestion process into an expression of electrical energy, because the THP process requires considerable amounts of heat input. In practice the heat is commonly supplied via two approaches. As shown in the Figure 5-17, the heat is supplied from the heat-grade heat recovered from the Combined Heat and Power (CHP) generation. If insufficient heat is provided by the CHP the deficit is supplied from a boiler that uses supportive fuel, such as natural gas or oil (Bowen et al., 2010). Thus, the input to the system is not only the sludge energy, but also the chemical energy from the support fuel. This energy usage needs converting to electrical energy in the approach used for the energy mass balance in this research. The second approach to the provision of heat, is to first divert some of the CH_4 to the boiler, and then the heat demand is met by combining the heat production from both the boiler and the CHP (Smyth et al., 2016). In this approach no support fuel is needed. There is only one input to the system in this case. The ratio for splitting the CH_4 to the boiler and the CHP has to be calculated because it determines the quantity of CH_4 available to the CHP.

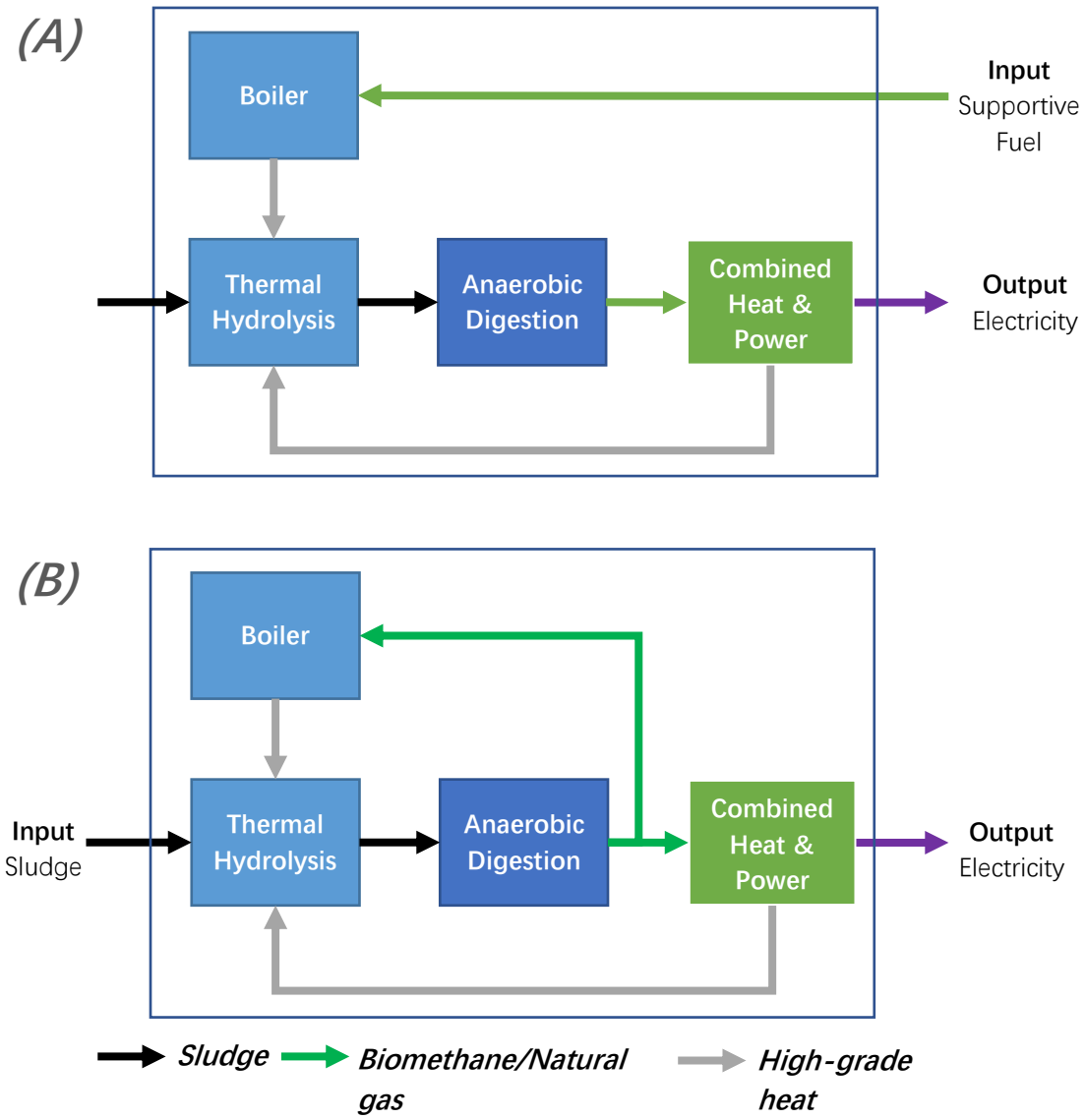

Figure 5-17 Schematic illustration of different approaches to heat supply to the THP

The ratio for splitting the CH_4 to the boiler and CHP for achieving heat self-sufficient can be calculated, beginning with the heat demand of the THP (η_{HtTHP}). The heat demand of THP (η_{HtTHP}) is considered as the unit heat required per unit sludge energy fed to the THP treatment unit and the subsequent digestion. Since the demand is met by high-grade heat from the CHP and the heat from the boiler, η_{HtTHP} can be calculated using Equation 5-3.

Equation 5-3

$$\eta_{HtTHP} = \eta_{CEfD} \times \eta_{CEtCHP} \times \eta_{HGHfCHP} + \eta_{CEfD} \times (1 - \eta_{CEtCHP}) \times \eta_{Boiler}$$

Where $\boldsymbol{\eta_{CEtCHP}}$ is the proportion of the produced chemical energy fed to the CHP

$\boldsymbol{\eta_{CEfD}}$is the chemical energy recovery efficiency of the digester,

$\boldsymbol{\eta_{HGHfCHP}}$ is the high-grade heat recovery efficiency from per unit energy fed to the CHP,

$\boldsymbol{\eta_{Boiler}}$ is the thermal efficiency of the boiler.

The η_{CEtCHP} can be calculated using Equation 5-3 which is rearranged from Equation 5-4.

Equation 5-4

$$\eta_{CEtCHP} = \frac{\eta_{HtTHP} - \eta_{CEfD} \times \eta_{Boiler}}{\eta_{CEfD} \times (\eta_{HGHfCHP} - \eta_{Boiler})}$$

Historical data shows 77.3 MWh/d heat as steam is used for the THP to treat feed sludge to anaerobic digestion process during the period of the sampling campaign conducted (*personal communication*, S Coverdale, Northumbrian Water, October 2017). As shown in Figure 5-14, the digester feed sludge contains 435.0 MWh chemical energy. Thus, the η_{HtTHP} (heat demand of THP) of the sludge treatment of WWTP C is 77.3÷435.0 = 17.8% which is in agreement with the reported range of 13.6-17.2% (Smyth et al., 2016, Mills et al., 2014). A value for $\eta_{HGHfCHP}$ (heat recovery efficiency) of 20.0% is assumed since the reported range is 18-22% (Mills et al., 2014, Smyth et al., 2016, Bowen et al., 2010). The boiler efficiency (η_{Boiler}) is taken the reported value of 85% (Vanwortswinkel and Nijs, 2010). From this, the η_{CEtCHP} is calculated as 0.821. To achieve self-sustaining heat generation at WWTP C, theoretical calculations suggest that 82.1% of the chemical energy produced via THP (as CH_4) at the plant should be fed to the CHP for electricity generation.

With a common heat to electricity conversion efficiency (η_{EfCHP}) of 38% in Combined Heat and Power (CHP) electricity generation (Banks, 2009, Mills et al., 2011), the electricity that could be produced from 1 m^3 of wastewater ($E_{ElecGen}$) can be calculated using Equation 5-5.

Equation 5-5

$$E_{ElecGen} = \left(E_{ww} \times \eta_{SfWW} \times \eta_{CErD} \times \eta_{CEfD}\right) \times \eta_{CEtCHP} \times \eta_{EfCHP}$$

The estimated $E_{ElecGen}$ of WWTP A, C and D, and their electrical balances are shown in Table 5-6.

Table 5-6 The estimated electricity production of different wastewater

	Flow, m^3/d^*	WWTP electricity consumption, kWh/d**	$E_{ElecCon}$, kWh/m^3	$E_{ElecGen}$, kWh/m^3
WWTP A	9,052	3,015	0.33	0.41
WWTP C	278,954	85,949	0.31	0.18
WWTP D	37,312	9,744	0.26	0.11

*: It is shown in Table 5-1

**: It is collected from Scottish Water and Northumbrian Water (*personal communication*, J McCowan, Scottish Water, June 2017 and *personal communication*, L Wilkinson, Northumbrian Water, July 2018)

In case of WWTPs A, C and D, the chemical energy contained in 1 m^3 raw wastewater (E_{ww}, 1.48-4.66 kWh, Table 5-5) is approximately 5-14 times higher than the electricity consumed in treating 1 m^3 of wastewater ($E_{ElecCon}$, 0.26-0.33 kWh, Table 5-6). However, the estimated $E_{ElecGen}$ are 0.11-0.41 kWh (Table 5-6), only 6 - 9% of the E_{ww} in the wastewater. With the exception of WWTP A the potential $E_{ElecGen}$ is less than $E_{ElecCon}$, and hence WWTPs C and D do not have the potential to be electricity self-sustaining. Although the potential $E_{ElecGen}$ of WWTP A is greater than its $E_{ElecCon}$, considering WWTP A has no onsite anaerobic digestion, if energy consumed on the sludge haulage is taken into account, the surplus $E_{ElecGen}$ compared to $E_{ElecCon}$ will be reduced or even eliminated.

5.3.3.2 Improving the electrical energy balance

The wastewater and subsequent sludge treatment with anaerobic digestion is considered as a set of reactors in sequence. The intermediate product is the sludge. The η_{SfWW} can be considered as the efficiency with which COD or chemical energy is captured in the wastewater treatment plant. A greater η_{SfWW} result in a greater amount of feedstock to the second reactor, the sludge treatment with anaerobic digestion. The sludge produced by the wastewater treatment consists of the primary sludge and SAS. However, the feed of the activated sludge is the effluent of the primary settlement. If the COD capture rate of the primary settlement is X, the COD capture rate of the activated sludge is Y, and the COD and chemical energy capturing rate of the WWTP, η_{SfWW}, can be expressed by Equation 5-6.

Equation 5-6

$$\eta_{SfWW} = X + (1 - X)Y = (1 - Y)X + Y$$

X, Y and η_{SfWW} are all between 0 to 1. According to the equation, if Y is given a set value, (1-Y) becomes a constant that is bigger than 0, then the Equation 5-6 becomes a linear function of X. Since the slope is bigger than 0, a greater X to can lead to greater η_{SfWW}. Improving the primary settlement process can potentially increase the η_{SfWW} (Equation 5-5) and lead to a greater $E_{ElecGen}$. Primary settlement aims to settle the particulate contaminant. In the four study WWTPs, approximately 26-60 % of the particulate COD remained in effluent of primary treatment (Table 5-3). The primary settlement can still be improved. Research suggests this can be done by dosing aluminum and ferric salts at the correct dosage rate and pH (Ismail et al., 2012, Sarparastzadeh et al., 2007).

The η_{CErD} (Equation 5-5) is the energy recovery efficiency of the sludge treatment. This consists of several stages of sludge thickening and dewatering prior to anaerobic digestion. As stated in Section 5.2.3, filtrates and centrates contain 31.1% of sludge energy. Among all four sludge filtrates and centrates, 1) primary sludge filtrate, 2) SAS filtrate, and 3) raw sludge centrate are formed prior to the anaerobic digestion. The formation of the filtrate and centrate does have an adverse effect on final energy production because sludge energy is kept in the filtrate rather than being sent for recovery. Therefore, reducing the chemical energy contained in the filtrates and centrates is a potential way of elevating the digestion feedstock and hence improving CH_4 production.

Recovering energy from the un-recovered chemical energy reserve is also a measure to promote the $E_{ElecGen}$. From the chemical energy balance study of the sludge treatment (Figure 5-16), the end product of the digestion, the dewatered digested cake, contains approximately 20% of the influent sludge energy fed to the sludge treatment. Although it is currently not used for energy application in WWTP C, has proven could produce energy via pyrolysis or gasification (Mills et al., 2014, Cao and Pawłowski, 2012). The energy recovery from digested cake could also leads to a greater energy recovery efficiency from sludge.

Apart from improving the energy balance of WWTPs by focusing on elevating the $E_{ElecGen}$, efforts could also be made to reduce $E_{ElecCon}$. Activated sludge process, which is used by all four WWTPs and is well applied in wastewater treatment, is reported to account for approximately 50% of the total process energy demand (Scherson and Criddle, 2014). Although aerobic activated sludge still produces SAS that can be used for energy production via digestion, it consumes energy to convert the energy material into CO_2 (Wan et al., 2016). As shown in Figure 5-12, the activate sludge processes suffered 23-52% of chemical energy loss. Activated sludge process is further wasting the chemical energy within the wastewater. Energy generating biological treatment, such as anaerobic treatment and microbial fuel/electrolysis cell, generates energy, for instance CH_4, H_2 and electricity, while simultaneously removing organic contaminants (Shoener et al., 2014, Stoll et al., 2018). The produced energy is then used for offsetting energy consumption. This could be an alternative to the current aerobic activated sludge treatment.

5.4 Case studies of energy recovery

Four case studies are presented in this section. They aim to illustrate how it may be possible to improve the electrical energy balance of the WWTP by:

1. Improving solids removal efficiency in the primary settlement (Section 5.4.1)
2. Reducing the sludge retention time prior to digestion (Section 5.4.2)
3. Recovering energy from the dewatered digested sludge via pyrolysis (Section 5.4.3), and
4. Replacing the activated sludge processes with an energy-generating anaerobic membrane reactor (Section 5.4.4).

Apart from case study 3, all case studies are founded on software modeling outputs from GPS-X. The conceptual models used are built on the model of WWTP C. That is because the model has been calibrated and is able to represent the real-life performance of the sludge thickening, dewatering and sludge digestion. As stated in Sections 5.3.3, the COD concentration of the raw wastewater is a key influence on the prediction of the chemical energy and electricity that might be recoverable from wastewater. Therefore, the case studies do not suggest the exact value of chemical energy or electricity that could be recovered but illustrate the relative merits of these approaches in terms of potential energy production and energy consumption.

It is worth noting that the electricity consumption and generation are not predicted via the GPS-X. This is because historical data collected from Northumbrian Water for WWTP C does not clearly show the electricity consumption of each individual unit process but shows electricity usage for groups of processes (*personal communication*, L Wilkinson, Northumbrian Water, July 2018). These include screening, odor control, wastewater pumping, primary settlement scraping, RAS and SAS pumping, aeration, and sludge treatment (as shown in Figure 5-18). Hence, it is not possible to model the electricity consumption of individual units in the software. It is worth noting that the activated sludge the RAS and SAS pumping and aeration contributed 32% of the total consumption. Whilst, only 1% of the consumption is for the primary settlement scrapping.

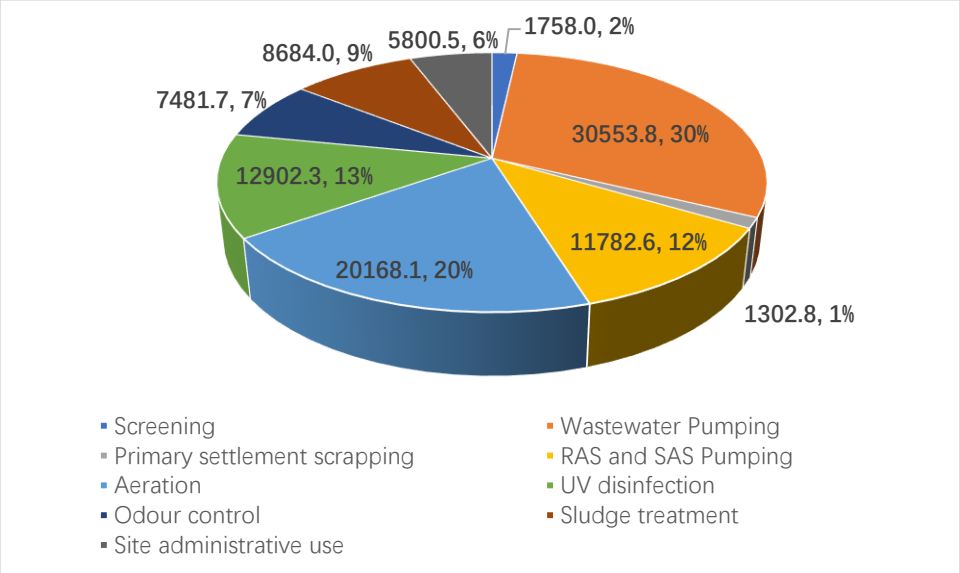

Figure 5-18 The breakdown of daily electricity consumption (kWh/d) of WWTP C

In this research, it is assumed that:

- Electricity consumption of primary settlement is proportional to the total solids content of the primary sludge,
- Electricity consumption of aeration is assumed proportional to total air flow required,
- Electricity consumption for sludge treatment (including pumping, thickening and dewatering) is proportional to the total TS fed to all four of the thickening and dewatering facilities (Mills et al., 2014),
- The other usage is considered as fixed consumption that will not change.

The per unit electricity consumption of the primary settlement, aeration and sludge treatment are calculated based on modelling results of the mass balance of WWTP C and are shown in Table 5-7.

Table 5-7 The per unit electricity consumption of the primary settlement, aeration, sludge treatment and fixed consumption of the WWTP C

	Total Consumption, kWh	Quantity	Per Unit Consumption
Primary Settlement	1302.8	54.2 tonnes TS	24.0 kWh/ton TS
Aeration	20,168.1	2,316,000 m^3 Air	0.0087 kWh/m^3 Air
Sludge treatment	8,684.0	261.8 tonnes TS	33.2 kWh/ton TS
Fixed Consumption	70,279	N/A	N/A

It is worth noting that the TS of the sludge is calculated from the predicted COD concentration of the sludge using Equation 5-7 which is derived from Equation 4-4 (in Section 4.2.3).

Equation 5-7

$$TS = (COD + 66.5) \div 1.3526 \div \frac{\text{VS}}{\text{TS}}\%$$

In Table 4-6, the mean observed VS/TS% of primary sludge, SAS, raw sludge, and digested sludge are 82.6±3.5%, 78.2±5.1%, 78.3±6.1%, and 67.8±1.6 %, respectively. For simplification, the VS/TS% of the primary sludge, SAS and raw sludge is taken as 80% and for digested sludge is taken as 70%.

5.4.1 Case study: Improving solids removal efficiency in primary settlement

5.4.1.1 Introduction

The sludge produced in the wastewater treatment becomes the feed stock to anaerobic digestion. As stated in Section 5.3.3, if the kinetic biological reactions of the secondary treatment remain constant, the wastewater treatment process will capture more chemical energy in the indigenous sludge if the primary settlement process is able to settle more chemical energy in its sludge. This study aimed to investigate the impact to the energy balance of the treatment works in a scenario in which solid removal efficiency of the primary settlement is improved.

5.4.1.2 Method

A conceptual model CM-4-1 (Figure 5-19) was constructed based on the model of WWTP C. Apart from transforming the model used for the primary settler from the "Simple1d" to an "empiric" model, the flow and concentrations of the raw wastewater and the configurations of the other processes remained the same. In the primary settler the settling model is changed to "empiric" and the sludge discharged is controlled by both the solid removal efficiency and the solid concentration of the primary sludge. The solid concentration is set to 26,360 mg/L which is the same as that in WWTP C.

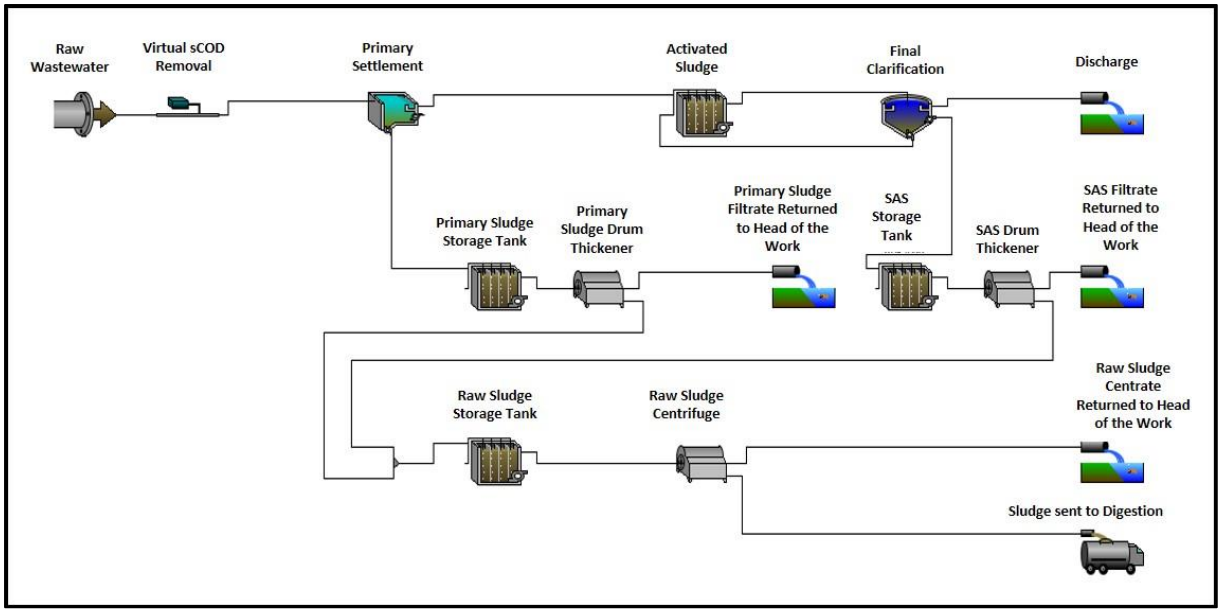

Figure 5-19 The conceptual model CM-4-1

For the sludge treatment modelling, it was assumed that there was no imported sludge, either before primary sludge thickening or after the raw sludge centrifuge. For modelling the digestion, to characterize the digester feed COD, TKN, TP, NH_4^+-N, PO_4^{3-}-P, VSS/TSS are required input variables. The study fixed the COD concentration of the digester feed (COD_{DF}) at 113,13780,280 mg/L which is the same as the original model. The flow of the digester feed (Q_{DF}) was calculated using Equation 5-8

Equation 5-8

$$Q_{DF} = \frac{Q_{DRS} \times COD_{DRS}}{COD_{DF}}$$

Where $\boldsymbol{Q_{DRS}}$ is the predicted flow of the dewatered raw sludge

$\boldsymbol{COD_{DRS}}$ is the predicted COD concentration of the dewatered raw sludge.

The TKN, TP, NH_4^+-N, PO_4^{3-}-P, VSS and TSS concentrations are then calculated using Equation 5-9.

Equation 5-9

$$C_{DF} = \frac{Q_{DRS} \times C_{DRS}}{Q_{DF}}$$

Where $\boldsymbol{C_{DF}}$ is the concentration of a parameter in the digester feed

$\boldsymbol{C_{DRS}}$ is the concentration of the corresponding parameter in the dewatered raw sludge.

The solid removal efficiency of primary settlement (SRE_{PS}) was incrementally changed from 0.40 to 0.70 at an interval of 0.05, to directly evaluate the influence of improved primary settlement efficiency on the energy balance. Changing the solid removal rate will affect the volume of sludge produced, which in turn may change the HRT in the raw sludge tank and in the digester. For the purposes of modelling, in order to make sure that the sludge undergoes fermentation to approximately the same extent during hydrolysis and digestion, in this study HRT was fixed at 410 hours and 505 hours in the raw sludge tank and the digester, respectively. The kinetics and model stoichiometry of the biological reaction in the activated sludge, all the sludge storage and anaerobic digestion will not be changed. Neither are the fractions of COD, nitrogen and phosphorus of the raw wastewater and the digester feed. The operational parameters at WWTP C were used in the models, and that they were always the same.

5.4.1.3 Results and discussion

The greater SRE_{PS} first results in a greater percentage of chemical energy captured in the primary sludge. It also results in a smaller percentage of chemical energy flowing to the activated sludge. In this case study, the stoichiometry and kinetics of the biological reactions in the activated sludge process stays the same, a smaller percentage of chemical energy is therefore captured in the SAS. However, the overall percentage chemical energy captured in the combined sludge increases from 50.3% to 58.6%. More chemical energy from the wastewater is captured and sent to the sludge treatment. The chemical energy balances are shown in Table 5-8.

Table 5-8 The chemical energy balance of the models with different SRE_{PS}

	SRE_{PS}						
	0.40	**0.45**	**0.50**	**0.55**	**0.60**	**0.65**	**0.70**
Final Effluent	15.1%	14.9%	14.9%	14.8%	14.8%	14.7%	14.7%
Loss in Activated sludge	34.7%	33.8%	32.5%	31.2%	29.7%	28.2%	26.7%
Primary Sludge	29.6%	33.2%	36.9%	40.6%	44.2%	47.9%	51.5%
SAS	20.7%	18.1%	15.7%	13.4%	11.3%	9.2%	7.1%
Primary sludge filtrate	2.8%	3.1%	3.4%	3.8%	4.1%	4.5%	4.8%
SAS filtrate	3.9%	3.1%	2.5%	2.1%	1.7%	1.3%	1.0%
Raw sludge centrate	8.1%	8.0%	7.7%	7.5%	7.2%	7.0%	6.6%
Dewatered Raw Sludge (as Digester Feed)	32.8%	34.7%	36.7%	38.7%	40.8%	42.9%	45.0%
CH_4	21.3%	22.5%	23.8%	25.1%	26.5%	27.8%	29.2%
Dewatered Digested Sludge	9.7%	10.3%	10.9%	11.5%	12.1%	12.8%	13.4%
Digested Sludge Centrate	1.7%	1.8%	1.9%	2.0%	2.1%	2.2%	2.3%

As shown in Table 5-8, in the subsequent thickening, the greater SRE_{PS} increases the percentage chemical energy retained in the primary sludge filtrate because the flow of primary sludge increases and reduces the percentage chemical energy in the SAS filtrate because there is less production of SAS. Because the reduction of chemical energy in the SAS filtrate is greater than the increase in chemical energy in the primary sludge filtrate, when the SRE_{PS} increases, the percentage chemical energy lost in the two combined filtrates still reduces from 6.7% (SRE_{PS}=0.4) to 5.8% (SRE_{PS}=0.7).

In addition, with an increase in SRE_{PS}, the proportion of the proportion of SAS in the combined sludge decreases. As shown in Table 5-9, when the SRE_{PS} increases, the predicted total COD fed to raw sludge increases slightly. At the same time, the substrate COD can be increased up to 45.7% whilst the heterotrophic biomass COD (originally produced in the activated sludge process) can be reduced up to 52.2%.

Table 5-9 COD, Substrate COD and Heterotrophic biomass COD of the sludge fed to the raw sludge storage tank

	SRE_{PS}						
	0.40	**0.45**	**0.50**	**0.55**	**0.60**	**0.65**	**0.70**
COD of the sludge fed to the raw sludge storage tank, mg/L	56280	57460	58350	59050	59670	60180	60570
Substrate COD of the sludge fed to the raw sludge storage tank, mg/L	27870	30050	32270	34450	36610	38660	40610
Heterotrophic biomass COD of the sludge fed to the raw sludge storage tank, mg/L	13450	12630	11530	10310	9036	7746	6435

The biological model used in the "Mantis2" model is developed from the activated sludge model No.2 d (ASM2d) (Hydromantis, 2017). In ASM2d, the extent of hydrolysis and fermentation are positively related to the concentration of heterotrophic biomass COD (Henze et al., 1999). As the HRT of the sludge storage time is fixed, because less heterotrophic biomass presents, hence less fermentation and hydrolysis happened in the raw sludge storage tank. Therefore, less COD is converted into sCOD which would be lost in the subsequent sludge dewatering. When the SRE_{PS} is changed from 0.4 to 0.7, the percentage COD loss due to raw sludge dewatering is reduced from 8.1% to 6.6%, and the overall percentage COD loss prior to digestion is 14.8% to 12.4%. Since more energetic COD is available to the digester, more chemical energy is therefore available to the digester and leads to more biogas is produced. Meanwhile, the extent of digestion of sludge is fixed in all cases, a greater digester feed leads to a greater percentage chemical energy captured in the dewatered digested sludge.

With respect to electricity, although the increase of SRE_{PS} results in less energy consumption during aeration (from 20,203 kWh/d to 16,180 kWh/d), the electricity consumption for primary settlement and sludge treatment also increases due to a greater production of primary sludge (from 6,417 kWh/d to 7,671 kWh/d). Overall, the electricity consumption is only reduced slightly, by up to 1.9%. However, the electricity production could increase by up to 32.2%. The electricity deficit is substantially reduced, and the reduction is up to 39.3%. The electricity balance is shown in Table 5-10.

Table 5-10 The electricity balance of the models with different SRE_{PS}

	SRE_{PS}						
	0.40	**0.45**	**0.50**	**0.55**	**0.60**	**0.65**	**0.70**
Primary Settlement, kWh/d	1217	1368	1519	1670	1821	1971	2122
Aeration, kWh/d	20203	20046	19541	18836	18026	17129	16180
Fixed consumption, kWh/d	70279	70279	70279	70279	70279	70279	70279
Sludge Treatment, kWh/d	6417	6572	6763	6974	7196	7433	7671
Total Consumption, kWh/d	98116	98265	98102	97759	97322	96812	96252
Electricity Generation, kWh/d	51352	53619	56348	59251	61900	64944	67872
Electricity Deficit, kWh/d	46764	44647	41754	38507	35422	31868	28380

Improving the SRE_{PS} may result in elevated biogas production, slightly reduced electricity consumption, and consequently an improvement in the overall energy balance of the wastewater treatment works.

The uncertainty in this case study is how to actually improve the SRE_{PS} operationally. It has been suggested that SRE can be improved by dosing aluminum and ferric salts (Ismail et al., 2012, Sarparastzadeh et al., 2007). However, in this case study the SRE_{PS} is adjusted by tuning the operational parameter of the "empiric" model that controls the primary settlement. There is no chemical dosing involved since the chemical dosing in the GPS-X is not able to enhance the SRE_{PS}. Meanwhile, Diamantis et al. (2013) reports that a high dosage of aluminium or ferric coagulant may reduce the digestibility. Therefore, if chemical dosing is applied to elevate the SRE_{PS}, a thorough investigation of possible changes to the dewaterability or digestibility of the sludge is recommended.

5.4.2 Case study: Reducing the sludge retention time prior to digestion

5.4.2.1 Introduction

Sludge thickening and dewatering aims to reduce water content of the feed sludge for various purposes, such as reducing sludge volume or raising the TS content to meet requirements for subsequent treatment. Inevitably some of the solid, both volatile and fixed, will remain in the filtrate or centrate rather than being retained in the thickened or dewatered sludge. From a waste recovery perspective, considering that the sludge will ultimately be fed to the digester for energy recovery, that portion of the solid that remains in the filtrate or centrate will not be

available for energy production. The loss of solids in the filtrate or centrate should therefore be minimized.

The loss of solid can be influenced by the solids retention capability of the sludge thickening and dewatering process, but also by biological activity in the sludge before thickening and dewatering. In the case of WWTP C, considerable amounts of the particulate COD of the feed sludge to the raw centrifuge are solubilized due to the long storage time, effectively resulting in greater solid loss in the centrate. This case study investigates the impact of reducing the size of the sludge storage tank to reduce the loss of potential energy during the raw sludge dewatering.

5.4.2.2 Method

The conceptual model CM-4-1 is applied in this case study. The sludge retention time of the raw sludge storage tank was decrementally changed from its original level of 410 hour to 0 hour at a percentage interval of 20%, to directly evaluate the influence of sludge storage time on the energy balance. The raw sludge storage tank was therefore assumed as a virtual unit. Its tank size was given values of 26,086 m^3 (100%), 20,869 m^3(80%), 15,652 m^3(60%), 10,434 m^3(40%), 5,217 m^3(20%), 0 m^3(0%). When the tank size is 0 m^3, it means the raw sludge will not be stored.

As in Section 5.4.1, the tank size of the digester will be adjusted to ensure approximately constant HRT. The solid removal efficiency of the primary settlement tank will also be fixed at 0.40. The kinetics and model stoichiometry of the biological reaction in the activated sludge, all the sludge storage tanks and anaerobic digestion will not be changed. The fractions of COD, nitrogen and phosphorus of the raw wastewater and the digester feed also remain the same. Finally, the operational parameters of the sludge dewatering unit remain unchanged in this study.

5.4.2.3 Results and discussion

The chemical energy balance of the wastewater treatment, primary sludge thickening, and SAS thickening is not influenced by the change in volume of the raw sludge storage tank.

When the effects of a decrease in volume of the raw sludge storage tank are modelled, the retention time of sludge reduces, and hence the degree to which raw sludge solubilizes decreases. As a result, the sCOD of the raw sludge centrate decreases. As shown in Table 5-11, there may be an approximately 62-fold variation in sCOD concentration, with a consequent variation of the COD in the raw sludge centrate.

Table 5-11 The change of sCOD, pCOD and COD over different raw sludge storage time

Tank Volume, m^3	sCOD, mg/L	pCOD, mg/L	COD, mg/L
26086	7305	5073	12378
20869	6628	5247	11875
15652	6351	5422	11773
10434	5631	5695	11326
5217	3719	6128	9847
0	117	6872	6989

The reduction of tank size reduces the percentage COD (also chemical energy) lost in the raw sludge centrate and simultaneously increases the percentage of COD (and chemical energy) fed to the digester, from 34.9% up to 41.4%. Ultimately, this leads to a greater biomethane production up to 23.3% of the chemical energy can be recovered as. The chemical energy balances are shown in Table 5-12.

Table 5-12 The chemical energy balance of models with different raw sludge storage time

	Tank volume, m^3					
	26086	**20869**	**15652**	**10434**	**5217**	**0**
Final Effluent	13.7%	13.7%	13.7%	13.7%	13.7%	13.7%
Loss in Activated sludge	31.6%	31.6%	31.6%	31.6%	31.6%	31.6%
Primary Sludge	29.5%	29.5%	29.5%	29.5%	29.5%	29.5%
SAS	25.3%	25.3%	25.3%	25.3%	25.3%	25.3%
Primary Sludge Filtrate	2.8%	2.8%	2.8%	2.8%	2.8%	2.8%
SAS Filtrate	5.7%	5.7%	5.7%	5.7%	5.7%	5.7%
Raw Sludge Centrate	8.7%	8.3%	8.2%	7.9%	6.9%	4.9%
Dewatered Raw Sludge (as Digester Feed)	34.9%	35.5%	36.3%	37.4%	39.0%	41.4%
CH_4	19.6%	19.9%	20.4%	21.0%	21.9%	23.3%
Dewatered Digested Sludge	10.7%	10.9%	11.2%	11.5%	12.0%	12.8%
Digested Sludge Centrate	1.7%	1.7%	1.8%	1.8%	1.9%	2.0%

With respect to electricity, a decrease in size of the raw sludge storage tank has no impact on the processes prior to the raw sludge dewatering, as shown in Table 5-13. Because solids

solubilization is reduced, more solid is fed to the raw sludge dewatering and the subsequent digester sludge dewatering. The predicted total sludge solid treated could increase from 193.5 tonnes to 203.0 tonnes. As shown in Table 5-13, the total electricity consumption therefore increases very slightly, by up to 0.3%. For the electricity production, the percentage increase could be up to 18.8%. The electricity deficit could also be substantially reduced by up to 20.0%.

Table 5-13 The electricity balance of models with different Raw sludge storage time

	Tank volume, m^3					
	27248	**21798**	**16349**	**10899**	**5450**	**0**
Primary Settlement, kWh/d	1217	1217	1217	1217	1217	1217
Aeration, kWh/d	20203	20203	20203	20203	20203	20203
Fixed consumption, kWh/d	70279	70279	70279	70279	70279	70279
Sludge Treatment, kWh/d	6417	6446	6510	6583	6651	6735
Total Consumption, kWh/d	98116	98145	98209	98282	98350	98434
Electricity Generation, kWh/d	51352	52012	53281	54917	57251	61020
Electricity Deficit, kWh/d	46764	46132	44928	43365	41099	37414

The conclusion from this is that reducing the sludge storage time could prevent loss of energy-containing material during sludge dewatering, and therefore enable greater energy recovery. In the example of WWTP C, the raw sludge storage tank is built for contingency if the downstream processes of THP or digester is shut down due to broken down or being maintained (*personal communication*, L Wilkinson, Northumbrian Water, October 2018). The long sludge storage time is not intentional but is due to the building up of sludge is because of the occasionally shut down of certain THP and digester (*personal communication*, L Wilkinson, Northumbrian Water, October 2018). Therefore, it is possible to reduce the sludge storage time.

5.4.3 Case study: Recovering energy from the dewatered digested sludge via pyrolysis

5.4.3.1 Introduction

As shown in the previous Section 5.3.2 in WWTP C, approximately 20% of the sludge chemical energy is stored in the dewatered digested sludge. This case study investigates the use of pyrolysis to recover this energy for electricity production.

5.4.3.2 Method

This pyrolysis modelling is built on the model CM-4-1, in which a solid removal efficiency of primary settlement of 0.4 is assumed. The TS content of the dewatered digested sludge is estimated using Equation 5-7.

The design of the pyrolysis module is based on Mills et al. (2014). The module has three units:

1. sludge drying, which utilizes low-grade heat to dry the sludge to reach 90% DS (Mills et al., 2014)
2. fast pyrolysis to convert biosolids into syngas
3. CHP for combusting the syngas to produce electricity and heat production.

A schematic illustration of the process is shown in Figure 5-20.

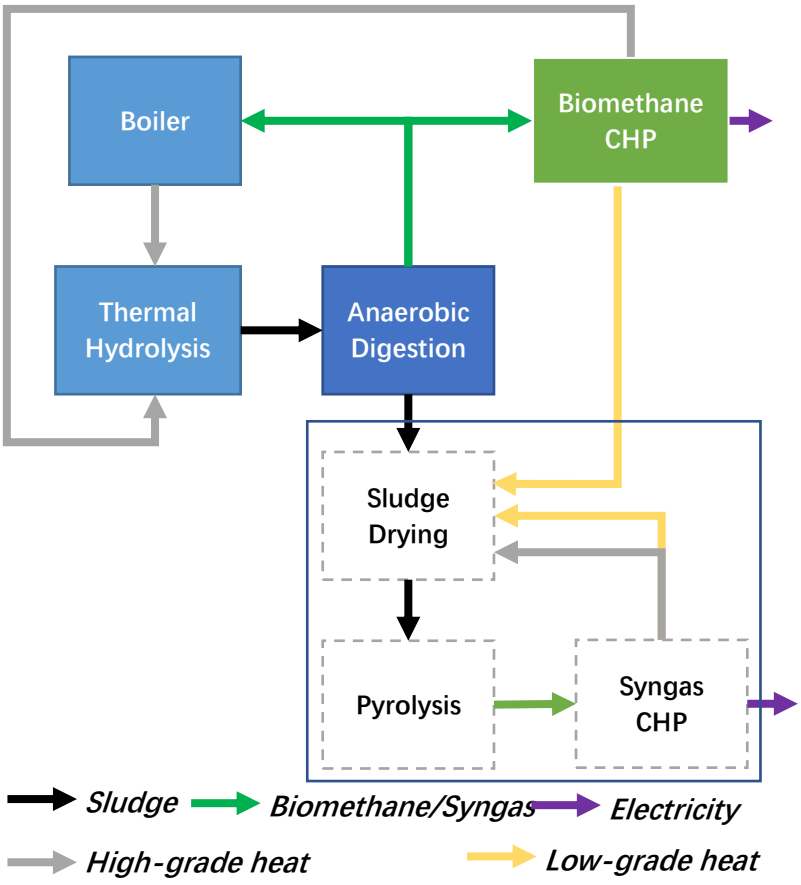

Figure 5-20 Schematic illustration of the dewatered digested sludge pyrolysis module

The key assumptions made for this case study are as follows:

- In the sludge drying, 0.9 MWh heat is required per tonne of water evaporated (Mills et al., 2014). 0.055 MWh electricity is required to process each tonne of TS content (Mills et al., 2014). Both high-grade heat and low-grade heat can be used for the heat supply
- In the pyrolysis, 80% of the chemical energy stored in the sludge will be converted into syngas (Mills et al., 2014, Cao and Pawłowski, 2012). Meanwhile, 0.4 MWh electricity is required to treat each tonne of DS (Mills et al., 2014).
- In both CHP units, the electricity conversion ratio is 38%, and both the high grade heat conversion ratio and low grade heat conversion ratio is 20% (Bowen et al., 2010, Smyth et al., 2016).

5.4.3.3 Results and discussion

When the solid removal efficiency of primary settlement is 0.4, conceptual model CM-4-1 predicts the dewatered digested sludge has a COD concentration of 257,417.2 mg/L and a predicted flow of 78.9 m^3/d. Via Equation 5-7, TS concentration is estimated as 265,655.8 mg/L. Since the density of sludge is assumed to be 1,000,000 mg/L in this study (explanation shown in Appendix C). The TS% of the dewatered digested sludge is estimated as 26.5%. The TS loading is 21.0 tonnes. Via Equation 4-2, chemical energy loading of the dewatered digested sludge is estimated as 87.1 MWh.

In the sludge drying process the electricity consumption is 19.0×0.055 = 1.155 MWh and the heat consumption is 0.9×[(21.0÷26.5%)-(19.0÷90.0%)] = 52.3 MWh. For the pyrolysis, 0.4×21.0=8.4 MWh electricity is required. Therefore, the total energy consumption of the module is 52.3 MWh heat and 9.6 MWh electricity.

For energy production, 87.1×80%=69.7 MWh syngas is produced. In the subsequent CHP application, 69.7×38%=26.4 MWh electricity and 69.7×20%+69.7×20%=27.9 MWh heat (combines the high-grade heat and low-grade heat) are produced. Therefore, the net electricity production is 16.8 MWh but there is a heat deficit of 24.4 MWh. The predicted biomethane production is 159.7 MWh in conceptual model CM-4-1, when the solid removal efficiency of primary settlement of 0.4. The heat deficit will be supplemented by the low-grade heat produced in the biomethane CHP since the production is 159.7 MWh×85%×20%=27.1 MWh.

As stated in Section 5.4.1, the electricity deficit of the WWTP is approximately 46.7 MWh. With the net electricity output from the pyrolysis module is 16.8 MWh, the gap is reduced by 35.9% to 29.9 MWh.

Unlike the previous two case studies, in which the process modification is upstream of the digestion, the pyrolysis targets the end product, and hence has the advantage that it would have no impact on upstream processes or energy recovery of the digestion. The key to success of this approach is to meet the low-grade heat demand for the sludge drying. Moreover, the two case studies focused on operational adjustments, whereas the sludge pyrolysis would require capital investment for installation of sludge drying, pyrolysis and the CHP infrastructure.

5.4.4 Case study: Replacing the activated sludge processes with an energy-generating anaerobic membrane reactor unit

5.4.4.1 Introduction

This case study investigates the benefits of replacement of the aerobic activated sludge treatment process with an anaerobic membrane reactor (AnMBR) for reducing the energy consumption of biological treatment of the wastewater.

5.4.4.2 Method

A conceptual model CM-4-2 is built on CM-4-1 in GPS-X (as shown in Figure 5-21). The predicted result generated by the CM-4-2 will be used to construct an energy balance. The newly obtained energy balance will be compared to the baseline case energy balance obtained from the CM-4-1 while the SRE_{PS} is 0.4. There are several key adjustments made in the model CM-4-2 comparing to CM-4-1:

- The "Anaerobic MBR" is used to replace the existing activated sludge process. According to Gimenez et al. (2011) and Gouveia et al. (2015), the tank size is given 66,406 m^3 for achieving the HRT to approximately 6 hours, and the mixed liquor suspended solid (MLSS) is set as 20,000 mg/L and is control by a PID controller. The stoichiometry and kinetics of the biological reactions of the "Anaerobic MBR" remain at their default value in the model. The treated effluent of the AnMBR will be discharged as final effluent.
- The solid removal efficiency of the primary settlement remains fixed at 0.40. The

surplus AnMBR sludge (SAnS) produced will be thickened in a similar way to the SAS thickening in model CM-4-1. However, because the MLSS of the AnMBR is set as 20,000 mg/L instead of the 2,805 mg/L used in CM-4-1, the "fraction of influent flow" of the SAnS drum thickener is changed to 0.35 in order to obtain thickened SAnS with similar COD content of the thickened SAS (in the original model CM-4-1).

- The kinetics and model stoichiometry of the biological reactions of all of the sludge storage tanks, and the rest of the thickening and dewatering facilities, will not be changed.
- In anaerobic digestion, the fraction of "P content of the inert particulate material" of the digester feed is changed from 0.021947 to 0.01794 in order to allow the feed sludge to have the same extent of digestion as in the baseline case.

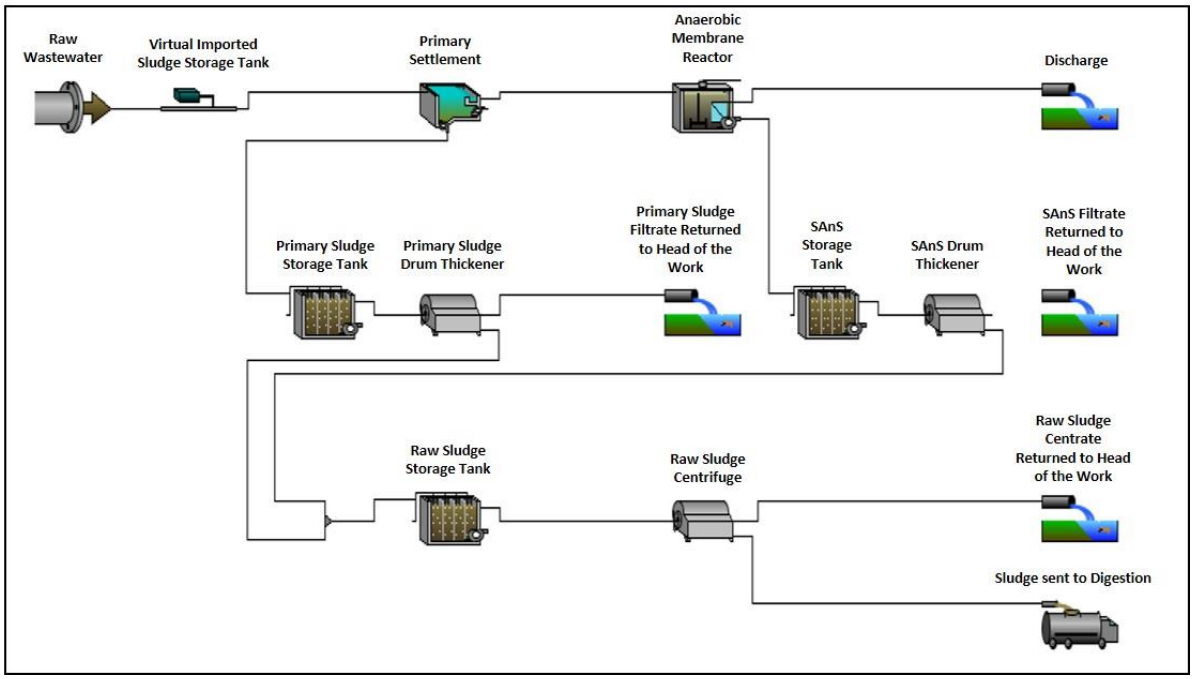

Figure 5-21 The conceptual model CM-4-2

For electricity consumption, the AnMBR is assumed to be energy self-sustaining and the original activated sludge related electricity consumption, including the consumption on aeration, RAS and SAS pumping will be ignored in the calculation

5.4.4.3 Result and discussion

The chemical energy balance of the baseline case (uses aerobic activated sludge as secondary treatment) and the AnMBR model are listed in Table 5-14.

Table 5-14 The chemical energy balance of the baseline model outputs and the AnMBR model outputs

	Baseline	AnMBR
Final Effluent	13.7%	10.8%
Ends Gaseous Product	31.6%	45.8%
Primary Sludge	29.5%	29.5%
SAS/SAnS	25.3%	13.9%
Primary Sludge Filtrate	2.8%	2.8%
SAS Filtrate	5.7%	2.3%
Raw Sludge Centrate	8.7%	3.9%
Dewatered Raw Sludge (as Digester Feed)	34.9%	30.7%
CH_4	19.6%	17.2%
Dewatered Digested Sludge	10.7%	9.3%
Digested Sludge Centrate	1.7%	1.5%

Using AnMBR results in a lower COD concentration in the final effluent, and hence the percentage chemical energy in the final effluent is less (10.8%) than if activated sludge is used (15.1%). Moreover, the percentage chemical energy captured in the SAnS is less than what is captured in the SAS. Therefore, in the AnMBR model, less chemical energy is fed to sludge treatment. Anaerobic treatment is reported to produce less sludge than aerobic treatment (Gimenez et al., 2011, Gouveia et al., 2015). The predicted COD and TSS loading of the SAS of base line model are 46.9 tonnes and 40.3 tonnes, respectively. The predicted COD and TSS loading of the SAnS are approximately half of the SAS loading and are 25.8 tonnes and 25.0 tonnes, respectively. Regarding the TSS produced per g COD removed, the predicted result is 0.23g TSS/g $COD_{Removed}$ which is in the reported range of 0.16-0.55g TSS g $COD_{Removed}$ (Gouveia et al., 2015). Modelling the use of AnMBR, 45.7% of the inflowing chemical energy ends up as gaseous product. Unlike the model results for the activated sludge process, the product is CH_4 rather than CO_2. The CH_4 production is 22,710 m^3 and results in a specific methane yield of 0.21L CH_4/g $COD_{Removed}$ which is also in the reported range of 0.13-0.24 L CH_4/g $COD_{Removed}$ (Gouveia et al., 2015, Gimenez et al., 2011). Although the model uses the default kinetic and stoichiometry of biological reaction in the AnMBR model, the predicted result is in agreement with the literature value.

During the sludge treatment prior to digestion, the major difference is in the raw sludge centrate. The AnMBR process has a weaker raw sludge centrate because the biomass contained in the

SAnS has very little heterotrophic biomass and hence the solubilization of the particulate COD is weaker. In the digestion, less CH_4 is produced in the AnMBR model because the sludge produced from the wastewater side is less, but the difference is small.

With respect to electricity, the generation from CH_4 produced from the sludge of AnMBR is approximately 12% less than if the activated sludge process (the baseline model) was used, as shown in Table 5-15. However, this study disregards the electricity consumption of the original activated sludge process, whilst the AnMBR is primarily assumed energy self-sustaining. In this sense, the electricity consumption is reduced substantially by 33.9%, as is the electricity deficit (by 57.7%).

Table 5-15 The electricity balance of the activated sludge and the AnMBR processes

	Activated Sludge	**AnMBR**
Primary Settlement, kWh/d	1217.1	1217.1
Aeration, kWh/d	20202.9	0.0
Fixed consumption, kWh/d	70278.9	58496.3
Sludge Treatment, kWh/d	6417.2	5143.6
Total Consumption, kWh/d	98116.1	64857.0
Electricity Generation, kWh/d	51352.2	45065.1
Electricity Deficit, kWh/d	46763.9	19791.9

The biggest uncertainty that affects the energy balance is whether the AnMBR process is able to be energy self-sustaining. Martin et al. (2011) reported that the energy demand of the submerged AnMBR varies from 0.03-3.57 kWh/m^3. In this case study, the CH_4 produced from the AnMBR is 22,710m^3×0.651kg/m^3×55,500kJ/kg÷3600kJ/kWh=227,923 kWh. While the flow of raw wastewater is 277,236 m^3/day, the energy produced from 1 m^3 wastewater is 0.82 kWh. Therefore, there is a possibility that the AnMBR is not energy self-sustaining. In the case if the AnMBR requires 3.57 kWh energy to treat 1 m^3 influent, 989,732 kWh heat energy is required. The heat deficit of the AnMBR will be 761,709 kWh. The implementation of the AnMBR process would have a high degree of uncertainty. Moreover, although full scale application has been reported, the requirement for COD concentration of the feed wastewater is measurable in tens of thousands (Basile et al., 2015); in all four investigated WWTPs the COD of the raw wastewater is no greater than 1,200 mg/L(Table 5-1), and of the settled wastewater is no greater than 700 mg/L (Table 4-1).

5.5 Chapter summary

This study constructed, calibrated and validated models for the wastewater and sludge treatment processes of four WWTPs. In all cases the predicted results differed from the observed results by no more than ± 15%. These predicted results were then used to construct COD and chemical energy mass balances for the WWTPs. Finally, the potential to improve the energy efficiency of the WWTPs was investigated by modelling the impact of various operational and process changes to the WWTPs.

The mass and energy balance of the four WWTPs shows that:

- the primary settlement captured 46.3 ± 12.0% of influent COD and chemical energy in the primary sludge. The remainder flowed into the secondary treatment.
- Activated sludge as the secondary biological treatment captured 44.4 ± 15.5% of its own influent COD and chemical energy in the SAS. Meanwhile, 42.2 ± 13.0% of the influent COD and chemical energy to the activated sludge is lost, potentially as CO_2. The remaining 13.6 ± 5.4% will leave the treatment works as final effluent.
- Overall, 69.7 ± 12.8% of COD and chemical energy flowing into the works can be captured in the sludge and sent for sludge treatment via digestion, and the rest is lost, either to atmosphere or in the final effluent.

In the sludge treatment, due to several stages of thickening and dewatering prior to the digestion, only 65.3% of the influent sludge energy actually reaches the digester, on average. Since the digester has a 57.0% of energy recovery efficiency, 38.8% of the chemical energy fed to the sludge treatment can be recovered as CH_4, whilst 20.4% of the sludge energy remains in the dewatered digested sludge, and approximately 30% of the sludge energy is left in the filtrates and centrates.

On this basis, approximately 20-30% of the chemical energy in the raw wastewater has the potential to be recovered as CH_4. However, only 6-9% of the chemical energy in the raw wastewater can be potentially recovered as electricity. In this study, even though the chemical energy within the raw wastewater of the investigated WWTPs is 5-14 times higher than its electricity consumption, the WWTPs are not always electricity self-sustaining.

The results of this research suggest that it should be feasible to improve the energy balance at WWTPs by:

- improving the efficiency of solids removal in primary settlement
- reducing the sludge retention time prior to the digestion
- recovering energy from the dewatered digested sludge via pyrolysis, and
- reducing the electricity consumption by replacing the activated sludge processes with energy-generating anaerobic membrane reactor (AnMBR) units.

Modelling case studies were undertaken around these four areas, and results indicated that the electricity deficit could be reduced by implementing operational and/or process changes. However, some approaches have significant drawbacks and uncertainties. For example, the coagulant used for improving the settling performance of the primary treatment may have adverse effects on sludge digestion, and the energy balance of AnMBR units is highly uncertain. The implementation in the real world needs further investigation.

Chapter 6 Results and Discussion: Nitrogen and Phosphorus Mass Balances of Wastewater Treatment Plants

This chapter presents the nitrogen and phosphorus balances of each process of the four WWTPs studied (Section 6.1). Based on these balances the nutrient recovery opportunities from wastewater and sludge are discussed in Section 6.2. Case studies are also presented, which investigate the potential to improve nutrient recovery from sludge at WWTPs. In Section 6.3 the impact of implementing energy recovery technologies on the effectiveness of nutrient recovery is discussed.

6.1 Nitrogen and phosphorus mass balance of individual treatment processes

6.1.1 Nitrogen and phosphorus mass balances of primary settlement units

The flow and concentration data predicted via modelling were used in the construction of the nitrogen and nitrogen and phosphorus mass balances of primary settlement units.

In the case of WWTP A and D which have reactive settler, the sum of the total nitrogen (TN) and total phosphorus (TP) of the sludge and effluent wastewater from the primary settlement are >99% of the inflowing. The amount of TN and TP cannot be accounted for is considered as loss but is negligible i.e.<1.0%. Therefore, even there is the biological sludge is recirculated back to the primary settlement, the TN and TP loss caused by the biological reaction can be ignored. The difference of the inflowing and outflowing TN and TP is smaller than 1.0%, and hence both the nitrogen and phosphorus mass balance is considered reliable. The mass balance is shown in Figure 6-1.

In terms of the distribution pattern, after primary settlement, 8-22.8 % of inflowing TN and 16.1-50.5 % of inflowing TP is captured in the primary sludge and 76.7-92.0% of the inflowing TN and 49.6-83.9% of inflowing TP remains in the primary effluent.

The TN and TP captured by the primary sludge is positively related to the COD captured by the primary sludge (shown in Figure 5-5). The main removal mechanism in the primary

settlement tanks is physical settling of particulates (Tchobanoglous et al., 2003). The particulate nitrogen and phosphorus settled and captured in the primary sludge is proportional to the COD settled in primary sludge. In the case of WWTP A, the TP captured by the primary sludge is substantially higher than in the other three treatment plants. That is because this site has ferric dosing and hence part of the soluble phosphate is converted into particulate ferric phosphate which then settles (Tchobanoglous et al., 2003).

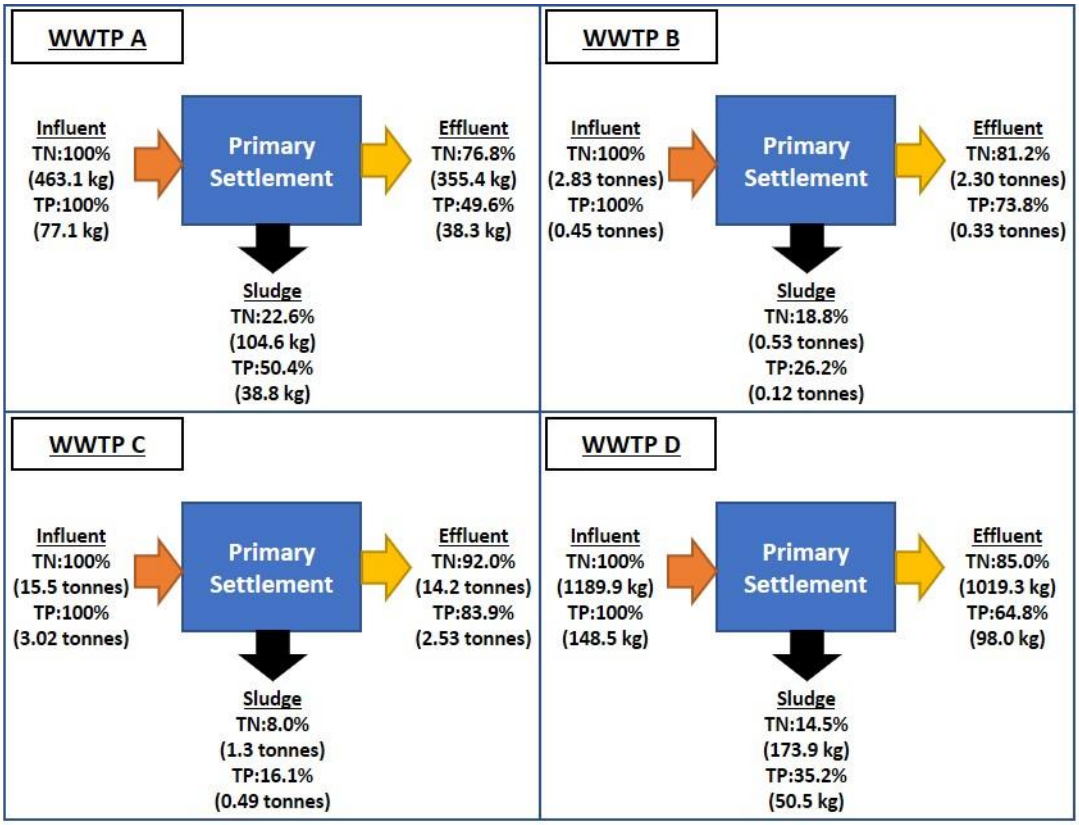

Figure 6-1 The nitrogen and phosphorus mass balances of primary settlement in a daily basis at the four WWTPs investigated

At the four study WWTPs the percentage of the influent TP captured in the primary sludge is greater than the percentage of TN. That is likely because in the raw wastewater of each plant the ratio of the estimated particulate phosphorus to TP is greater than the ratio of the estimated particulate nitrogen to TN (consists of mainly the total Kjeldahl nitrogen (TKN)), as shown in Table 6-1. Using WWTP C and D (which have no ferric dosing for phosphate removal) as examples, particulate phosphorus is 36.2% of TP for WWTP C and 58.3% for WWTP D. This is approximately twice the particulate nitrogen percentage of TN (16.3% for WWTP C and 21.8% for WWTP D).

Table 6-1 The particulate phosphorus, TP, the particulate nitrogen and TN of the raw wastewater of the four study WWTPs

	particulate TKN	TKN, mg/L	TN, mg/L	particulate phosphorus	TP
WWTP A	13.3	50.9	51.16	4.38	8.52
WWTP B	15.1	56.93	56.93	1.82	9.13
WWTP C	9.06	55.5	55.5	3.92	10.82
WWTP D	6.93	31.83	32.13	2.32	3.98

Literature values suggest that the percentage of nitrogen captured in primary sludge is only 10-25 % (Kristensen et al., 2004, Sötemann et al., 2006). Therefore, 75-90 % of nitrogen in wastewater treatment works flows to the secondary treatment process. For phosphorus removal, if there is no chemical dosing, 75-80 % of the phosphorus to the treatment works will flow to secondary treatment. If chemical dosing is used then 18-80% of the phosphorus mass entering primary settlement will flow to secondary treatment (Kristensen et al., 2004, Grizzetti and Bouraoui, 2006) and Grizzetti and Bouraoui (2006). The nitrogen and phosphorus mass balances reported in this study are similar to these literature values.

6.1.2 Nitrogen and phosphorus mass balance of secondary biological treatment as activated sludge

The flow and concentration data predicted via modelling were used in the construction of the nitrogen and nitrogen and phosphorus mass balances of activated sludge.

In all four activated sludge systems the differences between inflowing and outflowing phosphorus mass are negligible. The phosphorus mass balance is considered reliable. The nitrogen mass balance of the activated sludge process of WWTP B and C are also considered reliable because the inflowing nitrogen loading equals the outflowing. For WWTP A and D, their nitrogen balances are not closed because part of nitrogen is missing from the sludge and wastewater effluent suggested by the modelling results. The missing nitrogen loading is assumed left as gaseous product to the atmosphere. The nitrogen and phosphorus mass of the activated sludge process and its subsequent clarification is shown in Figure 6-2.

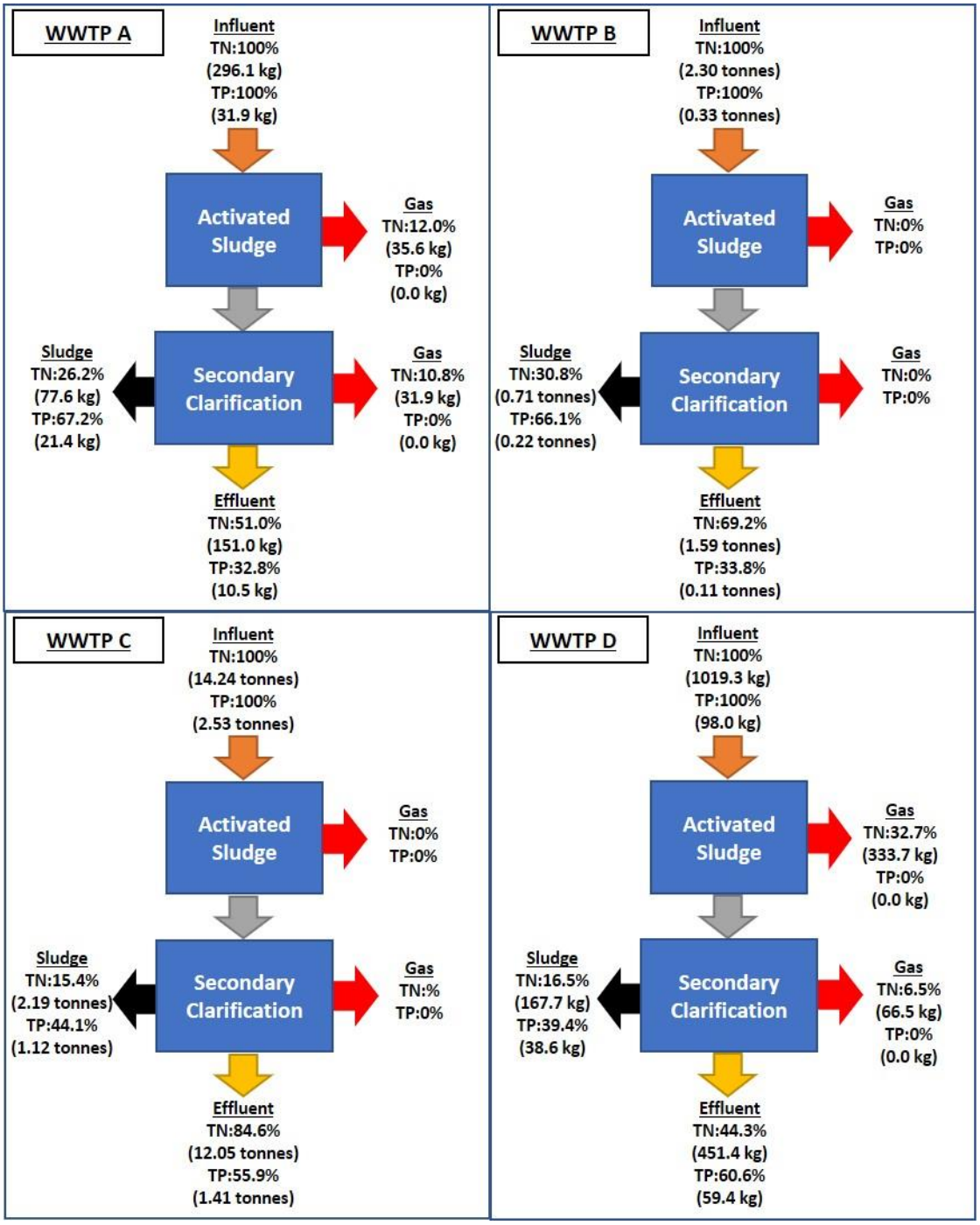

Figure 6-2 The nitrogen and phosphorus mass balances of secondary biological treatment in a daily basis at the four WWTPs investigated

The percentages of TN and TP captured by the surplus activated sludge (SAS) are also positively proportional to the COD captured by the SAS (Figure 5-12). However, the reason for this relationship does not appear to be the same as in the primary settlement (the proportion of TN and TP that is in particulate form). The proportion of nutrient captured in the SAS appears mainly to be because of biomass assimilation. The biomass requires carbon, nitrogen

and phosphorus to grow (Droste, 1997, Tchobanoglous et al., 2003). The biomass grown is generally expressed as $C_5H_7O_2NP_{0.074}$ (Droste, 1997), and the GPS-X model expresses it as $C_5H_7O_2N_{0.8}P_{0.1}K_{0.02}Mg_{0.02}Ca_{0.01}$. Thus, if more biomass is produced, a greater percentage of TOC (also COD) is captured in the SAS in the form of biomass, and the same applies to the nitrogen and phosphorus.

This study found that a considerable amount of nitrogen is lost in the aeration and final clarification units in WWTPs A and D, whereas this is not the case in WWTPs B and C. Unintentional denitrification during aeration and final clarification has been reported previously (Flores-Alsina et al., 2010, Ji et al., 2015, Satoh et al., 2003), and that may be the reason for N loss in WWTPs A and D. For denitrification to occur there must be a good source of nitrate and an anoxic environment (Tchobanoglous et al., 2003). WWTPs B and C do not include a nitrification process. Hence no nitrate is produced and there is no denitrification. WWTPs A and D do have nitrification, and hence nitrate is available and denitrification is possible.

The anoxic environment is formed differently in the activated sludge tank than in the final clarification. Denitrification occurs in the aerated activated sludge due to a low DO concentration, which means that the inner core of the biomass floc remains in an anoxic condition (Tchobanoglous et al., 2003, Ji et al., 2015). Wilson and Bouwer (1997) reported the threshold DO that inhibits denitrification ranges from 0.08-7.9 mg/L. In this study, the DO concentrations of WWTP A and WWTP D are 2.0 mg/L and 0.66 mg/L respectively. They both smaller than the highest reported threshold DO of 7.9 mg/L. Therefore, denitrification could take place. In the final clarification, since there is has no aeration involved, anoxic or anaerobic condition is formed naturally (Flores-Alsina et al., 2010). This also potentially enables the denitrification.

Denitrification requires not only nitrate but also a source of readily biodegradable substrate (Tchobanoglous et al., 2003). The activated sludge tank is likely to have sufficient substrate for more denitrification to occur because it is where the substrate rich primary effluent first flows. But the final clarification, which is after the activated sludge process, may have less available substrate. Thus, less denitrification is likely during final clarification than in the activated sludge process.

The nitrogen loss can also be attributed to nitrous oxide (N_2O), which is an intermediated product of the denitrification process (Foley et al., 2010). However, because the gaseous product was not collected in the sampling campaign, it was not possible to confirm the production of N_2O during this study.

Apart from causing potential nitrogen loss, the nitrification also affects the composition of the nitrogen compounds in the activated sludge treated effluent. As shown in Table 6-2, for WWTPs A and D with nitrification, the nitrate and nitrite nitrogen (NO_3^--N and NO_2^--N) contributes 42.6-78.4% of the TN, whilst for WWTPs C and D, the ammonium nitrogen (NH_4^+-N) contributed 85.5-93.9% of the TN.

Table 6-2 The predicted concentrations of different types of nitrogen of the activated sludge treated effluent at the four WWTPs investigated

	NH_4^+-N, mg/L	NO_2^--N, mg/L	NO_3^--N, mg/L	TN, mg/L
WWTP A	0.9	2.4	13.7	20.5
WWTP B	31.9	0.0	0.0	33.9
WWTP C	38.0	0.0	0.0	44.4
WWTP D	3.0	0.6	4.7	12.2

6.1.3 Nitrogen and phosphorus mass balance of sludge thickening and dewatering

The flow and concentration data predicted via modelling were used in the construction of the nitrogen and nitrogen and phosphorus mass balances of sludge thickening and dewatering.

The differences between inflowing and outflowing nitrogen and phosphorus mass of each sludge thickening and dewatering facility were <0.5% and were negligible. Therefore, the mass balances are considered closed. The nitrogen and phosphorus mass balances of each thickening and dewatering processes in WWTP C are shown in Figure 6-3.

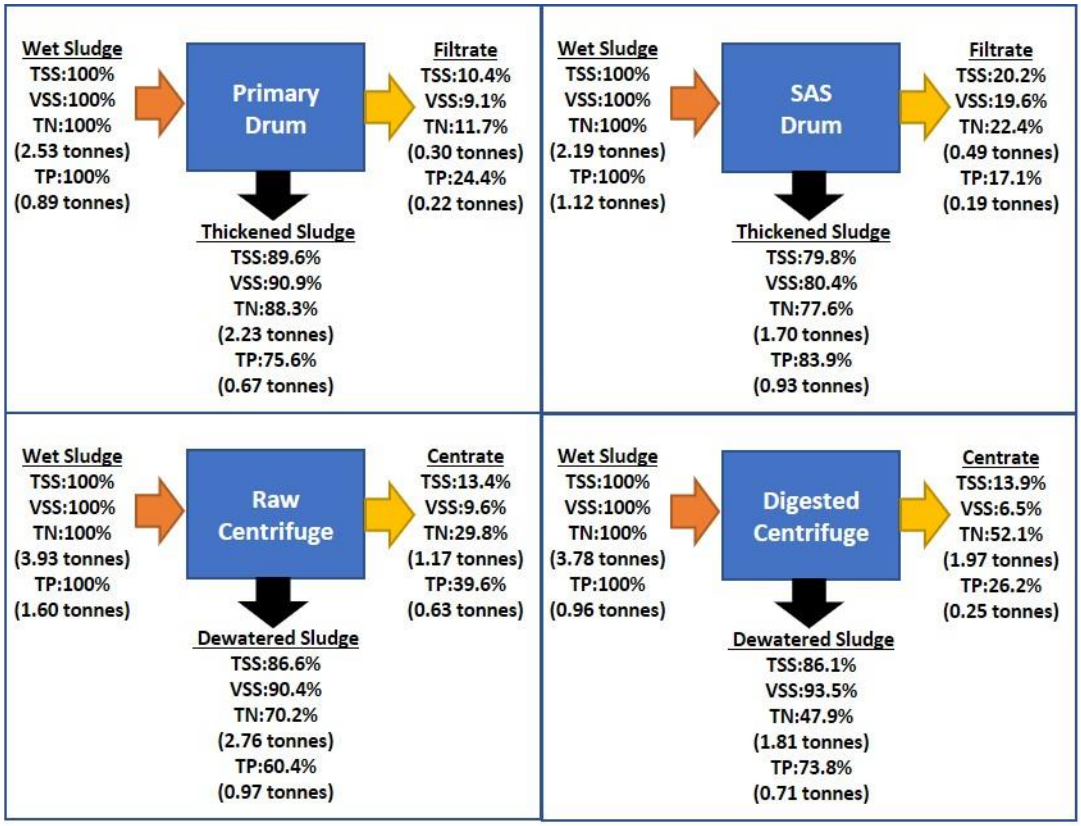

Figure 6-3 The nitrogen and phosphorus mass balances of the sludge thickening and dewatering processes in WWTP C

The percentage TN, TP, TSS and VSS mass distributed in the filtrates or centrates and in the thickened sludge are similar to each other in the drum thickening of primary sludge and SAS, particularly in the case of the SAS thickening. In both cases, the numerical differences of the percentage mass distributed in the filtrates and in the thickened sludge between the four substances are relatively small. However, the difference becomes substantial in the dewatering of the raw sludge and digested sludge. As shown Figure 6-3, in the raw centrifuge and digested centrifuge, the percentage TN and TP mass distributed in the centrate were 188%-801% of the percentage TSS and VSS mass distributed in the centrate. This is because the portion of the particulate TN and TP supposed to be captured in the sludge is solubilized in to ammonium and phosphate due to the hydrolysis and fermentation after long storage times or digestion, and hence remains in the centrate (Bouzas et al., 2007, Münch and Barr, 2001). Therefore, the composition of the TN and TP in different filtrates or centrates is highly varied, as shown in Table 6-3. In the primary sludge filtrate and SAS filtrate, the soluble fraction accounts commonly for no more than 60% of the total nutrient. But in the raw sludge centrate, the soluble PO_4^{3-}- P accounts for 55.5% of TP and soluble NH_4^+-N accounts 82.2% of the TN. In the

digested sludge centrate, the soluble PO_4^{3-}- P accounts for 68.5% of the TP and the soluble NH_4^+-N accounts 85.8% of the TN.

Table 6-3 Nutrient concentration of different filtrates or centrates

	NH_4^+-N, mg/L	TN, mg/L	PO_4^{3-}- P, mg/L	TP
Primary sludge filtrate	164.6	273.9	31.7	200.3
SAS filtrate	40.6	88.5	5.7	34.4
Raw sludge centrate	491.3	597.8	178.7	322.0
Digested sludge centrate	2238.7	2608.7	228.5	333.7

6.1.4 Nitrogen and phosphorus mass balance of anaerobic digestion

The flow and concentration data predicted via modelling were used in the construction of the nitrogen and nitrogen and phosphorus mass balances of anaerobic digestion.

After anaerobic digestion, the inflowing nitrogen and phosphorus remain in the digested sludge. This matches the reported findings that almost all of the nutrient content remains in the digestate (Shi, 2011, Rasi, 2009).

6.2 Discussion of the recovery opportunities based on plant wide mass balances

6.2.1 Nutrient product of wastewater treatment

The nitrogen and phosphorus balances of all four WWTPs were constructed from the result predicted via modelling and are presented in Figure 6-4. The nitrogen and phosphorus missing from the outflowing sludge and wastewater are considered loss.

As shown in Figure 6-4, WWTPs can be considered as reactors with three outputs: the gas, the final effluent, the sludge. Generally, the recovered nutrient is for fertilizer use (Mayer et al., 2016). To evaluate whether WWTP outputs are a product or not depends on whether the nitrogen and phosphorus contained within the products of wastewater treatment are fertile and whether there is potential to recover them.

If a WWTP includes a nitrification or denitrification process a portion of the nitrogen could end in the output gas (Siegrist et al., 1995, Foley et al., 2010, Tchobanoglous et al., 2003). In this study, WWTP A and WWTP D both possess a nitrification process. 17.9 % of the inflowing TN to WWTP A ends in the gas, and for WWTP D is 33.9% is lost as gas. The main ingredient

of this nitrogen stream is expected to be nitrogen, although sometimes N_2O will occur as well (Kim, 2013, Flores-Alsina et al., 2010, Tchobanoglous et al., 2003). Although the nitrogen in the gas output is considerable in WWTPs A and D, irrespective of whether it is present as N_2 or N_2O it will have no fertility (Mayer et al., 2016). Hence, for nitrogen recovery from wastewater the gas output is not considered a product and may even be considered a loss since the denitrification process converts the valuable ammonium into N_2, which has no value.

The predicted phosphorus mass balance suggests that the phosphorus only exists in the outflowing sludge and wastewater but not present in the gas output.

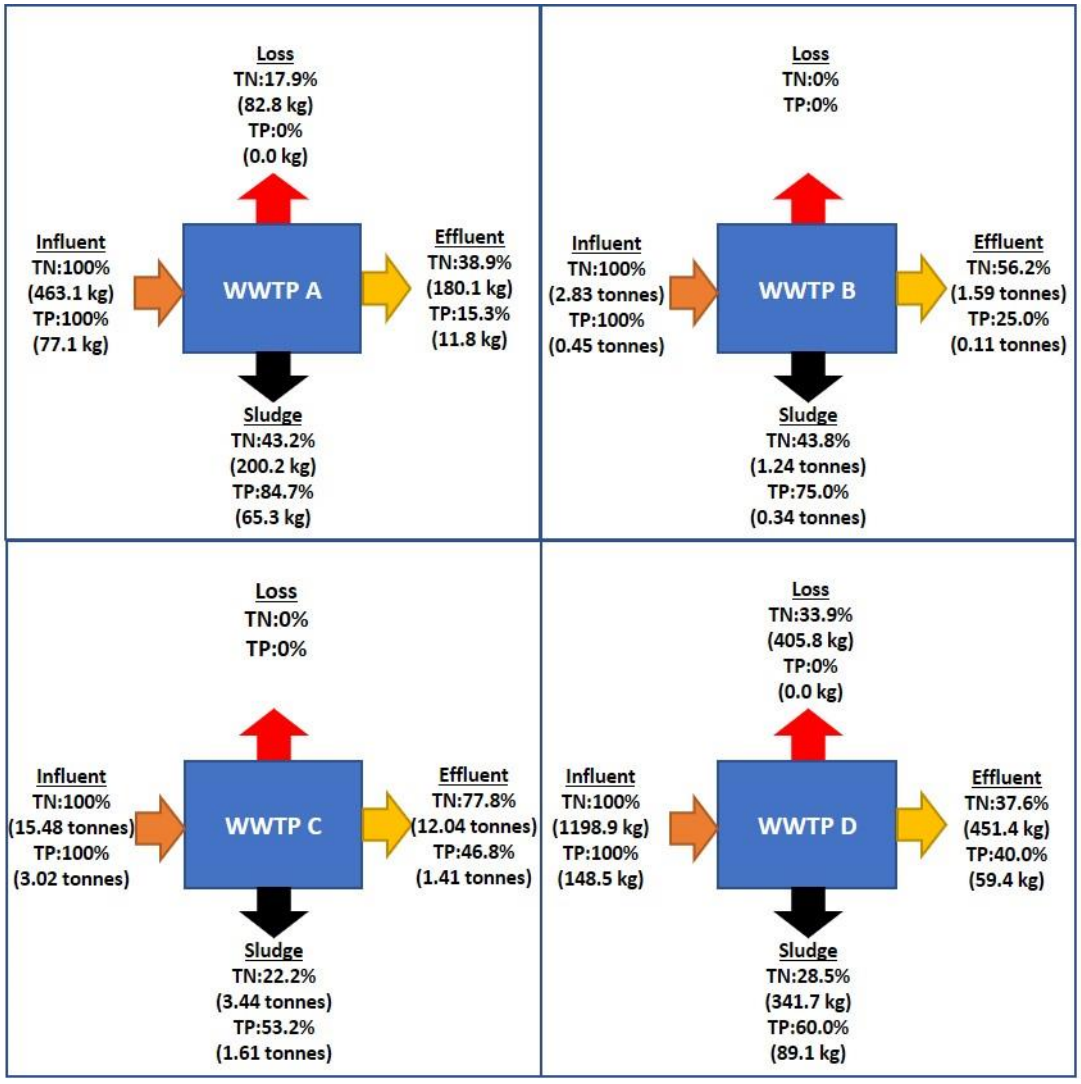

Figure 6-4 The nitrogen and phosphorus balances of the four WWTPs investigated

Unlike the COD mass balance and chemical energy balance, the percentage of influent nitrogen and phosphorus left in the final effluent is considerable, especially for WWTP B and C which do not have nitrification processes (more than 55% of the inflowing nitrogen remains in the final effluent). Therefore the final effluent represents a good reserve of nutrient.

Nutrients can be recovered from secondary effluent via ion exchange or in an algal reactor. Both technologies are able to recover the cation NH_4^+ and the anions PO_4^{3-} and NO_3^- simultaneously (Wang et al., 2010, Kim and Benjamin, 2004, Liberti et al., 1981).

For ion exchange, a resin or zeolite is first used to capture the nutrient ion. Resin or zeolite have functional groups with electric charges. The resin or zeolite with a positive charge captures anions, and those with negative charges capture the cations. When the functional group of the resin or zeolite is completely replaced by the nutrient ion, they will are washed with strong ionic strength solution, such as NaOH or H_2SO_4, to restore the ion exchange capacity by removing the nutrient from the functional group (Deng, 2014). The volume of the washing solution is commonly much less than the volume of the wastewater treated. Hence, the concentration of nutrient is elevated and is suitable for fertilizer production, such as in the form of Struvite (Deng, 2014).

Algal reactors can uptake nitrogen and phosphorus nutrients simultaneously if the correct algal species are in place (Wang et al., 2010). After the algae is harvested, dewatered, and chemically or thermally destroyed, the nutrient stored in the algal cell either ends up in the liquid product or in the solid residue (Shakya et al., 2017, Cai et al., 2013). The liquid product has a high concentration of NH_4^+ and PO_4^{3-}. As with the wash solution from ion exchange, it is suitable for struvite production (Shakya et al., 2017). The solid residue can be used as a bio-solid and applied on land for agricultural usage (Cai et al., 2013).

As shown in Table 6-2, the nitrification affects the composition of ammonium, nitrate and nitrite in activated sludge treated effluent. Although the three nitrogen compounds can all be recovered from the wastewater directly via algal reactor or ion exchange, the production of nitrate and nitrite may cause nitrogen loss. In the case of WWTP A and D, part of the nitrogen is lost as nitrogen gas in the activated sludge and subsequent final clarification processes, likely due to unintentional denitrification (Foley et al., 2010, Siegrist et al., 1995, Ji et al., 2015). But

WWTPs B and C, which have no denitrification, do not suffer such losses. Therefore, removing the nitrification process might prevent the nitrogen loss. Moreover, in the modelling of WWTP B, changing the adjusted growth rate of ammonium oxidizers from 0.91 (calibrated value) to 1.20 enables nitrification, and the ammonium concentration changes from the original predicted value of 31.9 mg/L to just 2.6 mg/L. Modelling results therefore suggest that this amendment to the treatment process increases the predicted airflow to the activated sludge tank from 152,400 m^3/d to 331,500 m^3/d, because nitrification requires extra oxygen to oxidize the ammonium to nitrate. Consequently, the electricity consumption for aeration would likely be increased. Removing the nitrification process not only prevents nitrogen loss, allowing greater amounts of nutrient available for potential recovery, but also saves energy.

However, such ion exchange and algal reactor technologies are not widely applied. For ion exchange, it has not yet been applied at full scale, and its adaptability to variable flows regime is uncertain (Bunce et al., 2018). For algal reactors the bottleneck is their long HRT and high temperature requirement (Wang et al., 2010). HRT values measurable in days require much larger footprints than existing treatment processes which require HRT values of only a matter of hours, or up to a day. Moreover, the optimal algal growth rate requires high temperatures and extra heat input in cold climates (Wang et al., 2010).

The remaining output of the wastewater treatment is the sludge. 22.2-43.8% of nitrogen and 53.2-84.7% of the phosphorus flowing into the works are captured in the sludge in the four studied WWTPs (shown in Figure 6-4). The sludge produced can be a product as it can be applied on land directly (DEFRA, 2018), or it can be deemed as an intermediate product because in some cases the sludge is subjected to anaerobic digestion before the final product is utilized (Münch and Barr, 2001).

6.2.2 Nutrient product of sludge treatment

A mass balance for the sludge treatment was only investigated for treatment plant WWTP C. This mass balance constructed from the predicted result obtained via modelling is shown in Figure 6-5.

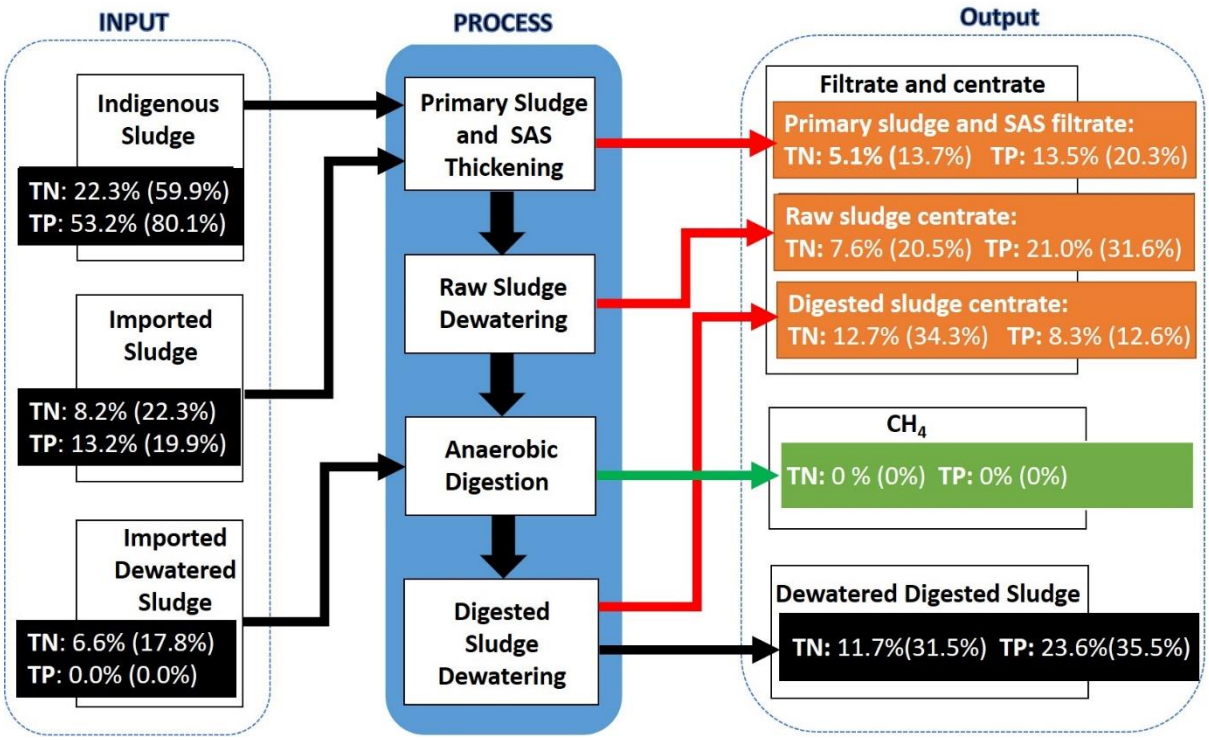

Figure 6-5 The nutrient balance for the sludge treatment process of WWTP C

(The value shows in the () are the percentage mass balance using the TN and TP inputted to the sludge treatment as reference)

The TN and TP input to the sludge treatment process are from the indigenous sludge, imported sludge and imported dewatered sludge, and are equivalent to 37.1% of the TN and 66.3% of the TP flowing into WWTP C. As shown in Figure 6-5, during sludge treatment 68.5% of the sludge TN and 64.5% of the sludge TP ends up in the filtrates and centrates, and 31.5% of the sludge TN and 35.5 % of the sludge TP remain in the dewatered digested sludge. Similar same proportions of TN and TP are found end up in filtrates and centrates and digested sludge respectively. Shi (2011) studied the nutrient mass balance of a sludge treatment only has sludge thickening of SAS and digested sludge and a conventional sludge anaerobic digestion. It suggested that 50.4 % of the sludge TN and 47.5 % of the sludge TP ends up in the filtrates and centrates, and the rest the sludge TN and TP remain in the dewatered digested sludge. It is likely that more sludge thickening and dewatering process will increase the proportion of nutrient distributed in the filtrates and centrates, though this is based on two studies and would therefore need further investigation.

Although energy and nutrient recovery occur in the same sludge treatment process, the definition of product varies in the two recovery processes. Biogas is categorized as a product from an energy recovery perspective. However, biogas contains very little nutrient, which largely remains in the filtrates, centrates and dewatered digested sludge (as shown in Figure 6-5). The filtrates and centrates can be processed for nutrient recovery and the sludge is already a nutrient product (DEFRA, 2018, Münch and Barr, 2001). Therefore, the filtrates and centrates are considered an intermediate product and the dewatered digested sludge is categorized as a product.

6.2.3 Nutrient recovery potential from wastewater

Since the dewatered digested sludge contains appreciable amounts of nitrogen and phosphorus it can be applied to land as fertilizer (DEFRA, 2018). Therefore, it is still a product. In 2010, approximately 80% of the UK sewage sludge was reused on land (DEFRA, 2012). As shown Figure 6-5, 31.5% of the sludge TN and 35.5 % of the sludge TP remain in the dewatered digested sludge in the sludge treatment process of WWTP C. Although WWTPs A, B and D has no sludge digestion treatment, assuming their sludge produced from the wastewater treatment will share the same distribution pattern as found in the sludge treatment of WWTP C, the percentage TN and TP could be kept in their dewatered digested sludge are estimated empirically and shown in Table 6-4

Table 6-4 The estimated percentage TN and TP kept in the dewatered digested sludge

	%TN captured in sludge from wastewater treatment*	**Estimated %TN ends in digested sludge****	**%TP captured in sludge from wastewater treatment***	**Estimated %TP ends in digested sludge*****
WWTP A	43.2%	13.6%	84.7%	30.1%
WWTP B	43.8%	13.8%	75.0%	26.6%
WWTP C	22.2%	7.0%	53.2%	18.9%
WWTP D	53.2%	16.8%	60.0%	21.3%

*: Collected from Figure 6-4
**: Estimated TN ends in digested sludge = TN captured in sludge from wastewater treatment ×31.5%
**: Estimated TP ends in digested sludge = TP captured in sludge from wastewater treatment ×35.5%

The result shown in Table 6-4 suggested that approximately 7-17 % of the TN and 19-30% of the TP inflowing to the four WWTPs could be kept in the dewatered digested sludge. The result also suggested that the dewatered digested sludge retain greater percentage TP inflowing to the WWTP than TN.

Besides applying the dewatered digested sludge on land, nutrient recovery from sludge can be via the most well-known struvite process, which converts NH_4^+-N and PO_4^{3+}-P into $Mg(NH_4)PO_4$ with the introduction of Mg^{2+} in a suitable pH range of 8-10 (Nelson et al., 2003). $Mg(NH_4)PO_4$ is a slow release fertilizer and its industrial-scale commercial production from sludge return liquor is proven (Ostara, 2010). For a WWTP with a more stringent nutrient consent, the additional nutrient loading (due to the recirculation of nutrient rich filtrates and/or centrates back to head of the work) might cause problems. Moreover, it may increase the operational cost since, for example, more oxygen would be needed for the nitrification of the ammonium and hence there would energy consumption for aeration (see Section 6.2.1). Also, extra chemicals (e.g.iron or aluminum salts) may be needed for removal of the additional phosphate (Ivanov et al., 2009). Nutrient recovery from sludge filtrates and/or centrates would have two benefits: (1) recovery of valuable nitrogen and phosphorus, and (2) relieving pressure on the wastewater treatment process, especially where a stringent nutrient effluent consent is enforced (Jaffer et al., 2002, Münch and Barr, 2001).

Although both dewatered digested sludge and struvite are products of nutrient recovery, the nutrient contained per unit weight of the product is different. The dewatered digested sludge collected in the sampling campaign of this research has a TS% of 28.4%, a TN/TS% of 5.2% and a TP/TS% of 1.8% (shown in Table 4-6). A gram of dewatered digested sludge contains 28.4%×5.2%×1g=0.015 g nitrogen and 28.4%×1.8%×1g=0.005g phosphorus. A according to the chemical composition of struvite ($Mg(NH_4)PO_4 \cdot 6H_2O$), a gram of struvite contains 0.057g nitrogen and 0.126g phosphorus. The nutrient content in the struvite is denser than the dewatered sludge, which could save the haulage of the product. Moreover, struvite is not only a fertiliser, but is also a chemical product for which there are industrial uses, such as the production of fire-resistant panels and cement (Mayer et al., 2016).

The struvite process is viable if at least 20 mg/L NH_4^+ (15.6 mg/L NH_4^+-N) and 106 mg/L PO_4^{3-} (34.6 mg/L PO_4^{3-}-P) are present simultaneously (Stratful et al., 2001). From the data shown in Table 6-3 and Figure 6-5, among the four filtrates and centrates, raw sludge centrate and digested sludge centrate are the ideal reserves for recovery because (1) >40% of the sludge TN and TP are retained in these centrates and (2) the NH_4^+-N and PO_4^{3-}-P concentration of both centrates are typically hundreds or even thousands of mg/L. In contrast the NH_4^+-N and $PO_4^{3—}$ P concentrations of the primary sludge filtrate and SAS filtrate are only just enough to meet the

minimum requirement for the struvite process (shown in Table 6-3). Struvite recovery therefore commonly targets the digested sludge centrate (Münch and Barr, 2001). Nevertheless, as shown in Figures 6-5, digested sludge centrate has the highest TN loading, and raw sludge centrate has the highest TP loading.

From the data shown in Table 6-3 and Figure 6-5,

- 20.4% of sludge TN is kept in the raw sludge centrate and 82.2% of it is NH_4^+-N, then the NH_4^+-N in the raw sludge centrate accounts for 20.4%×82.2% =16.8% of sludge TN feed to the sludge treatment
- 31.6% of sludge TP is kept in the raw sludge centrate and 55.5% of it is PO_4^{3-}-P, then the PO_4^{3-}-P accounts in the raw sludge centrate for 31.6%×55.5% =17.5% of sludge TP feed to the sludge treatment
- 34.3% of sludge TN is kept in the digested sludge centrate and 85.8% of it is NH_4^+-N, then the NH_4^+-N of the digested sludge centrate accounts for 34.3%×85.8% =29.4% of sludge TN feed to the sludge treatment
- 12.6% of sludge TP is kept in the digested sludge centrate and 68.5% of it is PO_4^{3-}-P, then the PO_4^{3-}-P of the digested sludge centrate accounts for 12.6%×68.5% =8.6% of sludge TP feed to the sludge treatment

On this basis, similar to the approach of estimating the percentage TN and TP kept in the dewatered digested sludge, the percentage of TN and TP inflowing to the work and existing as NH_4^+-N and PO_4^{3-}–P in the centrate can be estimated. The estimations of four WWTPs are shown in Table 6-5.

Table 6-5 The estimated percentage TN and TP (existing as NH_4^+-N and PO_4^{3-}–P) kept in the raw sludge centrate and digested sludge centrate

	%TN as NH_4^+-N in RSC[1]	**%TN as NH_4^+-N in DSC[2]**	**%TN as NH_4^+-N in RSC and DSC**	**%TP as PO_4^{3-}-P in RSC**	**T%P as PO_4^{3-}-P in DSC[1]**	**%TP as PO_4^{3-}-P in RSC and DSC[1]**
WWTP A	7.2%	12.7%	20.0%	14.9%	7.3%	22.2%
WWTP B	7.3%	12.9%	20.2%	13.2%	6.5%	19.6%
WWTP C	3.7%	6.5%	10.3%	9.3%	4.6%	13.9%
WWTP D	8.9%	15.7%	24.6%	10.5%	5.2%	15.7%

1: RSC =Raw sludge centrate
2: DSC = Digested sludge centrate

The result shown in Table 6-5 suggested that approximately 10-20 % of the TN and 14-22% of the TP inflowing to the four WWTPs could exist as NH_4^+-N and PO_4^{3-}–P and be kept in the raw sludge centrate and digested sludge centrate for potential struvite recovery.

According to the chemical composition of $Mg(NH_4)PO_4$, the mass ratio between the nitrogen (molar mass=14) and phosphorus (molar mass=31) is 1:2.2. Thus, not all the available TN and TP could be recovered into the struvite simultaneously. In some cases the remaining NH_4^+-N will be treated using the Anammox process, which converts the NH_4^+-N back to non-fertile N_2 gas (Desloover et al., 2011). However, further recovery can be achieved. Due to the instability of NH_4^+-N in alkaline conditions and its thermal instability, the redundant ammonium can be stripped from the sludge filtrate and/or centrate in the presence of heat and at a suitable pH (Bonmatı and Flotats, 2003). After the NH_3 gas is stripped off the liquid, it will contact the acidic solution which converts NH_3 back to NH_4^+. This s kept and concentrated in the solution. The NH_4^+ rich solution can then be further processed for fertilizer production (Bonmatı and Flotats, 2003, Deng, 2014).

Based on the data shown in Table 6-4 and 6-5, approximately 17-41% of TN and 33-52% of TP inflowing to the work could be kept in the dewatered digested sludge for later land application or ends as NH_4^+-N and PO_4^{3-}–P in the raw sludge centrate and digested sludge centrate for fertilizer recovery. Table 6-4 and 6-5 also suggest that the greater percentage of nutrient captured in the sludge in the wastewater treatment leads to a greater nutrient recovery potential, for instance, among four WWTPs, WWTP D captured the greatest percentage TN inflowing to the work, this leads to WWTP D has the greatest nutrient recovery potential of the dewatered digested sludge and of the raw sludge centrate and digested sludge centrate.

6.3 Case studies of nutrient recovery

As stated in section 6.2, nutrient recovery is current conducted in the sludge treatment, from the sludge dewatering centrates and the dewatered digested sludge. Therefore, this study first examines the potential impact of greater nutrient being captured from the sludge via chemical dosing or enhanced biological process prior to it being fed to the sludge treatment (Section 6.3.1).

Moreover, implementation of a particular recovery technology may impact the overall material mass balances of WWTPs. In Section 5.4, three case studies are presented in which options for improving the energy balance and they are:

- Improving solids removal efficiency in the primary settlement (Section 5.4.1)
- Reducing the sludge retention time prior to digestion (Section 5.4.2) and
- Replacing the activated sludge processes with an energy-generating anaerobic membrane reactor (Section 5.4.4).

Since these three case studies are found will impact both the wastewater and the sludge COD mass balance, Section 6.3.2 to 6.3.4 study their potential impact to the nutrient recovery.

The key criteria used to evaluate each of the improved energy recovery options case studies is the change in NH_4^+-N and PO_4^{3-}-P loading in the raw sludge centrate and digested sludge centrate where the struvite recovery could be implemented. Also, the change of nutrient mass distribution pattern between the final effluent and digested dewatering sludge will be examined for identifying the potent nutrient reserves.

6.3.1 Case study: Benefits to nutrient recovery of enhancing nutrient removal during wastewater treatment

6.3.1.1 Introduction

This study aims to capture more nutrient into the sludge. This study mainly focuses on the phosphorus since applications of the chemical dosing in primary settlement or an Enhance Biological Phosphorus Removal (EBPR) activated sludge process can improve capturing of phosphorus into the sludge (Tchobanoglous et al., 2003).

6.3.1.1 Method

A conceptual model named CM-5-1 is developed from the conceptual model CM-4-1 (Section 5.4.1.2, shown in Figure 5-19) which has a solid removal efficiency (of primary settlement) of 0.4. A chemical dosing unit using ferric sulphate is added for enabling the chemical phosphate removal. Moreover, a virtual anaerobic "Plug Flow Tank" with a set DO of 0 mg/L is added in front of the original "Plug Flow Tank" for enabling the EBPR process. The volume of the original "Plug Flow Tank" is set as 99,609 m^3 instead of the original volume of 33,203 m^3.

Moreover, the maximum growth rate of ammonia oxidizer of the original "Plug Flow Tank" is set to 0.001 to prevent nitrification. Other settings all remain the same. The model of the CM-5-1 is shown in Figure 6-6.

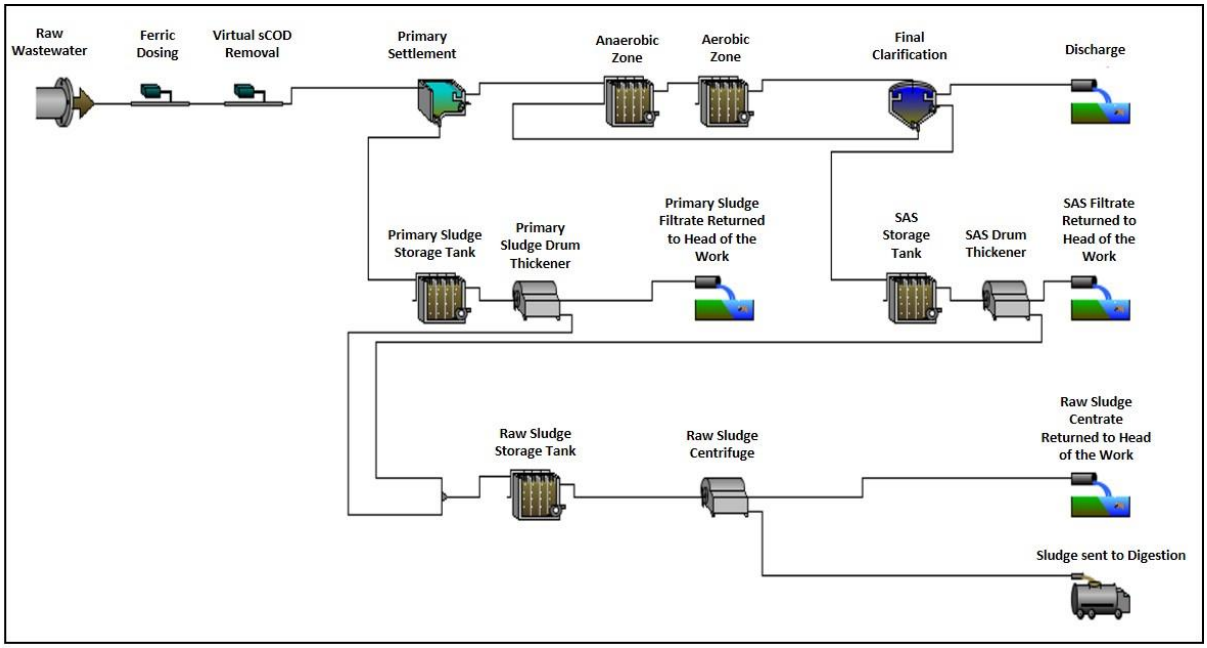

Figure 6-6 The CM-5-1 model

Three scenarios are investigated in this case study. The variables adjusted are the chemical dosing rate and the volume of the anaerobic tank.

- In the baseline scenario, the model used is called the baseline model and is with a zero chemical dosing rate and the volume of the anaerobic tank is set as only 1 m^3.
- In the second scenario, the model used is called the ferric dosing model and is with 8,900 kg/d of ferric sulphate dosing and the volume of the anaerobic tank is set as only 1 m^3. Hence, the extra phosphorus captured in the primary sludge is purely from the chemical dosing.
- In the third scenario, the model used is called the EBPR model and is with a zero chemical dosing rate and the volume of the anaerobic tank is set as only 33,203 m^3. The extra phosphorus captured in the sludge is all contained the biological sludge.

The predicted flow and concentrations are then used to demonstrate the influence to nutrient mass balance of the system.

6.3.1.3 Results and discussion

The modelling result shows that the Ferric dosing and EBPR are both able to capture more phosphorus in the sludge in the wastewater treatment process (as shown in Table 6-6). In both cases, approximately 75-80% of the phosphorus to the WWTP is captured in the sludge whilst the baseline model only captures approximately 46%. Meanwhile, there is no substantial impact to the nitrogen as the percentage of nitrogen captured in the sludge remains at approximately 21% in all three cases.

Table 6-6 The TN and TP percentage mass balance of the baseline, ferric dosing and EBPR models

	Baseline Model	**Ferric dosing model**	**EBPR model**
Percentage TN in final effluent	80.4%	79.0%	79.2%
Percentage TN loss in biological treatment	0.0%	0.0%	0.0%
Percentage TN in primary sludge	7.5%	7.7%	7.5%
Percentage TN in SAS	12.1%	13.2%	13.3%
Percentage TP in final effluent	54.0%	20.7%	24.4%
Percentage TP loss in biological treatment	0.0%	0.0%	0.0%
Percentage TP in primary sludge	15.1%	29.9%	15.1%
Percentage TP in SAS	31.0%	49.5%	60.6%

Although chemical dosing and EBPR capture similar amounts of phosphorus in the sludge, they impact the phosphate content in the raw sludge centrate differently. As shown in Table 6-7, the chemical dosing does not have a substantial impact nutrient content on the raw sludge centrate or digested sludge centrate. This is because the phosphorus removed is present as phosphate. This is bonded with the ferric iron as ferric phosphate which will rarely decomposed during hydrolysis, fermentation and digestion. But for EBPR, the captured phosphorus is stored in poly-phosphate accumulative organisms (PAOs). It will be released back to the liquid phase as phosphate in an anaerobic condition, like in the raw sludge tank. Hence, the PO_4^{3-}-P content of the raw sludge centrate of the EBPR model is about a third higher than the baseline model and the model with Ferric dosing.

Table 6-7 The concentration and loading of NH_4^+-N and PO_4^{3-}-P in the raw sludge centrate and digested sludge centrate of models with different phosphate removal scenarios

Model	NH_4^+-N in RSC[1], mg/L	PO_4^{3-}-P in RSC[1], mg/L	NH_4^+-N in DSC[2], mg/L	PO_4^{3-}-P in DSC[2], mg/L	NH_4^+-N in both centrate, kg/d	PO_4^{3-}-P in both centrate, kg/d
Baseline	539.8	212.5	1235.2	177.9	1191.6	326.7
With Chemical Dosing	514.5	190.7	1330.2	189.5	1298.9	337.4
With EBPR	410.9	324.7	1168.9	155.4	1055.4	471.6

1: RSC stands for Raw sludge centrate

2: DSC stands for digested sludge centrate

The chemical dosing and EBPR have an impact on the TP distribution on the output of the process but do not substantially influence the TN distribution as shown in Tables 6-8 and 6-9. Noticeably, a substantial increase in TP loading is shown in the SAS filtrate in both cases. For the chemical dosing, the increase of TP loading in the SAS filtrate and other filtrates and centrates is because solids retained in the filtrates and centrates contain ferric phosphate (the predicted concentration was 740.9 mg$FePO_4$/L), but this is not present in the baseline model nor the EBPR model. For EBPR, the TP loading increase is because the solid kept in the SAS filtrate contains PAOs which is rich in phosphorus. The predicted concentration of poly-phosphate in PAOs is 107.6 mg/L, but this is not present in the baseline model nor the ferric dosing model. However, in both cases, the PO_4^{3-}-P content of the SAS filtrate is still no greater than 10 mg/L.

Table 6-8 The TN distribution in the output of the combined wastewater and sludge treatment in models with different phosphate removal scenarios

Model	Primary Sludge Filtrate	SAS Filtrate	Raw Sludge Centrate	Digested Sludge Centrate	Dewatered Digested sludge
Baseline Model	0.5%	2.5%	5.0%	6.7%	4.8%
Ferric dosing model	0.5%	2.8%	5.4%	7.0%	5.3%
EBPR model	0.5%	4.0%	4.5%	7.0%	4.8%

Table 6-9 The TP distribution in the output of the combined wastewater and sludge treatment in models with different phosphate removal scenarios

Model	Primary Sludge Filtrate	SAS Filtrate	Raw Sludge Centrate	Digested Sludge Centrate	Dewatered Digested sludge
Baseline Model	3.7%	5.0%	14.3%	5.5%	17.5%
Ferric dosing model	5.7%	9.2%	21.2%	10.9%	32.4%
EBPR model	3.7%	24.7%	20.8%	6.1%	20.3%

It is also worth noting that the EBPR does not increase the TP loading in the dewatered digested sludge because considerable amounts of it has entered into the filtrates and centrates. But chemical dosing does increase the TP loading in the dewatered digested sludge as the ferric phosphate is stable during the biological reaction and thus it remains in the solid fraction throughout the process (Mayer et al., 2016). It therefore appears as though chemical dosing will not boost the struvite recovery but will result in greater capture of influent TP in the digested dewatered sludge. In contrast, the EBPR model predicts that slightly higher percentage of TP would be captured in the digested dewatered sludge, but struvite recovery may be boosted in the EBPR process.

In energy wise, as shown Table 6-10 and 6-11, the EBPR and chemical dosing have very mild impact on the chemical energy and the electricity balance.

Table 6-10 The chemical energy balance of the models with different phosphate removal scenarios

	Baseline Model	**EBPR model**	**Ferric dosing model**
Final Effluent	12.7%	12.3%	11.7%
Loss in Activated sludge	39.9%	38.9%	39.2%
Primary Sludge	29.5%	29.5%	29.8%
SAS	17.9%	19.3%	19.3%
Primary Sludge Filtrate	2.8%	2.8%	2.8%
SAS Filtrate	2.2%	3.9%	2.3%
Raw Sludge Centrate	7.5%	5.5%	7.9%
Dewatered Raw Sludge (as Digester Feed)	32.7%	33.4%	33.6%
CH_4	18.3%	18.7%	18.9%
Dewatered Digested Sludge	10.0%	10.2%	10.3%
Digested Sludge Centrate	1.6%	1.6%	1.6%

Table 6-11 The electricity balance of the models with different phosphate removal scenarios

	Baseline Model	EBPR model	Ferric dosing model
Primary Settlement, kWh/d	1217	1217	1230
Aeration, kWh/d	25393	22197	24958
Fixed consumption, kWh/d	70279	70279	70279
Sludge Treatment, kWh/d	6417	5775	5949
Total Consumption, kWh/d	103306	99468	102415
Electricity Generation, kWh/d	51352	48958	49393
Electricity Deficit, kWh/d	51954	50510	53023

6.3.2 Case study: Impact on nutrient recovery of improved primary settlement

6.3.2.1 Introduction

Struvite is recovered from the sludge centrates, which arises from the combined primary sludge and the SAS. A change in solid removal efficiency would influence the production of primary sludge and SAS, and hence may also influence how much phosphate and ammonium is available in the return liquor.

6.3.2.2 Method

The flow and concentration data predicted in conceptual modelling conducted in the Case Study: Improving solids removal efficiency in primary settlement (Section 5.4.1) are used to study the influence of improving solids removal efficiency in primary settlement on the nutrient mass balance.

6.3.2.3 Results and discussion

An increase in solid removal efficiency in primary settlement (SRE_{PS}) will increase the percentage of nutrient captured in the primary sludge as more particulate nutrient settles. However, less substrate COD will flow to the activated sludge process, and hence less nutrient would be assimilated in the biological sludge. In this case study, a greater solid removal rate in primary settlement will slightly reduce the percentage of nutrient captured in the sludge. As shown in Table 6-12, when the SRE_{PS} is increased from 40% to 70% the percentage of influent TN and TP captured in the combined sludge is only reduced from 22% to 20% and 54% to 46%, respectively. Simultaneously the concentration of ammonium and phosphate of both centrates

reduces substantially, as shown in Table 6-6. With the increase of SRE_{PS} from 0.4 to 0.7, although the predicted flow of the raw sludge increases from 1,264.1m^3 to 1393.7 m^3 and the predicted flow of digested sludge increases from 395.3 m^3 to 502.6 m^3, the loading of both NH_4^+-N and PO_4^{3-}-P kept in the two centrates reduces.

Table 6-12 The concentration and loading NH_4^+-N and PO_4^{3-}-P of raw sludge centrate and digested sludge centrate under different solid removal efficiency of primary settlement

SRE_{PS}	NH_4^+-N in RSC[1], mg/L	PO_4^{3-}-P in RSC[1], mg/L	NH_4^+-N in DSC[2], mg/L	PO_4^{3-}-P in DSC[2], mg/L	NH_4^+-N in both centrate, kg/d	PO_4^{3-}-P in both centrate, kg/d
0.40	581.8	237.2	1352.6	499.9	1422.5	554.6
0.45	551.4	219.3	1252.4	430.7	1370.1	510.1
0.50	509.7	195.7	1153.0	357.4	1304.0	454.4
0.55	461.5	169.3	1059.6	285.1	1229.1	392.0
0.60	410.5	142.7	974.0	217.0	1149.0	326.9
0.65	358.0	116.9	898.3	154.8	1067.7	262.1
0.70	303.9	92.5	828.8	98.9	981.2	198.3

1: RSC stands for Raw sludge centrate

2: DSC stands for digested sludge centrate

As stated in Section 5.4.1.3, less heterotrophic biomass is produced in the activated sludge process while the SRE_{PS} increases. This will leads to less fermentation and hydrolysis take place in the raw sludge tank because the modelling of extent of fermentation and hydrolysis is positively related to the content of heterotrophic biomass (Henze et al., 1999). It is likely the cause of the reduction of the ammonium and phosphate concentration and loading in the raw sludge centrate.

The cause of the reduction of the ammonium and phosphate in the dewatered digested sludge centrate is likely because of the ratio of nitrogen and phosphorus contained in per unit of COD reduces. Although more nutrient is fed to the digestion process, the amplification of it is smaller than amplification of the COD. When the SRE increases from 0.4 to 0.7, the percentage of influent COD content retained in the dewatered raw sludge increases by 32.6%, but the percentage of influent TN retained in the dewatered raw sludge only increases by only 13.6%, and TP retained in the dewatered raw sludge decrease by 8.5%. Since the conversion rate of COD to biomethane constantly stays at approximately 50%, less nitrogen and phosphorus is

solubilized when the solid removal efficiency increases. Consequently, even more nutrient is kept in the digester feed, and less ammonium and phosphate end in the digested centrate.

A greater SRE in the primary settlement process leads to a greater percentage of nutrient in the final effluent and digested sludge cake, but less ammonium and phosphate in the raw sludge and digested centrate available for struvite recovery. Improving the SRE of the primary settlement aims to elevate the CH_4 production. However, if struvite is a target product, then its production will be compromised. The TN and TP distribution in the output of the combined wastewater and sludge treatment is shown in Tables 6-13 and 6-14.

Table 6-13 The TN distribution in the output of the combined wastewater and sludge treatment under different solid removal efficiency of primary settlement

SRE_{PS}	Final Effluent	Primary Sludge Filtrate	SAS Filtrate	Raw Sludge Centrate	Digested Sludge Centrate	Dewatered Digested sludge
0.40	77.6%	0.5%	3.4%	6.0%	5.5%	7.0%
0.45	77.9%	0.6%	3.0%	5.7%	5.4%	7.3%
0.50	78.3%	0.6%	2.7%	5.4%	5.3%	7.7%
0.55	78.7%	0.7%	2.4%	5.0%	5.2%	8.0%
0.60	79.1%	0.8%	2.1%	4.5%	5.2%	8.4%
0.65	79.5%	0.8%	1.8%	4.1%	5.1%	8.7%
0.70	79.8%	0.9%	1.5%	3.6%	5.1%	9.1%

Table 6-14 The TP distribution in the output of the combined wastewater and sludge treatment under different solid removal efficiency of primary settlement

SRE_{PS}	Final Effluent	Primary Sludge Filtrate	SAS Filtrate	Raw sludge Centrate	Digested Sludge Centrate	Dewatered Digested Sludge
0.40	46.3%	3.7%	6.8%	17.2%	9.9%	16.1%
0.45	47.3%	4.2%	6.0%	16.6%	9.2%	16.6%
0.50	48.5%	4.7%	5.4%	15.9%	8.3%	17.2%
0.55	49.8%	5.1%	4.8%	15.0%	7.4%	17.9%
0.60	51.2%	5.6%	4.3%	14.1%	6.4%	18.5%
0.65	52.7%	6.0%	3.8%	13.2%	5.3%	19.0%
0.70	54.2%	6.5%	3.3%	12.2%	4.3%	19.5%

The uncertainty embedded in this case study is whether the increase of SRE will affect the nutrient balance, especially the phosphorus balance. Literature suggests that SRE can be improved by dosing with aluminium and ferric salts (Ismail et al., 2012, Sarparastzadeh et al., 2007). However, both aluminum and ferric iron are able to react with phosphate. Thus, more phosphorus is captured in the primary sludge, and it is also likely that less phosphorus will remain in the final effluent if the SRE is raised by dosing with metal salt coagulants. However, this will not affect the nitrogen balance since the nitrogen derivatives do not react with aluminum and ferric ion.

6.3.3 Case study: Impact on nutrient recovery of reducing sludge storage time

6.3.3.1 Introduction

The approach to reducing the particulate energy containing COD loss in the sludge dewatering is to reduce the sludge storage time of the raw sludge. As stated in Section 5.4.2.3, less particulate COD is solubilized by fermentation when the sludge storage time is reduced. Since particulate nitrogen and phosphorus can also be solubilized into ammonium and phosphate during sludge hydrolysis and fermentation (Tchobanoglous et al., 2003), reducing the sludge storage time may affect the ammonium and phosphate content in the raw sludge centrate and the digested sludge centrate.

6.3.3.2 Method

The flow and concentration data predicted in conceptual modelling conducted in the Case Study: Reducing the sludge retention time prior to digestion (Section 5.4.2) are used to study the influence of the reducing the sludge retention time prior to digestion on the nutrient mass balance

6.3.3.3 Results and discussion

A smaller tank volume leads to a shorter sludge storage time. With a reduced sludge storage time the extent of hydrolysis and fermentation in the raw sludge reduces. The ammonium and phosphate produced from the hydrolysis and fermentation of the raw sludge also reduces. Since more TN and TP remain and fed to the digester, the content of ammonium and phosphate of the digested sludge centrate increases (as shown in Table 6-15). However, with sludge storage time reduces, the loading of the ammonium and phosphate of the combined raw sludge centrate and digested sludge centrate reduces.

Table 6-15 The concentration and loading NH_4^+-N and PO_4^{3-}-P of raw sludge centrate and digested sludge centrate under different raw sludge tank volume scenarios

Tank volume, m^3	NH_4^+-N in RSC[1], mg/L	PO_4^{3-}-P in RSC[1], mg/L	NH_4^+-N in DSC[2], mg/L	PO_4^{3-}-P in DSC[2], mg/L	NH_4^+-N in both centrate, kg/d	PO_4^{3-}-P both centrate, kg/d
26086	581.7	237.2	1352.6	499.9	1422.4	554.5
20869	533.5	210.8	1385.4	521.7	1387.7	535.4
15652	473.9	177.5	1420.4	546.0	1344.8	510.8
10434	387.3	132.9	1474.3	576.3	1283.4	477.7
5217	254.2	75.8	1565.9	608.9	1193.5	434.1
0	41.1	6.1	1708.1	627.6	1053.9	375.5

1: RSC stands for Raw sludge centrate

2: DSC stands for digested sludge centrate

The upstream process of the wastewater treatment and sludge thickening of primary sludge and SAS stay the same. With the same input to the raw sludge dewatering and its subsequent treatment, as less TP and TN are kept in the centrate, a greater proportion of nutrient will remain in the dewatered digested sludge. Reducing the raw sludge storage tank volume aims to elevate the CH_4 production. However, if the struvite recovered from the raw sludge centrate and digested sludge centrate is a target product, then its production will be compromised. The TN and TP distribution in the output of the combined wastewater and sludge treatment are shown in Tables 6-16 and 6-17.

Table 6-16 The TN distribution in the output of the combined wastewater and sludge treatment under different raw sludge tank volume scenarios

Tank volume, m^3	Final Effluent	Primary Sludge Filtrate	SAS Filtrate	Raw sludge Centrate	Digested Sludge Centrate	Dewatered Digested Sludge
26086	77.6%	0.5%	3.4%	6.0%	5.5%	7.0%
20869	77.6%	0.5%	3.4%	5.6%	5.7%	7.2%
15652	77.6%	0.5%	3.4%	5.2%	5.9%	7.4%
10434	77.6%	0.5%	3.4%	4.5%	6.3%	7.7%
5217	77.6%	0.5%	3.4%	3.6%	6.9%	8.0%
0	77.6%	0.5%	3.4%	2.0%	7.9%	8.7%

Table 6-17 The TP distribution in the output of the combined wastewater and sludge treatment under different raw sludge tank volume scenarios

Tank volume, m^3	Final Effluent	Primary Sludge Filtrate	SAS Filtrate	Raw sludge Centrate	Digested Sludge Centrate	Dewatered Digested Sludge
26086	46.3%	3.7%	6.8%	17.2%	9.9%	16.1%
20869	46.3%	3.7%	6.8%	16.3%	10.5%	16.4%
15652	46.3%	3.7%	6.8%	15.2%	11.1%	16.9%
10434	46.3%	3.7%	6.8%	13.7%	12.0%	17.5%
5217	46.3%	3.7%	6.8%	11.7%	13.1%	18.4%
0	46.3%	3.7%	6.8%	9.3%	14.3%	19.6%

6.3.4 Case study: Impact on nutrient recovery of using an anaerobic membrane reactor as secondary biological treatment

6.3.3.1 Introduction

In Section 5.4.4, anaerobic membrane reactor (AnMBR) treatment was found to produce less sludge compared to an activated sludge process. Moreover, anaerobic treatment is normally not efficient for nutrient removal (Chernicharo, 2006). Therefore, the nutrient distribution pattern in the wastewater treatment may change dramatically if AnMBR is substituted for the activated sludge process.

6.3.3.2 Method

The flow and concentration data predicted in conceptual modelling conducted in the Case Study: Replacing the activated sludge processes with an energy-generating anaerobic membrane reactor unit (Section 5.4.4) are used to study the influence of replacing the activated sludge processes with an energy-generating anaerobic membrane reactor unit on the nutrient mass balance.

6.3.3.3 Results and discussion

Compared to the baseline model that uses activated sludge, the application of AnMBR substantial reduces the amount of NH_4^+-N and PO_4^{3-}-P in the centrates (as shown in Table 6-18). This can be attributed to the sludge production of the AnMBR being much smaller than the activated sludge model used by the baseline model, and hence less nutrient is captured in the sludge that is fed to the sludge treatment. Moreover, since the AnMBR does not produce the same quantity of heterotrophic biomass as the activated sludge process, the extent of

fermentation in the raw sludge tank is far smaller than the activated sludge process, and hence content of NH_4^+-N and PO_4^{3-}-P of the raw sludge filtrate reduces substantially.

Table 6-18 The concentration and loading NH_4^+-N and PO_4^{3-}-P of raw sludge centrate and digested sludge centrate of models with different secondary biological treatment

Model	NH_4^+-N in RSC[1], mg/L	PO_4^{3-}-P in RSC[1], mg/L	NH_4^+-N in DSC[2], mg/L	PO_4^{3-}-P in DSC[2], mg/L	NH_4^+-N in both centrate, kg/d	PO_4^{3-}-P in both centrate, kg/d
Activated Sludge	581.8	237.2	1352.6	499.9	1422.5	554.6
AnMBR	152.3	22.6	1281.4	19.1	715.0	31.9

1: RSC stands for Raw sludge centrate

2: DSC stands for digested sludge centrate

The application of AnMBR also impacts on the TN and TP distribution in the outputs from the treatment process (shown in Table 6-19 and 6-20). However, the impact is greater for TP. This is because in the baseline model 38.6% of the TP to the WWTP is captured in the biological sludge. But the figure is reduced to 9.7%% in the AnMBR case. This leads to the percentage of TP captured in the sludge reducing from 53.7% to 24.8%. Meanwhile the percentage of TN captured in the sludge only reduces from 22.4% to 15.9%. The most noticeable change in the TP distribution pattern of the application of AnMBR is that the percentage of influent TP kept in the final effluent increases from 46.3% to 75.2%. If struvite recovered from the raw sludge centrate and digested sludge centrate is a target product, applying AnMBR may improve the energy balance (stated in Section 5.4.4.3) but will compromise the struvite production. In addition, more nutrient will remain in the final effluent.

Table 6-19 The TN distribution in the output of the combined wastewater and sludge treatment in different scenarios of secondary biological treatment

Model	Final Effluent	Primary Sludge Filtrate	SAS Filtrate	Raw Sludge Centrate	Digested Sludge Centrate	Dewatered Digested Sludge
Baseline	77.6%	0.5%	3.4%	6.0%	5.5%	7.0%
AnMBR	84.1%	0.5%	2.1%	2.6%	4.6%	6.1%

Table 6-20 The TP distribution in the output of the combined wastewater and sludge treatment of models with different secondary biological treatment

Model	Final Effluent	Primary Sludge Filtrate	SAS Filtrate	Raw sludge Centrate	Digested Sludge Centrate	Dewatered Digested Sludge
Baseline	46.3%	3.7%	6.8%	17.2%	9.9%	16.1%
AnMBR	75.2%	3.7%	2.9%	5.8%	1.6%	10.8%

6.4 Chapter Summary

This chapter first presents the nitrogen and phosphorus mass balance of the studied WWTPs. In primary settlement, 8-23% of the inflowing nitrogen and 16-50% of inflowing phosphorus will be settled in the primary sludge and the rest will flow into the secondary treatment. Since the studied WWTP treatment works have no enhanced biological phosphorus removal technology, 32-60% of phosphorus flowing to the secondary treatment is stored in the SAS and the rest will leave the treatment works within the final effluent. Meanwhile, approximately 15-30% of the nitrogen flowing to the secondary treatment is captured in the SAS. Where nitrification is occurring, this will affect the distribution pattern of the remaining nitrogen content. If there is no nitrification the remaining nitrogen will leave the system and is present mainly as NH_4^+-N. For the WWTPs with nitrification, only approximately 50% of the nitrogen flowing to the secondary treatment process remains in the effluent, mainly as nitrate or nitrite. The rest is denitrified and emitted to the atmosphere due to unexpected denitrification occurring in the aeration tank and in the final clarifier. After the whole treatment process, approximately 22-44% of the nitrogen and 53-85% of phosphorus is captured in the sludge. The rest of the phosphorus will leave the WWTPs in the final effluent. For nitrogen, if nitrification does not occur the remaining 55-78% of nitrogen will leave the WWTPs within the final effluent. Where nitrification does occur, 18-34% of the nitrogen will be emitted to atmosphere and the rest (approximately 40%) will leave the works in the final effluent. The distribution pattern of the nitrogen and phosphorus are substantially different during the wastewater treatment process: the majority of the phosphorus is captured in the sludge, but the majority of the nitrogen is either emitted to the atmosphere or is discharged in the final effluent.

During sludge treatment with sludge thickening, dewatering and anaerobic digestion, the distribution patterns of nitrogen and phosphorus are similar. Approximately 30-35% of the sludge nitrogen and phosphorus remain in the dewatered digested sludge, but no nitrogen or

phosphorus is present in the biogas. The rest of the nitrogen and phosphorus is found in the filtrates and centrates of the sludge thickening and dewatering. A large proportion of the nitrogen and phosphorus, in the form of NH_4^+-N and PO_4^{3-}-P, are typically found in the filtrate and/or centrate of the biological treated sludge, or sludge that has been stored for a long time. This is because the particulate nutrient content in the sludge is solubilized and therefore enters into the liquid phase.

Regarding nutrient recovery, although the final effluent contains substantial amounts of nitrogen, its recovery is focused mainly on the sludge treatment side. Current practice is to recover nutrients by either by (1) sending the sludge to land for agricultural application or (2) producing struvite, which is recovered from the filtrates and/or centrates which have high concentrations of NH_4^+-N and PO_4^{3-}-P. Since struvite has a greater per unit mass nutrient content, struvite recovery appears to be a promising approach to nutrient recovery. Struvite recovery potential case studies were therefore undertaken to examine how to increase the efficiency of production and to investigate what other modifications could be made in the upstream treatment process to increase the loading of the NH_4^+-N and PO_4^{3-}-P in the filtrates and/or centrates.

The first case study was aimed at evaluating the impact of capturing greater amounts of phosphorus in the sludge. Modelling of chemical dosing and enhanced biological phosphorus removal (EBPR), to increase the loading of nutrient in the sludge dewatering centrates, was undertaken. The case study suggests that EBPR is able to increase nutrient content in the sludge centrate but that chemical dosing would not. This is because the chemically bonded phosphorus is stable during sludge treatment. The majority of the extra phosphate captured will end up in the dewatered digested sludge. In the EBPR process, the extra phosphorus captured in the biological sludge is stored in the form of poly-phosphate, which will be released as phosphate back to liquid phase under anaerobic conditions such as during sludge storage. Therefore, the EBPR process is found to be able to boost the loading of the PO_4^{3-}-P in the centrate.

There are also three case studies conducted in Section 5.4 that aim to improve the energy balance via modifying the wastewater treatment and sludge dewatering treatment. The approaches are 1) improving the solid removal efficiency of the primary settlement process, 2) reducing the sludge storage time, and 3) using energy generating secondary treatment. All

three were found to reduce the loading of the NH_4^+-N and PO_4^{3-}-P in the centrate. Approach 1) and 3) reduced the nutrient captured in the secondary biological sludge and therefore, less nutrient would be fed to the sludge treatment, and a greater percentage of nutrient would be discharged with the final effluent. Approach 2) maintains the same amount of nutrient fed to the sludge treatment. The reduction of sludge storage time, however, reduces the extent of solubilization of the particulate nutrient and leads to a reduction of NH_4^+-N and PO_4^{3-}-P loading in the centrate, but a greater nutrient reserve in the dewatered digested sludge.

Chapter 7 Business case study: pyrolysis of the biosolid for further energy recovery

7.1 Introduction

Based on the mass and chemical energy balance constructed, the recovery opportunities for nutrient and chemical energy are identified and examined in Section 5.4 and 6.3. This chapter aims to choose the most promising approach and subsequently to develop a business case for it.

The nutrient recovery from wastewater and sludge mainly focuses on struvite recovery from the centrate from sludge dewatering. It can create income due to the fertilizer production and may also reduce operational cost since chemical dosing for removal of the pipe scaling issue is prevented (Khunjar et al., 2013, Ostara, 2010, de Vries et al., 2017, Molinos-Senante et al., 2010). The economic feasibility of this has already been well demonstrated in different case studies (Ostara, 2010, Kleemann et al., 2015).Thus, this study will not make further discussion on it .

On the energy recovery side, Section 5.4 suggests that, improving the solid removal efficiency of the primary settlement, pyrolysis of the dewatered digested sludge (called biosolid in this chapter), and applying energy generating biological treatment can all potentially deliver a better energy balance. But some approaches come with high uncertainty.

For primary settlement improvement, if it is delivered by metal chemical dosing, the stability and digestibility of the sludge will be compromised (Diamantis et al., 2013).

For the energy generating biological treatment, no matter whether by AnMBR, or microbial electrolysis cells and microbial fuel cells, none are yet proven to be completely energy self-sustaining (Martin et al., 2011). In some cases, they even required a considerable amount of energy input (Martin et al., 2011). Moreover, these technologies require a high influent COD concentration but have limited ability in nutrient removal (Chernicharo, 2006). Therefore, they are not a universal solution to all the treatment work, especially if the WWTP has a stringent

nutrient consent. They have not been previously implemented at full scale (Cotterill et al., 2017, Williams et al., 2015, Shoener et al., 2014).

Among the proposed approaches for energy recovery, the biosolid pyrolysis has the least direct impact to the current wastewater and sludge treatment process because it targets the end of the sludge treatment and will not recirculate any waste stream back to the upstream treatment. Moreover, because the agricultural land bank for anaerobic digestate is limited, the biosolid has to compete with other organic source, i.e. food waste digestate (Bhogal et al., 2017). The biosolid pyrolysis can reduce the volume of the digestate and hence reduce the land bank stress (Paz-Ferreiro et al., 2018). Therefore, the biosolid pyrolysis is chosen as an example for development into a business case study.

Brief of Base Case

The Base Case of this business case is the energy recovery system of WWTP C. WWTP C is a district sludge treatment center having advanced anaerobic digestion (AAD). There is an onsite combined heat and power (CHP) unit which is able to use the produced biomethane (CH_4 in the following content in this chapter) to produce electricity for the onsite wastewater treatment and sludge treatment. But since 2014, the majority of the produced CH_4 has been upgraded and injected back to the gas grid. The drive for this act is that the renewable heat incentive (RHI) claimed on the CH_4 injected to the grid brings better cost benefit to the WWTP (*personal communication*, L Wilkinson, Northumbrian Water, December 2016). Meanwhile, since CH_4 is upgraded and sold, the CHP unit is mainly fed with imported natural gas. Also, part of the electricity demand of the site is met by the import of electricity.

The aim of this business case study is to explore both the technical and economic feasibility of the implementation of the biosolid pyrolysis to the Base Case energy recovery system.

7.2 Method

This study uses the payback period, net present value (NPV) and internal return rate (IRR) to conduct the economic evaluation of the installation of the biosolid pyrolysis. This study considers an economic feasible project should have a payback period shorter than the asset life, an NPV that is greater than 0, and an IRR that is smaller than the nominal return rate.

7.2.1 The calculation of cash flows

The cash flow is the key for determining the payback period, the NPV and the IRR. The initial cash flow is the capital expenditure (CAPEX) spent on the installation of the biosolid pyrolysis system. The annual cash flow is determined by subtracting the operational expenditure from the income. The operational expenditure (OPEX) considers the maintenance cost, labor and the purchase of energy. The income considers the sale of the energy produced and the incentives claimed. Both of the OPEX and income are related to the energy balance of the system.

The biosolid pyrolysis module is proposed to be installed at 2019 and is assumed to have an asset life of 20 years, from 2019 to 2039. It worth noting that, the RHI for the CH_4 injected to the grid is valid for 20 years, from 2014 to 2034. This study assumes that after the RHI for the CH_4 injected to the grid expires after the first 15 years of asset life of biosolids pyrolysis, the use of CH_4 will change due to the economics of carrying on grid injection becoming weaker (details will be explained in Section 7.3.3). This will result in a different energy balance from the Base Case. Therefore, four energy balances are constructed for calculating the cash flow based on whether the RHI for the CH_4 injected to the grid is available or not, and they are

- $\boldsymbol{EB_{GtG}}$ is the energy balance of the Base Case
- $\boldsymbol{EB_{GtG+FP}}$ is the energy balance of the Base Case after the proposed fast pyrolysis is installed
- $\boldsymbol{EB_{CHP}}$ is the energy balance of the Base Case that has no CH_4 grid injection and feeds majority of CH_4 to the CHP for electricity generation
- $\boldsymbol{EB_{CHP+FP}}$ is the energy balance of the Base Case that has no CH_4 grid injection, feeds majority of CH_4 to the CHP for electricity generation, and has a biosolid pyrolysis

Thus, four cash flow will then be constructed based on the above balance.

- $\boldsymbol{CF_{GtG(I)}}$ is the cash flow calculated based on $\boldsymbol{EB_{GtG}}$ and incentives being available
- $\boldsymbol{CF_{GtG+FP(I)}}$ is the cash flow calculated based on $\boldsymbol{EB_{GtG+FP}}$ and incentives being available
- $\boldsymbol{CF_{CHP}}$ is the cash flow calculated based on $\boldsymbol{EB_{CHP}}$ and no incentive is considered to be available
- $\boldsymbol{CF_{CHP+FP(I)}}$ is calculated based on $\boldsymbol{EB_{CHP+FP}}$ and RHI incentive being only available to be claimed on syngas produced by the biosolid pyrolysis

The real cash flow after the installation of biosolid pyrolysis for the first 15 years is $\boldsymbol{CF_{GtG+FP(I)} - CF_{GtG(I)}}$. From the 16th year, after the current RHI for the CH4 injected to the GtG is no longer available, the real cash flow becomes $\boldsymbol{CF_{CHP+FP(I)} - CF_{CHP}}$.

7.2.2 The calculation of payback period, NPV and IRR

Payback period

The payback period is the expected time required to recover the capital expenditure (CAPEX). Therefore, it is calculated by Equation 7-1.

Equation 7-1

$$Payback\ period = \frac{CAPEX}{Real\ cash\ flow}$$

A shorter payback period means the project has greater a liquidity (San Ong and Thum, 2013). However, the payback period approach focuses solely on the capital recovery but ignore the profit generate after the payback period (San Ong and Thum, 2013).

It is worth noting that the income is generated from the sale of energy or the incentive generated from it, rather than from a fixed promised sum of cash given annually. The income, also the OPEX, will be affected by the inflation. So is the cash flow. The payback period calculated in this study has considered the time value of the money.

NPV

The core concept of NPV approach is to consider the time value of the money (Žižlavský, 2014). In most of the cases, it considers the same amount of money is worth less in the future than today (Žižlavský, 2014) . This approach calculates the difference between the present value of the inflowing cash and the present value of the outflowing cash of the investment to be made (Žižlavský, 2014). If the NPV is greater than or equals to zero, the investment is considered economic viable. If the NPV is negative, the investment is considered not economic viable (Mack, 2012). The NPV is calculated via Equation 7-2 (Žižlavský, 2014).

Equation 7-2

$$\text{NPV} = \sum_{t=0}^{n} \frac{NCF_t}{(1+r)^t}$$

Where $\boldsymbol{NCF_t}$ in year *t*, $\boldsymbol{r}$ is the real discount rate. In this study, the propose biosolid pyrolysis system is assumed to have an asset life of 20 years. Therefore, the *t* is 20.

It is worth noting that the NPV is commonly used as a ranking tool to compare the cost benefits of different proposed projects (Puchongkawarin et al., 2015). Because this study only proposes one project, the NPV is only used as an economic indicator but not a ranking tool.

In the calculation of NPV, the real discount rate is an influential factor since it is used to discount the cash inflow to today's value. The real discount rate (r_{real}) is decided by the interest rate ($r_{interest}$) and the inflation rate ($r_{inflation}$) via Equation 7-3 (Mack, 2012).

Equation 7-3

$$r_{real} = \frac{r_{nominal\ discount\ rate} - r_{inflation}}{1 + r_{inflation}}$$

The interest rate is so called "the return on the investment" or "nominal cost of capital". It is named as nominal discount rate in this study. If the nominal discount rate is 20%, it means, the minimum profit (made from the investment) required by the investor is 20% (Juhász, 2011). The sponsor company commonly uses 12% as the interest rate for its investment project (*personal communication*, Andrew Moore, Northumbrian Water, October 2017). Therefore, this study uses 12% for the initial NPV calculation.

Inflation is a phenomenon that the prices of goods and services increases over time (Mack, 2012). According to Office of for National Statistics, the mean monthly inflation rate of the UK during Jan 2017 to Dec 2018 is 2.43%. Therefore, this study takes 2.50% as the inflation rate in all calculation.

IRR

The NPV only shows the increase in assets due to the investing during its life span but no information about the yield of the profitability of the investment (Juhász, 2011). Meanwhile, the IRR can (Juhász, 2011). IRR is the real discount rate when the NPV equals zero and then a

return of the investment is promised (Gallo, 2019). If the IRR is greater or equal to the nominal discount rate, the investment is worthwhile (Gallo, 2019). In this study, the IRR is calculated with the “irr” function of Microsoft Excel.

7.2.3 Sensitivity study on the uncertainty

As stated in Section 7.2.1, the cash flow calculation is based on the energy balance. The energy balance construction in study is based on mass balance. Puig et al. (2008) reported that poor data quality will results in erroneous mass balance. As stated in Section 5.4, the mass balance could also change due to the modification of the process operation. Thus, there is uncertainty embed in the mass balance. Besides, uncertainty also exist in the cost estimation. Therefore, this study conducts sensitivity analysis to study how the uncertainty could impact the economic evaluation.

This case study conducts sensitivity study on the following ten parameters,

(1) the amount of total solid in the biosolid
(2) the TS% of the biosolid
(3) the chemical energy content of the dried biosolid
(4) the electricity consumed on the fast pyrolysis of biosolid
(5) the efficiency of recovering syngas from biosolid. This will be called pyrolysis efficiency in the following of content of this chapter
(6) the CAPEX
(7) the cost factor to estimate the maintenance cost,
(8) the additional labor
(9) the sale price of the surplus electricity
(10) the RHI claimed on the syngas

And the uncertainty of them are considered comes from

- For parameter (1), as stated in Section 5.4.3, the change of the upstream wastewater and sludge process may affect the production of biosolid.
- For parameter (2), the TS% of biosolid is impacted by the dewatering process. For parameter (3), the reported chemical energy content of the dried biosolid varies (Shizas and Bagley, 2004, Schaum et al., 2016, Smyth et al., 2016).

- For parameter (4)-(8), they are estimated from literature value.
- For parameter (9), the sale price surplus electricity can vary depend on the deal with the electricity supplier (*personal communication*, L Begg, OFGEM, January 2018).
- For parameter (10), this project did not propose an exact date for installation whilst the RHI could change in the future.

A spider plot, which is a visualization aid, is used to present their impact to the pay back, NPV and the IRR (El-Temtamy and Gendy, 2014). The approach is to give a ±20% variation on one parameter once at a time, and then the newly obtained payback period, NPV and IRR will be used to plot against the ratio of the changed value to the original value of that parameter (El-Temtamy and Gendy, 2014, Lipu and Jamal, 2013). If a line of the corresponding parameter has a steep slope, then the parameter is considered to have a big influence on the predicted pay back, NPV and IRR (Lipu and Jamal, 2013, El-Temtamy and Gendy, 2014).

The found most influential parameter(s) will be chosen for being further studied the payback period, NPV, and IRR under a pessimistic scenario and an optimistic scenario (Rysanek and Choudhary, 2013). In this study, the pessimistic scenario is that parameter(s) is(are) at the worst condition, and the optimistic condition is that all three parameter(s) is(are) at the best condition. The scenario study is for deeply understand the impact from the uncertainty to the economic evaluation.

7.3 Result and Discussion

7.3.1 Energy balance

The data shown below in this Sub-section 7.3.1 is the daily average collected from sludge treatment of WWTP C from 01/03/2016 to 31/08/2016. The data is collected from Northumbrian Water (*personal communication*, S Coverdale, Northumbrian Water, October 2017 and *personal communication*, L Wilkinson, Northumbrian Water, October 2018).

7.3.1.1 Energy balance of the energy recovery system (EB_{GtG}) of the Base Case

In the Base Case, the energy recovery system of the WWTP C consist of three major components, the boiler, the CHP, and the Gas to Grid (GtG) upgrade plant. The input energy containing materials are the indigenously produced biomethane (CH_4), the natural gas purchased from the grid, and the purchased propane. Also, a certain amount of electricity is purchased for meeting the demand of the sludge treatment and wastewater treatment. There are four outputs of the system, the steam from the boiler, the low-grade heat from the CHP, the electricity produced from the CHP, and the upgraded gas from the GtG upgrade plant. The produced steam will be used for the thermal hydrolysis process (THP) process of the AAD. The electricity will be consumed onsite for sludge and wastewater treatment. The low-grade heat is usually wasted. The produced upgrade gas will be injected to the gas grid.

In detail, The CH_4 produced from the AD was measured as 245.5 MWh. Since the CH_4 flared was measured as 20.7 MWh, only 224.8 MWh CH_4 enters into the system, along with 257.1 MWh natural gas and 23.7 MWh propane.

27.6 MWh of CH_4 and 212.8 MWh of natural gas are fed to the CHP. The electricity production is measured as 83.2 MWh. The heat to electricity conversion is 34.6%. It is worth noting that, 9.6 out of 83.2 MWh electricity is generated from the 27.6 MWh CH_4. Based on the literature, the conversion ratio of both high-grade heat and low-grade heat is assumed as 20% (Smyth et al., 2016, Bowen et al., 2010). Therefore, 48.1 MWh of high-grade heat and 48.1 MWh of low-grade heat are then produced.

48.1 MWh of high-grade heat made up with 44.3 MWh of natural gas are fed to the boiler. The heat production is measured as 77.3 MWh of steam. The energy recovery ratio is 83.7% which agrees with the reported value approximately 85% (Vanwortswinkel and Nijs, 2010).

The rest 197.2 CH_4 is fed to the GtG upgrade plant along with 23.7 MWh propane. 220.9 MWh upgrade gas is injected into the grid.

In the end, the system produces 77.3 MWh steam which meets the demand of the THP, 48.1 MWh low-grade heat, 220.9 MWh upgrade gas, and 83.2 MWh electricity which is still 18.8

MWh short to fulfil the daily electricity demand measured as 102.0 MWh. The energy balance of the Base Case is shown in Figure 7-1.

The cash flow related energy flow on a daily basis is summarized as

- Purchase: 257.1 MWh natural gas, 23.7 MWh propane, and 18.8 MWh electricity
- Sale: 220.9 MWh upgrade gas
- Incentives received: 197.2 MWh CH_4 for the RHI claim, and 9.6 MWh electricity for the Renewable Obligation Certificate (ROC) trade (*personal communication*, Steve Coverdale, Northumbrian Water, October 2017).

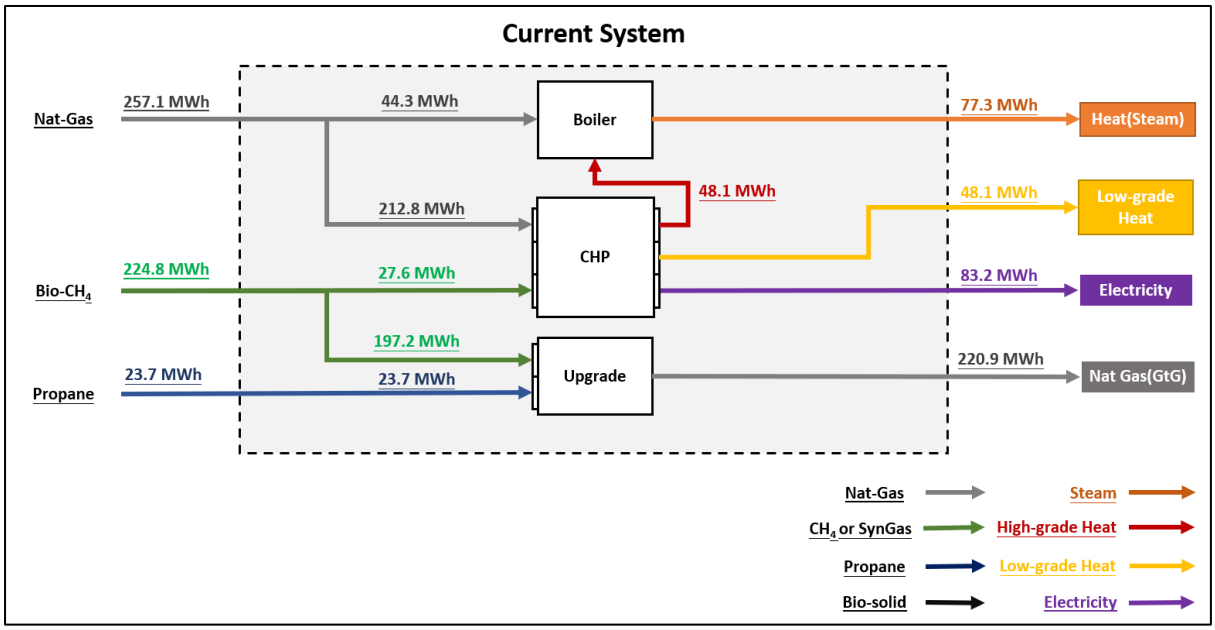

Figure 7-1 The energy balance ($\boldsymbol{EB_{GtG}}$) of the Base Case

7.3.1.2 Energy balance of the Base Case energy recovery system with the addition of biosolid pyrolysis (EB_{GtG+FP})

The design of sludge fast pyrolysis has three units; the sludge drying, which utilizes the low-grade heat to dry the sludge to reach 90% DS (Mills et al., 2014), the fast pyrolysis to convert biosolid into syngas, and the CHP for combusting the syngas produced for electricity and heat production. Apart from the original three inputs, CH_4, natural gas, and the propane, the energy containing biosolid is fed to the system. The installation of the pyrolysis requires no modification of the Base Case energy system and its operation. The output remains the same for, steam, low-grade heat, upgrade gas, and electricity.

The energy balance is presented on a daily basis. 41 tonnes dried solid (DS) biosolid with 177.7 MWh of chemical energy is fed to pyrolysis. Reportedly, 0.77-1.09 MWh heat is required to evaporate 1 ton of water (Mills et al., 2014). The heat supplied can be from the low-grade heat from the CHP (Mills et al., 2014). This study assumes the ratio is 0.9 MWh heat per ton water evaporated. In the sampling campaign conducted in the mass and chemical energy balance investigation, 5 times the TS% of the biosolid were measured all were 28.5%. When the TS of the biosolid is increased from 28.5% to 90.0%, 41÷28.5%-41÷90.0%= 98.3 tonne water is removed and hence 0.9×98.3=88.5 MWh of low-grade heat is required. Whilst 0.055 MWh electricity is required to process each tonne DS content (Mills et al., 2014). Therefore, 88.5 MWh/day of low-grade heat and 2.3 MWh/day electricity is required for drying the sludge.

Approximately 60%-90% of the chemical energy within the biosolid can be recovered as syngas and fed to the CHP, the rest is lost or remains in the bio-char (Mills et al., 2014, Cao and Pawłowski, 2012). This study assumes the conversion ratio is 80%. Therefore, the thermal energy within the syngas is 177.7×80.0% = 142.1 MWh. The pyrolysis does require electricity input for the heating. According to Mills et al. (2014), this study assumes the ratio is 0.4 MWh electricity per ton DS. Therefore 16.4 MWh electricity is required.

The produced syngas is then fed to the CHP. Assuming using the CHP for the syngas recovers 38% of the 142.1 MWh of influent energy as electricity, then electricity production is 54.0 MWh/day (Mills et al., 2014). Meanwhile, the conversion ratio of both high-grade heat and low-grade heat are assumed to be 20% (Smyth et al., 2016, Bowen et al., 2010). Therefore, 28.4 MWh of high-grade heat and 28.4 MWh of low-grade heat are also produced.

The sludge pyrolysis produces 54.0 MWh electricity from the daily 41.0 tonnes DS biosolid. After offsetting the 2.3+16.4=18.7 MWh parasitic load of electricity consumed in sludge drying and pyrolysis unit, the net electricity output of the biosolid pyrolysis module is 35.3 MWh. The system also produces 56.8 MWh heat, but it is not able meet the demand of 88.5 MWh for sludge drying. The heat deficit of the biosolid pyrolysis module is 31.6 MWh per day.

With integration to the Base Case energy recovery unit, the unused 48.1 MWh low-grade heat from the original system can be used to fulfil the 31.6 MWh heat deficit of the gasification

system, with still 16.5 MWh surplus. Meanwhile, the total electricity output is increase to 118.5 MWh. After offsetting the 102.0 demand, there is still 16.5 MWh net electricity output which can be sold to the electricity grid. The production of the steam and upgrades gas is remained at 77.3 MWh and 220.9 MWh upgrade gas, respectively.

The cash flow related energy flow on a daily basis becomes:

- Purchase: 257.1 MWh natural gas and 23.7 MWh propane,
- Sale: 220.9 MWh upgrade gas and 16.5 MWh electricity
- Incentives received: 197.2 MWh CH_4 for the original RHI claim, and 9.6 MWh electricity for the Renewable Obligation Certificate (ROC) trade (*personal communication*, Steve Coverdale, Northumbrian Water, October 2017), and142.1 MWh of syngas for the new RHI claim.

The energy balance of the Base Case with biosolid pyrolysis is shown in Figure 7-2.

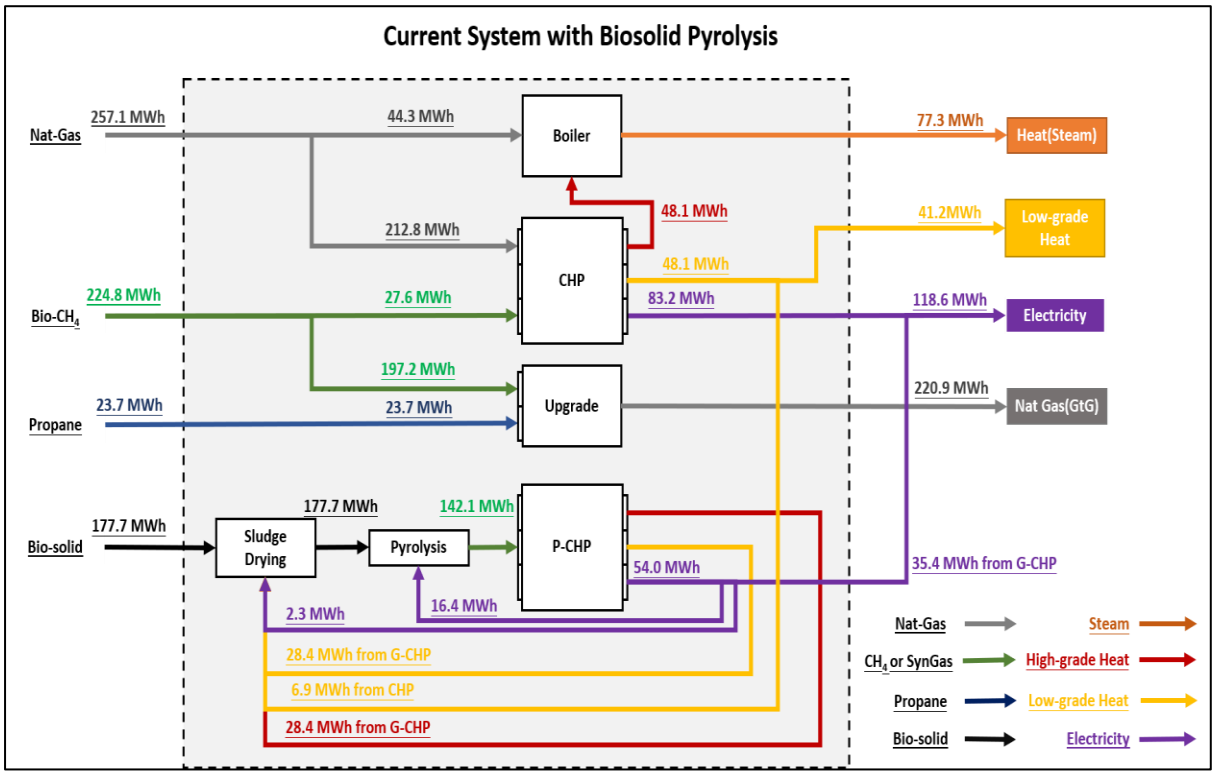

Figure 7-2 The energy balance ($\boldsymbol{EB_{GtG+FP}}$) of the Base Case system with biosolid pyrolysis

7.3.1.3 Energy balance of the Base Case energy recovery system with no GtG (EB_{CHP})

Since the RHI will end within the project life time of pyrolysis unit, modification of the Base Case system is likely to occur. This study assumes the change will be diverting the CH_4 back to the CHP for electricity production. The reason is that, the buying price of the natural gas which current used for electricity production is £13/MWh, but the sale price of the upgrade gas is £10/MWh while the extra cost for the purchase of propane is involved (*personal communication*, Steve Coverdale, Northumbrian Water, October 2017).

However, in the original $\boldsymbol{EB_{GtG}}$, the natural gas usage is 212.8 MWh and the CH_4 fed to the GtG upgrade of only 197.2 MWh. There is a shortage of 15.6 MWh chemical energy for the CHP. Based on the energy conversion ratio of the current CHP is 34.6%, 15.6 MWh heat energy is equivalent to 5.4 MWh electricity. Either 15.6 MWh natural gas or 5.4 MWh electricity has to be brought from the grid. The buying price of natural gas is only £13/MWh but of electricity is £114/MWh. Thus, in a daily basis, the import of natural gas costs £15.6×13=£202.8, but the import of electricity costs £114×5.6=£615.6. It is therefore more economic to buy 15.6 MWh natural gas to produce electricity on site. Therefore, this study assumes 15.6 MWh natural gas will be brought from the grid per day.

After the route of GtG is abandoned at the end of the RHI incentive to the CH_4 to grid, the input to system are only the 59.9 MWh natural gas and 224.8 MWh CH_4. The output of the system becomes 77.3 MWh steam which still meets the demand of the THP, 48.1 MWh low-grade heat, and 83.2 MWh electricity which is still 18.8 MWh short of fulfilling the daily electricity demand measured as 102.0 MWh.

The cash related energy flow on a daily basis is summarized as

- Purchase: 59.9 MWh natural gas and 18.8 MWh electricity

The energy balance of the Base Case system with no GtG is shown in Figure 7-3.

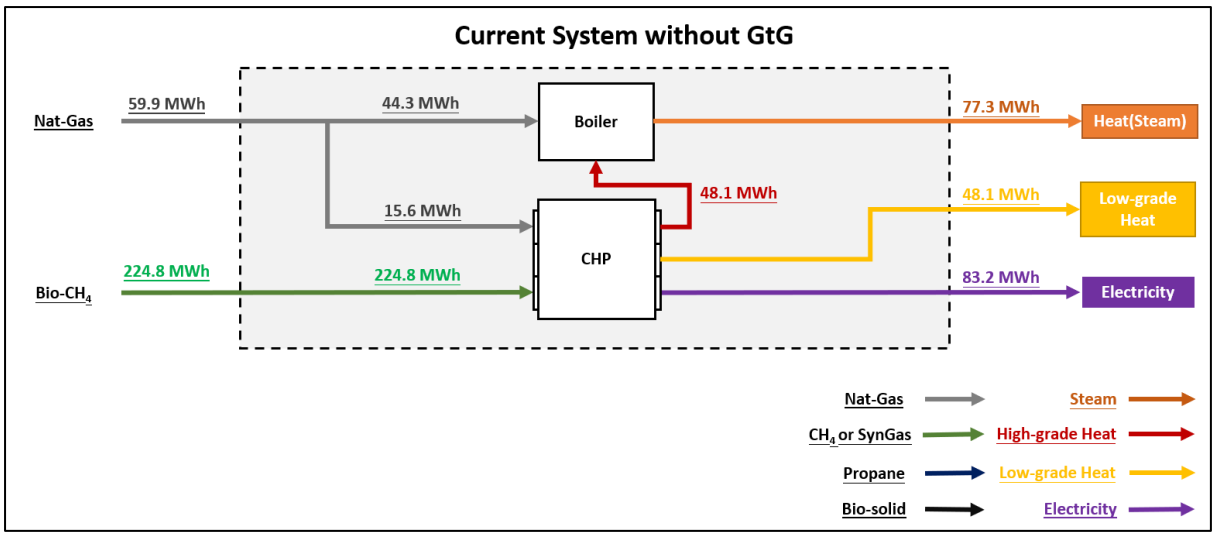

Figure 7-3 The energy balance (EB_{CHP}) of the system has no CH_4 grid injection

7.3.1.4 Energy balance of the Base Case energy recovery system with biosolid pyrolysis but with no GtG (EB_{CHP+FP})

The end of the GtG route does not affect low grade heat production and hence will not affect the performance of the energy balance of the pyrolysis module as stated in Section 7.3.1.4. The pyrolysis module still has a net output of the electricity of 35.3 MWh per day and suffers a heat deficit is 31.6 MWh per day. Once the module is added on to the system with no GtG, the heat deficit will be rectified, and the net electricity output will offset the 18.8 MWh electricity import. Although there is still surplus electricity after the offset, this electricity is preferable to be sold to the grid rather than supplementing the gap due to the CH_4 shortage stated in Section 7.3.1.3. This is because 2.9 MWh of natural gas is needed for generating 1 MWh electricity (based on the heat to electricity conversion ratio is 34.6%) and the cost is only £13×2.9= 37.7, whilst the sale price of 1 MWh of electricity is £48.5. Therefore, it is more economic to carry on importing the natural gas for electricity production.

After the route of GtG is abandoned but a pyrolysis module is added in, the input to system are still 59.9 MWh natural gas and 224.8 MWh CH_4. The output of the system becomes 77.3 MW of steam, 16.5 MWh low-grade heat, and 16.5 MWh electricity.

The cash related energy flow on a daily basis is summarised as

- Purchase: 59.9 MWh natural gas
- Sale: 16.5 MWh electricity

- Incentives received: 142.1 MWh of syngas for the new RHI claim.

The energy balance of the Base Case system with no GtG but has biosolid pyrolysis is shown in Figure 7-4.

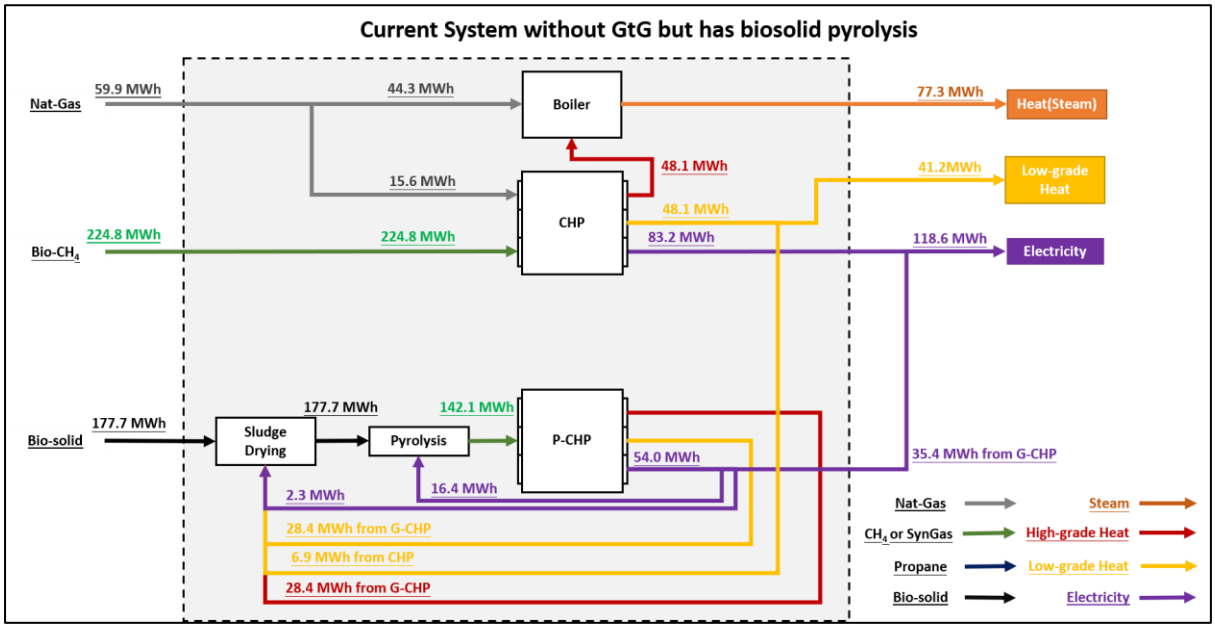

Figure 7-4 The energy balance ($\boldsymbol{EB_{CHP+FP}}$) of the system has no CH_4 grid injection but with biosolid pyrolysis

7.3.2 Cash flow

This subsection will first present the estimation and calculation approach to the CAPEX, OPEX and income, per equipment or, per unit of energy as in Section 7.3.2.1, 7.3.2.2, and 7.3.2.3, respectively. Then the real cash flow will be shown in Section 7.3.2.4.

7.3.2.1 Capital Expenditure

This study assumes there is no CAPEX involved in the Base Case with no pyrolysis module. The CAPEX of the pyrolysis module is spent on the installation of the sludge drying plant, the gasifier, and the CHP for Syn-Gas. The CAPEX of the unit ($Capex_p$) is estimated via Equation 7-4 (Jones et al., 2013).

Equation 7-4

$$Capex_p = Capex_r \times \left(\frac{Capacity_p}{Capacity_r}\right)^n$$

Where $\boldsymbol{Capex_r}$ is capital cost of the similar process unit reported in literature, $\boldsymbol{Capacity_p}$ is the capacity of the proposed unit, $\boldsymbol{Capacity_r}$is the capacity of the similar process unit reported

in literature, and ***n*** is the scale factor, commonly, 0.6-0.7 (Jones et al., 2013). This study takes the ***n*** as 0.65.

As stated in Section 7.3.1.2, 98.3 tonnes water is expected to be evaporated, 41 tonnes of TDS are expected to be treated, and 54 MWh electricity (equivalent to a power rating of 54,000kWh÷24h=2250 kW) is expected to be produced. The estimated capital cost of the three process units are listed in Table 7-1.

Table 7-1 The estimated CAPEX of the components of the biosolid pyrolysis

Reference	$Capex_r$, £	$Capacity_r$	$Capacity_p$	$Capex_p$, £
Sludge Drying				
Mills et al. (2014)	3,676,922	77 tH_2O/d*	98.3 tH_2O/d	4,309,600
Fast Pyrolysis				
Mills et al. (2014)	8,120,331	60 tds/d*	41 tds/d	6,339,937
Jones et al. (2013)	123,120,000	2000 tds/d	41 tds/d	9,839,400
CHP				
Mills et al. (2014)	7,504,802	4000 kW	2250 kW	5,163,862
BEIS (2017a)	5,300,000	7700 kW	2250 kW	2,382,491
BEIS (2017b)	2,700,000	1400 kW	2250 kW	3,675,826
BEIS (2017c)	7,300,000	4000 kW	2250 kW	5,022,943

*: tH_2O/d stands for ton water evaporated per day, and tds/d stands for ton dried solid per day.

The estimated CAPEX of the sludge drying plant is £ 4,309,600. The estimated capital cost of the fast pyrolysis and the CHP are taken from the mean value of the multiple estimated values, and they are £8,089,668 and £4,060,281, respectively. Therefore, the total CAPEX of the biosolid pyrolysis system is estimated as £16,460,549 but could vary from £13,032,028 to £19,312,862

7.3.2.2 Operational expenditure

In this study, the operational expenditure (OPEX) includes maintenance, labour cost, and the material, namely the purchase of natural gas, propane and electricity.

Maintenance

The typical maintenance costs can be estimated as 1-3% of the capital cost. This study assumes the ratio is 2% since the energy consumption and the labor cost is calculated separately. The

investment in the gas to grid facility at WWTP C is reported to have amounted to £8,000,000 (WWT online, 2015). The annual maintenance cost is estimated as £160,000. For the original CHP, its maintenance is calculated based on a ratio of £6 per MWh electricity produced. Therefore, the maintenance cost per annum is 6×83.2×365= £182,208 (DECC, 2008).

For the biosolid pyrolysis module, based on the CAPEX estimated in Section 7.3.2.1, the maintenance cost of the drying plant is £86,190, of the fast pyrolysis is £161,793, and of the syngas CHP is £81,215, respectively.

Labor

The annual salary of a wastewater operator is from £14,500 to 32,000 (OECD, 2017). The labor cost of a GtG process is suggested as £31,000 (DECC, 2014). Thus, their wages are assumed to be £30,000 per person per annum.

Currently, there are 18 operators working for this Base Case energy system that processes 85 tonnes DS per day (based on the average from 10/03/2016 to 31/08/2016) (*personal communication*, John Robinson, Northumbrian Water, October 2017). This study assumes the labor needed is proportional to the amount of dried solid processed. Hence, the 9 additional operators could be required for the sludge gasification system that treats 41 tonnes DS. Considering the operators could be allocated from other operation teams, this study assumes 5 instead of 9 operators will be added to the operation team of the energy recovery system (*personal communication*, A Moore, Northumbrian Water, January 2019).

Material

The buying price of natural gas is £ 13.0 per MWh and the buying price of propane is £100.0 per MWh (*personal communication*, S Coverdale, Northumbrian Water, October 2017). According to statistic “Prices of fuels purchased by non-domestic consumers in the UK” published by Department for Business, Energy & Industrial Strategy, the electricity sale price to a medium size (2,000-19,999 MWh) consumer is 114.4 per MWh. Since the electricity import of WWTP C is 18.8×365=6,862 MWh per annum, it should be categorized as medium size consumer. Therefore, the buying price of electricity is assumed as £114.4 per MWh.

7.3.2.3 Income

The income includes the sale of exported gas and electricity to the gas grid, and the incentives received.

The upgrade gas injected to grid is sold at £ 10.0 per MWh (*personal communication*, S Coverdale, Northumbrian Water, October 2017). Moreover, the sale of electricity to the grid is estimated as price £52.4 per MWh, the same as the export price of the Feed-In-Tariff (OFGEM, 2019a).

The Renewable Heat Incentive (RHI) is available to claim on the CH_4 injected to the grid. The unit price for WWTP C is £ 76.2 per MWh (*personal communication*, S Coverdale, Northumbrian Water, October 2017). It is also available to claim on the syngas produced by the biosolid pyrolysis and injected to the CHP (OFGEM, 2018). Therefore, this study assumes the pyrolysis and CHP is accredited for the RHI, and £11.6 per MWh is gained for the syngas fed to the CHP (OFGEM, 2019b).

A Renewable Obligation Certificate (ROC) can be granted for the electricity produced from the CH_4 in the exiting CHP. The trade price of ROC is £ 42 per MWh electricity (*personal communication*, S Coverdale, Northumbrian Water, October 2017).

The biosolid produced at WWTP C is currently sold to the farmers. Considering the biochar, the resulting product of the pyrolysis, may have the similar fertility with biosolid, this study assumes the income generated from the sale of biosolid and from the sale of the biochar are the same, and hence are not considered in the cash flow.

7.3.2.4 Real cash flow

The annual cash flows of different energy balances are shown in Table 7-2.

Table 7-2 The annual cash flow of different energy balance and under different scenarios

	$CF_{GtG(I)}$	$CF_{GtG+FP(I)}$	CF_{CHP}	$CF_{CHP+FP(I)}$
Operational Expenditure				
Purchase of Electricity	£785,013	£0	£785,013	£0
Purchase of Natural Gas	£1,219,940	£1,219,940	£284,226	£284,226
Purchase of Propane	£865,050	£865,050	£0	£0
Labor cost	£540,000	£540,000	£540,000	£540,000
Maintenance (CHP)	£182,208	£182,208	£182,208	£182,208
Maintenance (GtG)	£160,000	£160,000	£0	£0
Labor cost (Fast Pyrolysis)	£0	£150,000	£0	£150,000
Maintenance (Sludge Drying Plant)	£0	£86,192	£0	£86,192
Maintenance (Fast Pyrolysis)	£0	£161,793	£0	£161,793
Maintenance (Fast Pyrolysis CHP)	£0	£81,226	£0	£81,226
Total Operational Expenditure:	£3,752,210	£3,446,408	£1,791,446	£1,485,644
Income				
Sale of Upgraded Gas	£806,285	£806,285	£0	£0
RHI claimed on the CH4 of Upgraded Gas	£5,484,724	£5,484,724	£0	£0
ROC claimed on Electricity produced by Biomethane	£146,433	£146,433	£0	£0
Sale of Electricity	£0	£316,644	£0	£316,644
RHI claimed on the Syngas to CHP	£0	£601,793	£0	£601,793
Total Income:	£6,437,442	£7,355,878	£0	£918,436
Cash flow:	**£2,685,232**	**£3,909,470**	**-£1,791,446**	**-£567,208**

No matter whether the GtG exists or not, the installation of the biosolid pyrolysis is able to reduce the OPEX by £305,802 per annum which is attributed to the scrapping of the purchase of electricity. Also, it can bring in an extra income of £918,436 from the sale of surplus electricity and the RHI claimed in the syngas. Therefore, the real cash flow of the first 15 years and last 5 years remains the same as £1,224,238.

It is worth noting that, apart from CF_{CHP}, 65.5-87.5% of the income comes from the incentives (Figure 7-5). As shown in Table 7-2, if the incentives are scrapped, both $CF_{GtG(I)}$ and $CF_{GtG+FP(I)}$ will become negative because the income from the sale of the upgrade gas and electricity is far too low to cover the OPEX. The incentives are vital to the cash flow.

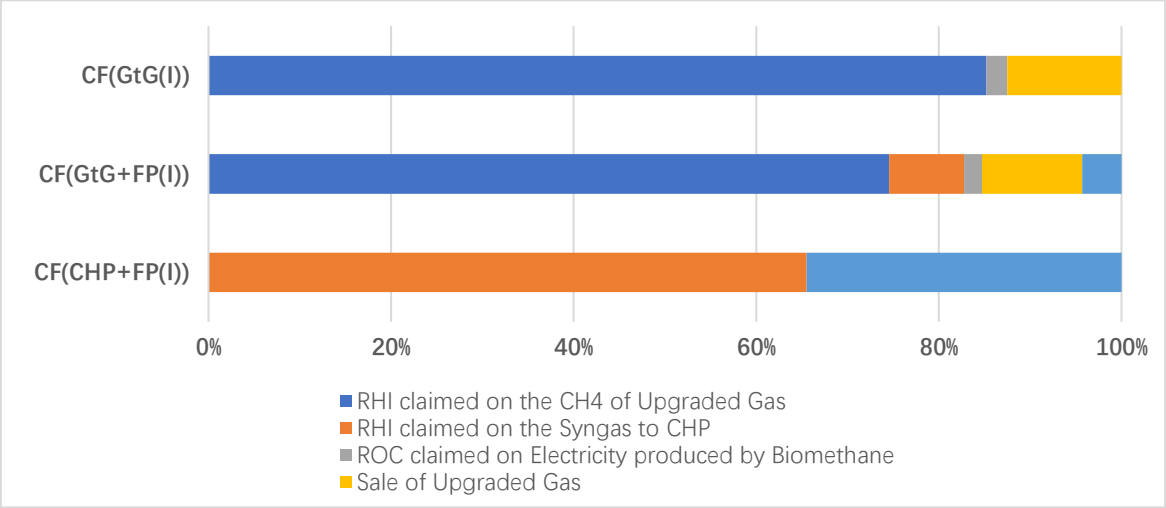

Figure 7-5 The percentage breakdown of income of different cash flow

7.3.3 The economic evaluation and the sensitivity study on the uncertainties

7.3.3.1 The economic evaluation

Base on the real cash flow, the payback period, the NPV and the IRR of the installation of the biosolid pyrolysis system are calculated as 13.4 years, -£5,495,459, and 4.12%, respectively. Although the payback period suggests the investment could be recovered during the asset life, the negative NPV and an IRR that smaller than the nominal discount rate (12%) both suggesting that the installation of biosolid pyrolysis is not currently economically feasible.

7.3.3.2 The sensitivity study on the uncertainties

Ten parameters with uncertainties are studied for their impact to the economic evaluation. Figure 7-6 to 7-8 shows the spider plot of the sensitivity study.

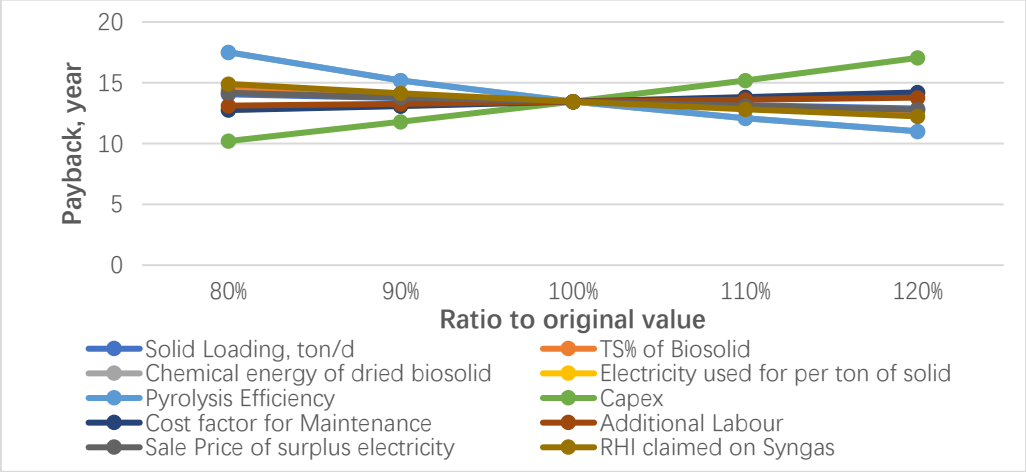

Figure 7-6 The spider chart of payback period

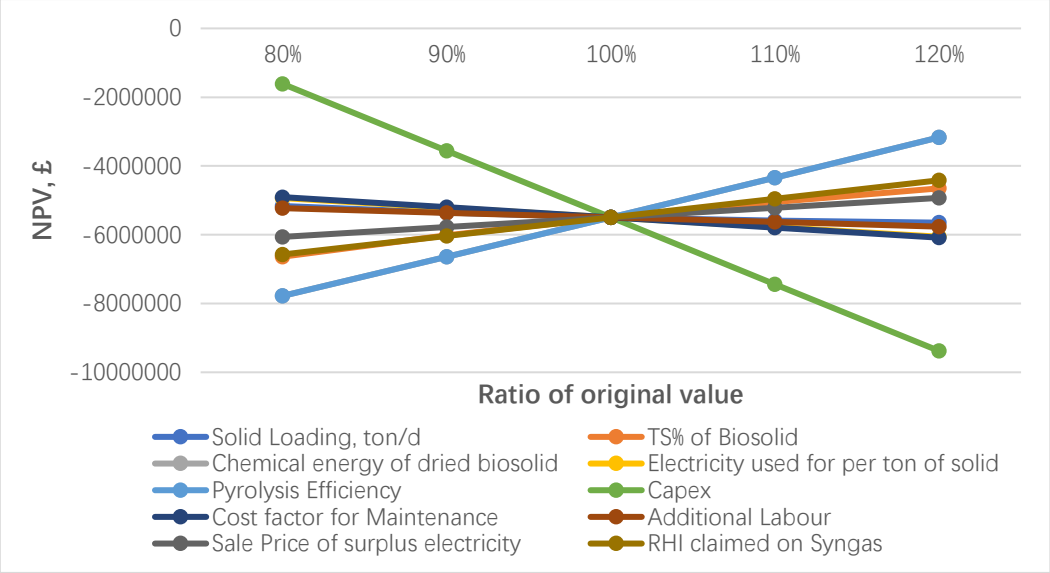

Figure 7-7 The spider chart of the NPV

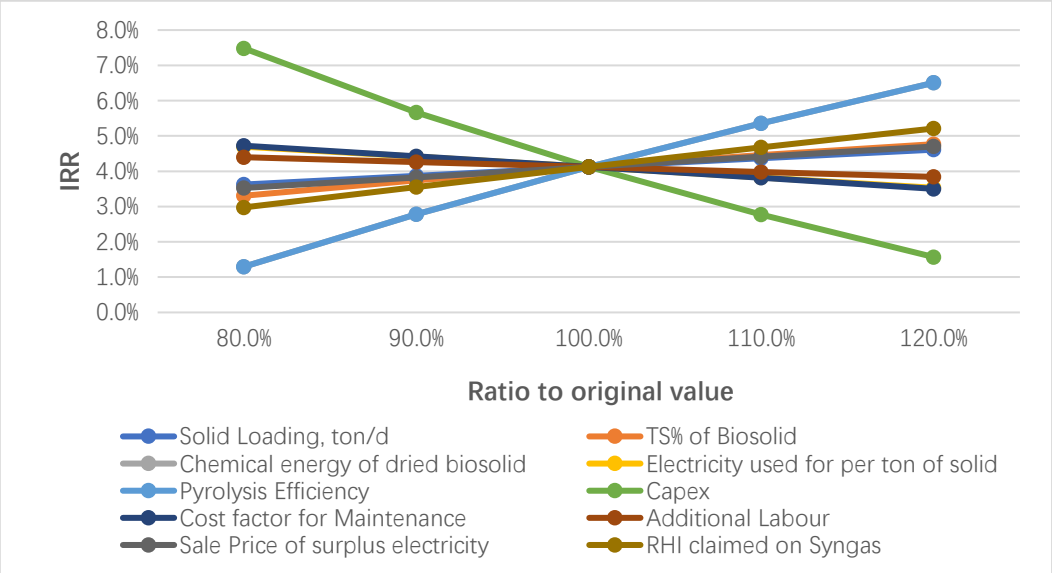

Figure 7-8 The spider chart of the IRR

The increase of TS% of biosolid, chemical energy of dried biosolid, pyrolysis efficiency, sale price of surplus electricity and RHI claimed on Syngas will leads to a higher NPV, a greater IRR and a shorter payback period. The impact caused by a 20% increase of these parameters (once at a time) to NPV, IRR and payback period are listed in Table 7-3.

Meanwhile, the decrease of electricity used for per ton of solid (in the pyrolysis), CAPEX, cost factor of maintenance, additional labour, sale price of surplus electricity and RHI claimed on Syngas will also leads to a higher NPV, a greater IRR and a shorter payback period. The impact

caused by a 20% decrease of these parameters (once at a time) to NPV, IRR and payback period are also listed in Table 7-3.

Interestingly, the increase of solid loading results in a lower NPV but a higher IRR and a shorter payback period. In the cash flow calculation, the CAPEX is estimated base of solid loading, water loading in the sludge, and the projected electricity production. The maintenance cost is then estimated from the CAPEX. The increase of the solid loading will increase the CAPEX and subsequently increase the maintenance cost. However, it also leads to a greater production of syngas and electricity. The income from the RHI claimed on the syngas and sale of surplus electricity is therefore elevated. In result, if the solid loading is increased by 20%, the CAPEX will be increased from £16,460,549 to £18,351,566 and the cash flow will also be increased to £1,224,238 to £1,438,419. The increase of both CAPEX and cash flow explains why a greater solid loading will lead to a lower NPV but a higher IRR and a shorter payback period. However, a 20% increase of the solid loading only leads to a 5% worse NPV, 12% better IRR and 4% shorter payback period.

Table 7-3 The impact to the NPV, IRR and Payback period if a ±20% change is given to the parameters tested for sensitivity

	NPV	Improvement on NPV*	IRR	Improvement on IRR*	Payback Period	Improvement on Payback*
TS% of Biosolid**	-4,651,032	15%	4.77%	16%	12.7	5%
Chemical energy of dried biosolid**	-3,169,498	42%	6.51%	58%	11.0	18%
Pyrolysis Efficiency**	-3,169,498	42%	6.51%	58%	11.0	18%
Sale Price of surplus electricity**	-4,928,245	10%	4.70%	14%	12.8	5%
RHI claimed on Syngas**	-4,417,448	20%	5.21%	26%	12.2	9%
Electricity used for per ton of solid***	-4,933,578	10%	4.70%	14%	12.8	5%
Capex***	-1,613,623	71%	7.48%	82%	10.2	24%
Cost factor for Maintenance***	-4,905,732	11%	4.72%	15%	12.8	5%
Additional Labor***	-5,226,759	5%	4.40%	7%	13.1	2%

*: The improvement is calculated by $\left|\frac{Updated\ NPV,IRR,or\ Payback - Original\ NPV,IRR,or\ Payback}{Original\ NPV,IRR,or\ Payback}\right| \times 100\%$

**: A 20% increase is given to each of these parameters

***: A 20% decrease is given to each of these parameters

For all three economic feasibility indicators, the CAPEX, the chemical energy content of dried biosolid and the pyrolysis efficiency are the most influential parameters, since their lines have the steepest slope as shown in Figure 7-6 to 7-8. This is because the calculation of the payback period, NPV and IRR are affected by three elements, the CAPEX, the OPEX and the income, and these three parameters are able to simultaneously influence two elements or have a double effect on one element. For the CAPEX, its change does not only affect the amount of investment needed to be paid but also affects the cash flow since the maintenance cost of the newly installed facility is estimated from the capital. For the chemical energy content of dried biosolid and the pyrolysis efficiency, they affect the production of the syngas, and hence influences the RHI that could be claimed from the syngas fed to the CHP. Moreover, the increased production of the syngas will also positively affect the production of electricity and hence the income of the sale of electricity. But the others can only affect one element at a time. The TS% of the biosolid only affects the CAPEX estimated for the sludge drying plant. The sale price of surplus electricity, RHI claimed on syngas and electricity used for pyrolysis affects the income only, whilst the cost factor for maintenance and additional labour just impacts the OPEX.

The pessimistic scenario and optimistic scenario study are conducted on the three most influential parameters, the CAPEX, the pyrolysis efficiency and the chemical energy content of dried biosolid are found as the most influential factors in the economic evaluation.

In literatures, the reported pyrolysis efficiency is between 60% to 90% (Cao and Pawłowski, 2012, Mills et al., 2014). For the chemical energy content of dried biosolid, the reported values range for 11.1 to 15.7 kJ/g (Shizas and Bagley, 2004, Mills et al., 2014, Schaum et al., 2016). In the CAPEX estimation shown in Section 7.3.2.1, the CAPEX of the CHP is estimated from electricity production which is influenced by the pyrolysis efficiency and the chemical energy content of dried biosolid. Different pyrolysis efficiency and the chemical energy content of dried biosolid will results in different estimated CAPEX. In this study, the CAPEX in the pessimistic scenario is its highest estimation based on the worst pyrolysis efficiency and the chemical energy content of dried biosolid. The CAPEX in the optimistic scenario is in the opposite. Therefore,

- In the pessimistic scenario, the CAPEX is assumed as £17,582,155, the pyrolysis is assumed as 60%, and the chemical energy content of dried biosolid is assumed as 11.1 kJ/g. Based on the pessimistic scenario, the payback period, NPV and IRR are calculated 40.0 years, -£13,646,391, and -5.86%, respectively.

- In the optimistic scenario, the CAPEX is assumed as £13,232,298, the pyrolysis is assumed as 90%, and the chemical energy content of dried biosolid is assumed as 15.7 kJ/g. Based on the optimistic scenario, the payback period is calculated 8.8 years, NPV becomes a positive value of £ 246,696, but the IRR is 9.53% which is still smaller that the nominal discount rate of 12% , respectively.

Although the economic feasibility is not proven in both pessimistic and optimistic scenarios, there can be a substantial difference in the predicted payback period, NPV and IRR in this proposed project. For managing this huge uncertainty, the Monte Carlo analysis can be used (Korytárová and Pospíšilová, 2015). The analysis first give numbers randomly chosen (from a reasonable range) to the influential parameter to obtain large amount of the predicted economic indicators, and then work out the probabilistic distribution of the economic indicators (as shown in Figure 7-9) (Korytárová and Pospíšilová, 2015). The result can then demonstrate the economic feasibility under consideration of risks. However, since the economic feasibility is not proven in the optimistic scenario, the Monte Carlo analysis is not performed in this study.

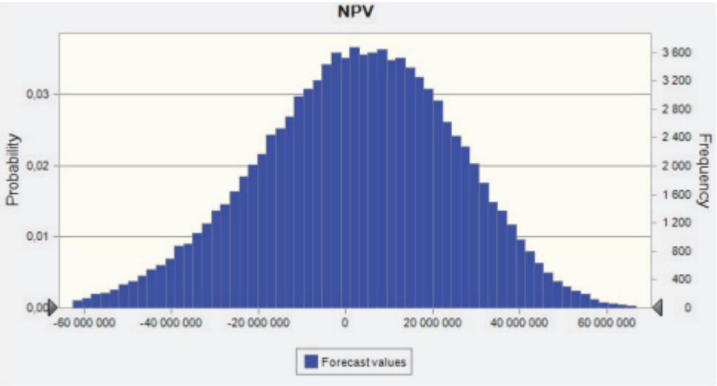

Figure 7-9 The probabilistic distribution of NPV obtained from Monte Carlo Analysis (Korytárová and Pospíšilová, 2015)

7.3.3.3 Future opportunities

This section is to discuss at what circumstance the economics of this proposed project will become feasible. The discussion is made on the optimistic scenario discussed in Section 7.3.3.2. Each of the three most influential parameters will be adjusted once at a time till a payback period within 20 years, a positive NPV and an IRR greater than 12% are achieved simultaneously.

For the CAPEX, the economic feasibility will be achieved if it is reduced to lower than £11,499,245 which is £1,739,052 less than the optimistic estimation of £13,232,298. Potentially this may happen because the future technology improvement can reduce the CAPEX of the facility, for example, the capital cost of wind turbine electricity generators at present has fallen by approximately 20% comparing to in 2008 due to the technology improvement (IRENA, 2016).

For the pyrolysis efficiency, even it is raised from the optimistic estimation of 90% to 100%, the IRR obtained is still 11.22%. It is not able to achieve the economic feasibility. Pyrolysis efficiency is sensitive to the economic evaluation. But in this study, it has been assumed at high level (80%) and is with less room to improve. It cannot single-handedly elevate the economic of the proposed project to the desired level.

For the chemical energy content of the biosolid, if it is raised to 18.3 kJ/g, the economic feasibility will be achieved. However, the chemical energy content of the dried digested sludge is reported 11.1 to 15.7 kJ/g and is not likely to be as high as 18.3 kJ/g (Schaum et al., 2016, Smyth et al., 2016, Shizas and Bagley, 2004). But such a high kJ/g value can be found on the non-digested sludge as shown in Table 4-6. This implies that non-digested sludge may be a more suitable feed of the pyrolysis.

Besides, although incentive are not classified as the most influential parameter in this study, it plays an important role in determining the economics of high capital related projects (Mills et al., 2014). The best example is the current operating GtG in the Base Case whose economics substantially relies on the RHI claimed on the CH_4 injected to the grid (*personnel communication*, L Wilkinson, Northumbrian Water, December 2016). Also, as stated in the Section 7.3.2, the 65.5% projected income of the proposed project is from the incentives

claimed on the syngas. If future market favors generating energy from biosolid or solid waste via pyrolysis, the better economics could be achieved. In particular, the change of incentives tariff is sometimes dramatic. According to the historical data publish by OFGEM, for the "Large biogas combustion" applied in this project, the highest ever announced tariff was £24.3 per MWh for the CH_4 combusted and the lowest was £8.9 per MWh (OFGEM, 2019b). Applying the £24.3 per MWh incentive to the optimistic scenario, the projected payback period becomes 5.5 years, the NPV is improved to £6,035,248, and the IRR is 15.65%. The biosolid pyrolysis may have a future if incentives will become better.

7.3.4 Environmental Benefit

The greatest environmental benefit brought about by the biosolid pyrolysis plant is the improved energy balance of the Base Case. The energy balance $\boldsymbol{EB_{CHP}}$ (stated in Section 7.3.1.3) and $\boldsymbol{EB_{CHP+FP}}$ (stated in Section 7.3.1.3) that are shown without GtG are used for further demonstration. These two comparative balances are in a unified energy type, electricity. All the input or outputs of natural gas will be converted into electricity at the conversion ratio of 38%. The energy figures shown in the following content is given on a daily basis.

In $\boldsymbol{EB_{CHP}}$, the system has to import 59.9 MWh natural gas and 18.8 MWh electricity but generates no output energy. Therefore, the Base Case is a net energy importer and the electricity balance is -59.9×38%+(-18.8)= -41.6 MWh. For $\boldsymbol{EB_{CHP+FP}}$, the system with biosolid pyrolysis still imports 59.9 MWh natural but no electricity. Moreover, the system can even export 16.6 MWh electricity back to the grid. Although the system is still a net energy importer, the electricity balance is improved to -59.9×38%+16.6= -6.2 MWh. The total electricity saving is 35.4 MWh electricity. In 2017, the CO_2 emitted from per MWh electricity supplied is 0.2 ton (BEIS, 2018). Hence, the annual CO_2 emission reduction will be 35.4×0.2×365=2584.2 tonnes. Furthermore, the biochar comes with smaller volume than the biosolid (Paz-Ferreiro et al., 2018). Implementation of biosolid pyrolysis can also reduce the energy consumption of the biosolid haulage.

Moreover, currently biosolid is mainly sent for land application due to its nutrient content. But it also has some potential environmental issues, such as the ammonia gas emission and the concern of possible pathogen regrowth on land, etc.(Paz-Ferreiro et al., 2018, Higgins and

Murthy, 2006). The biochar, the resulting product of pyrolysis, still has a comparable fertility to biosolid but is free from these issues since pyrolysis is a high temperature treatment which can evaporate the free ammonia and kill pathogen (Paz-Ferreiro et al., 2018, Wang et al., 2012). Pyrolysis can unlock the energy reserve of the biosolid, prevent any adverse effect of its land application, but still retain its advantageous fertility.

7.4 Chapter Summary

Since the biosolid pyrolysis potentially has the least impact to the upstream wastewater and sludge treatment process and could potentially help to reduce the landbank stress, this chapter investigated the technical and economic feasibility of its implementation on to the existing energy recovery system of WWTP C.

This chapter first studied the energy balance of the Base Case system and the system with the addition of the biosolid pyrolysis. The economic evaluation considering the payback period, NPV and IRR were then made according to the energy balance. The result suggested that the installation of biosolid pyrolysis is not currently economically feasible.

In the sensitivity study of the uncertainty, CAPEX, pyrolysis efficiency and the chemical energy content of the dried biosolid were found the most influential parameters to the economic evaluation. Even the three were given an optimistic estimation, but the economic feasibility is still not achieved. However, if the CAPEX can be further reduced or better incentives will be granted in the future, the installation of biosolid pyrolysis could become economically feasible.

Although biosolid pyrolysis is not currently economically feasible, it can still bring in environmental benefits of 1) a better energy balance of the system, 2) a reduced energy consumption on sludge haulage, and 3) the prevention of the ammonia gas emission and the possible pathogen regrowth from the biosolid.

Chapter 8 Conclusion and Recommendation

8.1 Conclusion

The overall aim of this project is to reliably determine the chemical energy and mass balances of wastewater treatment plants in the UK to inform possible options for recovery of organic carbon (for energy), nitrogen and phosphorus.

To fulfil this overall aim, the objectives were set, as follows:

1. Develop a reliable and practical method for determination of the chemical energy content of wastewater, and identify a reliable surrogate of the chemical energy in wastewater and in sludge

2. Construct chemical energy and mass balances for 4 actual wastewater treatment plants (WWTPs) to determine the fate of chemical energy, organic carbon (expressed as COD), nitrogen and phosphorus in the wastewater and sludge treatment (via modelling)

3. Identify potential waste recovery opportunities and explore the impact of their implementation on the existing treatment process (via modelling)

8.1.1 Chemical energy of wastewater and sludge

The first objective of this study is to develop a reliable and practical method for determination of the chemical energy content of wastewater and identify a reliable surrogate of the chemical energy in wastewater and in sludge.

This research successfully developed a new wastewater drying method that is at least as good as the proven method of freeze-drying for retaining the energy-containing material but is able to shorten the drying time for 1 L of wastewater sample from 2-4 weeks to 3 days. Having developed the drying method, 46 spot samples and 61 composite samples of raw wastewater, 20 composite samples of primary effluent, and 17 composite samples of secondary effluent collected from four WWTPs were measured for chemical energy content (kJ/L) in this study. Subsequently, this research conducted statistical analysis (correlation and Best Subset of

regression) to investigate the relationship between chemical energy (E_{ww}, kJ/L) and commonly analyzed wastewater variables. COD was found to be the best surrogate of the energy content of wastewater. It has a ubiquitously (across the four WWTPs) strong linear relationship (r^2= 77 -93%, $p<0.05$, excluding the spot raw) with E_{ww}. An empirical mathematical relationship between E_{ww} and COD is found 15.8 kJ/g COD.

A similar statistical study was also conducted for understanding the relationship between sludge chemical energy (E_s, kJ/L) and the other commonly analyzed sludge variables, Strong linear relationships ($r^2>85\%$, $p<0.05$) were found between the E_s and sludge total solid (TS_s), sludge volatile solid (VS_s), based on 87 sludge samples collected from various treatment processes, such as primary settlement, activated sludge, anaerobic digestion, of four WWTPs . The empirical mathematical relationships between E_s and, TS_s and VS_s are found 17.1 kJ/g TS_s and 21.9 kJ/g VS_s. Via assuming the wastewater and sludge share the same relationship between COD and VS, the sludge COD was estimated. A similar relationship between chemical energy and COD is found in both sludge and wastewater.

The objectives of developing a quick but reliable method of estimating wastewater energy content using routinely analyzed variables has been fulfilled. Since the chemical energy of wastewater and sludge can be estimated much more quickly via COD, TS_s and/or VS_s, an energy audit of a treatment process or a treatment works can now be easily conducted. The energy recovery performance can be better monitored. This also helps discover potential opportunities for improvement in energy recovery.

8.1.2 Investigation of chemical energy balance and COD, nitrogen and phosphorus mass balance

The second objective of this study is to construct chemical energy and mass balances for four actual WWTPs to determine the fate of chemical energy, organic carbon (expressed as COD), nitrogen and phosphorus in the wastewater and sludge treatment via modelling.

This study constructed, calibrated and validated models for the wastewater and sludge treatment processes of four WWTPs with a range of population equivalents, wastewater treatment processes, and sludge treatment processes. In all cases, the difference between the

predicted results from the observed results was no more than ± 15%. Hence, these predicted results were used to build the chemical energy balance and COD, nitrogen and nitrogen mass balance for the four WWTPs.

8.1.2.1 COD mass balance and chemical energy balance

The COD mass and chemical energy balance of the four WWTPs shows that:

- 69.7 ± 12.8% of wastewater COD and chemical energy flowing into the works can be captured in the sludge and sent for sludge treatment via digestion,
- 24.8 ± 5.5% of wastewater COD and chemical energy flowing into the works is lost to the atmosphere, potentially as CO_2
- 7.5 ± 4.4 % of wastewater COD and chemical energy flowing into the works remains in the final effluent and is discharged to the water bodies.

The COD mass balance and chemical energy balance of the four WWTPs suggest that majority of the COD and chemical energy loading were captured during the wastewater treatment. Only a small proportion of COD and chemical energy loading remain in the final effluent.

The COD mass balance and chemical energy balance of the sludge treatment of WWTP C shows that,

- 21.3 % of the sludge COD and chemical energy ends in the dewatered digested sludge
- 31.1% of the sludge COD and chemical energy is retained in the filtrates and centrates
- 43.7% of the sludge COD and 38.4% of the sludge chemical energy is recovered as CH_4.

On this basis, approximately 20-30% of the chemical energy in raw wastewater has the potential to be recovered as CH_4. However, only 6-9% of the chemical energy in raw wastewater can be potentially recovered as electricity. In this study, even though the chemical energy within the raw wastewater of the investigated WWTPs is 5 - 14 times higher than its electricity consumption, the WWTPs are not always electricity self-sustaining.

8.1.2.2 Nitrogen and Phosphorus mass balance

The phosphorus mass balance of the four WWTPs shows that:

- 68.2 ± 14.3% of wastewater phosphorus flowing into the works can be captured in the

sludge and sent for sludge treatment via digestion,

- 31.8 ± 14.3 % of wastewater phosphorus energy flowing into the works remains in the final effluent and is discharged to the water bodies,
- No wastewater phosphorus flowing into the works is lost to the atmosphere.

The nitrogen mass balance of the four WWTPs shows that:

- For WWTPs A and D has nitrification in the activated sludge process,
    - 35.9 ± 10.4% of wastewater nitrogen flowing into the works can be captured in the sludge and sent for sludge treatment via digestion,
    - 25.9 ± 11.3 % of wastewater nitrogen flowing into the works is lost to the atmosphere, potentially as N_2 or N_2O,
    - 38.3 ± 0.9 % of wastewater phosphorus energy flowing into the works remains in the final effluent and is discharged to the water bodies,
- For WWTPs B and C has nitrification in the activated sludge process,
    - 33.0 ± 10.4% of wastewater nitrogen flowing into the works can be captured in the sludge and sent for sludge treatment via digestion,
    - No wastewater nitrogen flowing into the works is lost to the atmosphere, potentially as N_2 or N_2O,
    - 67.0 ± 15.3 % of wastewater phosphorus energy flowing into the works remains in the final effluent and is discharged to the water bodies,

The nitrogen and phosphorus mass balance of the four WWTPs suggests that the approximately two-thirds of the wastewater phosphorus and one-third of wastewater nitrogen are captured in the sludge during the wastewater treatment. Unlike the COD and chemical energy, the final effluent could contain a substantial proportion of 30-70% of the nutrient mass flowing into the work. Moreover, this study finds nitrification may cause nitrogen lost to the atmosphere due to the unexpected denitrification in the activated sludge process and the subsequent final clarification.

The nitrogen and phosphorus mass balance of the sludge treatment study of the sludge treatment of WWTP C shows that,

- 68.5% of the sludge nitrogen and 64.5% of the sludge nitrogen is distributed in the filtrates and centrates of the sludge thickening and dewatering, and

- 31.5% of the sludge nitrogen and 35.5 % of the sludge nitrogen remain in the dewatered digested sludge.

On this basis, approximately 20-30% of the nitrogen and 35-55% of the nitrogen flowing into the works are estimated to end up in the filtrates and centrates which will be recirculated back to the head of the work. Meanwhile, approximately 7-14% of the nitrogen and 19-30% of the nitrogen flowing into the work are estimated to be kept in the digested sludge.

8.1.3 Investigation of chemical energy balance and COD, nitrogen and phosphorus mass balance

The third objective of this study is to identify potential waste recovery opportunities and explore the impact of their implementation on the existing treatment process (via modelling)

Based on the chemical energy and COD mass balance study, this study found that even though the chemical energy within the raw wastewater of the investigated WWTPs is 5-14 times higher than its electricity consumption, the WWTPs are not always electricity self-sustaining.
The energy recovery opportunities are 1) to increase the chemical energy feed to the anaerobic digestion, 2) to recover the unrecovered chemical energy kept in the dewatered digested sludge (biosolid), and 3) to recover energy from wastewater directly.

Therefore, according to the opportunities discovered, four measures are proposed

- improving the efficiency of solids removal in primary settlement
- reducing the sludge retention time prior to the digestion
- recovering energy from the dewatered digested sludge via pyrolysis, and
- reducing the electricity consumption by replacing the activated sludge processes with energy-generating anaerobic membrane reactor (AnMBR) units.

The current nutrient recovery focused on the agricultural land application of the dewatered digested sludge and fertilizer recovery of the phosphate and ammonium from the raw sludge centrate and digested sludge centrate, based on the nitrogen and phosphorus balance studied, this study considers the opportunity is to improve the capturing of phosphorus to the sludge in order to increase the nutrient loading distrusted to sludge filtrates and centrates and digested

sludge. Thus, it proposed a measure of adding ferric dosing or enhanced biological phosphorus removal (EBPR) to the current system.

The five proposed measures are built into case studies. The impact of their implementation on the holistic energy balance and nutrient balance are explored mainly via modelling (exclude the dewatered digested sludge pyrolysis) and are listed as followed:

- Improving the efficiency of solids removal in the primary settlement is able to increase the feed chemical energy to the digester. Moreover, it also reduces the energy consumption on the aeration process. Therefore, a better energy balance is achieved. However, the uncertainty of this measure is that, if metal coagulant is used, it could bring adverse effect to the digester. In nutrient wise, it the phosphate and ammonium loading distributed to the raw sludge centrate and digested sludge centrate but increases total nitrogen and total phosphorus loading in the digested sludge. Furthermore, it increases the nitrogen and phosphorus loading distributed to the final effluent.

- Reducing the sludge retention time prior to the digestion reduces the chemical energy lost to centrate and hence increaser the feed chemical energy to the digester. It delivers a better energy balance. It also reduces the phosphate and ammonium loading distributed to the raw sludge centrate and digested sludge centrate but increases total nitrogen and total phosphorus loading in the digested sludge.

- Recovering energy from the dewatered digested sludge via pyrolysis leads to a better energy balance since the chemical energy with dewatered digested sludge is unlocked. It makes no impact on the phosphate and ammonium loading distributed to the raw sludge centrate and digested sludge centrate.

- Replacing the activated sludge processes with energy-generating AnMBR units can lead to a better energy balance if the AnMBR can be energy self-sufficient. That is because substantial amount of the aeration energy is saved. However, this is highly uncertain depending of the energy consumption (including both heating and pumping) on the process itself (Martin et al., 2011). Meanwhile, this measure reduces both the phosphate and ammonium loading distributed to the raw sludge centrate and digested sludge centrate and

the total nitrogen and total phosphorus loading in the digested sludge. More nitrogen and phosphorus are therefore distributed to the final effluent.

- Implementation of both ferric dosing and EBPR to improve the phosphorus capturing barely impacts the energy balance. The implementation of EBPR substantially improves the phosphate loading distributed to the raw sludge centrate and digested sludge centrate but barely impacts the phosphorus loading to the digested sludge. The implementation of ferric dosing is in the opposite: it barely changes phosphate loading distributed to the raw sludge centrate and digested sludge centrate but substantially increases the phosphorus loading to the digested sludge. The nitrogen mass balance is only slightly impacted in this case.

The five case studies suggest that the measures aim to promote the energy balance is likely to increase the nutrient loading distributed to the dewatered digested sludge or to the final effluent but reduce the phosphate and ammonium loading distributed to the raw sludge centrate and digested sludge centrate. This is adverse to the fertilizer recovery from the raw sludge and digested sludge centrate but provides an opportunity of recovering nutrient directly from wastewater. However, the measures aim to promote the nutrient recovery from sludge treatment barely impacts the energy balance

Since the biosolid pyrolysis potentially has the least impact to the upstream wastewater and sludge treatment process and could potentially reduce the landbank stress, the technical and economic feasibility of its implementation on to the existing energy recovery system of WWTP C is studied. The economic evaluation considering the payback period, NPV and IRR suggest that the installation of biosolid pyrolysis is not currently economically feasible. From the sensitivity study, the capital expenditure (CAPEX), pyrolysis efficiency and chemical energy content are the most influential parameters to economic evaluation. This study considers economic feasibility could be achieved in the future if CAPEX becomes lowered due to the technology development, and/or incentive granted will be elevated as pyrolysis is encouraged by the government.

8.2 Recommendation

The breakdown of energy material in wastewater and sludge

This study has demonstrated that the chemical energy content of wastewater can be estimated by multiplying its COD concentration by a value of 15.8 kJ/g COD. This 15.8 kJ/g COD only represents the relationship between COD concentration and the total chemical energy contained in wastewater, but not the energy content of a gram of COD because part of the chemical energy is from the TKN (Scherson and Criddle, 2014). Therefore, understanding the energy content of a gram of COD is a potential research area. So is recovering energy from TKN.

Wastewater and sludge are both mixtures. Their chemical energy is from different groups of chemicals. This research did not investigate the breakdown of the energy contribution from each chemical as it was not a primary aim of the research. Nevertheless, that is an area recommended for future research because it may help target energy recovery technologies to specific energy containing materials that are not recovered using current methods.

The establishing model of the innovative value recovery technology

In the nutrient recovery, a substantial proportion of nutrient remains in the final effluent discharged. Recovery opportunity is, therefore, to recover this nutrient directly from wastewater. However, the modelling software does not contain such a unit of ion exchange or algal reactor. And hence, the modelling of the nutrient recovery directly from wastewater is therefore hampered. Moreover, the microbial fuel/electrolysis cell is another promising energy generating biological treatment (Stoll et al., 2018, Cotterill et al., 2018). Since it produces different products of H_2 or electricity, it would be useful to model its implementation and then compare to the CH_4 generating anaerobic treatment. Therefore, it would be useful to has such innovative recovery technologies programmed into the modelling software.

Chemical energy recovery

Although improving the solid removal efficiency of primary settlement is found beneficial to the energy balance, the uncertainty of this measure is how to improve the solid removal efficiency. If metal coagulant is used and is in high dosage, harmful effect may be caused to the digester (Diamantis et al., 2013). Therefore, it is worth to discover effective coagulant for improving the solid settling without harming the downstream digestion.

As mentioned in Section 5.2.2, WWTP B has a high percentage of chemical energy captured in the SAS. The reason of it is considered as that the high ferric content of the inflowing wastewater causes bio-flocculation which reduce the chemical energy loss due to COD oxidation. Therefore, coagulant dosing in the activated sludge process could be a potential approach to improve the capturing of chemical energy in the activated sludge.

As stated in Section 8.1.2.1, approximately 30% of the sludge energy entered into the sludge treatment ended in the filtrates and centrates. This study suggested reducing the sludge retention time to reduce the chemical energy loading. This measure mainly focuses on reducing the soluble energetic COD formed from the hydrolysis, fermentation and digestion of the sludge. However, as shown in Table 5-4, majority of the COD in the primary sludge filtrate and in the SAS filtrate are pCOD. Therefore, improving the solid retaining efficiency of the sludge thickening and dewatering process could also leads to greater feed chemical energy to the digestion.

Moreover, apart from reducing the energy loading in the filtrates and centrates for promoting energy production, effort could be made on recovering the chemical energy directly from the filtrates and/or centrates. As shown in Table 5-4, the COD content of the filtrates varies from 1,000-10,000 mg/L. Such a high concentration is favored by the anaerobic treatment or microbial fuel cells (Stoll et al., 2018). Therefore, it is worth to investigate the treatability of the filtrates and centrates in the anaerobic treatments and energy balance.

The recovery of nutrient and energy directly from wastewater requires a concentrated feed wastewater (Stoll et al., 2018, Münch and Barr, 2001). The measure for promoting value recovery proposed in this study mainly focus on modifying the process inside the WWTPs and is unable to change to concentration of the valuable COD, nitrogen and phosphorus in the raw wastewater. Therefore, effort could potentially be made on recovering the valuable from its source via decentralized treatment (Capodaglio, 2017).

Appendix A. TN Adjustment for Sludge Sample

In this study, Total Nitrogen content (TN%) was measured by the scientific service of Scottish Water. Due to the logistical constraints the sludge was dried prior to the test. However, Ammonia can be lost during the sludge drying (Maurer and Müller, 2012, Huett, 1997), and hence leads to the lower TN% of the sludge. Therefore, this study firstly adjusts the TN% of the sludge.

TN% of the feed and thickened or dewatered sludge of WWTP C's thickening and dewatering facilities was adjusted via Equation 3-8 (shown in Section 3.2.2.4). The adjusted TN% (as $TN\%_{Adjusted}$) and the experimentally measured TN% (as $TN\%_{Measured}$) were compared. Results are shown in Table A-1.

Table A-1 Adjusted TN% of different type of sludge of Howdon WWTP

Type of Sludge	No. of Sampling	$TN\%_{Measured}$, %	$TN\%_{Adjusted}$, %	$TN\%_{Measured}$:$TN\%_{Adjusted}$
Primary Sludge	3	2.66 ±0.46	3.18 ±0.68	1.19 ±0.08
Thickened Primary Sludge	3	2.58 ±0.25	2.90 ±0.67	1.12 ±0.06
SAS	4	5.27 ±0.60	5.88 ±0.64	1.12 ±0.01
Thickened SAS	4	6.67 ±0.78	6.75 ±0.79	1.01 ±0.00
Raw Sludge	5	3.60 ±1.24	4.58 ±1.27	1.28 ±0.12
Raw Centrifuged Cake	5	3.67 ±0.56	3.82 ±0.55	1.05 ±0.01
Digested Sludge	5	4.63 ±1.55	8.62 ±1.87	1.89 ±0.37
Digested Cake	5	4.65 ±0.20	5.21 ±0.30	1.12 ±0.02

In Chapter 4 to 6, the TN% used is adjusted according to the $TN\%_{Measured}$: $TN\%_{Adjusted}$ of the corresponding type of sludge. For WWTP A and D, even though their primary sludge was mixed with SAS and humus, since the $TN\%_{Measured}$: $TN\%_{Adjusted}$ of the primary sludge and SAS is close the TN% of their primary sludge is adjusted by just multiplying by 1.19, which is the $TN\%_{Measured}$: $TN\%_{Adjusted}$ of primary sludge.

Appendix B. The value range of the kinetic and stoichiometry of the biological models.

Table B-1 The value range of the kinetic and stoichiometry of the biological models

Parameter	Defaul Value	Lower boundary	Upper Boundary
Model Stoichiometry			
Heterotrophic yield on soluble substrate			
Aerobic heterotrophic yield on soluble substrate	0.6250	0.3800[1]	0.7500[1]
Anoxic heterotrophic yield on soluble substrate	0.5330	0.4264	0.6250[2]
Methylotrophic Biomass			
Aerobic methylotroph yield on methanol	0.4500	0.3600	0.5400
Anoxic methylotroph yield on methanol	0.3600	0.2880	0.4320
Fermentative Biomass			
Yield of fermentative biomass	0.1800	0.1440	0.2160
Ammonia-Oxidizing Biomass			
Ammonia-oxidizer yield	0.1800	0.0500[3]	0.3000[3]
Nitrite-Oxidizing Biomass			
Nitrite-oxidizer yield	0.0600	0.0480	0.0720
Anammox Biomass			
Biomass yield on NH4-N	0.1675	0.1340	0.2010
Poly-Phosphate-Accumulating Biomass (PAOs)			
Aerobic yield on PAO growth	0.6250	0.5000	0.7500
Anoxic yield on PAO growth	0.5110	0.4088	0.6250[2]
PHA storage yield	0.4000	0.1000[4]	0.6000[4]
Xpp storage yield	0.2000	0.1000[4]	0.3000[4]
Acetogenic Biomass			
Acetogenic yield on propionate	0.0400	0.0320	0.0480
Hydrogenotrophic Methanogenic Biomass			
Methanogenic yield on H2	0.0600	0.0480	0.0720

Acetoclastic Methanogenic Biomass			
Methanogenic yield on acetate	0.0500	0.0400	0.0600
Unbiodegradable fraction from biomass decay			
Unbiodegradable fraction from cell decay	0.1000	0.0800	0.2500[5]
Soluble inert COD fraction			
Fraction of inert COD during slowly biodegradable organic hydrolysis	0.0000	0.0000	0.0000
Fraction of inert COD during inert residue hydrolysis	0.0000	0.0000	0.0000
Fraction of inert COD during inert organic hydrolysis	0.0000	0.0000	0.0000
Kinetics			
Absorption of colloidal COD			
Specific adsoprtion rate	0.1000	0.0800	0.1200
Saturation/inhibition coefficient for Xs/Xbh	0.0500	0.0400	0.0600
Heterotrophic biomass			
Maximum specific growth rate on substrate	6.0000	0.6000[1]	13.2000[1]
Saturation/inhibition coefficient for SS	4.0000	3.2000[5]	15.0000
Saturation coefficient for oxygen	0.2000	0.0100	0.5000[1]
Saturation coefficient for nitrogen as nutrient	0.0500	0.0400[1]	0.2000
Saturation coefficient for Nox-N as nutrient	0.5000	0.1000[3]	0.5500[3]
Saturation coefficient for phosphorus (nutrient)	0.0100	0.0050[4]	0.0150[4]
Saturation/inhibition coefficient for Sac	4.0000	3.5000[4]	4.5000[4]
Saturation/inhibition coefficient for Spro	4.0000	3.2000	4.8000
Reduction factor for denitrification on nitrate-N	0.3200	0.2560	0.9000[4]
reduction factor for denitrification on nitrite-N	0.4800	0.3840	0.5760
Saturation coefficient for nitrite	0.1000	0.0800	0.1200
Saturation coefficient for nitrate	0.5000	0.4000	0.6000
Oxygen inhibition coefficient for denitrification	0.2000	0.1600	0.2400
Aerobic heterotrophic decay rate	0.4000	0.0200	1.6000[5]
Anoxic reduction factor fro decay rate	0.9000	0.7200	1.0800
Anaerobic reduction factor for decay rate	0.6000	0.4800	0.7200
Methylotrophic Biomass			
Maximum growth rate fro methylotrophs	1.3000	1.0400	1.5600
Methanol saturation coefficient for methyltrophs	0.5000	0.4000	0.6000
Saturation coefficient of nitrite for methyltrophs	0.1000	0.0800	0.1200

Saturation coefficient of nitrate fro methyltrophs	0.1000	0.0800	0.1200
Oxygen saturation for methyltrophs	0.2000	0.1600	0.2400
Reduction factor for denitrification on nitrate-N	0.4000	0.3200	0.4800
Reduction factor for denitrification on nitrite-N	0.6000	0.4800	0.7200
Oxygen inhibition ocefficient for denitrification	0.2000	0.1600	0.2400
Aerobic methylotrophic decay rate	0.2000	0.1600	0.2400
Anoxic recution factor fro decay rate	0.9000	0.7200	1.0800
Anearobic methylotrophic decay rate	0.6000	0.4800	0.7200
Ammonia-Oxidizing Biomass			
Maximum growth rate for ammonia oxidizer	1.0000	0.2000[7]	1.2000
Ammonia saturation coefficient for ammonia oxidizer	1.0000	0.2000[1]	1.5000[1]
Oxygen saturation for ammonia oxidizer	0.5000	0.2000[2]	3.0000[1]
Inhibition coefficient of FA for ammonia oxidizer	50.0000	40.0000	60.0000
Inhibition coefficient of FNA for ammonia oxidizer	0.2000	0.1600	0.2400
ammonia oxidizer aerobic decay rate	0.1500	0.0200[1]	0.2300[6]
anoxic reduction factor for decay rate	0.5000	0.4000	1.5000[1]
anaerobic recution factor for decay rate	0.3000	0.2400	0.3600
Nitrite-Oxidizing Biomass			
Maximum growth rate for nitrite oxidizer	1.0000	0.8000	1.2000
NItrite saturation coefficient for nitrite oxidizer	0.5000	0.0400[2]	0.6000
Oxygen saturation for nitrite oxidizer	0.6800	0.1000[2]	0.8160
Inhibition coefficient of FA for nitrite oxidizer	1.0000	0.8000	1.2000
Inhibition coefficient of FNA for nitrite oxidizer	0.0900	0.0720	0.1080
nitrite oxidizer aerobic decay rate	0.1700	0.1360	0.2040
anoxic reduction factor for decay rate	0.5000	0.3000[2]	0.6000
anaerobic recution factor for decay rate	0.3000	0.2400	0.3600
Anammox Biomass			
Maximum growth rate for anammox bacteria	0.0186	0.0148	0.0223
Ammonia saturation coefficient for anammox bacteria	0.7300	0.5840	0.8760
Nitrite saturation for anammox bacteria	0.5000	0.4000	0.6000
Oxygen saturation/inhibition for anammox bacteria	0.1000	0.0800	0.1200
aerobic decay rate of anammox bacteria	0.0058	0.0046	0.0070
anoxic reduction factor for decay rate	0.5000	0.4000	0.6000
anaerobic recution factor for decay rate	0.3000	0.2400	0.3600
Poly-Phosphate-Accumulating Biomass (PAOs)			

Rate constant for storage of PHA	3.0000	2.0000[4]	6.0000[4]
Saturation coefficient of PAO for Sac	4.0000	2.0000[2]	4.8000
Saturation coefficient for Xpp/Xbp	0.0100	0.0080	0.0200[4]
Saturation coefficient of PAO for Spro	4.0000	3.2000	4.8000
Maximum growth rate of PAO	1.0000	0.6700[4]	1.2000
Saturation coefficient for PHA	0.0100	0.0070[4]	0.0150[4]
Saturation coefficient for oxygen	0.2000	0.1600	0.2400
Rate constant for storage of poly-phosphate	1.5000	1.0000[4]	2.5000[2]
Maximum ratio of Xpp/Xpao	0.3400	0.2000[8]	0.5100[8]
Inhibition coefficient for Xpp/Xbp	0.0200	0.0100[4]	0.0300[4]
P saturation for uptake	0.2000	0.1000[4]	0.3000[4]
Reduction factor for denitrification on nitrate-N	0.2400	0.1920	0.2880
Reduction factor for denitrification on nitrite-N	0.3600	0.2880	0.4320
Saturation coefficient of nitrite for PAO	0.5000	0.4000	0.6000
Saturation coefficient of nitrate for PAO	0.5000	0.4000	0.6000
Oxygen inhibition coefficient for denitrification	0.2000	0.1600	0.2400
aerobic decay rate for PAO	0.2000	0.1000[4]	0.2400
anoxic reduction factor for decay rate	0.9000	0.6000[2]	1.0800
anaerobic reduction factor for decay rate	0.6000	0.4800	0.7200
Poly-P lysis coefficient	0.2000	0.1000[4]	0.3000[4]
PHA lysis coefficient	0.2000	0.1000[4]	0.2400
Fermentative Biomass			
Maximum fermentation rate	3.0000	1.5000[4]	3.6000
Oxygen saturation for obligate anaerobic biomass	0.1000	0.0800	0.1200
Nitrate saturation forobligate anaeobic biomass	0.1000	0.0800	0.1200
Substrate saturation for fermentative biomass	4.0000	3.2000	4.8000
Hydrogen saturation/inhibition for acidifier	10.0000	8.0000	12.0000
Aerobic decay rate for fermentative biomass	0.1333	0.1066	0.1600
Anoxic reduction factor for decay rate	0.5000	0.4000	0.6000
anaerobic reduction factor for decay rate	0.3000	0.2400	0.3600
Acetogenic Biomass			
Maximum growth rate of propionate degrading bacteria	0.3500	0.2800	0.4200
Undissociated propionate saturation for propionate degrading bacteria	10.0000	8.0000	12.0000
Hydrogen inhibition for propionate degrader	5.0000	4.0000	6.0000
Aerobic decay rate for acetogens	0.0670	0.0536	0.0804
Anoxic reduction factor for decay rate	0.5000	0.4000	0.6000
Anaerobic reduction factor for decay rate	0.3000	0.2400	0.3600

Hydrogenotrophic Methanogenic Biomass			
Maximum growth rate of H2-utilizing bacteria	0.3680	0.2944	0.4416
Hydrogen saturation for hydrogenotrophic methanogens	2.5000	2.0000	3.0000
Aerobic decay rate for hydrogenotrophic methanogens	0.0330	0.0264	0.0396
Anoxic reduction factor for decay rate	0.5000	0.4000	0.6000
Anaerobic reduction factor for decay rate	0.3000	0.2400	0.3600
Acetoclastic Methanogenic Biomass			
Maximum growth rate of acetate utilizing bacteria	0.1500	0.1200	0.1800
Acetate saturation for hydrogenotrophic methanogens	75.0000	60.0000	90.0000
Aerobic decay rate for acetoclastic methanogens	0.0670	0.0536	0.0804
Anoxic reduction factor for decay rate	0.5000	0.4000	0.6000
Anaerobic reduction factor for decay rate	0.3000	0.2400	0.3600
Hydrolysis			
Hydrolysis rate constant for xs	3.0000	0.9600[1]	3.6000
Saturation coefficient for particulate COD	0.1000	0.0100[7]	0.2000[2]
Anoxic hydrolysis reduction factor	0.6000	0.4000[5]	1.0000[5]
Anaerobic hydrolysis reduction factor	0.4000	0.1000[2]	0.4500[4]
Saturation /ihibiton coefficient for NOx	0.5000	0.4000	0.6000
Hydrolysis rate constant for inert residue	0.0300	0.0240	0.0360
Saturation coefficient for inert residue	1.0000	0.8000	1.2000
Hydrolysis rate constant for inert organic	0.0300	0.0240	0.0360
Saturation coefficient for inert organic	1.0000	0.8000	1.2000
Ammonification			
Ammonification rate	0.0800	0.0640	0.0960

1: The value is reported in Jeppsson (1996)
2: The value is reported in Drewnowski et al. (2018)
3: The value is reported in Weijers and Vanrolleghem (1997)
4: The value is reported in Henze et al. (2000)
5: The value is recommended by GPS-X 7.0
6: The value is reported in Liwarska-Bizukojc et al. (2011)
7: The value is reported in Petersen et al. (2002)
8: The value is reported in Rieger et al. (2001)

Appendix C. Sludge density calculation

Sludge consists water, fix solid (FS) and volatile solid (VS). The latter two compose the total solid (TS). Thus, both mass or volume of sludge is the total mass or volume of the three. As volume is calculated by diving the mass (m) with specific density, thus

Equation C-1

$$\frac{m_{Sludge}}{\rho_{Sludge}} = \frac{m_{Water}}{\rho_{Water}} + (\frac{m_{VS}}{\rho_{VS}} + \frac{m_{FS}}{\rho_{FS}})$$

where $\boldsymbol{m_{Sludge}}$, $\boldsymbol{m_{Water}}$, $\boldsymbol{m_{VS}}$ and $\boldsymbol{m_{FS}}$ are the mass of the sludge, water content, volatile solid and fixed solid, respectively; $\boldsymbol{\rho_{Sludge}}$, $\boldsymbol{\rho_{Water}}$, $\boldsymbol{\rho_{VS}}$ and $\boldsymbol{\rho_{FS}}$ are the density of the sludge, water content, volatile solid and fixed solid, respectively

By diving the m_{Sludge} on both side of Equation B-1, gets

Equation C-2

$$\frac{1}{\rho_{Sludge}} = \frac{m_{Water}/m_{Sludge}}{\rho_{Water}} + (\frac{m_{VS}/m_{Sludge}}{\rho_{VS}} + \frac{m_{FS}/m_{Sludge}}{\rho_{FS}})$$

where $\boldsymbol{m_{Water}/m_{Sludge}}$ is the percentage water content of the sludge which is calculated by subtracting the TS% from 100%, $\boldsymbol{m_{VS}/m_{Sludge}}$ is the percentage VS content of the sludge which can be calculated by multiplying the TS% with the VS%, $\boldsymbol{m_{FS}/m_{Sludge}}$ is the percentage FS content of the sludge which can be calculated by multiplying the TS% with (1-VS%). Thus,

Equation C-3

$$\frac{1}{\rho_{Sludge}} = \frac{1 - TS\%}{\rho_{Water}} + (\frac{VS\% \times TS\%}{\rho_{VS}} + \frac{(1 - VS\%) \times TS\%}{\rho_{FS}})$$

The specific density of water is 1 g/cm^3, and the specific density of VS and FS are commonly taken as 1 g/cm^3 and 2.5 g/cm^3 (Andreoli, C.V., et al, 2007), respectively. Therefore, the specific density of sludge is

Equation C-4

$$\rho_{Sludge} = \frac{1}{\frac{1 - TS\%}{1} + (\frac{VS\% \times TS\%}{1} + \frac{(1 - VS\%) \times TS\%}{2.5})}$$

where ***TS%*** is the total solid percentage, ***VS%*** is the volatile solid percentage (to total solid).

Sewage sludge collected in this study commonly has TS% varies from 0.5% to 24.0%, and VS% varies from 60% to 80%. In this range of TS% and VS%, the specific density of sludge increases with the increase of TS% and the decrease of VS% but is within range of 1.001 to 1.061 ton/m^3. Thus, the specific density of all the sludge in this study were assumed as 1 ton/m^3 (1,000 g/L).

Appendix D. Model calibration

The most important parameters of influent fraction, kinetic and stoichiometric that influence the modelling results, and are therefore subject to adjustment in the model for each WWTP, are listed in the Tables D-1 to D-4. The table also presents the δ_j^{msqr} (that indicates the influence of the parameter to the entire model), the adjusted value, the order of adjustment, and the category each adjusted parameter belongs to.

Table D-1 The calibrated parameters of the wastewater treatment model of WWTP A

Ranking	Category*	Parameters	δ_j^{msqr}	Adjusted Value	Tuning Order
1	ASM	Aerobic heterotrophic yield on soluble substrate	1.682	0.4277	Step 2
2	ASM	Maximum growth rate for ammonia oxidizer	1.083	1.1306	Step 3
3	ASM	Aerobic heterotrophic decay rate	0.741	0.0282	Step 2
4	Pri-ASM	Anoxic heterotrophic yield on soluble substrate	0.388	0.4680	Step 3
5	Inf	Soluble inert fraction of total COD	0.350	0.1768	Step 1
6	Final-ASM	Aerobic heterotrophic decay rate	0.282	0.6955	Step 2
7	ASM	Anoxic heterotrophic yield on soluble substrate	0.257	0.4320	Step 3
8	Pri-Set	Flocculant zone settling parameter	0.213	0.0012	Step 2
9	Final-ASM	Saturation coefficient for phosphorus (nutrient)	0.196	0.0085	Step 2
10	Final-ASM	Maximum specific growth rate on substrate	0.192	3.9115	Step 2
11	Final-ASM	Aerobic heterotrophic yield on soluble substrate	0.182	0.7491	Step 2
12	Inf	Readily biodegradable fraction of total COD	0.182	0.0501	Step 1
13	Pri-Set	Maximum Vesilind settling velocity	0.181	263.1532	Step 2
14	Final-Set	Flocculant zone settling parameter	0.180	0.0020	Step 2
15	Final-Set	Maximum Vesilind settling velocity	0.166	233.7769	Step 2
16	Pri-ASM	Reduction factor for denitrification on nitrate-N	0.154	0.3001	Step 3
17	Pri-ASM	Maximum specific growth rate on substrate	0.154	6.2283	Step 3
18	Pri-ASM	Saturation coefficient for nitrate	0.150	0.5717	Step 3
19	Pri-Set	Maximum non-settleable solids	0.144	16.4233	Step 2
20	ASM	Saturation coefficient for nitrate	0.115	0.4301	Step 3
21	Inf	P content of soluble inert material	0.115	0.0063	Step 1
22	Final-ASM	Anoxic heterotrophic yield on soluble substrate	0.115	0.4507	Step 3
23	ASM	Reduction factor for denitrification on nitrate-N	0.109	0.2889	Step 3
	ASM	Ammonia oxidizer aerobic decay rate**		0.0239	Step 3
	Inf	Colloidal fraction of slowly biodegradable COD		0.0494	Step 1
		Chemical dosage for sCOD removal (kg/d)		0.7410	Step 1

*:"Inf" stands for influent fraction, "Pri-ASM" stands for the biological model of the primary settlement, "Pri-Set" stands for the settling model of the primary settlement, "ASM" stands for the biological model of the activated sludge process, "Final-ASM" stands for biological model of the final clarification, "Final-Set" stands the settling model of the final clarification, "V-sCOD" stands for the virtual chemical dosing for sCOD removal, and "SYS-BMS" stands for the biochemical model settings in the system setting of the model.
**: Based on the modeller's knowledge, Ammonia oxidizer aerobic decay rate was added in the step 3 calibration in order to adjust the predicted NH_4^+-N concentration close to the observed value.

Table D-2 The calibrated parameters of the wastewater treatment model of WWTP B

Ranking	Category*	Parameters	δ_j^{msqr}	Adjusted Value	Tuning Order
1	Pri-Set	Maximum Settleable TSS Fraction	1.006	0.6892	Step 2
2	ASM	Aerobic heterotrophic yield on soluble substrate	0.572	0.7499	Step 2
3	ASM	Maximum growth rate for ammonia oxidizer	0.388	0.9081	Step 3
4	Inf	Readily biodegradable fraction of total COD	0.380	0.1972	Step 1
5	ASM	ammonia oxidizer aerobic decay rate	0.296	0.1714	Step 3
6	Inf	Soluble inert fraction of total COD	0.254	0.0655	Step 1
7	ASM	Ammonia saturation coefficient for ammonia oxidizer	0.233	1.0501	Step 3
8	Final-Set	Flocculant zone settling parameter	0.188	0.0039	Step 2
9	Final-Set	Maximum Vesilind settling velocity	0.171	372.6467	Step 2
10	ASM	Anoxic heterotrophic yield on soluble substrate	0.148	0.5485	Step 2
11	ASM	Aerobic heterotrophic decay rate	0.116	0.0206	Step 2
12	ASM	Unbiodegradable fraction from cell decay	0.114	0.1537	Step 2
13	ASM	Anoxic reduction factor for decay rate	0.111	0.5796	Step 3
14	Inf	Colloidal fraction of slowly biodegradable COD	0.106	0.1307	Step 1
15	ASM	Ammonia-oxidizer yield	0.097	0.1708	Step 3
16	Pri-ASM	Rate constant for storage of poly-phosphate	0.095	1.6220	Step 3
17	Inf	N content in soluble inert material	0.082	0.0516	Step 3
18	ASM	Oxygen saturation for ammonia oxidizer	0.070	0.6622	Step 3
	V-sCOD	Chemical dosage for virtual sCOD removal		2.7956	Step 1
	V-P	Chemical dosage for virtual phosphate removal		1250.6702	Step 1

*:“Inf” stands for influent fraction, “Pri-ASM” stands for the biological model of the primary settlement, “Pri-Set” stands for the settling model of the primary settlement, “ASM” stands for the biological model of the activated sludge process, “Final-ASM” stands for biological model of the final clarification, “Final-Set” stands the settling model of the final clarification, “V-sCOD” stands for the virtual chemical dosing for sCOD removal, V-P stands for the virtual chemical dosing for phosphate removal, and “SYS-BMS” stands for the biochemical model settings in the system setting of the model.

Table D-3 The calibrated kinetics and stoichiometry of the wastewater treatment model of WWTP C

Ranking	Category*	Parameters	δ_j^{msqr}	Adjusted Value	Tuning Order
1	Inf	Readily biodegradable fraction of total COD	0.545	0.1943	Step 1
2	ASM	Aerobic heterotrophic yield on soluble substrate	0.324	0.3830	Step 3
3	Final-Set	Flocculant zone settling parameter	0.207	0.0025	Step 3
4	Final-Set	Maximum Vesilind settling velocity	0.194	211.0880	Step 3
5	Inf	Soluble inert fraction of total COD	0.151	0.0752	Step 1
6	ASM	Hydrolysis rate constant for xs	0.144	2.8962	Step 3
7	Pri-Set	Flocculant zone settling parameter	0.093	0.0012	Step 2
8	ASM	Aerobic heterotrophic decay rate	0.081	0.1529	Step 3
9	Pri-Set	Maximum Vesilind settling velocity	0.079	249.9797	Step 2
10	Pri-Set	Maximum non-settleable solids	0.073	99.1407	Step 2
	Inf	Colloidal fraction of slowly biodegradable COD		0.0453	Step 1
	V-sCOD	Chemical dosage for sCOD removal (kg/d)		5.3398	Step 1
	SYS-BMS	N content of heterotrophic biomass**		0.0593	Step 3
	SYS-BMS	N content of unbiodegradable biomass**		0.0651	Step 3
	SYS-BMS	P content of heterotrophic biomass**		0.0411	Step 3
	SYS-BMS	P content of unbiodegradable biomass**		0.0323	Step 3

*:"Inf" stands for influent fraction, "Pri-ASM" stands for the biological model of the primary settlement, "Pri-Set" stands for the settling model of the primary settlement, "ASM" stands for the biological model of the activated sludge process, "Final-ASM" stands for biological model of the final clarification, "Final-Set" stands the settling model of the final clarification, "V-sCOD" stands for the virtual chemical dosing for sCOD removal, V-P stands for the virtual chemical dosing for phosphate removal, and "SYS-BMS" stands for the biochemical model settings in the system setting of the model.

**: In order to adjust the predicted total nitrogen and total phosphorus concentration of the surplus activated sludge close to the observed value. The range given to the N content of heterotrophic biomass, N content of unbiodegradable biomass, P content of heterotrophic biomass, P content of unbiodegradable biomass were 0.05-0.087 gN/g, 0.035-0.087 gN/gCOD, 0.015-0.056 gP/gCOD and 0.011-0.056 gP/COD, respectively. The range is determined from the value reported in Brdjanovic et al. (2015) and Labelle et al. (2017)

The parameter of influent fraction (of digester feed sludge), kinetic and stoichiometric parameters that influence the biological modelling results of the sludge storage, sludge thickening and dewatering processes, and the anaerobic digestion, and are therefore subject to adjustment in the model for each WWTP, are listed in the Tables D-5 to D-8. The table also presents the adjusted value and the category those adjusted parameter belongs to.

Table D-4 The calibrated kinetics and stoichiometry of the wastewater treatment model of WWTP D

Ranking	Category*	Parameters	δ_j^{msqr}	Adjusted Value	Tuning Order
1	ASM	Aerobic heterotrophic yield on soluble substrate	0.486	0.7341	Step 2
2	Inf	Readily biodegradable fraction of total COD	0.360	0.1626	Step 1
3	ASM	Anoxic heterotrophic yield on soluble substrate	0.310	0.5427	Step 2
4	ASM	Maximum growth rate for ammonia oxidizer	0.250	0.4778	Step 3
5	Inf	Soluble inert fraction of total COD	0.247	0.0946	Step 1
6	ASM	Ammonia oxidizer aerobic decay rate	0.198	0.2068	Step 3
7	ASM	Ammonia saturation coefficient for ammonia oxidizer	0.184	1.0525	Step 3
8	Final-Set	Flocculant zone settling parameter	0.180	0.0044	Step 2
9	ASM	Reduction factor for denitrification on nitrite-N	0.168	0.5737	Step 3
10	Final-Set	Maximum Vesilind settling velocity	0.163	489.9424	Step 2
11	Pri-Set	Flocculant zone settling parameter	0.123	0.0012	Step 2
12	ASM	Oxygen inhibition coefficient for denitrification	0.111	0.2400	Step 3
13	Inf	N content of soluble inert material	0.105	0.1500	Step 3
14	Inf	Colloidal fraction of slowly biodegradable COD	0.105	0.1508	Step 1
15	Pri-Set	Maximum Vesilind settling velocity	0.105	263.3874	Step 2
16	ASM	Oxygen saturation for ammonia oxidizer	0.097	0.2023	Step 3
17	Pri-Set	Maximum non-settleable solids	0.096	17.1448	Step 2
18	ASM	Aerobic heterotrophic decay rate	0.082	0.9471	Step 2
19	ASM	Unbiodegradable fraction from cell decay	0.080	0.1841	Step 2
20	ASM	Maximum growth rate for nitrite oxidizer	0.075	0.8041	Step 3
	V-sCOD	Chemical dosage for sCOD removal (kg/d)		0.9992	Step 1

*:“Inf” stands for influent fraction, “Pri-ASM” stands for the biological model of the primary settlement, “Pri-Set” stands for the settling model of the primary settlement, “ASM” stands for the biological model of the activated sludge process, “Final-ASM” stands for biological model of the final clarification, “Final-Set” stands the settling model of the final clarification, “V-sCOD” stands for the virtual chemical dosing for sCOD removal, V-P stands for the virtual chemical dosing for phosphate removal, and “SYS-BMS” stands for the biochemical model settings in the system setting of the model.

Table D-5 The calibrated kinetics and stoichiometry of the primary sludge storage, thickening and dewatering

Category*	Parameters	Adjusted Value
I-ASM	Yield of fermentative biomass	0.1441
I-ASM	Aerobic heterotrophic decay rate	0.8848
I-ASM	Anaerobic reduction factor for decay rate (in Heterotrophic Biomass section)	0.6788
I-ASM	Hydrolysis rate constant for xs	3.5989
I-ASM	Anaerobic reduction factor for decay rate (in Hydrolysis section)	0.2680
PS-ASM	Yield of fermentative biomass	0.1685
PS-ASM	Aerobic heterotrophic decay rate	0.1498
PS-ASM	Anaerobic reduction factor for decay rate (in Heterotrophic Biomass section)	0.5508
PS-ASM	Hydrolysis rate constant for xs	3.3313
PS-ASM	Saturation coefficient for particulate COD	0.1070
PS-ASM	Anaerobic reduction factor for decay rate (in Hydrolysis section)	0.3913
PS-Drum	Fraction of influent flow	0.5602
PS-Drum	Removal efficiency of particulate inert material	0.9938
PS-Drum	Removal efficiency of slowly biodegradable substrate	0.8141
PS-Drum	Removal efficiency of nitrogen in slowly biodegradable substrate	0.7325

*: I-ASM and PS-ASM stands for the biological model of the virtual imported sludge tank and of the primary sludge storage tank, respectively. Meanwhile, PS-Drum stands for the operational parameters of the drum thickener of primary sludge.

Table D-6 The calibrated parameters of the SAS storage, thickening and dewatering

Category*	Parameters	Adjusted Value
SAS-ASM	Yield of fermentative biomass	0.1461
SAS-ASM	Aerobic heterotrophic decay rate	0.4044
SAS-ASM	Anaerobic reduction factor for decay rate (in Heterotrophic Biomass section)	0.5436
SAS-ASM	Hydrolysis rate constant for xs	0.9679
SAS-ASM	Anaerobic reduction factor for decay rate (in Hydrolysis section)	0.1005
SAS-Drum	Fraction of influent flow	0.1050
SAS-Drum	Removal efficiency of particulate inert material	0.9980
SAS-Drum	Removal efficiency of nitrogen in slowly biodegradable substrate	0.8143
SAS-Drum	Removal efficiency of heterotrophic biomass	0.8198

*: SAS-ASM stands for the biological model of the virtual surplus activated sludge (SAS) tank. Meanwhile, SAS-Drum stands for the operational parameters of the drum thickener of SAS.

Table D-7 The calibrated parameters of the raw sludge storage, thickening and dewatering

Category*	Parameters	Adjusted Value
Raw-ASM	Yield of fermentative biomass	0.1921
Raw-ASM	Aerobic heterotrophic decay rate	0.4401
Raw-ASM	Anaerobic reduction factor for decay rate (in Heterotrophic Biomass section)	0.5162
Raw-ASM	Hydrolysis rate constant for xs	2.2344
Raw-ASM	Saturation coefficient for particulate COD	0.1179
Raw-ASM	Anaerobic reduction factor for decay rate (in Hydrolysis section)	0.1778
Raw-Drum	Fraction of influent flow	0.1643
Raw-Drum	Removal efficiency of particulate inert material	0.9707
Raw-Drum	Removal efficiency of slowly biodegradable substrate	0.9048
Raw-Drum	Removal efficiency of nitrogen in slowly biodegradable substrate	0.9048
Raw-Drum	Removal efficiency of phosphorus in slowly biodegradable substrate	0.9664
Raw-Drum	Removal efficiency of heterotrophic biomass	0.9943

*: RAW-ASM stands for the biological model of the virtual raw sludge tank. Meanwhile, SAS-Drum stands for the operational parameters of the centrifuge of raw sludge.

Table D-8 The calibrated parameters of the anaerobic digestion process and subsequent sludge storage, thickening and dewatering

Category*	Parameters	Adjusted Value
DF-Inf	Particulate inert fraction of total COD	0.1994
DF-Inf	N content of inert particulate material	0.0377
DF-Inf	P content of inert particulate material	0.0263
AD-ASM	Yield of fermentative biomass	0.2149
AD-ASM	Fraction of inert COD during slowly biodegradable organic hydrolysis	0.0419
DS-Drum	Fraction of influent flow	0.1296
DS-Drum	Removal efficiency of particulate inert material	0.9983
DS-Drum	Removal efficiency of unbiodegradable cell product	0.4952
DS-Drum	Removal efficiency of fermentative biomass	0.9657
DS-Drum	Removal efficiency of acetogenic biomass	0.6823
DS-Drum	Removal efficiency of acetolactic methanogenic biomass	0.6823
DS-Drum	Removal efficiency of hydrogenotrophic methanogenic biomass	0.7067
Sys-BMS	C content of inert particulate material	0.3092
Sys-BMS	C content of slowly biodegradable substrate	0.3167

*: DF-Inf stands for influent fraction of the digester feed, AD-ASM stands for the biological model of the anaerobic digestion, DS-Drum stands for the operational parameters of the drum thickener of digested sludge, and Sys-BMS the biochemical model settings in the system setting of the model.

Appendix E. The observed and predicted flow and concentration data

Table E-1 The observed and predicted flow and concentration of the modelling of wastewater treatment of four WWTPs

		WWTP A		WWTP B		WWTP C		WWTP D	
Stream	**Unit**	Observed Value	Predicted Value	Observed Value	Predicted Value	Observed Value	Predicted Value	Observed Value	Predicted Value
Primary Effluent	sCOD, mg/L	193.4	200.1	193.2	187.4	180.8	180.7	86.5	87.1
Primary Effluent	pCOD, mg/L	227.9	206.4	199.0	197.8	276.9	276.9	82.3	92.9
Primary Effluent	NH_4^+-N, mg/L	27.6	29.4	34.6	37.7	43.1	41.8	20.8	19.5
Primary Effluent	TKN, mg/L	34.7	38.9	42.0	46.6	58.6	51.3	27.9	26.7
Primary Effluent	PO_4^{3-}-P, mg/L	1.8	2.3	4.9	5.3	7.1	6.7	1.6	1.5
Primary Sludge	COD, mg/L	34844.1	34843.9	43951.2	43120.0	*	*	24212.7	24210.8
Primary Sludge	TN, mg/L	1125.7	945.8	1130.0	1336.0	*	*	835.8	1013.8
Primary Sludge	TP, mg/L	518.2	308.5	379.0	298.7	*	*	243.2	264.4
Final Effluent	sCOD, mg/L	21.3	19.6	29.0	24.6	47.0	46.5	23.5	21.9
Final Effluent	pCOD, mg/L	19.9	19.8	16.8	13.9	46.8	46.2	5.0	5.8
Final Effluent	NH_4^+-N, mg/L	0.20	0.88	30.1	31.9	37.9	38.0	2.3	3.0
Final Effluent	TKN, mg/L	4.1	4.4	30.5	33.9	40.7	44.4	8.7	7.0
Final Effluent	Nitrate-N, mg/L	13.4	13.7	0.0	0.0	0.0	0.0	2.9	4.7
Final Effluent	TN, mg/L	17.5	20.6	30.5	33.9	40.7	44.4	11.8	12.2
Final Effluent	Op, mg/L	0.9	1.0	3.0	2.1	3.8	3.8	1.6	1.4
Surplus Activated Sludge	Flow, m3/d	204.0	222.9	2712.4	2460.5	6041.0	6238.2	1032.0	888.7
Surplus Activated Sludge	COD, mg/L	6159.5	5425.4	5053.1	5195.8	6389.5	6949.5	2522.4	2809.3
Surplus Activated Sludge	TN, mg/L	377.9	348.1	284.0	287.3	358.0	351.6	163.6	188.8
Surplus Activated Sludge	TP, mg/L	99.8	96.1	121.0	89.9	183.0	179.1	39.2	43.4

*: No sample was collected, and hence no observed value was obtained.

Table E-2 The observed and predicted flow and concentration of the modelling of sludge thickening, dewatering and digestion of WWTP C

		Primary sludge thickening		SAS thickening		Raw sludge dewatering		Digested sludge dewatering	
Stream	**Unit**	Observed Value	Predicted Value	Observed Value	Predicted Value	Observed Value	Predicted Value	Observed Value	Predicted Value
Feed Sludge	COD, mg/L	37917.7	37472.7	*	*	41780.8	46870.5	49061.1	40834.3
Feed Sludge	TN, mg/L	1051.0	1051.1	*	*	1857.1	1705.0	4797.3	4315.0
Feed Sludge	TP, mg/L	368.0	367.9	*	*	629.2	691.4	1082.2	1099.1
Filtrate/Centrate	COD, mg/L	9775.0	9780.6	1598.3	1609.3	10595.0	10582.5	6520.0	6471.3
Filtrate/Centrate	sCOD, mg/L	2657.9	2648.4	34.9	47.7	6072.5	6062.9	4074.6	3993.1
Filtrate/Centrate	pCOD, mg/L	7117.1	7132.2	1563.4	1561.6	4522.5	4519.6	2445.4	2478.3
Filtrate/Centrate	NH_4^+-N, mg/L	164.5	164.6	32.9	40.6	428.8	491.3	2243.1	2238.7
Filtrate/Centrate	TKN, mg/L	273.5	273.9	88.5	88.5	530.3	597.8	3244.3	2608.7
Filtrate/Centrate	PO_4^{3-}-P, mg/L	66.2	31.7	16.6	5.7	203.8	178.7	228.5	228.5
Dewatered Sludge	COD, mg/L	59813.1	60021.3	47741.7	50480.8	244210.7	253699.5	276618.2	255423.9
Dewatered Sludge	TN, mg/L	1646.4	1684.0	2972.1	2496.9	8127.4	8015.9	14991.3	14970.8
Dewatered Sludge	TP, mg/L	547.0	504.4	1359.4	1359.6	2796.7	2796.6	5281.9	5879.1
Biogas, m3/d	m3/d	*	*	*	*	*	*	39633.1	39940.0
CO2, m3/d	m3/d	*	*	*	*	*	*	15853.3	15500.0
CH4, m3/d	m3/d	*	*	*	*	*	*	23779.9	24360.0

*: No sample was collected, and hence no observed value was obtained.

Appendix F. Conceptual modelling for investigating the impact of population equivalent to energy and mass balance

Introduction

This case study is to investigate the impact of population equivalent on the COD, total nitrogen (TN) and total phosphorus (TP) mass balance and the chemical energy balance.

Method

To a wastewater treatment plant (WWTP), the most noticeable impact of the population equivalent is on the flow. Therefore, this case study investigates the chemical and energy balance of four scenarios with different flow conditions of 10,000 m^3/d, 50,000 m^3/d, 150,000 m^3/d, and 250,000 m^3/d, respectively. The mass balance and chemical energy balance construction is based on the predicted result from conceptual modelling.

A conceptual wastewater treatment work consists of primary settlement, activated sludge, and final clarification are constructed. The primary sludge and surplus activated sludge (SAS) are discharged separately. The conceptual model CM-F-1 is shown in Figure F-1.

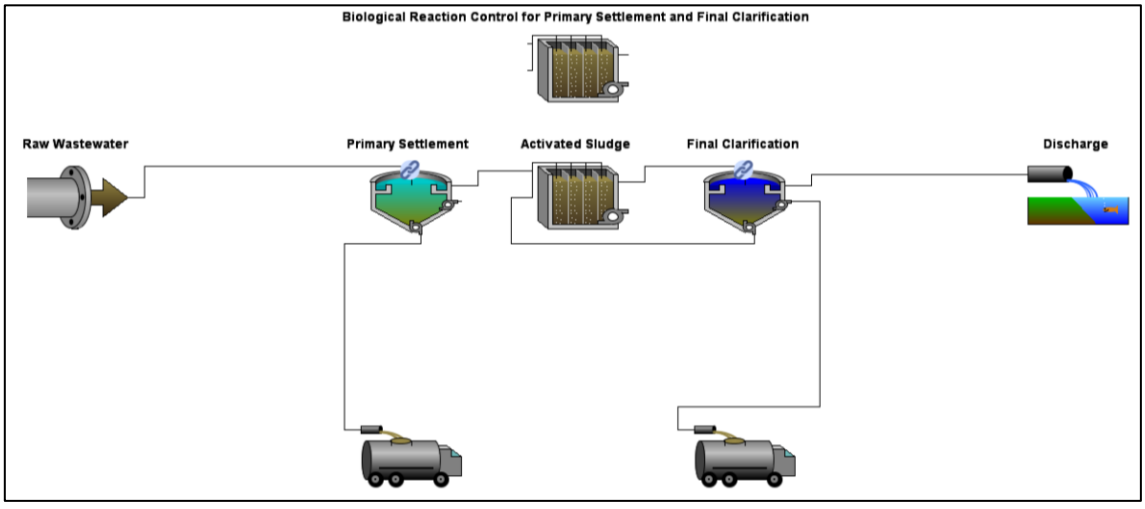

Figure F-1 The conceptual model CM-F-1

The key features of the model are listed:

- For dimension wise, in order to provide the same extent of treatment, the hydraulic retention time of the primary settlement, activated sludge, and final clarification are

assumed 3 hours, 2.4 hours, and 3 hours, respectively, according to the HRT of the corresponding process of the four investigated WWTPs (calculated via tank size stated in Table 3-2 and 3-3 and flow data stated in Table 5-1). Therefore, the tank sizes are varied accordingly as shown in Table F-1

Table F-1 Dimensions of the primary settler, aeration tank and final clarifier

Flow, m3/d	Primary Settler*			Aeration Tank**		Final Clarifier*		
	Side Wall Depth, m	Centre Depth, m	Surface Area, m^2	Depth, m	Tank Volume, m^3	Side Wall Depth, m	Centre Depth, m	Surface Area, m^2
10000	2.0	3.6	500	4.0	2000	2	3.5	1000
50000	2.0	3.6	2500	4.0	10000	2	3.5	5000
150000	2.0	3.6	7500	4.0	30000	2	3.5	15000
250000	2.0	3.6	12500	4.0	50000	2	3.5	25000

*: The Sloping bottom circular primary clarifier is used in both the primary settlement and final clarification
**: The plug flow tank unit is used in the activated sludge.

- For control wise, in all four scenarios,
  - The proportional–integral–derivative (PID) controller is applied to the discharge of primary sludge. The total suspended solid (TSS) content of the discharged primary sludge is the control variable and is set as 30,000 mg/L,
  - The dissolved oxygen (DO) setpoint is 2.0 mg/L,
  - The PID controller is applied to the discharge of SAS. The mixed liquor suspended solid is the control variable and is set as 2,000 mg/L.

- For mechanical and biological reaction wise,
  - The kinetics of the settling of the primary settlement and final clarification remains the default value,
  - Both primary settlement tank and final clarification tank are biological reactive and are control by the same virtual “Plug Flow Tank” unit as shown in Figure F-1,
  - The stoichiometry and kinetics of the biological reactions are the same as the value stated in the “Initial Value” column of Table B-1.

- The influent characterization of the raw wastewater remains the software default value, expect the total phosphorus content and ortho-phosphate content are adjusted to 5.0 mg/L and 3 mg/L, respectively.

Results and discussions

The COD, TN and TP mass balance and the chemical energy balance of four scenarios four scenarios with different flow conditions are constructed based on the predicted result and are shown in Table F-2.

Table F-2 Chemical energy balance and COD, TN and TP mass balance of the conceptual treatment work in different flow condition

Flow, m3/d	Subject	Captured in Primary Sludge	Captured in SAS	Remained in Final Effluent	Loss
10,000	COD	30.3%	28.3%	8.3%	33.1%
50,000	COD	30.3%	29.9%	7.0%	32.8%
150,000	COD	30.3%	28.3%	8.3%	33.1%
250,000	COD	30.3%	28.4%	8.3%	33.1%
10,000	Chemical Energy	30.3%	28.3%	8.3%	33.1%
50,000	Chemical Energy	30.3%	29.9%	7.0%	32.8%
150,000	Chemical Energy	30.3%	28.3%	8.3%	33.1%
250,000	Chemical Energy	30.3%	28.4%	8.3%	33.1%
10,000	TN	14.3%	20.2%	46.3%	19.2%
50,000	TN	14.3%	21.5%	47.2%	17.1%
150,000	TN	14.3%	20.2%	46.3%	19.2%
250,000	TN	14.3%	20.3%	46.3%	19.2%
10,000	TP	16.8%	41.5%	41.7%	0.0%
50,000	TP	16.8%	43.7%	39.5%	0.0%
150,000	TP	16.8%	41.5%	41.8%	0.0%
250,000	TP	16.8%	41.6%	41.6%	0.0%

The data stated in Table F-2 shows that the mass balance and chemical energy balance are more or less identical in different flow conditions. This suggest that, if the HRT, kinetic of the settling process, stoichiometry and kinetic of biological reaction, and the quality of the influent wastewater are the same, the mass balance and chemical energy balance will not be influenced by the change of flow of the raw wastewater.

References

AGU, C. E., HJULSTAD, Å., ELSETH, G. & LIE, B. 2017. Algorithm with improved accuracy for real-time measurement of flow rate in open channel systems. *Flow Measurement and Instrumentation,* 57**,** 20-27.

AIC 2011. AIC Fertiliser Statistics Report 2011. Peterborough, UK: Agricultural Industries Confederation.

AINGER, C., BUTLER, D., CAFFOR, I., CRAWFORD-BROWN, D., HELM, D. & STEPHENSON, T. 2009. A Low Carbon Water Industry in 2050. Bristol, UK: Environment Agency.

APHA 2012. *Standard methods for the examination of water and wastewater,* Washington, DC, USA, Clearway Logistics Phase 1a.

BANKS, C. 2009. Optimising anaerobic digestion. *Anaerobic digestion workshop.* University of Reading.

BASILE, A., CASSANO, A. & RASTOGI, N. K. 2015. *Advances in membrane technologies for water treatment: materials, processes and applications,* Elsevier.

BATSTONE, D. J., KELLER, J., ANGELIDAKI, I., KALYUZHNYI, S., PAVLOSTATHIS, S., ROZZI, A., SANDERS, W., SIEGRIST, H. & VAVILIN, V. 2002. The IWA anaerobic digestion model no 1 (ADM1). *Water Science and Technology,* 45**,** 65-73.

BEIS 2017a. CHPQA case study - Coventry Energy from Waste. UK: Department for Business, Energy & Industrial Strategy.

BEIS 2017b. CHPQA case study - Lister Hospital. UK: Department for Business, Energy & Industrial Strategy.

BEIS 2017c. CHPQA case study - University of Liverpool. UK: Department for Business, Energy & Industrial Strategy.

BEIS 2018. 2017 UK Provisional Greenhouse Gas Emissions. London, UK: Department for Business, Energy & Industrial Strategy

BHOGAL, A., ROLLETT, A. & WILLIAMS, J. 2017. Use of food-based PAS110 digestate to grow energy grasses on brownfield land as an AD feedstock. UK: WRAP.

BONMATı, A. & FLOTATS, X. 2003. Air stripping of ammonia from pig slurry: characterisation and feasibility as a pre-or post-treatment to mesophilic anaerobic digestion. *Waste management,* 23**,** 261-272.

BOUZAS, A., RIBES, J., FERRER, J. & SECO, A. 2007. Fermentation and elutriation of primary sludge: Effect of SRT on process performance. *Water Research,* 41**,** 747-756.

BOWEN, A., EVANS, B., OLIVER, B., EVANS, R. & MERRY, J. Advanced Digestion at Cardiff and Afan; Dwr Cymru Welsh Water drive for lowest sustainable cost of sludge treatment and 15% reduction in carbon footprint. 15th Biosolids Conference, 2010.

BOYLES, W. 1991. The Science of CHEMICAL OXYGEN DEMAND. USA: Hach Company.

BRDJANOVIC, D., MEIJER, S. C., LOPEZ-VAZQUEZ, C. M., HOOIJMANS, C. M. & VAN LOOSDRECHT, M. C. 2015. *Applications of Activated Sludge Models,* Iwa Publishing.

BRUN, R., KÜHNI, M., SIEGRIST, H., GUJER, W. & REICHERT, P. 2002. Practical identifiability of ASM2d parameters—systematic selection and tuning of parameter subsets. *Water research,* 36**,** 4113-4127.

BUNCE, J. T., NDAM, E., OFITERU, I. D., MOORE, A. & GRAHAM, D. W. 2018. A Review of Phosphorus Removal Technologies and Their Applicability to Small-Scale Domestic Wastewater Treatment Systems. *Frontiers in Environmental Science,* 6.

CAI, T., PARK, S. Y. & LI, Y. 2013. Nutrient recovery from wastewater streams by microalgae: Status and prospects. *Renewable and Sustainable Energy Reviews,* 19**,** 360-369.

CAO, Y. & PAWŁOWSKI, A. 2012. Sewage sludge-to-energy approaches based on anaerobic digestion and pyrolysis: Brief overview and energy efficiency assessment. *Renewable and Sustainable Energy Reviews,* 16**,** 1657-1665.

CAPODAGLIO, A. 2017. Integrated, decentralized wastewater management for resource recovery in rural and peri-urban areas. *Resources,* 6**,** 22.

CHERNICHARO, C. D. 2006. Post-treatment options for the anaerobic treatment of domestic wastewater. *Reviews in Environmental Science and Bio/Technology,* 5**,** 73-92.

COLBERT, J., XIHENG, H. & KIRKLIN, D. 1981. Enthalpy of combustion of microcrystalline cellulose. *JOURNAL OF RESEARCH of the National Bureau of Standards,* 86.

COSENZA, A., MANNINA, G., VANROLLEGHEM, P. A. & NEUMANN, M. B. 2014. Variance-based sensitivity analysis for wastewater treatment plant modelling. *Sci Total Environ,* 470-471**,** 1068-77.

COTTERILL, S. E., DOLFING, J., CURTIS, T. P. & HEIDRICH, E. S. 2018. Community Assembly in Wastewater-Fed Pilot-Scale Microbial Electrolysis Cells. *Frontiers in Energy Research,* 6.

COTTERILL, S. E., DOLFING, J., JONES, C., CURTIS, T. P. & HEIDRICH, E. S. 2017. Low Temperature Domestic Wastewater Treatment in a Microbial Electrolysis Cell with 1 m2

Anodes: Towards System Scale-Up. *Fuel Cells*.

DE VRIES, S. C., POSTMA, R., VAN SCHOLL, L., BLOM-ZANDSTRA, G., VERHAGEN, J. & HARMS, I. 2017. Extractive Nutrient Recovery as a Green Option for Managing Phosphorus in Sidestreams and Biosolids Netherland: Wageningen University & Research

DECC 2008. CHP Finance. UK: Department of Energy & Climate Change.

DECC 2014. RHI Biomethane Injection to Grid Tariff Review. UK: Department of Energy & Climate Change.

DEFRA 2012. Waste water treatment in the United Kingdom – 2012. London, UK: Department for Environment, Food and Rural Affairs.

DEFRA 2018. Sewage sludge in agriculture: code of practice for England, Wales and Northern Ireland. *In:* DEPARTMENT FOR ENVIRONMENT, F. R. A. A. E. A. (ed.). UK: Department for Environment, Food & Rural Affairs and Environment Agency.

DEMIRBAS, A. 2016. Calculation of higher heating values of fatty acids. *Energy Sources, Part A: Recovery, Utilization, and Environmental Effects,* 38**,** 2693-2697.

DENG, Q. 2014. *Ammonia Removal and Recovery from Wastewater Using Natural Zeolite: An Integrated System for Regeneration by Air Stripping Followed Ion Exchange.* Master, University of Waterloo.

DESLOOVER, J., DE CLIPPELEIR, H., BOECKX, P., DU LAING, G., COLSEN, J., VERSTRAETE, W. & VLAEMINCK, S. E. 2011. Floc-based sequential partial nitritation and anammox at full scale with contrasting N2O emissions. *Water Research,* 45**,** 2811-2821.

DIAMANTIS, V., VERSTRAETE, W., EFTAXIAS, A., BUNDERVOET, B., SIEGFRIED, V., MELIDIS, P. & AIVASIDIS, A. 2013. Sewage pre-concentration for maximum recovery and reuse at decentralized level. *Water Sci Technol,* 67**,** 1188-93.

DONG, Y. 2015. *ENZYME PRETREATMENT OF FATS, OIL AND GREASE FROM RESTAURANT WASTE TO PROLONG DRAIN FIELD EFFECTIVENESS.* Master, Michigan State University.

DREWNOWSKI, J., ZABOROWSKA, E. & DE VEGA, C. H. Computer Simulation in Predicting Biochemical Processes and Energy Balance at WWTPs. E3S Web of Conferences, 2018. EDP Sciences, 03007.

DROSTE, R. L. 1997. *Theory and practice of water and wastewater treatment,* New York, New York : J. Wiley.

EL-TEMTAMY, S. A. & GENDY, T. S. 2014. Economic evaluation and sensitivity analysis of some fuel oil upgrading processes. *Egyptian Journal of Petroleum,* 23**,** 397-407.

EL SHEIKH, R., GOUDA, A., SALEM, A. & HENDY, I. 2016. Analysis and Characterization of Wastewater Nitrogen Components for using in Wastewater Modeling and Simulation. *International Journal of Advanced Research in Chemical Science,* 3.

EUROPEAN COMMISSION. 2019. *Implementation of the Circular Economy Action Plan* [Online]. European Commission. [Accessed 06-02-2019].

EVANS, F. W. & SKINNER, H. A. 1959. The heat of combustion of acetic acid. *Transactions of the Faraday Society,* 55**,** 260-261.

EVANS, T. D. Recovering ammonium and struvite fertilisers from digested sludge dewatering liquors. Proc. IWA Specialist Conference: Moving Forward–Wastewater biosolids sustainability, 2007.

FABIYI, M., MENNITI, A., SCHAUER, P., BRITTON, A. & GOEL, R. 2016. Modeling & Operational Case Study of a Full Scale Phosphorus Recovery System Coupled with WASSTRIP®: Factors to Consider in Model Development & Insights for Optimal P Recovery. *Proceedings of the Water Environment Federation,* 2016**,** 1506-1521.

FALL, C., ESPINOSA-RODRIGUEZ, M., FLORES-ALAMO, N., VAN LOOSDRECHT, M. & HOOIJMANS, C. 2011. Stepwise calibration of the activated sludge model no. 1 at a partially denitrifying large wastewater treatment plant. *Water Environment Research,* 83**,** 2036-2048.

FATTAH, K. P. 2012. Assessing struvite formation potential at wastewater treatment plants. *International Journal of Environmental Science and Development,* 3**,** 548.

FLORES-ALSINA, X., COMAS, J. & RODRÍGUEZ-RODA, I. 2010. Analysis of rising sludge risk in Activated Sludge Systems: from operational strategies to clarifier design.

FOLADORI, P., ANDREOTTOLA, G. & ZIGLIO, G. 2010. *Sludge reduction technologies in wastewater treatment plants*, IWA publishing.

FOLEY, J., DE HAAS, D., YUAN, Z. & LANT, P. 2010. Nitrous oxide generation in full-scale biological nutrient removal wastewater treatment plants. *Water Res,* 44**,** 831-44.

GALLO, A. 2019. *A Refresher on Internal Rate of Return* [Online]. Available: https://hbr.org/2016/03/a-refresher-on-internal-rate-of-return [Accessed 20 Dec 2018].

GANS, N., MOBINI, S. & ZHANG, X. 2007. *Mass and energy balances at the Gaobeidian wastewater treatment plant in Beijing, China.* MSc

GASSO, K., MOUROT, G. & RAGOT, J. 2002. Environmental systems modelling and

diagnosis using a multiple model approach. *Computational Intelligent Systems For Applied Research.* World Scientific.

GERNAEY, K., VANROLLEGHEM, P. & LESSARD, P. 2001. Modeling of a reactive primary clarifier. *Water Science and Technology,* 43**,** 73-81.

GERNAEY, K. V., VAN LOOSDRECHT, M. C., HENZE, M., LIND, M. & JØRGENSEN, S. B. 2004. Activated sludge wastewater treatment plant modelling and simulation: state of the art. *Environmental Modelling & Software,* 19**,** 763-783.

GIMENEZ, J. B., ROBLES, A., CARRETERO, L., DURAN, F., RUANO, M. V., GATTI, M. N., RIBES, J., FERRER, J. & SECO, A. 2011. Experimental study of the anaerobic urban wastewater treatment in a submerged hollow-fibre membrane bioreactor at pilot scale. *Bioresour Technol,* 102**,** 8799-806.

GOUVEIA, J., PLAZA, F., GARRALON, G., FDZ-POLANCO, F. & PENA, M. 2015. Long-term operation of a pilot scale anaerobic membrane bioreactor (AnMBR) for the treatment of municipal wastewater under psychrophilic conditions. *Bioresour Technol,* 185**,** 225-33.

GRIZZETTI, B. & BOURAOUI, F. 2006. Assessment of nitrogen and phosphorus environmental pressure at European scale. *EUR Report,* 22526**,** 66.

GU, Y., LI, Y., LI, X., LUO, P., WANG, H., WANG, X., WU, J. & LI, F. 2017. Energy Self-sufficient Wastewater Treatment Plants: Feasibilities and Challenges. *Energy Procedia,* 105**,** 3741-3751.

HEIDRICH, E., CURTIS, T. & DOLFING, J. 2010. Determination of the internal chemical energy of wastewater. *Environmental Science & Technology,* 45**,** 827-832.

HENZE, M. & COMEAU, Y. 2008. Wastewater characterization.

HENZE, M., GUJER, W., MINO, T., MATSUO, T., WENTZEL, M. C., MARAIS, G. V. R. & VAN LOOSDRECHT, M. C. M. 1999. Activated Sludge Model No.2d, ASM2D. *Water Science and Technology,* 39**,** 165-182.

HENZE, M., GUJER, W., MINO, T. & VAN LOOSDRECHT, M. C. 2000. *Activated sludge models ASM1, ASM2, ASM2d and ASM3*, IWA publishing.

HIGGINS, M. J. & MURTHY, S. 2006. Examination of Reactivation and Regrowth of Fecal Coliforms in Centrifuge Dewatered, Anaerobically Digested Sludges. *Water Environment Research Foundation Report*.

HUANG, M.-H., LI, Y.-M. & GU, G.-W. 2010. Chemical composition of organic matters in domestic wastewater. *Desalination,* 262**,** 36-42.

HUETT, D. O. 1997. Fertiliser use effciency by containerised nursery plants 2. Nutrient leaching. *Australian Journal of Agricultural Research,* 48**,** 259-265.

HULSBEEK, J. J. W., KRUIT, J., ROELEVELD, P. J. & VAN LOOSDRECHT, M. C. M. 2002. A practical protocol for dynamic modelling of activated sludge systems. *Water Science and Technology,* 45**,** 127-136.

HYDROMANTIS 2015. Webinar: Modelling Anaerobic Digestion Processes in GPS-X. Youtube.

HYDROMANTIS 2017. GPS-X Technical Reference (GPS-X version 7). Canada.

IRENA 2016. The Power to Change: Solar and Wind Cost Reduction Potential to 2025. International Renewable Energy Agency.

ISMAIL, I. M., FAWZY, A. S., ABDEL-MONEM, N. M., MAHMOUD, M. H. & EL-HALWANY, M. A. 2012. Combined coagulation flocculation pre treatment unit for

municipal wastewater. *Journal of Advanced Research,* 3**,** 331-336.

IVANOV, V., KUANG, S., STABNIKOV, V. & GUO, C. 2009. The removal of phosphorus from reject water in a municipal wastewater treatment plant using iron ore. *Journal of Chemical Technology & Biotechnology,* 84**,** 78-82.

IWA 2016. Water Utility Pathways in a Circular Economy. London, UK: International Water Association.

JAFFER, Y., CLARK, T. A., PEARCE, P. & PARSONS, S. A. 2002. Potential phosphorus recovery by struvite formation. *Water research,* 36**,** 1834-1842.

JARDIN, N., THÖLE, D. & WETT, B. 2006. Treatment of sludge return liquors: experiences from the operation of full-scale plants. *Proceedings of the Water Environment Federation,* 2006**,** 5237-5255.

JEPPSSON, U. 1996. *Modelling aspects of wastewater treatment processes*.

JI, B., YANG, K., ZHU, L., JIANG, Y., WANG, H., ZHOU, J. & ZHANG, H. 2015. Aerobic denitrification: A review of important advances of the last 30 years. *Biotechnology and Bioprocess Engineering,* 20**,** 643-651.

JIMENEZ, J., MILLER, M., BOTT, C., MURTHY, S., DE CLIPPELEIR, H. & WETT, B. 2015. High-rate activated sludge system for carbon management – Evaluation of crucial process mechanisms and design parameters. *Water Research,* 87**,** 476-482.

JONES, R., MACGREGOR, J. & MURPHY, K. 1989. State estimation in wastewater engineering: application to an anaerobic process. *Environmental monitoring and assessment,* 13**,** 271-282.

JONES, S. B., MEYER, P. A., SNOWDEN-SWAN, L. J., PADMAPERUMA, A. B., TAN, E., DUTTA, A., JACOBSON, J. & CAFFERTY, K. 2013. Process design and economics for the conversion of lignocellulosic biomass to hydrocarbon fuels: fast pyrolysis and hydrotreating bio-oil pathway. Pacific Northwest National Lab.(PNNL), Richland, WA (United States).

JUHÁSZ, L. 2011. Net present value versus internal rate of return. *Economics & Sociology,* 4**,** 46-53.

KHUNJAR, W., LATIMER, R., BILYK, K., ROHRBACHER, J. & PITT, P. 2013. *Extractive Nutrient Recovery as a Green Option for Managing Phosphorus in Sidestreams and Biosolids* [Online]. Available: https://static1.squarespace.com/static/54806478e4b0dc44e1698e88/t/548619fae4b0af073c8d429c/1418074618937/Khunjar-NutrientRecovery-29Oct13.pdf [Accessed 10-10-2017].

KIM, D.-J. 2013. Effect of Aeration on Nitrous Oxide (N2O) Emission from Nitrogen-Removing Sequencing Batch Reactors. *Journal of Microbiology and Biotechnology,* 23**,** 99-105.

KIM, D., YOUNG PARK, K. & YOSHIKAWA, K. 2017. Conversion of Municipal Solid Wastes into Biochar through Hydrothermal Carbonization. *In:* HUANG, W.-J. (ed.) *Engineering Applications of Biochar.* London, UK: IntechOpen Limited.

KIM, J. & BENJAMIN, M. M. 2004. Modeling a novel ion exchange process for arsenic and nitrate removal. *Water research,* 38**,** 2053-2062.

KLEEMANN, R., CHENOWETH, J., CLIFT, R., MORSE, S., PEARCE, P. & SAROJ, D. 2015. Evaluation of local and national effects of recovering phosphorus at wastewater treatment plants: Lessons learned from the UK. *Resources, Conservation and Recycling,* 105**,** 347-359.

KORTH, B., MASKOW, T., GÜNTHER, S. & HARNISCH, F. 2017. Estimating the Energy Content of Wastewater Using Combustion Calorimetry and Different Drying Processes. *Frontiers in Energy Research,* 5**,** 23.

KORYTÁROVÁ, J. & POSPÍŠILOVÁ, B. 2015. Evaluation of investment risks in CBA with Monte Carlo method. *Acta Universitatis Agriculturae et Silviculturae Mendelianae Brunensis,* 63**,** 245-251.

KRISTENSEN, P., FRIBOURG-BLANC, B. & NIXON, S. 2004. Outlooks on Nutrient Discharges in Europe from Urban Waste Water Treatment Plants.

LABELLE, M.-A., DOLD, P. L., GADBOIS, A., DÉLÉRIS, S. & COMEAU, Y. 2017. Activated Sludge Production Parameters and Nutrient Content of Organic Sludge Components. *Water Environment Research,* 89**,** 51-61.

LANGERGRABER, G., RIEGER, L., WINKLER, S., ALEX, J., WIESE, J., OWERDIECK, C., AHNERT, M., SIMON, J. & MAURER, M. 2004. A guideline for simulation studies of wastewater treatment plants. *Water Science and Technology,* 50**,** 131-138.

LI, L., ZHANG, S., LI, G. & ZHAO, H. 2012. Determination of chemical oxygen demand of nitrogenous organic compounds in wastewater using synergetic photoelectrocatalytic oxidation effect at TiO2 nanostructured electrode. *Analytica chimica acta,* 754**,** 47-53.

LIBERTI, L., BOARI, G., PETRUZZELLI, D. & PASSINO, R. 1981. Nutrient removal and recovery from wastewater by ion exchange. *Water research,* 15**,** 337-342.

LIPU, M. S. H. & JAMAL, T. 2013. Techno-economic Analysis of Solar Concentrating Power (CSP) in Bangladesh. *Int. J. Adv. Renew. Energy Res,* 2**,** 750-762.

LIWARSKA-BIZUKOJC, E., OLEJNIK, D., BIERNACKI, R. & LEDAKOWICZ, S. 2011. Calibration of a complex activated sludge model for the full-scale wastewater treatment plant. *Bioprocess Biosyst Eng,* 34**,** 659-70.

LU, J. 2006. *Optimization of anaerobic digestion of sewage sludge using thermophilic anaerobic pre-treatment.*

MACK, J. 2012. Accounting for material-specific inflation rates in life-cycle cost analysis for pavement type selection. *Transportation Research Record: Journal of the Transportation Research Board***,** 86-96.

MANNINA, G., COSENZA, A., VANROLLEGHEM, P. A. & VIVIANI, G. 2011. A practical protocol for calibration of nutrient removal wastewater treatment models. *Journal of Hydroinformatics,* 13**,** 575-595.

MARIA, A. Introduction to modeling and simulation. Proceedings of the 29th conference on Winter simulation, 1997. IEEE Computer Society, 7-13.

MARTIN, I., PIDOU, M., SOARES, A., JUDD, S. & JEFFERSON, B. 2011. Modelling the energy demands of aerobic and anaerobic membrane bioreactors for wastewater treatment. *Environmental technology,* 32**,** 921-932.

MAURER, C. & MÜLLER, J. 2012. Ammonia (NH3) emissions during drying of untreated and dewatered biogas digestate in a hybrid waste‐heat/solar dryer. *Engineering in Life Sciences,* 12**,** 321-326.

MAYER, B. K., BAKER, L. A., BOYER, T. H., DRECHSEL, P., GIFFORD, M., HANJRA, M. A., PARAMESWARAN, P., STOLTZFUS, J., WESTERHOFF, P. & RITTMANN, B. E. 2016. Total Value of Phosphorus Recovery. *Environ Sci Technol,* 50**,** 6606-20.

MCCARTY, P. L., BAE, J. & KIM, J. 2011. Domestic wastewater treatment as a net energy producer–can this be achieved? : ACS Publications.

MEIJER, S. C. F., VAN LOOSDRECHT, M. C. M. & HEIJNEN, J. J. 2001. Metabolic modelling of full-scale biological nitrogen and phosphorus removing WWTP's. *Water research,* 35**,** 2711-2723.

MILLS, N., PEARCE, P., FARROW, J., THORPE, R., KIRKBY, N. & WATER, T. The influence of heat balance on the economics of advanced anaerobic digestion processes. 16th Biosolids Conference: Organic Resources. Exhibition. Aquaenviro, Leeds, 2011.

MILLS, N., PEARCE, P., FARROW, J., THORPE, R. B. & KIRKBY, N. F. 2014. Environmental & economic life cycle assessment of current & future sewage sludge to energy technologies. *Waste Manag,* 34**,** 185-95.

MINITAB BLOG EDITOR. 2013. *How to Interpret Regression Analysis Results: P-values and Coefficients* [Online]. Minitab. Available: http://blog.minitab.com/blog/adventures-in-statistics-2/how-to-interpret-regression-analysis-results-p-values-and-coefficients [Accessed 06-06-2018].

MINITAB INC. 2017a. *Create a fitted line plot and regression model that go through the origin* [Online]. Minitab Inc. . Available: https://support.minitab.com/en-us/minitab/18/help-and-how-to/modeling-statistics/regression/supporting-topics/regression-models/create-models-that-go-through-the-origin/ [Accessed 06-06-2018 2018].

MINITAB INC. 2017b. *Model summary table for Fit Regression Model* [Online]. Available: https://support.minitab.com/en-us/minitab/18/help-and-how-to/modeling-statistics/regression/how-to/fit-regression-model/interpret-the-results/all-statistics-and-graphs/model-summary-table/ [Accessed].

MINITAB INC. 2017c. *Should I use Bonett's method or Levene's method for 2 Variances?* [Online]. Minitab Inc. Available: https://support.minitab.com/en-us/minitab/18/help-and-how-to/statistics/basic-statistics/supporting-topics/tests-of-proportions-and-variances/bonett-s-method-or-levene-s-method/ [Accessed].

MOLINOS-SENANTE, M., HERNÁNDEZ-SANCHO, F., SALA-GARRIDO, R. & GARRIDO-BASERBA, M. 2010. Economic Feasibility Study for Phosphorus Recovery Processes. *Ambio,* 40**,** 408-416.

MÜNCH, E. V. & BARR, K. 2001. Controlled struvite crystallisation for removing phosphorus from anaerobic digester sidestreams. *Water research,* 35**,** 151-159.

MUSVOTO, E., WENTZEL, M. & EKAMA, G. 2000. Integrated chemical–physical processes modelling—II. simulating aeration treatment of anaerobic digester supernatants. *Water Research,* 34**,** 1868-1880.

NADEN, P., BELL, V., CARNELL, E., TOMLINSON, S., DRAGOSITS, U., CHAPLOW, J., MAY, L. & TIPPING, E. 2016. Nutrient fluxes from domestic wastewater: A national-scale historical perspective for the UK 1800-2010. *Sci Total Environ,* 572**,** 1471-1484.

NELSON, N. O., MIKKELSEN, R. L. & HESTERBERG, D. L. 2003. Struvite precipitation in anaerobic swine lagoon liquid: effect of pH and Mg: P ratio and determination of rate constant. *Bioresource technology,* 89**,** 229-236.

NIH. 2018a. *Compound Summary for CID 222* [Online]. National Institute of Health. Available: https://pubchem.ncbi.nlm.nih.gov/compound/222#section=Heat-of-Combustion [Accessed 01-07-2018 2018].

NIH. 2018b. *Compound Summary for CID 1049* [Online]. National Institute of Health. Available: https://pubchem.ncbi.nlm.nih.gov/compound/1049#section=Heat-of-Combustion [Accessed 01-07-2018 2018].

NIST. 2018a. *Benzene* [Online]. National Institute of Science and Standard. Available: https://webbook.nist.gov/cgi/cbook.cgi?ID=C71432&Mask=2 [Accessed 01-07-2018 2018].

NIST. 2018b. *Toluene* [Online]. National Institute of Standards and Technology. Available: https://webbook.nist.gov/cgi/cbook.cgi?ID=C108883&Type=HCOMBL#HCOMBL [Accessed 01-07-2018 2018].

NOWAK, O., SVARDAL, K., FRANZ, A. & KUHN, V. 1999. Degradation of particulate organic matter—A comparison of different model concepts. *Water science and technology,* 39**,** 119-127.

OECD. 2017. *Average annual hours actually worked per worker* [Online]. Organisation for Economic Co-operation and Development. Available: https://stats.oecd.org/Index.aspx?DataSetCode=ANHRS [Accessed 14-10-2017 2017].

OFGEM 2018. Non-domestic Renewable Heat Incentives, Guidance Volume 1: Eligibility and how to apply. *In:* MARKETS, T. O. O. G. A. E. (ed.). UK.

OFGEM. 2019a. *Feed-In Tariff (FIT) rates* [Online]. Available: https://www.ofgem.gov.uk/environmental-programmes/fit/fit-tariff-rates [Accessed 16 Dec 2018].

OFGEM. 2019b. *Tariffs and payments: Non-Domestic RHI* [Online]. Available: https://www.ofgem.gov.uk/environmental-programmes/non-domestic-rhi/contacts-guidance-and-resources/tariffs-and-payments-non-domestic-rhi [Accessed].

OFWAT 2016. Water 2020: our regulatory approach for water and wastewater services in England and Wales Appendix 2 Moving beyond waste - further evidence and analysis. UK: Office of Water Services.

OGILVIE, D. 1998. National Study of the Composition of Sewage Sludge. Auckland, New Zealand: The New Zealand Water and Wastes Association.

OSTARA 2010. Case Study York Wastewater Treatment Plant, City of York Vancover, Canada: Ostara.

OWEN, W. F. 1982. *Energy in wastewater treatment*.

PAZ-FERREIRO, J., NIETO, A., MÉNDEZ, A., ASKELAND, M. & GASCÓ, G. 2018. Biochar from biosolids pyrolysis: A review. *International journal of environmental research and public health,* 15**,** 956.

PEARCE, D. W. & TURNER, R. K. 1990. *Economics of natural resources and the environment*, JHU Press.

PEARCE, P., MILLS, N. & WINTER, P. 2014. Novel sludge management options for a large UK water company. *Water Practice and Technology,* 9**,** 179-185.

PETERSEN, B., VANROLLEGHEM, P. A., GERNAEY, K. & HENZE, M. 2002. Evaluation of an ASM1 model calibration procedure on a municipal–industrial wastewater treatment plant. *Journal of Hydroinformatics,* 4**,** 15-38.

POST 2007. ENERGY AND SEWAGE UK: Parliamentary Office of Science and Technology.

POWER, C., MCNABOLA, A. & COUGHLAN, P. 2014. Development of an evaluation method for hydropower energy recovery in wastewater treatment plants: Case studies in Ireland and the UK. *Sustainable Energy Technologies and Assessments,* 7**,** 166-177.

PUCHONGKAWARIN, C., GOMEZ-MONT, C., STUCKEY, D. C. & CHACHUAT, B. 2015. Optimization-based methodology for the development of wastewater facilities for energy and nutrient recovery. *Chemosphere,* 140**,** 150-8.

PUIG, S., VAN LOOSDRECHT, M., COLPRIM, J. & MEIJER, S. 2008. Data evaluation of full-scale wastewater treatment plants by mass balance. *Water research,* 42**,** 4645-4655.

RABONI, M., TORRETTA, V. & URBINI, G. 2013. Influence of strong diurnal variations in sewage quality on the performance of biological denitrification in small community wastewater treatment plants (WWTPs). *Sustainability,* 5**,** 3679-3689.

RASI, S. 2009. *Biogas composition and upgrading to biomethane*, University of Jyväskylä.

RAWLINSON, D., COVERDALE, S., OLIVER, B. & ORD, J. 2012. Howdon & Bran Sands STWs using advanced anaerobic digestion to improve operational efficiency and environmental sustainability in Northumbrian Water. *UK Water Projects Online.* 2012 ed. UK.

REDDY, M., LEENHEER, J. & MALCOLM, R. 1989. Elemental analysis and heat of combustion of fulvic acid from the Suwannee River. *In: Humic Substances in the Suwannee River, Georgia: Interactions, Properties, and Proposed Structures. Open-File Report 87-557, 1989. p 147-161, 4 fig, 4 tab, 11 ref.*

RIBEIRO DA SILVA, M. A. V., RIBEIRO DA SILVA, M. D. M. C., LOBO FERREIRA, A. I. M. C., SHI, Q., WOODFIELD, B. F. & GOLDBERG, R. N. 2013. Thermochemistry of α-D-xylose(cr). *The Journal of Chemical Thermodynamics,* 58**,** 20-28.

RIEGER, L., GILLOT, S., LANGERGRABER, G., OHTSUKI, T., SHAW, A., TAKACS, I. & WINKLER, S. 2012. *Guidelines for using activated sludge models*, IWA publishing.

RIEGER, L., KOCH, G., KÜHNI, M., GUJER, W. & SIEGRIST, H. 2001. The EAWAG Bio-P module for activated sludge model No. 3. *Water Research,* 35**,** 3887-3903.

ROELEVELD, P. J. & VAN LOOSDRECHT, M. C. M. 2002. Experience with guidelines for wastewater characterisation in The Netherlands. *Water Science and Technology,* 45**,** 77-87.

RYSANEK, A. & CHOUDHARY, R. 2013. Optimum building energy retrofits under technical and economic uncertainty. *Energy and Buildings,* 57**,** 324-337.

SAN ONG, T. & THUM, C. H. 2013. Net present value and payback period for building integrated photovoltaic projects in Malaysia. *International Journal of Academic Research in Business and Social Sciences,* 3**,** 153.

SARKAR, U., DASGUPTA, D., BHATTACHARYA, T., PAL, S. & CHAKROBORTY, T. 2010. Dynamic simulation of activated sludge based wastewater treatment processes: Case studies with Titagarh Sewage Treatment Plant, India. *Desalination,* 252**,** 120-126.

SARPARASTZADEH, H., SAEEDI, M., NAEIMPOOR, F. & AMINZADEH, B. 2007. Pretreatment of municipal wastewater by enhanced chemical coagulation. *International Journal of Environmental Research,* 1**,** 104-113.

SATO, M. 1990. Thermochemistry of the formation of fossil fuels. In R.J. Spencer and I.M. Chou (Eds) Fluid-Mineral Interactions: A Tribute to HP Eugster. *Geol. Soc. Am. Spec. Publ. ,* 2**,** 271-283.

SATOH, H., NAKAMURA, Y., ONO, H. & OKABE, S. 2003. Effect of oxygen concentration on nitrification and denitrification in single activated sludge flocs. *Biotechnol Bioeng,* 83**,** 604-7.

SCHAUM, C., LENSCH, D. & CORNEL, P. 2016. Evaluation of the energetic potential of sewage sludge by characterization of its organic composition. *Water Sci Technol,* 73**,** 3072-9.

SCHERSON, Y. D. & CRIDDLE, C. S. 2014. Recovery of freshwater from wastewater: upgrading process configurations to maximize energy recovery and minimize residuals.

Environmental science & technology, 48**,** 8420-8432.

SEDLAK, R. I. 1991. *Phosphorus and nitrogen removal from municipal wastewater: principles and practice*, CRC press.

SHAKYA, R., ADHIKARI, S., MAHADEVAN, R., SHANMUGAM, S. R., NAM, H., HASSAN, E. B. & DEMPSTER, T. A. 2017. Influence of biochemical composition during hydrothermal liquefaction of algae on product yields and fuel properties. *Bioresource Technology,* 243**,** 1112-1120.

SHI, C. Y. 2011. *Mass flow and energy efficiency of municipal wastewater treatment plants*, IWA Publishing.

SHIZAS, I. & BAGLEY, D. M. 2004. Experimental determination of energy content of unknown organics in municipal wastewater streams. *Journal of Energy Engineering,* 130**,** 45-53.

SHOENER, B. D., BRADLEY, I. M., CUSICK, R. D. & GUEST, J. S. 2014. Energy positive domestic wastewater treatment: the roles of anaerobic and phototrophic technologies. *Environ Sci Process Impacts,* 16**,** 1204-22.

SIEGRIST, H., KREBS, P., BÜHLER, R., PURTSCHERT, I., RÖCK, C. & RUFER, R. 1995. Denitrification in secondary clarifiers. *Water Science and Technology,* 31**,** 205-214.

SIN, G., GERNAEY, K. V., NEUMANN, M. B., VAN LOOSDRECHT, M. C. & GUJER, W. 2011. Global sensitivity analysis in wastewater treatment plant model applications: prioritizing sources of uncertainty. *Water Res,* 45**,** 639-51.

SINGH, H. 2007. Interactions of milk proteins during the manufacture of milk powders. *Le Lait,* 87**,** 413-423.

SMYTH, M., MINALL, R., STEAD, T. & WALKER, J. 2016. Optimising the energy yield from anaerobic digestion through calorific value analysis: case studies from davyhulme and seafield. *21st Biosolids Conference.* Edinburgh, UK: Aqua Enviro.

SNF FLOERGER 2003. Sludge Dewatering. *In:* FLOERGER, S. (ed.). France.

SÖTEMANN, S. W., WENTZEL, M. C. & EKAMA, G. A. 2006. Mass balance-based plant-wide wastewater treatment plant models–Part 4: Aerobic digestion of primary and waste activated sludges. *Water SA,* 32**,** 297-306.

STOICA, A., SANDBERG, M. & HOLBY, O. 2009. Energy use and recovery strategies within wastewater treatment and sludge handling at pulp and paper mills. *Bioresource technology,* 100**,** 3497-3505.

STOLL, Z., DOLFING, J. & XU, P. 2018. Minimum Performance Requirements for Microbial Fuel Cells to Achieve Energy-Neutral Wastewater Treatment. *Water,* 10**,** 243.

STRATFUL, I., SCRIMSHAW, M. D. & LESTER, J. N. 2001. Conditions influencing the precipitation of magnesium ammonium phosphate. *Water research,* 35**,** 4191-4199.

SUNNER, S. & MÅNSSON, M. 1979. *Combustion Calorimetry: Experimental Chemical Thermodynamics*, Elsevier.

SUTTON, P. M., MELCER, H., SCHRAA, O. J. & TOGNA, A. P. 2011. Treating municipal wastewater with the goal of resource recovery. *Water Science and Technology,* 63**,** 25-31.

TAKÁCS, I., PATRY, G. G. & NOLASCO, D. 1991. A dynamic model of the clarification-thickening process. *Water research,* 25**,** 1263-1271.

TAS, D. O., KARAHAN, Ö., ÖVEZ, S., ORHON, D. & SPANJERS, H. 2009. Biodegradability and denitrification potential of settleable chemical oxygen demand in

domestic wastewater. *Water Environment Research,* 81**,** 715-727.

TCHOBANOGLOUS, G., BURTON, F. L. & STENSEL, H. D. 2003. *Wastewater engineering treatment and reuse*, Boston, US: McGraw-Hill Higher Education.

THORNTON, I., BUTLER, D., DOCX, P., HESSION, M., MAKROPOULOS, C., MCMULLEN, M., NIEUWENHUIJSEN, M., PITMAN, A., RAUTIU, R. & SAWYER, R. 2001. Pollutants in urban waste water and sewage sludge. Luxembourg: European Commission.

TSUZUKI, T. & HUNT, H. 1957. Heats of Combustion. VI. The Heats of Combustion of Some Amino Acids. *The Journal of Physical Chemistry,* 61**,** 1668-1668.

UBAY-COKGOR, E., OKTAY, S., ZENGIN, G., ARTAN, N. & ORHON, D. 2005. Effect of primary sludge fermentation products on mass balance for biological treatment. *Water Science and Technology,* 51**,** 105-114.

VAN DER HOEK, J., DUIJFF, R. & REINSTRA, O. 2018. Nitrogen Recovery from Wastewater: Possibilities, Competition with Other Resources, and Adaptation Pathways. *Sustainability,* 10.

VAN DER HOEK, J. P., DE FOOIJ, H. & STRUKER, A. 2016. Wastewater as a resource: Strategies to recover resources from Amsterdam's wastewater. *Resources, Conservation and Recycling,* 113**,** 53-64.

VANHOOREN, H., MEIRLAEN, J., AMERLINCK, Y., CLAEYS, F., VANGHELUWE, H. & VANROLLEGHEM, P. A. 2003. WEST: modelling biological wastewater treatment. *Journal of Hydroinformatics,* 5**,** 27-50.

VANWORTSWINKEL, L. & NIJS, W. 2010. Industrial Combustion Boilers. International Energy Agency.

WAN, J., GU, J., ZHAO, Q. & LIU, Y. 2016. COD capture: a feasible option towards energy self-sufficient domestic wastewater treatment. *Scientific reports,* 6**,** 25054.

WANG, L., MIN, M., LI, Y., CHEN, P., CHEN, Y., LIU, Y., WANG, Y. & RUAN, R. 2010. Cultivation of green algae Chlorella sp. in different wastewaters from municipal wastewater treatment plant. *Applied biochemistry and biotechnology,* 162**,** 1174-1186.

WANG, T., CAMPS-ARBESTAIN, M., HEDLEY, M. & BISHOP, P. 2012. Predicting phosphorus bioavailability from high-ash biochars. *Plant and Soil,* 357**,** 173-187.

WEIJERS, S. R. & VANROLLEGHEM, P. A. 1997. A procedure for selecting best identifiable parameters in calibrating activated sludge model no. 1 to full-scale plant data. *Water science and technology,* 36**,** 69-79.

WETT, B., BUCHAUER, K. & FIMML, C. Energy self-sufficiency as a feasible concept for wastewater treatment systems. IWA Leading Edge Technology Conference, 2007. Singa-pore: Asian Water, 21-24.

WILLIAMS, A. T., ZITOMER, D. H. & MAYER, B. K. 2015. Ion exchange-precipitation for nutrient recovery from dilute wastewater. *Environmental Science: Water Research & Technology,* 1**,** 832-838.

WILSON, L. & BOUWER, E. 1997. Biodegradation of aromatic compounds under mixed oxygen/denitrifying conditions: a review. *Journal of Industrial Microbiology and Biotechnology,* 18**,** 116-130.

WU YANG, X., RUI LIU, J., LI GAO, S., DONG HOU, Y. & ZHEN SHI, Q. 1999. Determination of combustion energies of thirteen amino acids. *Thermochimica Acta,* 329**,** 109-115.

WWT ONLINE. 2015. *Northumbrian Water creates gas from sewage for the national grid*

[Online]. Available: http://wwtonline.co.uk/news/northumbrian-water-creates-gas-from-sewage-for-the-national-grid#.WeJlhFXyvIU [Accessed 10-10-2017].

YESHI, C., LENG, L. C., LI, L., YINGJIE, L., SENG, L. K., GHANI, Y. A. & LONG, W. Y. 2013. Mass flow and energy efficiency in a large water reclamation plant in Singapore. *Journal of Water Reuse and Desalination,* 3**,** 402-409.

ZALAT, O. & ELSAYED, M. 2013. A study on microwave removal of pyridine from wastewater. *Journal of Environmental Chemical Engineering,* 1**,** 137-143.

ŽIŽLAVSKÝ, O. 2014. Net present value approach: method for economic assessment of innovation projects. *Procedia-Social and Behavioral Sciences,* 156**,** 506-512.